

CONFIDENTIAL

TNO report 2014 R10265
**Improved Sweet Spot Identification and smart
development using integrated reservoir
characterization**

Princetonlaan 6
3584 CB Utrecht
P.O. Box 80015
3508 TA Utrecht
The Netherlands

www.tno.nl

T +31 88 866 42 56
F +31 88 866 44 75

Date	July 2014
Author(s)	J.H. ten Veen R.M.C.H. Verreussel D. Ventra M.H.A.A. Zijp T.A.P. Boxem
Sponsor	Energie Beheer Nederland, GdFSuez, Wintershall Noordzee B.V.
Project name	IC Sweet Spot Identification
Project number	060.01401

All rights reserved.

No part of this publication may be reproduced and/or published by print, photoprint, microfilm or any other means without the previous written consent of TNO.

In case this report was drafted on instructions, the rights and obligations of contracting parties are subject to either the General Terms and Conditions for commissions to TNO, or the relevant agreement concluded between the contracting parties. Submitting the report for inspection to parties who have a direct interest is permitted.

© 2014 TNO

CONFIDENTIAL

Summary

In this report the results are presented of the project entitled 'Improved Sweet Spot Identification and Smart Development Using Integrated Reservoir Characterization'. This project was carried out within the *Innovation program Upstream Gas* as part of the Dutch Top Sector Policy 'Energy'. The aim of the project is to characterize the shale gas reservoir properties of the Posidonia Shale Formation (PSF), present in the Dutch subsurface. Particularly, the project aims at characterizing and quantifying lateral and vertical shale heterogeneities and their expressions in conventional well logs. In order to achieve this goal, an age-equivalent outcrop analogue to the PSF has been selected and studied in detail. The selected outcrop analogue is the informal 'Jet Rock', part of the Whitby Mudstone Formation, cropping out in coastal cliff sections in Yorkshire, Northern England. The analytical results from the Whitby outcrop study are applied to the Posidonia Shale Formation (PSF) in the West Netherlands Basin (WNB) and the outcome of this integration is subsequently discussed. In support of the analogy, it can be concluded that the 'Jet Rock' is very similar to the PSF with respect to overall thickness, depositional environment, mineralogy, and to a certain extent also in the Total Organic Carbon distribution. This suggests that on a trend parallel to a paleo-shoreline of the northwestern part of the Tethys Ocean, the PSF is laterally homogeneous over large distances (>50 km). It is expected that the PSF is less homogeneous over large distances on a trend perpendicular to the paleo-shoreline, but this could not be investigated further.

The observed vertical heterogeneity is expressed on a meter scale and allows a stratigraphic subdivision for both the Jet Rock and PSF of 6 to 10 units. The observed variation in geochemistry, sedimentology and organic matter composition appear closely related considering the correspondence of the individual analytical zonations. For the WNB, a detailed zonation based on the wire-line logs has been established, but here, detailed geochemical analyses are missing. Fortunately, a comparison of the geochemistry and mineralogy of the Jet Rock and the PSF via pseudologs. Geochemical and mineralogical data of the Whitby outcrops were used to produce pseudo GR and RHOB, which were then compared with GR and RHOB well-logs from the WNB. It appears that both show a similar subdivision characterized by a high GR - low RHOB interval related to very high TOC content and low GR zone in the upper part of the succession related to relatively high carbonate content. The elevated carbonate content in the upper Jet Rock is also reflected in a high Brittleness Index and in a high fracture density. This observation is quite interesting, especially since the gas logs in the WNB often show a peak at or near this interval. In the interval considered carbonates levels have not been encountered in the available cores available, but it is suggested that in the WNB, low GR-high RHOB log zones reflect the (near) presence of carbonate concretions, identical to the stratigraphically defined dogger occurrences in the Yorkshire outcrops.

Apart from the similarities, there is a striking and important difference in the TOC trend. In the Jet Rock, the TOC quickly rises from 4 to 14% and after 1,5 m falls back to 4%. Both in the WNB and offshore L05 and F11 blocks, the TOC of the PSF also rises quickly to values around 15% and remains quite high (between 5 and 8%) the next ~25 m. In order to understand these diverging TOC trends, additional

inconspicuous differences between the two localities are scrutinized. First of all, the WNB succession is almost twice as thick as the Yorkshire succession and contains more quartz and has a higher fossil content. Thin section analysis from both localities indicate a similar paleowaterdepth, ranging between 20 to 100 meters. Therefore, it is assumed that the amount of clastic input in the WNB was much higher than in the Cleveland Basin. In other words, the catchment area of the river(s) that provided the clastic input, must have differed in terms of e.g. the catchment size, the hinterland topography, the composition of the exposed rocks and soils, and so on. Based on the TOC trends, it can be concluded that the organic matter flux was concurrent with the siliciclastic riverine input and was much higher in the WNB than in the Cleveland Basin. It is a well-established fact, both from the literature and from the results of this study, that the anoxia of the Toarcian are triggered by a change in climate, in particular by an increase in the amount of precipitation. Most papers connect the occurrence of freshwater surface layers with the development of stratified water columns and impoverished circulation, eventually leading to bottom water anoxia and enhanced TOC content. In this study, careful comparison of the geochemical and palynological results indicates that for the Toarcian black shale, primary production is a more critical factor for TOC than the redox conditions. Almost all organic matter is of marine origin and is represented by fecal pellets or organic aggregates, which are mainly composed of structureless organic matter derived from microbial activity.

In summary, the Jet Rock and PSF were deposited in sub-basins, belonging to the same shallow marine, epeiric sea, which was influenced by 1) regional and global environmental change, and 2) by local factors. The regional and global changes are primarily related to climate and are reflected in the synchronous onset of the TOC increase, in the synchronous changes in carbonate preservation style, in the assumed (but not yet confirmed) synchronous stratigraphic position of the concretion horizons, in the assumed (but not yet confirmed) synchronous changes in the geochemical composition, and in the synchronous development of other sedimentary features such as trends in quartz and clay content and bed forms. The local factors are primarily related to paleogeography and influenced the amount and extent of primary production at the site of deposition. It is concluded here that paleogeography is the underlying driving mechanism for the TOC. In that respect, the paleogeographic setting for the WNB is much more prolific for shale gas or shale oil than the paleogeographic setting of the Cleveland Basin. In any case, a thorough understanding of the paleogeography is key. Because the Toarcian black shale is homogenous across large distances, basic knowledge derived for instance from just a few wells will probably be sufficient to predict the properties across a large area. In the West Netherlands Basin (WNB), the Posidonia Shale Formation (PSF) exhibits a 25 meters thick interval of relatively high (>5%) TOC, of which approximately 7 meters are (probably) enriched in carbonate. This carbonate-rich interval is the most brittle interval of the PSF and lies directly on top of the interval with the peak in TOC. As a consequence, this interval is the most prolific for shale gas and is regarded as the prime pay zone. Gas logs show that most peaks indeed occur in this interval.

Contents

Summary	2
Section 1 - Background	6
1 Introduction.....	7
1.1 Description of the Sweet Spot Identification project	7
1.2 Research approach	8
1.3 How to read this report	9
2 The Posidonia Shale Formation.....	10
2.1 Geological description	10
2.2 Sedimentology	13
2.3 The need for an analogue to the PSF in the WNB.....	17
3 The Whitby Mudstone Formation.....	20
3.1 Grounds of assumed equivalence	20
3.2 Geological context: the Cleveland (Yorkshire) Basin, the Whitby Mudstone Formation and the Toarcian Oceanic Anoxic Event (TOAE).....	22
3.3 Studied localities.....	27
Section 2 - Data	28
4 Sedimentology.....	29
4.1 Thin section analysis	29
4.2 Grey Shales	30
4.3 Jet Rock	32
4.4 Bituminous Shales	34
4.5 Synthesis and general insights.....	34
5 Palynology.....	37
5.1 Methodology	37
5.2 Organic Matter	38
5.3 Palynomorph assemblages	39
5.4 Results	39
5.5 Synthesis and general insights.....	43
6 Geochemical Analysis	45
6.1 Methodology	45
6.2 Results	46
6.3 Pseudo logs	52
6.4 Interpretation of geochemical analysis	55
6.5 Lateral variation of results	57
6.6 Synthesis and general insights.....	57
7 Fracture Analysis.....	59
7.1 Introduction	59
7.2 Methodology and Dataset.....	59
7.3 Fracture characteristics	63
7.4 Lithology-related fracture characteristics (DigiFract results)	69

7.5	Data interpretation	70
7.6	Data analysis/interpretation	74
7.7	Synthesis and general insights	78
8	Stable isotopes and stratigraphic correlation	79
8.1	Methodology	80
8.2	Stable isotope curves	80
8.3	Stratigraphic correlation.....	84
Section 3 – Integration.....		87
9	Integration of the analytical results from the Whitby outcrop study in the UK	88
9.1	Heterogeneity	88
9.2	Sea level	90
9.3	Mineralogy	90
9.4	Pseudologs	94
10	Compilation and review of data from the Posidonia Shale Formation (PSF) in the Netherlands.....	95
10.1	Review of existing data.....	95
10.2	New data: stable isotope analyses of well WED-01	98
11	Discussion and conclusions	99
12	Implications and recommendations	101
13	References	102

Appendices

- Appendix 1 Thin section results
- Appendix 2 Palynological charts
- Appendix 3 Outcrop photographs
- Appendix 4 Summary Whitby results
- Appendix 5 Well log correlations of the Posidonia Shale Fm in the Netherlands
- Appendix 6 Regional correlations
- Appendix 7 Log zonation of the Posidonia Shale Fm

Section 1 - Background

1 Introduction

This project is carried out within the *Innovation program Upstream Gas* and is part of the Dutch Top Sector Policy 'Energy'. Within the Innovation Program, the project at hand is called 'Improved Sweet Spot Identification and Smart Development Using Integrated Reservoir Characterization'. The total budget for the project is 200,000.- euro, 50,000.- of which is accounted for by the Dutch government. The remaining 150,000.- euro is funded by three industrial partners, all of which contribute an equal share of 50,000.-. The industrial partners are:

- **Energie Beheer Nederland (EBN)**
- **GDF SUEZ S.A.**
- **Wintershall Noordzee B.V.**

1.1 Description of the Sweet Spot Identification project

Given the long-term ambition to step up from trial-and-error to optimum design of fractures and considering the complexity of gas flow in tough gas reservoirs, predicting and planning reservoir stimulation (e.g. hydraulic fracturing) requires a comprehensive reservoir characterization. Understanding shale depositional processes and characterizing their vertical and lateral sedimentological variability is a fundamental premise to predict the character and stratigraphic position of sweet spots, and to characterize their geomechanical properties. Ideally, reservoir characterization should be carried out at different scales: from an analysis of fault networks and responses to local stress regimes at reservoir scale, to analyses of hydro-mechanical properties and fracture networks at bed scale, down to a characterization of compositional and sedimentological heterogeneity at the scale of laminae.

Since the scale at which reservoir heterogeneities occur is a priori unknown and not easily estimated from limited subsurface datasets, support of an outcrop-analogue study is essential, because it allows to obtain information at much more flexible resolution than those retrieved from vintage well data. In addition, an outcrop-based approach carries the benefit of direct control on the lateral variability of relevant formation properties. By comparing and integrating time-equivalent field and well/core data, we aim to derive a better conceptual model of heterogeneity in subsurface data and of its expression in conventional well logs.

In anticipation of new shale-gas exploration activities in the Netherlands, vintage well-log data is all that is available to date. Thus, the integrated sedimentological, biofacies, petrophysical and geomechanical analysis proposed here and based on palaeogeographical concepts represents the most promising conceptual framework for developing predictive models of sweet spot detection, and for assessing the quality and distribution of potential shale reservoirs.

In light of the most recent developments on deep-marine processes and shale sedimentology, the specific objective consists of exploring the relationships between processes and products of mud-grade sediment transport (at a scale from beds, i.e. individual sedimentary events, to laminae) and physical properties

(texture, sorting, flow properties, etc.), organic matter content and composition (mineralogy, geochemistry). Specific questions addressed herein are:

- Which depositional environments can provide hard/fraccable shales and where do these environments manifest in the Dutch subsurface?
- Subsequently, how is a sweet spot defined, and how can the lateral variability of relevant properties be used to better delineate the sweet spots in the Posidonia Shale Formation (PSF)?
- How are lateral gas-shale heterogeneities quantified and characterized at the reservoir scale, and how can these be applied to model properties of subsurface shale-gas occurrences in the Netherlands?
- In order to assess the (vertical) averaging effects of 'vintage' log resolution: what is the upscaling effect of measured and analysed properties from micro- to well-log scale, or how do small-scale heterogeneities in gas-shales contribute to 'log responses'? How are outliers represented in the data?
- What do zonations in log response mean in terms of relevant rock properties, and are they meaningful in shale-gas exploration?
- Establishing qualitative and quantitative relationships with TOC (gas potential) data, rock properties and fraccability: How do (micro)structures & rock properties determine productivity?

The initial activities of this project (phase 1) are aimed at the quantification and characterization of vertical gas-shale heterogeneities and how these can be inferred from conventional well logs. Insight into these heterogeneities, combined with predefined play concepts, will be utilized to model properties of subsurface shale-gas occurrences in the Netherlands. This should ultimately lead to a sharper definition of 'sweet spot', and consequently to a more reliable mapping of sweet spots for potentially prolific gas shales in the Netherlands.

1.2 Research approach

The extremely fine grain size of mudstones and their relative macroscopic homogeneity at outcrop require an integrated approach for their analysis. In most cases, research has amply demonstrated that outcrop observations are secondary in importance to a well-planned sampling strategy aimed at retrieving good-quality samples for standard petrographic (microscopic), compositional (mineralogy, geochemistry, organic matter) and petrophysical analysis.

The approach adopted for this project thus involved an informed choice for an ideal field analogue (see section 2.3), followed by preliminary field observations at outcrop scale and by a sampling campaign aimed at stratigraphic intervals of specific interest.

A preliminary reconnaissance trip was carried out in early March 2013, in order to appraise outcrop location, quality and accessibility. A follow-up mission took place in early May for rock sampling and for measurements of different rock properties at outcrop. In this second campaign priority was given to logging and sampling the stratigraphic interval from the upper part of the Grey Shale Member (upper *Dactyloceras tenuicostatum* ammonite zone) up to the basal portion of the Bituminous Shales (middle *Harpoceras falciferum* ammonite zone), including the Jet

Rock unit (basal *Harpoceras falciferum* zone). This stratigraphic interval extends within the chronological limits of the Posidonia Shale Fm on the continent, and it includes the most organic-rich stratigraphic unit of the WMF (the Jet Rock) as well as the transition from relatively coarser, organic-poor mudstones of the Grey Shales into the Jet Rock. It is thus considered highly representative for the most important paleoenvironmental, sedimentological and facies/compositional transition in the succession, which also represents the basic high-order heterogeneity within it.

Structural and image data for the analysis of fracture patterns at macro- and mesoscale is collected, together with a detailed sedimentological log and high-resolution collection of oriented samples (~20 cm interval; double samples for microfacies analysis and geochemistry).

1.3 How to read this report

This report is organized in three sections, each one describing a specific phase of the project. The first part gives background information on the Posidonia SF and discusses criteria for the selection of a chronological and sedimentological outcrop analogue, as there are no outcrops of the Posidonia Shale Formation in the Netherlands. The second part of this report concerns description and analysis of the collected data at the selected outcrop locality, i.e. the Whitby Mudstone Formation of the Cleveland Basin (UK). These data support the main research questions on how to better understand and characterize the heterogeneity. The final part three summarizes the results and subsequently describes the relevance of this study to understand reservoir heterogeneity in the Dutch subsurface PSF. It also highlights possible shortcomings of this study, the assumptions on which it is based, the significance of its results, and provides recommendations for next phases. The appendices contain background and accessory information derived from this study, which do not directly concern the research questions.

2 The Posidonia Shale Formation

The Posidonia Shale Formation is considered to be the main shale-gas prospect in the Netherlands, with a subsurface distribution throughout the central parts of the Broad Fourteens Basin, the West Netherlands Basin and the Central Netherlands Basin. Previous studies and technical reports have emphasised aspects of this formation related to its basinal context, such as structural setting, large-scale compositional and diagenetic trends, and thermal maturity. The present study adds particular attention to the depositional processes and environments of shales. The sedimentological history is the natural key to an understanding and thus prediction of internal compositional, structural (architectural) and textural trends in the formation, at scales from metric to millimetric. These, in turn, are responsible for the lateral and vertical distribution of properties critical to success in production, such as brittleness and fracture distribution, permeability, and organic matter.

Successful production of gas from shales varies per basin and is determined by several critical factors, among which the most important are generally considered to be: formation thickness, depth, thermal history, TOC content, maturity, geomechanical properties, porosity and adsorption capacity

<i>Property</i>	<i>Limit</i>	<i>Reference</i>
Depth	< 4 km	(AAPG EMD Annual Report 2010)
Thickness	> 20 m	(AAPG EMD Annual Report 2010)
TOC content	> 2 wt%	(Evans et al. 2003)
Organic Matter	Type II	(Kabula et al. 2003)
Hydrogen Index	> 250 mg/gTOC	(Kabula et al. 2003)
Maturity	1.4 – 3.3 % Vitrinite Reflectance	(Jarvie et al. 2007)

Table 2-1: Critical Values for prospective shale gas reservoirs

It must be emphasized that such values are still subject to debate and could vary per basin; therefore, they should be referred to as guidelines, and not as absolute criteria. The Antrim Shale in the US is a good example of a successful biogenic shale-gas play which nonetheless does not fit all of the criteria reported above.

2.1 Geological description

The Toarcian Posidonia Shale Formation is part of a very distinctive global stratigraphic interval with a present-day distribution from central to northwestern Europe comprising the surface and subsurface of the U.K. (Mulgrave Shale Member), Germany (Posidonienschiefer, or Ölschiefer, Figure 3) and France (Schistes Cartons). Given the relatively uniform lithological characters and thickness (mostly around 30-60 m of dark-grey to brownish-black, bituminous, fissile

claystones and siltstones) across these basins, it is commonly suggested that deposition of the Posidonia Shale took place over a large oceanic domain during a period of high eustatic level and restricted circulation in the water column. The present-day distribution of these stratigraphic units has been probably controlled by erosion at basin margins and non-deposition over bounding paleotectonic/geographic highs (Pletsch *et al.*, 2010). The official Dutch nomenclature (Van Adrichem Boogaert and Kouwe, 1993-1997) describes the formation as deposited in a low-energy pelagic realm under oxygen-deficient conditions partly controlled by a eustatic phase of high sea level; however; however, recent research suggests that this simplistic process and environmental framework should be reconsidered (e.g. Ghadeer and Macquaker, 2011; Trabucho-Alexandre *et al.*, 2012).

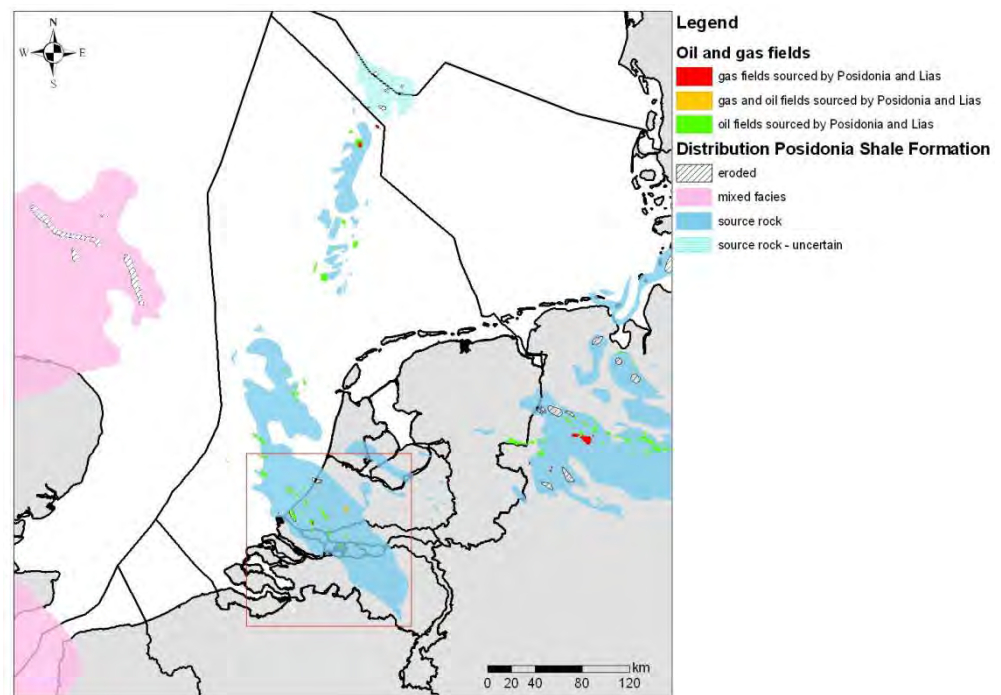


Figure 1: Map of the distribution and source rock quality of the Toarcian Posidonia Shale Formation (modified after Doornenbal and Stevenson, 2010). The red rectangle indicates the position of the detailed maps

In the Netherlands onshore, the formation is restricted to the axes of Late Jurassic rift basins (e.g. West Netherlands Basin and its extension into the Roer Valley Graben, the Central Netherlands Basin, and isolated locations in the Lower Saxony Basin, Figure 3). The greatest thickness is encountered at depths between 830 and 3055 m in the West Netherlands Basin (Figure 4), where, the Late Jurassic rifting and Cretaceous inversion produced a favourable horst-and-graben configuration. The common view is also that the sediments deposited outside the basin centres were eroded in parts of the Netherlands due to inversion events (Wong *et al.*, 2007), although this hypothesis is debated following observations of syn-sedimentary tectonics in the Early Jurassic. The Posidonia Shale Formation conformably overlies the non-bituminous claystones of the Lower Jurassic Aalburg Fm., although bituminous intervals have been identified also in the Aalburg Fm. (De Jager *et al.*, 1996), and it is conformably overlain by non-bituminous clay- and siltstones of the Middle Jurassic Werkendam Formation (Van Adrichem Boogaert and Kouwe 1993-1997; TNO-NITG, 2004), although hiatuses and unconformities

were identified at several locations. The formation consists of dark-grey to brownish-black bituminous fissile claystones and forms a very distinctive interval throughout the subsurface of the Netherlands, recognizable by its high gamma ray and resistivity readings on wire-line logs (Van Adrichem Boogaert and Kouwe, 1993-1997). Evaluation of the log responses showed that a subdivision can be made into distinct zones within the Posidonia Shale Formation, correlatable between wells throughout the basin (Figure 6). This internal variability can probably be referred to changing depositional mechanisms and conditions, which reflect on log responses through mineralogical and/or textural heterogeneities. A similar vertical zonation of the Posidonia Shale Fm. is observed also in Germany (Posidonienschiefer Formation) on the basis of both geochemical and sedimentological parameters (e.g. Röhl *et al.*, 2001; Frimmel *et al.* 2004; Schwark and Frimmel 2004;), and is evident in pseudo van-Krevelen diagrams (Figure 5) which show a wide range of kerogen types. Most measurements indicate a typical dominance of type II organic matter, while samples with a significant content of type III kerogen are probably the result of variations in depositional environment. Macroscopic and microscopic observations of core samples confirm this variability of depositional conditions. For example, textural alternations have been noted in cores from the onshore of the West Netherlands Basin and the offshore of the Central Graben; combined with the identification of erosional surfaces in the offshore, these characters indicate deposition in a dynamic environment with fluctuating energy conditions, probably well above the wave base at certain time intervals (e.g. Tabucho-Alexandre *et al.*, 2012).

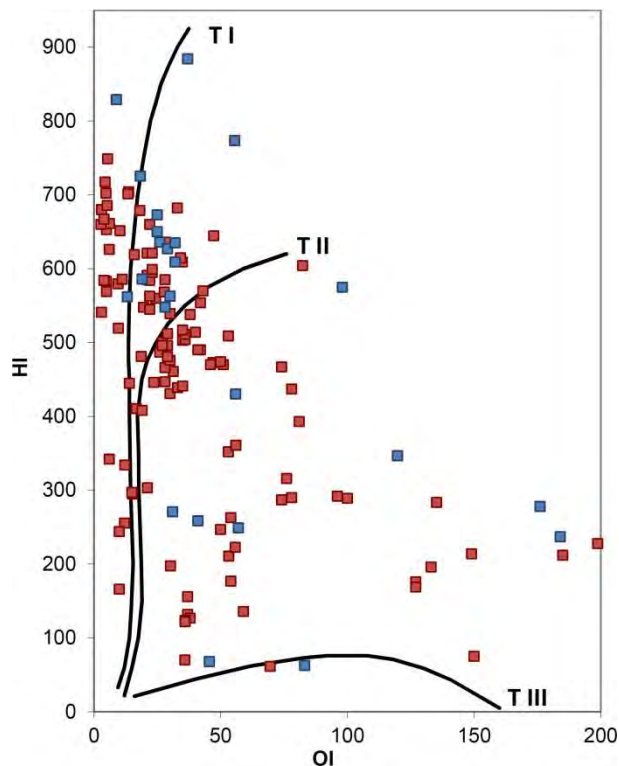


Figure 2: Pseudo van-Krevelen diagram for measurements from the Posidonia Shale formation onshore (blue) and offshore (red)

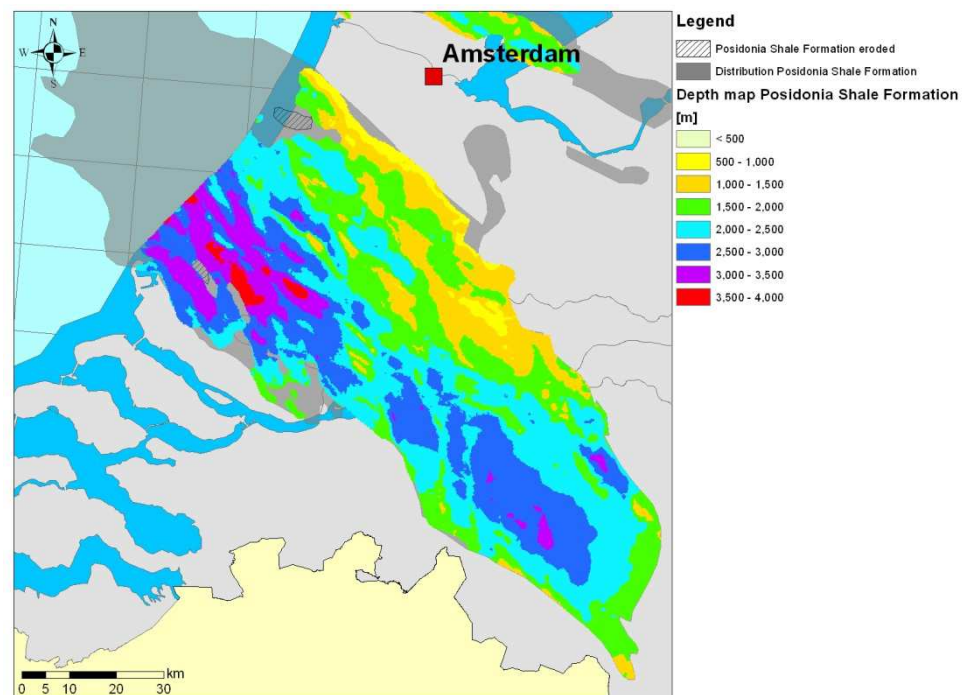


Figure 3: Map of the distribution and depth of the Posidonia Shale Formation (depth grid available on www.nlog.nl)

2.2 Sedimentology

Not much detailed sedimentological research has been carried out on the Posidonia Shale Formation in cores and outcrops of the Netherlands and Germany, most work being rather directed at analyses of geochemical and palaeoecological records. The recent resurgence of mudstone and shale sedimentology has brought some new data and interpretations to bear on the formation's depositional history and lithological characterization, but the available information is still relatively scarce.

So far the most detailed observations have been conducted on both outcrop and subsurface datasets of the Posidonienschiefer in Germany (e.g. Littke and Rullkötter, 1987; Littke *et al.*, 1988; Littke *et al.*, 1991; Prauss *et al.*, 1991; Littke, 1993; Röhl *et al.*, 2001; Frimmel *et al.*, 2004; Schmid-Röhl *et al.*, 2002; Röhl and Schmid-Röhl, 2005; Bour *et al.*, 2007; Klaver *et al.*, 2012) where the stratigraphic interval of interest here has been classically divided by essentially all authors into three superposed units (Fig. 4). These are defined on the basis of ammonite biozonation (from stratigraphic bottom to top: *Dactylioceras tenuicostatum*, *Harpoceras falciferum*, and *Hildoceras bifrons* zones; Riegraf, 1984), but show also an excellent correspondence with gross lithological and sedimentological changes vertically through the formation. In the field or in cores, visual reference for recognition of stratigraphic intervals can be made either to the dominant lithologies, or to a number of early-diagenetic horizons particularly rich in carbonate concretions and/or cement, which have been assigned informal names now long in use among workers (e.g. Inoceramenbank, Kubische bank, etc.; Fig. 4).

The basal '*tenuicostatum* zone' ranges in thickness between 2 and 3 m, composed of structureless, grey marlstones or clayey marlstones, with relatively low organic-

matter content (average TOC < 1%) and a high to pervasive degree of bioturbation. This interval commonly also preserves a diversified macrofauna in the form of both body fossils and recognizable ichnofossils. The overlying '*falciferum* zone' has been observed consistently to comprise of a so-called 'oil-shale facies' of dominantly organic-rich claystones and clayey marlstones, with variable thickness of 3-4 m and up to ~8 m. This facies presents a macroscopically evident millimetric lamination, a particularly high volume of preserved organic matter (TOC > 10%, up to 16%) with associated sulfur and pyrite, and thin, relatively coarse-grained interlayers (mostly silt to very fine sand). The topmost '*bifrons* zone' commonly reaches up to 6-8 m in thickness and consists of a dense alternation of claystones and bioclastic carbonates (wackestones and packstones) which give a coarse, millimetric lamination recognizable also macroscopically; organic content is intermediate between the two lower units (TOC = 1-10%).

From a compositional viewpoint, sediments of the Posidonienschiefer are consist of four fundamental components: terrigenous clastics (mainly clay- and silt-sized), carbonates of fine-grained bioclastic (nannoplanktonic) and subordinately diagenetic origin, organic matter, and pyrite, which is the dominant accessory mineral. Clastics and carbonates are consistently seen to be inversely covariant, frequently segregated in different laminae or beds. Illite is the dominant clay mineral, whereas silt-sized quartz is the most abundant clastic component of coarser granulometry.

Especially from borehole data, the thickness of the formation and of the defined stratigraphic intervals is generally seen to increase from about 10 m in SE Germany increase up to ~30 m in NW Germany; however, thickness trends are not regular and the location of distinct depocentres is tied to the distribution of local sub-basins of tectonic and/or palaeobathymetric origin.

Sample analyses show that most of the organic matter within the formation consists mostly of small alginite particles ($d < 20 \mu\text{m}$) and secondarily of bituminite particles of marine algal origin (phytoplankton), with only minor amounts of associated vitrinite and inertinite of land provenance (plants). However, the distribution of these organic components is not homogeneous throughout the Posidonienschiefer, and stratigraphic intervals with varying composition occur (Prauss *et al.*, 1991). Where laminae or beds with either dominant clastic (clay) or carbonate composition occur, organic matter is generally more abundant as dispersed within clastic laminae. Concentration of organic matter peaks in the basal interval of mudstones in the '*falciferum* zone' (particularly in the *elegantulum* and *exaratum* subzones). Rock-eval analyses show that type II kerogen of planktonic origin is dominant in the organic-rich units of the formation, with only minor contributions from material of terrestrial origin. Maturity, evaluated by vitrinite reflectance, generally corresponds to burial within a shallow to deep oil window. Carbonate-rich beds and stratigraphic units are generally the poorest in TOC, probably as a result of compositional dilution.

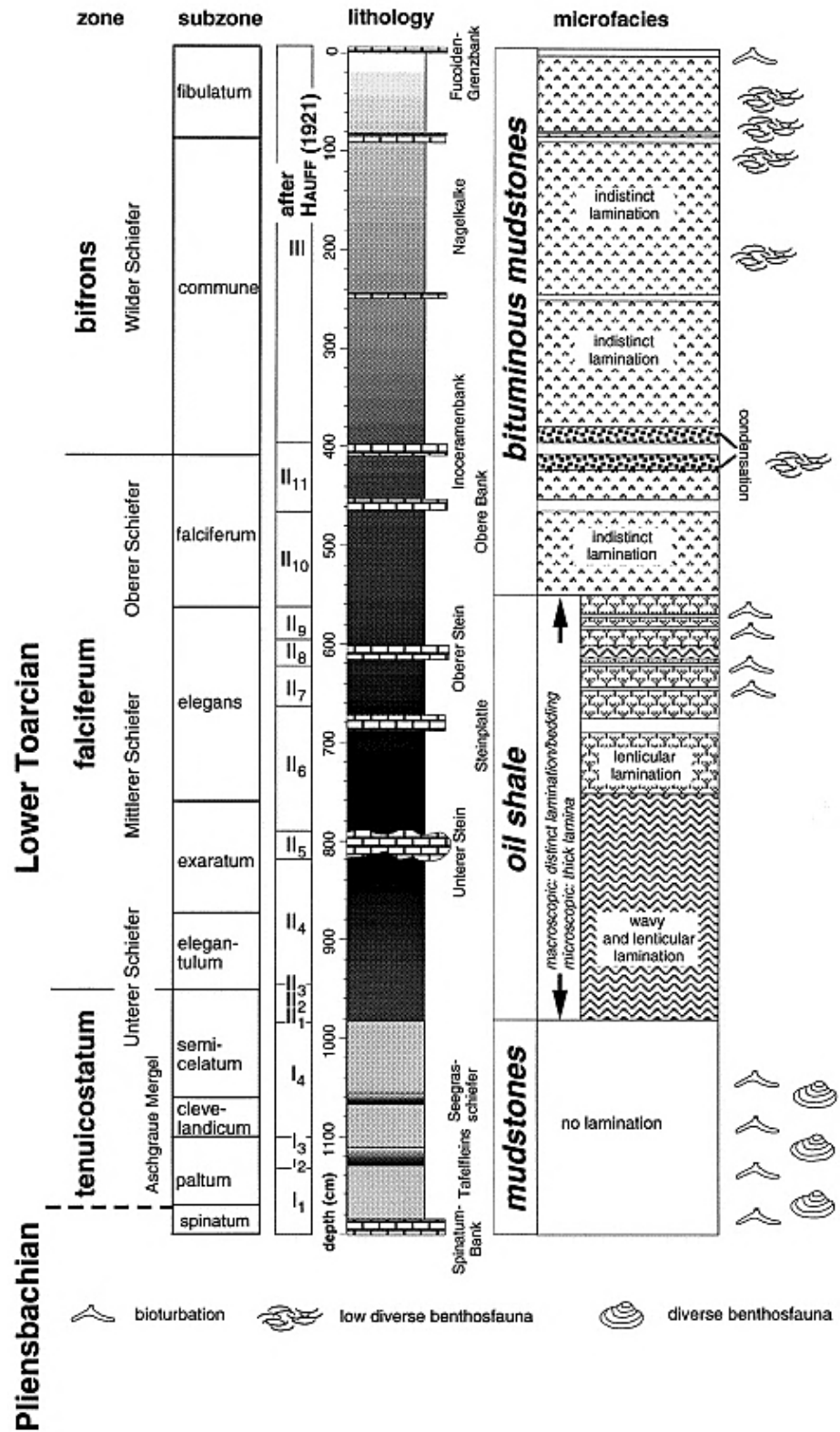


Figure 4: Classically tripartite lithological and biostratigraphic zonation recognized in all datasets from the German Posidonienschiefer (from Röhl *et al.*, 2001).

to silt) are dominant. Silt-sized quartz grains and clay minerals constitute most of the sediment, while the sand fraction is almost absent; diagenetic pyrite and dolomite are a secondary, minor component, abundant especially along specific stratigraphic horizons. Trends and absolute abundances in organic-matter content are substantially similar to those observed in German section, with maxima up to 15% recorded in the lower portion of the Posidonia Shale Fm in correspondence of the main negative carbon-isotope excursion (uppermost *tenuicostatum* and basal to middle *falciferum* zones; Fig. 5), and generally a significant variability in absolute TOC between different laminae and beds at millimetric to centimetric scales (Verreussel *et al.*, 2013). The same variability has been observed in sedimentological parameters such as composition and microfacies (Trabucho-Alexandre *et al.*, 2012), clearly showing that the formation is not composed of a relatively homogeneous stacking of uniformly fine-grained sediment, but rather comprises complex alternations of variously graded and laminated, clayey to silty depositional units, accompanied by erosional unconformities, deformed horizons, and local peaks in autogenic (syngenetic) minerals mostly related to the redox conditions at or immediately following the time of deposition. Petrographic studies show that organic matter is mostly represented by amorphous aggregates of marine planktonic origin ('marine snow'), preferentially segregated within densely laminated clastic-rich intervals with the highest degree of heterogeneity at the microscale.

2.3 The need for an analogue to the PSF in the WNB

The Posidonia Shale Formation has been penetrated in many wells, but rarely subject to sampling operations and analyses which could provide direct information on its composition and internal organization. Given the relative lack of data, one of the most effective strategies to inform a new evaluation of the Posidonia Fm consists in deriving relevant insights from outcrops of equivalent stratigraphic units, based on which useful geological concepts may be derived and applied to subsurface prediction and development. Five wells in the West Netherlands Basin (Fig. 3) have extracted PSF cores and samples: Andel-02 (AND-02; 54 samples available), Berkel-02 (BRK-02; 8 samples), Loon Op Zand-01 (LOZ-01; 85 samples), Werkendam-01 (WED-01; 14 samples) and Zoetermeer-02 (ZOM-02; 3 samples).

As this study focusses on a characterization of lateral formational heterogeneity in order to increase our understanding of inter-well areas, a geological setting is needed where rocks are accessible over significant distances for direct observation and sampling. For this reason, a sedimentologically equivalent formation is needed for which outcrops are extensive enough to make lateral correlations at reservoir scale. Given the peculiar sedimentological and geochemical character of the Posidonia Shale, tied to the particular palaeoceanographic conditions of the Toarcian, an additional requirement is the need to find a coeval shallow-/ deep-marine unit, deposited under identical forcing condition to the Posidonia, and over the same time interval.

2.3.1 The requirements for the analogue

Environmental factors which controlled the production and preservation of Toarcian organic-rich sediments in marine settings acted and interacted at regional to global scale, as now well established by an extensive scientific literature on Early Jurassic

paleoceanography (e.g. Jenkyns, 1988; Hesselbo *et al.*, 2000; Röhl *et al.*, 2001; Wignall *et al.*, 2005; Mattioli *et al.*, 2008; Al-Suwaidi *et al.*, 2010; Newton *et al.*, 2010). As a consequence, several stratigraphic units generically identifiable as 'black shales' have long been recognized in the stratigraphic records of various countries comprised within the former extent of the epeiric seaway that occupied northwestern Europe in the early Mesozoic. Such units are chronologically equivalent, as unambiguously ascertained through the high-resolution biostratigraphic framework of the Jurassic System; in addition, they are characterized by substantial sedimentological analogies at a scale of metres when comparisons are drawn between paleogeographically adjacent realms of the European seaway. A relatively broad set of options is thus available for a selection of potential outcrop analogues to the Dutch Posidonia Shale.

However, such a choice should be guided by several fundamental criteria, listed hereafter:

- given the articulated paleogeography of the Jurassic NW European epicontinental sea, comprising several (pen)insular landmasses and intervening oceanic corridors and sub-basins, the chosen succession should belong preferably to a paleogeographic realm adjacent to the Dutch one, and possibly not separated by extensive landmasses;
- outcrops should be characterized by good-quality, unobstructed exposure over relatively great distances (at least hundreds of metres, preferably up to several kilometres), while maintaining the access unrestricted by property limits or special regulations;
- a substantial body of knowledge on regional geology and stratigraphy should be available from easily retrievable literature, in order to inform preliminary observations and allow an immediate focus on specific aspects of interest, without spending much effort to decipher the local stratigraphic and palaeoenvironmental context;
- ideally, it should be possible to obtain subsurface datasets from local governmental/research institutions, in case further insights and comparisons were required for successive project phases.

2.3.2 Available alternatives and most suitable analogue

Although substantial research has been carried out on Toarcian shallow- to deep-marine successions in Europe, the erodible and easily weathered nature of mudstones restricts the choice for extensive surface exposures. One classical option is represented by the Schawische Alb region in southern Germany, where scattered outcrops of the Posidonienschiefer occur along a narrow belt extending approximately from Tübingen in the west to Würzburg in the east. However, the combination of low landscape relief and humid climate makes for poor-quality, small outcrops mostly comprising a rather reduced stratigraphic extent. The best opportunities are offered by quarries (active or abandoned), prominent among which is the Rohrback Zement Factory at Dotternhausen (near Tübingen), which offers a complete stratigraphic window on the early Toarcian actively exploited by academic geologists (e.g. Röhl *et al.*, 2001; Frimmel *et al.*, 2004). Recent changes in the quarry's administration and safety regulations have complicated preliminary planning, and this option is momentarily set aside, although still valid in terms of outcrop quality, physical access and available knowledge of the local geological/stratigraphic context.

Published research articles indicate that potential locations for field analogues exist also in north-central Germany (e.g. Littke *et al.*, 1991; Klaver *et al.*, 2012) and in various basins in France (e.g. Jenkyns, 1988; Rey *et al.*, 1994; Emmanuel *et al.*, 2006; Suan *et al.*, 2013), notably the Paris Basin and Aquitaine Basin. Similar considerations of generally lesser outcrop quality and rather restricted stratigraphic extent of available sections also lead us to classify such options as viable only for a successive project phase, in case detailed work were required on facies and compositional variations within specific stratigraphic intervals. Most important, the petrography of German and some of the French sections indicates a notably higher abundance of carbonate sediment, mostly of biogenic/bioclastic origin, than the Dutch Posidonia Shale, which is relatively richer in siliclastic components by volume.

Sections of possible interest on the Iberian Peninsula (e.g. Basque-Cantabrian Basin and Lusitanian Basin; Quesada *et al.*, 1997; Duarte, 1998) have not been considered given the greater distance from the northwestern realm of the Jurassic European seaway, and the consequent differences in sedimentology (especially the reduced volume of organic matter; Gómez and Goy, 2011; Suan *et al.*, 2013) and internal stratigraphy with the Dutch Posidonia Shale.

The Whitby Mudstone Formation, as exposed along the coast of NE England, is considered for now the most interesting option to fully characterize an outcrop analogue for the Posidonia Shale in the subsurface. In view of the guiding criteria listed above, the Whitby Mudstone Fm features an ideal combination of extensive outcrops of good to excellent quality, directly accessible over many kilometres along the northern Yorkshire coast (with only moderate hindrance due to cliff height, which may be solved in the field with the use of ladders or ropes) and exhaustively covered by numerous studies on international and local literature, which prove the stratigraphic completeness of exposed sections from the Pliensbachian to the Aalenian, including therefore the early Toarcian. The latter interval is furthermore described within a high-resolution bio-, chemo- and lithostratigraphic framework in northern Yorkshire, which has represented a type locality for biozone and stage correlations of European to global significance, and is thus ideal for comparisons with coeval sedimentary records anywhere else on the continent.

3 The Whitby Mudstone Formation

The Lower Jurassic successions of the southern and northeastern UK represent deposition in mostly shallow-marine and coastal environments which occupied the northwestern epicontinental margin of the then expanding Tethys Ocean. In the UK, these rocks formed a classical training ground for the development and application of basic concepts in litho- and biostratigraphy; as a consequence, the stratigraphic interval has long been one of the best characterized in the world, although various recent publications show that further refinements in our understanding of its sedimentary record are still possible. The Whitby Mudstone Formation (WMF; Barrow, 1988; Howarth, 1973; Powell, 1984) belongs to the Lias Group of the east-English Cleveland Basin (also known as Yorkshire Basin), and comprises ~90-105 m of mudstones of lower to late Toarcian age, with associated minor volumes of sandstones and carbonate rocks.

3.1 Grounds of assumed equivalence

Practical considerations supporting choice of the WMF as analogue to the Posidonia Shale Formation in the subsurface of the Netherlands are reported above, in section 2.3. From a more strictly geologic and stratigraphic perspective, the assumed validity of the WMF as outcrop equivalent to the Posidonia Shale is based on four main lines of evidence:

biostratigraphic: the organic-rich, shaly portion of the formation is comprised from the *D. tenuicostatum* to the *H. bifrons* zones, over the same standard biozones of the Lower Jurassic which define the chronology of the Dutch Posidonia Shale;

chemostratigraphic: coeval deposition is corroborated at even higher resolution by numerous published works demonstrating that trends in stable carbon isotopes ($\delta^{13}\text{C}$) are essentially identical for the two formations over the identified biozones;

paleogeographic: both stratigraphic units were deposited in relatively shallow, marginal to open marine conditions within the same sub-basin of the Jurassic European epicontinental seaway, relatively proximal to emergent land and broad shoaling blocks (Pennine High and London-Brabant Massif), and thus subject to substantially analogue base-level histories and paleoceanographic conditions;

sedimentological: sediments of the WMF are volumetrically dominated by siliciclastic components of mostly mud grade, in analogy to the Dutch Posidonia Shale, with only a limited percentage of carbonates and authigenic fractions, of which coeval successions (such as the German Posidonienschiefer and the French Schistes Carton) tend to be relatively rich; this implies more direct textural, compositional and potentially geotechnical analogies between the WMF and the Posidonia Shale over the considered stratigraphic interval, compared with other time-equivalent formations of more distal Tethyan domains;

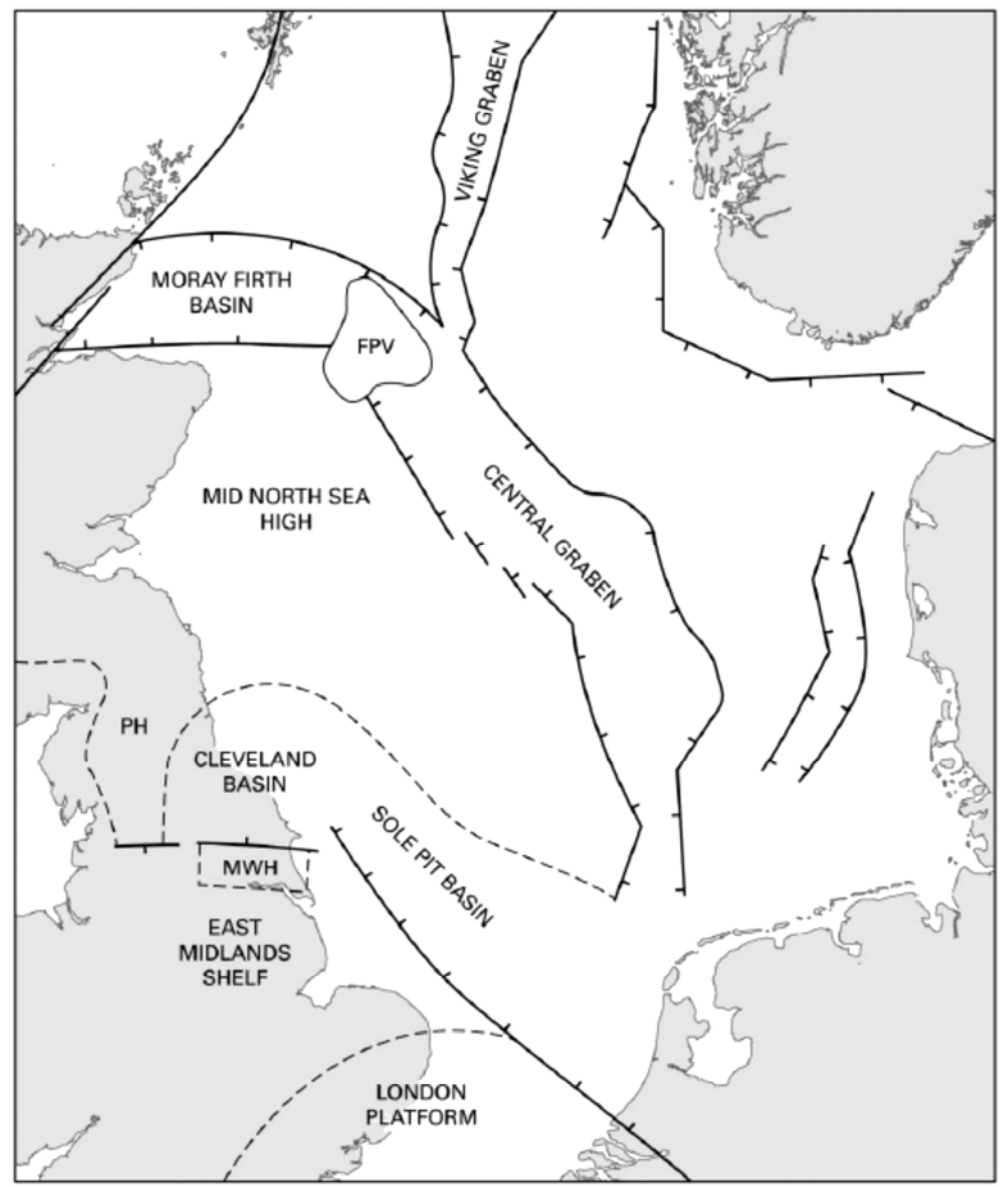


Fig. 3-1 Paleogeographic reconstruction of the eastern British coast at Early Jurassic times (modified from Powell, 2010; MWH – Market Weighton High, PH – Pennine High, FPV – Forties-Piper Volcanic Centre).

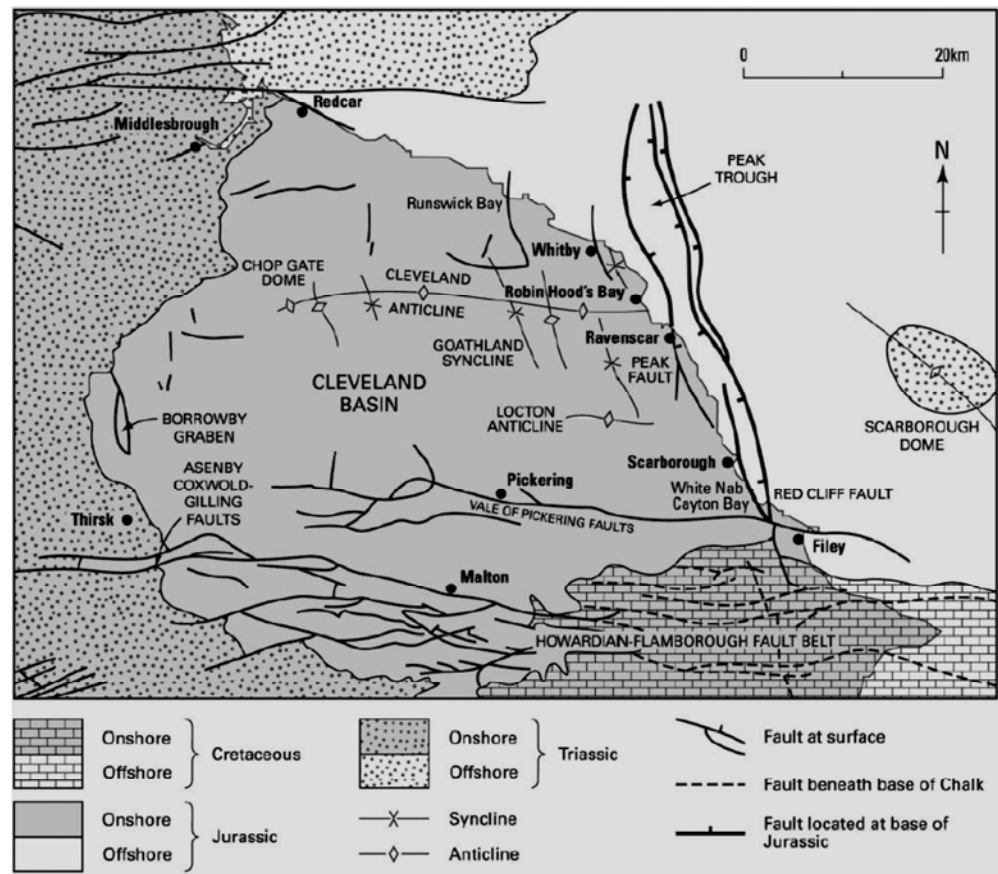


Fig. 3-2 Generalized geological map of the Cleveland Basin (from Powell, 2010, modified from Rawson and Wright, 2000). Faults at outcrop are bold solid lines; faults below the Cretaceous chalk are bold dashed lines. Dots – Triassic rocks at outcrop; brickwork – Cretaceous rocks at outcrop; grey – Jurassic at outcrop

tectonic: during and following the Jurassic, the Cleveland Basin was involved in the same regional stress field as the region where the Dutch Posidonia Shale was deposited, in the framework of extension and subsidence of the southern branch of the North Sea Rift; from the perspective of structural and fracture analysis, it is reasonable to expect that the WMF and the Posidonia Shale underwent a similar evolution.

3.2 Geological context: the Cleveland (Yorkshire) Basin, the Whitby Mudstone Formation and the Toarcian Oceanic Anoxic Event (TOAE).

In the early Mesozoic, the present NE English coast belonged to a group of large insular landmasses at the northwestern margin of the newly formed Tethys Ocean, enclosed by and disconnected from surrounding continental masses (**Fig. 3-1**). In the region, the Early Jurassic (Pliensbachian to Toarcian) saw the relative culmination of a gradual marine transgression that had initiated in the Late Triassic (Rhaetian) (Hesselbo and Jenkyns, 1998; Hallam, 2001). In the context of the early North Sea rifting, local extensional tectonics developed a series of physiographically disconnected basins along the present-day southern and eastern British margins

(Rawson and Wright, 1995; Powell, 2010). Among these, the relatively deep Cleveland Basin (frequently referred to as Yorkshire Basin in old literature) was separated from a generally shallow shelfal domain to the south (East Midlands Shelf) by a tectonically raised massif (the Market Weighton High), and flanked to the north by an extensive shallow shelf (the Mid-North Sea High), with a probably gradual bathymetric transition to a deeper oceanic realm farther east (the Sole Pit Basin). Landmasses of the Pennine High bounded the Cleveland Basin to the west and northwest, forming the main clastic sources. Over the long term, Aalenian to Bathonian relative uplift of the Mid-North Sea High region, related to the updoming and incipient rifting of the North Sea, would create a new major sediment source in the northeast and contribute to a normal regression in the Cleveland Basin, where fluvio-deltaic environments would partly supplant marginal-marine ones. The two principal tectonic lineaments along the northern Yorkshire coast (the Peak Fault, present in the south of the study area, and the Red Cliff Fault; Fig. 3-2) were activated since the Early Jurassic to accommodate extensional stresses (Milsom and Rawson, 1989; Powell, 2010); however, their activity was mostly concentrated in post-Toarcian times, and is not particularly relevant to the sedimentary history examined here.

In this framework, the stratigraphic evolution of the Cleveland Basin was strongly controlled by long-term regional changes in relative sea-level, accompanied by regional and global climatic events that influenced sediment supply, but especially the basinal oceanography. While the Middle-Late Jurassic peak in regional tectonics caused a discrepancy between local patterns of relative sea-level change and the commonly accepted global ones (e.g. Haq *et al.*, 1987; Hallam, 2001), the Hettangian to Toarcian interval in the Lower Jurassic shows a generally good correspondence with global trends.

The Lias Group (Powell, 1984; Fig. 3-3) comprises five formations deposited over two major regressive cycles (probably shoaling-up, normal regressive trends; Van Buchem and Knox, 1998), for an overall thickness of several hundreds of metres as measured from subsurface data and outcrops. Early-Jurassic stages comprise, in ascending stratigraphic order, the Hettangian to early Pliensbachian Redcar Mudstone Formation, the middle-Pliensbachian Staithes Sandstone Formation, the late-Pliensbachian Cleveland Ironstone Formation, and the Toarcian Whitby Mudstone Formation and Blea Wyke Sandstone Formation. The entire stratigraphic interval comprises sediments of marginal- to open-marine environments, wave- and storm-dominated, with generally continuous deposition as verified through ammonite zones and accompanied by equivalent lithostratigraphic units up to the late Toarcian in the adjacent Sole Pit Basin and East Midlands Shelf. The Whitby Mudstone Formation belongs to the younger regressive trend in the Lias Group (Van Buchem and Knox, 1998; Powell, 2010),

The middle Pliensbachian Staithes Sandstone Formation records a relative peak in the dispersal of coarse sediment at the top of the first Liassic shoaling cycle, and is composed mostly of fine- to medium-grained sandstones and siltstones with abundant bioturbation and an evident internal heterogeneity and organization (low- to high-angle cross-bedding, hummocky and swaley cross stratification, gutter casts and erosive surfaces, occasional shell beds, repeated textural cycles) testifying to relatively high-energy conditions on a well-oxygenated, open shoreface aggrading well above wave base (Howard, 1985; Knox *et al.*, 1991; Powell, 2010). Several upward-coarsening cycles recognized in the Staithes Sandstone are interpreted as

phases of shelfal accretion and progradation that managed to keep up with a steady increase in accommodation, mostly controlled by a rising sea level. The general east-west orientation of gutter casts and the eastward vergence of sedimentary structures from unidirectional currents (probably storm-surge and rip currents) suggest a clear dominance of currents and bathymetric deepening toward east, and a coastal domain landward to the west.

In spite of its name, the late Pliensbachian Cleveland Ironstone Formation contains only about 30% of early-diagenetic sideritic and chamositic ooids, mostly in laterally continuous levels, whereas its dominant muddy clastic content marks a distinct fining upward trend in comparison with the Staithes Sandstone. Clayey siltstones, claystones and subordinate fine sandstones are commonly interpreted as the result of a lengthening in the path of clastic dispersal following the start of a major transgressive trend, the upper one in the Lias Group (Macquaker and Taylor, 1996; Powell, 2010). The abundance of associated sediments of (bio)chemical origin confirms a reduced clastic supply and prolonged periods of stability and reworking at the sediment-water interface. However, shell beds, bioturbation and the internal organization into distinct ‘parasequences’ capped by relatively coarse facies with sedimentary structures, still indicate a shallow, storm-dominated, open-marine environment subject to energetic circulation and oxygenation.

	STAGE/ SUBSTAGE	AMMONITE ZONE	LITHOSTRATIGRAPHY				
			CLEVELAND BASIN		SOLE PIT BASIN	EAST MIDLANDS SHELF	
UPPER JURASSIC	175.6 Ma TOARCIAN	<i>Pleydellia aalensis</i>	Blea Wyke Sandstone Formation	Yellow Sandstone Mbr 9m	Phillips Member c. 60m		
		<i>Dumortieria levesquei</i>		Grey Sandstone Mbr 9m			
		<i>Grammoceras thouarsense</i>		Fox Cliff Siltstone Mbr 11m			
		<i>Haugia variabilis</i>	Peak Mudstone Mbr 13m	Cerdic Formation c. 120m			Whitby Mudstone Formation 50m
		<i>Hildoceras bifrons</i>	Alum Shale Member 37m				
		<i>Harpoceras falciferum</i>	Mulgrave Shale Member 32m				
		<i>Dactyloceras tenuicostatum</i>	Grey Shale Member 14m				
	183.0 Ma	<i>Pleuroceras spinatum</i>	Cleveland Ironstone Formation	Kettness Member 10m	Ida Formation 30m	Marlstone Rock Formation 13m	
	UPPER PLEINSBACHIAN	<i>Amaltheus margaritatus</i>		Penny Nab Member 19m			
	LOWER PLEINSBACHIAN	<i>Procdactyloceras davoei</i>	LIAAS GROUP	Staithes Sandstone Formation 25m		Charmouth Mudstone Formation 110m	
		<i>Tragophylloceras ibex</i>		"Ironstone Shales" (Banded Shales) 64m	Offa Formation 190m		
	189.6 Ma	<i>Uptonia jamesoni</i>		"Pyritous Shales" 27m		Penda Formation 250m	Scunthorpe Mudstone Formation 115m
	UPPER SINEMURIAN	<i>Echioceras raricostatum</i>	Redcar Mudstone Formation	"Siliceous Shales" 38m			
		<i>Oxynoticeras oxynotum</i>					
		<i>Asteroceras obtusum</i>					
	LOWER SINEMURIAN	<i>Caenesites turneri</i>		"Calcareous Shales" 127m			
		<i>Arnioceras semicostatum</i>					
	196.5 Ma	<i>Arietites bucklandi</i>					
HETTANGIAN	<i>Schlotheimia angulata</i>						
	199.6 Ma	<i>Alsatites liasicus</i>					
		<i>Psiloceras planorbis</i>					
(TRIASSIC)			(Penarth Group)				

Fig. 3-3 Litho- and biostratigraphic framework of the Lower-Jurassic Lias Group in the Cleveland Basin (after Powell, 1984, 2010).

The concentration of iron minerals especially in the fine units capping individual parasequences has recently been interpreted as deposition of solutes provenant from the adjacent lands, where tectonic stability and the Early-Jurassic climate warming intensified weathering and leaching of soils while at the same time cutting down on coarse clastic supply (Morgans *et al.* 1999; Dera *et al.*, 2009; Powell, 2010); this would have produced a typical (bio)chemical signature in sediments representing condensed intervals corresponding with the transgressive phase.

The Whitby Mudstone Formation comprises a thick association of mudstones and subordinate sandstones and carbonate rocks tied to the second Lower-Jurassic maximum transgression in NW Europe, and successive regression. It is historically well known for its high content in organic matter, and for its internal heterogeneity, which represents complex responses to environmental and oceanographic forcing in the Toarcian. The formation is subdivided into five formal members, as well as a number of informal stratigraphic intervals and individual layers which have established value for stratigraphy and correlation. The formation history is tied to the establishment of relatively more open oceanic conditions and probably slight further deepening of the water column during the Toarcian climatic altithermal phase whose consequences are well reported from global sedimentological, geochemical and palaeoecological records (e.g. Jenkyns, 1988; Little and Benton, 1995; Jenkyns *et al.*, 2002; Mattioli *et al.*, 2004; Wignall *et al.*, 2006; Hesselbo *et al.*, 2007; Cohen *et al.*, 2007; Caruthers *et al.*, 2011; Suan *et al.*, 2013; Danise *et al.*, 2013). The processes and stratigraphic expression of environmental change are variable between palaeogeographic domains, and the mechanisms and implications are still debated in the literature. The Toarcian Oceanic Anoxic Event (TOAE) has been studied with more attention in the NW European region, for which a moderately prevailing opinion exists that the combination of warming climate and transgression would have favoured variably intense stratification of the oceanic water column, especially in bathymetrically confined sub-basins, accompanied by enhanced organic productivity in the photic zone (Sælen *et al.*, 2000; Röhl *et al.*, 2001; Röhl and Schmid-Röhl, 2005; Wignall *et al.*, 2005; Jenkyns, 2010; Suan *et al.*, 2013). Alternating anoxic/dysoxic and oxic conditions were established for protracted periods along the bottoms of various shallow-marine regions worldwide, shelfal or epicontinental, which almost invariably accumulated organic-rich sediments. The record from more distal, deeper marine environments is virtually nonexistent, owing to the subduction of Early-Jurassic oceanic crust, but sparse observations suggest that organic-rich deposits might have been preserved also in pelagic realms (Hori, 1997; Jenkyns, 2010). Geochemical and petrographic records from the Toarcian of Yorkshire and NW Europe match with those of other successions worldwide, showing various peaks in the abundance of trace elements and disseminated pyrite, the first common indicators of anoxic to dysoxic conditions at least below the sediment-water interface, the second a possible indicator of reducing conditions also in the water column (Jenkyns and Clayton, 1997; Wignall and Newton, 1998; Frimmel *et al.*, 2004; McArthur *et al.*, 2008). As mentioned above, the WMF also shows an excellent parallel between trends in stable carbon isotopes ($\delta^{13}\text{C}$) with other sections in Europe and worldwide (Sælen *et al.*, 2000) McArthur *et al.*, 2008; Jenkyns, 2010). The broad negative peak in the isotopic signature of ^{13}C encountered in the most organic-rich intervals of the formation (see below) is accompanied by subdued positive trends. These isotopic patterns at present are at the center of a scientific debate between alternative explanations: 1) direct consequence of massive organic-carbon burial and preservation, enhanced by global warming and variably controlled by local oceanographic and bathymetric conditions in different basins; or 2) record of a disequilibrium in the concentration of atmospheric greenhouse gases (namely, methane from gas hydrates or protracted CO_2 exhalation from volcanic sources; e.g. Hesselbo *et al.*, 2000; Pálffy and Smith, 2000), which would actually have led to temporary global warming.

The basal member of the WMF, the 'Grey Shales' reaches up to about 13 m along the coastal outcrops of Yorkshire, and consists of pale grey siltstones to silty

claystones showing a generally scarce development of stratification and lamination at outcrop, with intercalated levels of diagenetic nodular carbonates (siderite and dolomite). The top half of this member is sedimentologically characterized by a coarsening-upward trend, dictated by an increase in the volume of silt-sized detrital quartz (Wignall *et al.*, 2005), which terminates approximately 1.5 m below the transition to the Mulgrave Shale Member. The Gret Shales represent deposition on an open, probably deeper shelf compared to the underlying Cleveland Ironstone Formation, as well as a marked increase in clastic sediment supply, particularly rich in fine (silt and clay) fractions. The coarsening trend toward the top of the unit is probably tied to a temporary decrease in relative sea-level identified in the *semicelatum* subzone (Wignall *et al.*, 2005) and superposed to the longer-term transgression of the Toarcian. Geochemical and palaeoecological evidence points to fluctuating oxic and dysoxic conditions, but never to full anoxia; TOC increases towards the top of the member (*semicelatum* subzone of the *tenuicostatum* zone), in the few metres preceding the stratigraphic transition to the Jet Rock unit.

The overlying 'Mulgrave Shale Member' is about 35 m thick along the coastal outcrops, and comprises three informal stratigraphic units long in use among stratigraphers and paleontologists, the basal Jet Rock (often improperly referred to as Jet Rock Member in the literature), the Bituminous Shales, and a relatively thick but laterally discontinuous, topmost level containing abundant diagenetic concretions and concentrations of cephalopods, called Ovatum Band. The Mulgrave Shale Member is distinguishable from the Grey Shales below for its finer clayey texture, finely laminated appearance at outcrop, and generally darker in unweathered exposures (whereas heavily weathered exposures tend to assume a yellow-red varnished appearance, due to the oxidation of iron, manganese and other trace elements of which the mudstones are rich). The Jet Rock unit (~5-7 m thick) is particularly enriched in organic matter, reaching up to 18% TOC from an average of ~6% up to the *exaratum* ammonite subzone of the *falciferum* zone; it is considered represent the most restricted conditions in mixing and circulation of the lower water column, with temporary anoxia to dysoxia below a generally still productive photic zone (as evidenced by the varied ammonite and belemnite faunas preserved). The thicker (more than 20 m) Bituminous Shales represent a gradual return to more frequent, effective mixing of the water column and slightly coarser sediment supply, with a markedly lower TOC (average 3%, and only slightly higher in the basal metres) compared to the Jet Rock, a slightly higher fraction of silt, and reduced preservation of primary stratification/lamination.

The 'Alum Shales' (~12 m) represent a gradual return to 'normal' oceanic conditions, and consist of poorly laminated (apparently massive at outcrop) claystones and siltstones with grey to pale colour, scattered concretions, and a notable increase in bioturbation and preserved benthic faunas.

The two members topping the WMF, 'Peak Mudstone Member' and 'Fox Cliff Siltstone Member', comprise together a little more than 20 m in stratigraphy, and consist of superposed textural cycles (claystones to siltstones) with a lower content in diagenetic concretions compared to the entire interval below, representing a marked return to progradation and aggradation of clastic 'parasequences' in an oceanic realm which tended to be more marginal during a gradual base-level lowering (shoaling) probably related to the incipient doming of the Mid-North Sea High. The coarse-clastic Blea Wyke Sandstone Formation, with analogue characters to the Pliensbachian Staithes Sandstone, overlies the WMF and forms resistant ledges capping most of the coastal cliffs in northern Yorkshire; it testifies to the relative bathymetric and accommodation minimum in the region.

3.3 Studied localities

In order to characterize heterogeneity at the scale of an average gas shale play, i.e. at km scale, several well exposed beach-cliff sections of the Whitby Mudstone were selected. The sections are taken at Port Mulgrave, Runswick Bay and Kettleiness, with a maximum separation of ~3 km (**Fig. 3-4**). At each locality it was attempted to study the entire Jet Rock Formation, including its lower transition with the Grey Shale Member and its upper transition with the Bituminous Shales. Because of the inaccessibility of the cliff sections this could only be achieved by lateral- instead of vertical logging and sampling. As such, each locality represents a composite section composed of lateral logs taken within a certain radius (< 200 m). Table 3-1 shows the analysis performed at studied localities.



Fig. 3-4 Locality of the studied (partial) sections

Table 3-1 Analysis performed at studied localities

	Name	Medusa	Fracture	Rock samples	
1	Runswick	SGR, runs 1, 2, 4, 5	WHI-1, WHI-3	RW	RW01-RW32
				RWN	RWN01-RWN33
2	Kettleiness	-	-		KL01-KL13
3	Kettleiness N	SGR, run 3	-		KLN01-KLN16
4	Port Mulgrave	SGR, runs 6+7	WHI-2, WHI-4		-
5	Port Mulgrave S	SGR, runs 8+9	-		PMS01-PMS12

Section 2 - Data

4 Sedimentology

4.1 Thin section analysis

As most sedimentological information on mudstones cannot be gained from outcrop, a number of thin sections were prepared at Utrecht University in order to derive more specific insights into depositional processes of the Whitby Mudstone Formation (WMF) and evaluate the (micro)facies and lithological heterogeneity at millimetric to submillimetric scales. The recent resurgent interest in the sedimentology of shales/mudstones has demonstrated that most of these rocks possess a much greater degree of textural, compositional and architectural complexity than was previously assumed. 'Classical' depositional models for mudstones and shales almost invariably envisaged deposition of fine clastic sediments as passive settling of mostly isolated particles through the water column; sedimentary environments which would favour this conceptual model were necessarily interpreted as relatively distal, low-energy domains of either marine or deep lacustrine basins, where the action of physical processes would be limited by depth below base-level or wave-base, and/or by the geographic distance from subaerial/shoreline environments. This interpretive framework lies at the base of the frequent extraction of geochemical and palaeobiological proxies from mudstone successions, thought to preserve continuous, high-resolution records of palaeoenvironmental conditions undisturbed by sediment erosion, reworking, mixing, etc., and it has been applied generally in particular to organic-rich mudstone successions (Tyson *et al.*, 1979; Demaison and Moore, 1980; Pye and Krinsley, 1986; Hesselbo *et al.*, 2000, 2007).

By converse, the last two decades of research in mud and mudstone sedimentology have witnessed a slowly rising critique and reevaluation of old concepts and an increasing number of workers are highlighting the importance of variable physical transport processes also for these very fine-grained sediments (e.g. Macquaker and Gawthorpe, 1993; Macquaker, 1994; Macquaker and Taylor, 1996; Schieber, 1998; Traykovski *et al.*, 2000; Lamb and Parsons, 2005; Schieber *et al.*, 2007; Bhattacharya and MacEachern, 2009; Ichnas and Dalrymple, 2009; Schieber, 2011; Ghadeer and Macquaker, 2011; Plint *et al.*, 2012; Egenhoff and Fishman, 2013). Consequently, major emphasis is now placed on the great heterogeneity in facies and composition that mudstones can show at multiple scales, previously overlooked by classical petrographic approaches more oriented toward a simple compositional analysis. Our preliminary observations of thin sections from the WMF confirm the relevance of modern concepts in mudstone sedimentology for a high-resolution characterization of gas-shales.

In this first project phase, sampling for sedimentological analysis was focused on a relatively restricted stratigraphic interval centered on the Jet Rock unit of the Mulgrave Shale Member, known to be the most organic-rich portion of the entire formation. Sample collection comprised the topmost metres of the Grey Shales Member, which underlie the Jet Rock unit in stratigraphy (Fig. 4-1), and further upward the basal two metres of the Bituminous Shales unit, which forms the upper interval of the Mulgrave Shale Member. The objective of this first sampling campaign was to ascertain the degree of microfacies heterogeneity within/between different units of the WMF. To this effect, unweathered or very poorly weathered samples were extracted at outcrop after noting their stratigraphic polarity (base/top); particularly thin sections (average thickness a long section's surface ideally targeted

at 20-30 µm in order to allow optical microscopy in transmitted light through clay-rich and organic-rich mixtures) were extracted after consolidating the samples with artificial resins for standard petrographic analysis.

A general overview of the sedimentological history and variability of the studied interval is reported below here and represented in Fig. 4-1; selected facies microphotographs that explain the most relevant details are presented in Appendix 1. For descriptive purposes, the facies terminology and codes adopted are a simplified version of the notation suggested by Macquaker and Adams (2003), as follows: a mudstone is defined as a siltstone if containing >50% silt-sized granules, or claystone if it contains >50% clay-sized material by volume (as identified at microscopic analysis); for secondary components between 50% and 20% a mudstone is described as 'rich' in those constituents; for secondary components <20% a mudstone is defined as 'bearing' them (example: bioclast-bearing, silt-rich claystone). Appropriate modifiers (massive, crudely bedded, finely bedded, bioturbated, pelleted, intraclastic, etc.) can be added to further integrate the microfacies description.

4.2 Grey Shales

At outcrop scale, the general sedimentology of the Grey Shales Member is characterized by a prevalence of grey to dark grey, non-fissile siltstones and subordinate claystones in single or frequently amalgamated millimetric to centimetric beds, with varying degree of bioturbation and sedimentary structures which are sometimes identifiable at macroscopic scale. Although diagenetic concretionary horizons are less numerous than in the overlying Jet Rock (see below), the Grey Shales are characterized by several shell pavements at different stratigraphic levels, distinguishable through detailed analysis of species occurrence and diversity. The overall evidence indicates deposition in a very dynamic submarine environment, probably at relatively shallow water depths (tens of metres) where various processes transported and reworked sediment forming wave ripples, current ripples, starved ripples, graded beds, erosional surfaces, and condensed lags.

Possible hummocky cross-stratification has been observed by Wignall *et al.* (2005) within the topmost metres of the Grey Shales at Kettlecess; however, the physical interpretation of such structures requires careful analysis, given the lack of experiment-based knowledge on their origin in very fine-grained sediment. Recent developments in marine sedimentology suggest that density stratification in the water column can result in stable interfaces between superposed water masses, which can be disturbed by storms, tides and other agents (Pomar *et al.*, 2012; Shanmugam, 2013). Waves and other periodic instabilities commonly form along such interfaces with the same potential to transport and rework sediment as common gravity waves and storm waves at the ocean's surface.

The overall stratigraphic trend within this unit is a general fining-upward (from silt-dominated to clay-rich mudstones), with an associated macroscopic reduction in the density and scale of structures related to physical processes. Thin sections of our samples from the topmost interval of the Grey Shales clearly demonstrate facies variability associated to a variety of physical processes of sediment advection (probably from proximal sources on the Toarcian shelf), rather than a simple dominance of (hemi)pelagic settling of fine particulates through the water column.

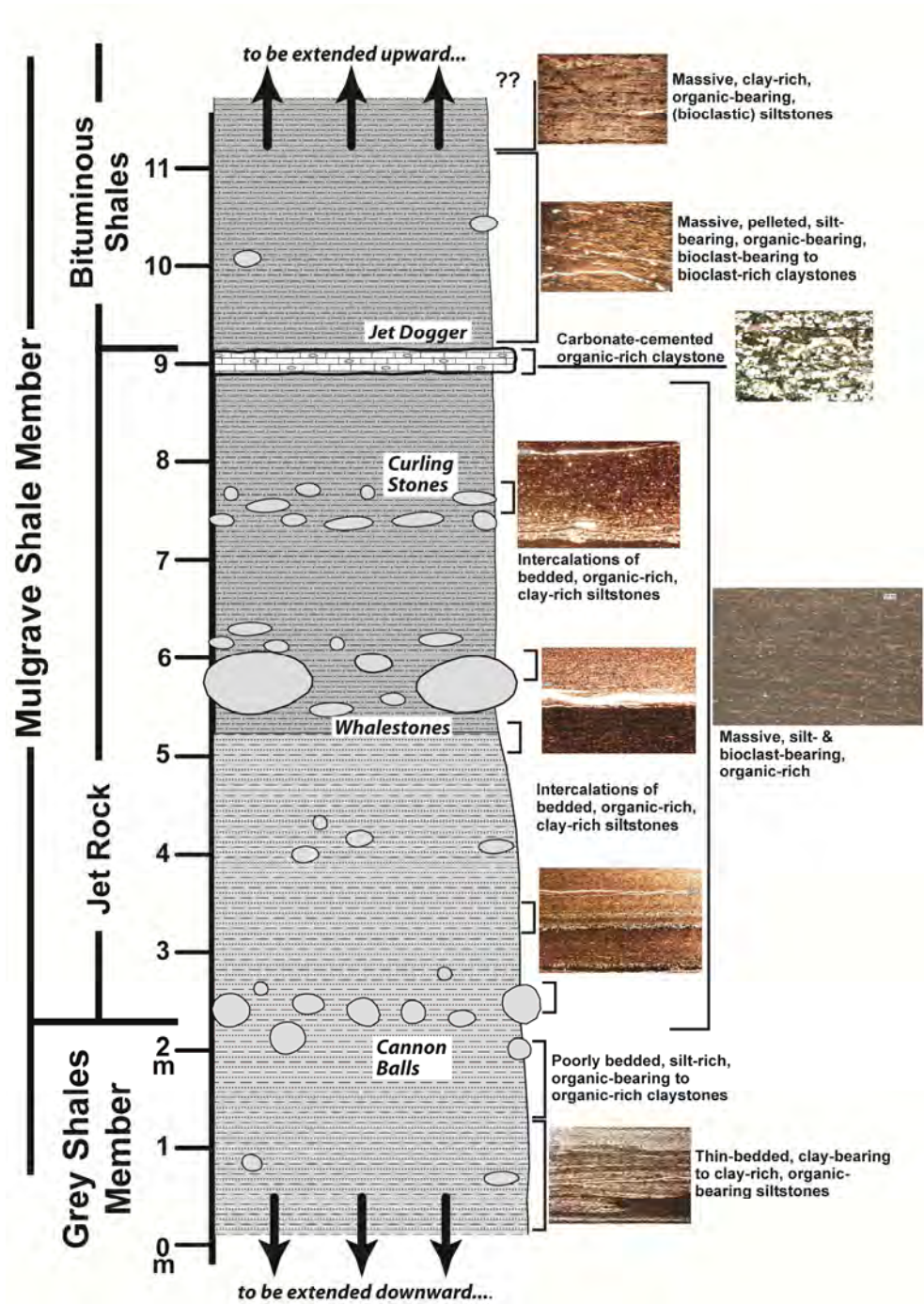


Fig. 4-1 Composite log of the Whitby Mudstone Formation, showing the main sedimentary and lithological variation. For detailed thin section descriptions reference is made to Appendix 1

The most important implications of these textural and microfacies variability within mudstones of the Grey Shales are:

- 1) geotechnical properties and geochemical signatures must be strongly variable, depending on the scale of internal heterogeneity and anisotropy of the original sediment;
- 2) the origin and concentration of dispersed organic-matter are quite variable on a scale of cm to mm, depending on which beds or divisions are examined.

The rarity or recurrence of certain microfacies thus may dictate the properties of the rock at a macroscale. The vertical facies distribution is inherently tied to the sedimentary and paleoenvironmental history of the rocks, and as such is predictable through an integrated reconstruction of basinal history, as is common practice with more 'conventional' rocks (i.e. sandstones, limestones, etc.).

4.3 Jet Rock

The 'Jet Rock' is an informal lithostratigraphic unit of long-established usage in British stratigraphic nomenclature, comprising the lower ~5 m of the Mulgrave Shale Member of the WMF (the upper informal unit being the 'Bituminous Shales'). At outcrop, this interval is typified by a rather uniform, featureless appearance, accompanied by the following distinctive traits:

- 1) a marked darkening in the colour of fresh samples, compared with the underlying Grey Shales;
- 2) a notable increase in yellow to light brown mottling and smearing at particularly weathered exposures, due to the leaching and surface reprecipitation of oxides and hydroxides of abundant trace elements (mostly Fe and Mn) in the rock;
- 3) a generally finer texture than the underlying Grey Shales, although alternations of relatively silt-rich and clay-rich domain are occasionally distinguishable in not too weathered exposures (fresh outcrop faces are commonly more uniform in appearance, whereas moderate weathering highlights compositional differences);
- 4) a reduction of the bioturbation index, which mostly results in a more continuous, better-defined 'lamination' (particularly in weathered exposures, where the rock develop a distinct fine fissility);
- 5) a lower abundance and diversity of macrofossils.

Note however that the evident lamination recognized at outcrop face does not necessarily correspond to an actual presence of distinct 'beds' within the rock (defined as layers produced by genetically distinct depositional events), but more often is the product of a mechanical reaction to weathering of the microscopically planar post-compaction fabric of the sediment.

The average TOC in the Jet Rock (5-6%) rises up to ~14% at some levels, and it is possible to distinguish organic stains in some exposures; samples with particularly high TOC are said to ignite when dried and exposed to a low-temperature flame. Thin sections reveal a sharp change in microfacies with respect to the Grey Shales, with a notable rise in the volume of sediment derived directly from primary organic production. A large percentage of sediment volume consists of relatively large (several tens of microns) organo-mineralic aggregates ('marine snow'), bioclastic debris (mollusk-shell fragments, phosphatic particles of probable Vertebrate origin, coccolithic plates, possible algal fragments), and amorphous organic matter, associated with dispersed pyrite (small opaque particles with well-defined boundaries). This evidence indicates high organic productivity in the water column,

especially in the photic zone, not consistent with classical interpretations of anoxic oceanic conditions and drastic biotic crisis for the Toarcian.

In thin sections, this abundant organic and organogenic component is dispersed in a dominant microfacies of massive, organic-rich, silt-bearing to silt-rich, pelleted to non-aggregated claystones, which is mostly indicative of suspended settling of very fine clastic debris through the water column, probably transported by buoyant hypopycnal plumes (riverine outflows, nepheloid layers, storm suspensions from the proximal shelf) and other low-energy processes. The overall interval is sedimentologically much more homogeneous than the Grey Shales in terms of components of microfacies/sedimentary microstructures. However, it is important to note the still continuous presence of event-beds and possible lag horizons with a dominant volume of silt and relatively coarse biogenic debris. These subordinate microfacies are less common than in the Grey Shales, but recurrent vertically over the entire stratigraphic interval of the Jet Rock, and clearly indicate that more energetic sediment advection and selective entrainment were active on the bottom at this time. The implications are that: 1) supporting the evidence from abundant biogenic debris, it is difficult to envisage permanently anoxic conditions for the lower water column given the periodic current activity and probable advection of oxygenated water masses from elsewhere in the basin: 2) although difficult to quantify, the water column was probably deeper at this stage, but not enough to isolate the bottom from physical processes for prolonged times.

Of particular relevance for the Jet Rock unit is the occurrence of numerous stratigraphic horizons characterized by major cementation and/or macroscopic diagenetic carbonate concretions (mostly siderite, calcite and secondary dolomite), mutually distinguishable because of the consistent development of concretions in size and shape. Outcrop analysis and available literature confirm that essentially all such horizons are traceable over distances of several kilometres between outcrops, that some are confidently used for basin-wide stratigraphic correlation, and that all of those observed in our surveys are stratigraphic markers of more immediate reliability than biofacies or lithofacies changes. Although still debated in detail, the early diagenetic origin of these concretions is demonstrated by lateral differential compaction of hosting mudstones around them (Appendix 3, Photo 9). The variability in size and shape of these chemical segregations is most likely related to the interplay of sedimentation rate and redox state at times when the hosting stratigraphic horizons were buried but remained close to the depositional interface for relatively long periods, allowing interstitial circulation and chemical or bio-mediated reactions between pore waters and sediment components (Curtis, 1995; Sageman and Lyons, 2004).

Bacterial metabolic processes are known to control chemical reduction of sulphates and Fe/Mn oxides within freshly deposited, uncompacted fine sediments in the presence of abundant organic matter (e.g. Raiswell, 1976; Curtis and Coleman, 1986; Curtis, 1987; Hendry *et al.*, 2006); the oxic vs. anoxic conditions of the overlying water column are not always an important factor in controlling these early diagenetic stages, but may favour the transfer of available organic debris from the depositional interface to burial within the sedimentary column if they limit the activity of bottom scavengers. In case of rapid depletion of dissolved interstitial O₂, marine waters are rich in sulphate ions which form the most abundant and efficient electron donor for organic-matter consumption by specialized microbial communities, producing dispersed sulphides (most typically pyrite; Raiswell and Berner, 1986; Sageman and Lyons, 2004) in the sediment. Sulphate depletion and/or restricted

water circulation at deeper burial trigger a shift to reduction of Fe or Mn, which in turn increase the local alkalinity of pore waters and favour multiple-stage accretion of carbonate concretions (Curtis, 1987; Canfield *et al.*, 1993). The pervasiveness and spatial extent of these early cementation processes are controlled by a complex interplay of burial depth, sediment composition and texture, TOC, water chemistry and circulation (Raiswell and Fisher, 2004; Hendry *et al.*, 2006). The latter factor for example is important in eliminating organic-acid byproducts of microbial metabolism from the reaction environment (Curtis, 1987; Curtis *et al.*, 1986), essential to maintain a relatively high pH and thus growth of carbonate concretions

4.4 Bituminous Shales

The 'Bituminous Shales' are informally defined as the topmost stratigraphic interval of the Mulgrave Shale Member in the WMF, with a thickness of ~7-8 m. At outcrop, this unit is sharply separated from the underlying Jet Rock by a laterally continuous, highly indurated, carbonate-rich marker bed called Jet Dogger in the classical regional lithostratigraphy. However, the sedimentological transition from the Jet Rock is gradual, and macroscopically the two units are poorly distinguishable at outcrop in the lower interval of the Bituminous Shales. The most distinctive differences between them consist in a very gradual increase in the modal grain size upwards through the stratigraphy (macroscopically recognizable as an increased granularity and induration of fresh bedrock samples), an upward decrease in the amount and colour intensity of secondary mottling by weathering, and a slight macroscopic increase in the sediment heterogeneity at millimetric to centimetric scales.

Samples from the basal few metres of the Bituminous Shales show a general change in microfacies from the underlying Jet Rock, signalled by the substantial lack of a (relatively) coarse, silt-sized clastic fraction, and by the frequent occurrence of pelleted fabrics of whose origin has not been possible to ascertain here. These are most likely of biologic origin, since the evidence for sediment transport and reworking along the sediment-water interface, which would commonly result in small clay aggregates, is rather minimal in this stratigraphic interval.

The organic-matter content remains relatively high in the Bituminous Shales, yet markedly lower than the underlying Jet Rock unit; TOC values range between 3 and 5%, with a peak in the lower part of the Bituminous Shales stratigraphically close to the Jet Rock, and a gradual decrease upward through the unit. Abnormally elevated values in excess of 5% are not registered in this unit. Thin-section analysis reveals a particular dominance of large organo-mineralic aggregates and dispersed calcitic debris of (micro)algal/coccolithic origin, whereas phosphatic particles and macroscopic shell fragments are less frequently recognized, although still present.

4.5 Synthesis and general insights

Our preliminary sedimentological analysis reveals definite trends in sediment structure, composition and heterogeneity over the studied interval, suggesting general insights applicable to the analysis of mudstone successions at field to basin

scale. Although the examined stratigraphic interval was relatively restricted in this preliminary project, a first-order heterogeneity is clearly recognizable between mudstones of the Grey Shales, relatively coarser-grained and dominated by advective clastic transport, and rocks of the Mulgrave Shale Member, which comprise a much higher primary component related to organic productivity diluted in a 'background' of finer-grained clastic debris. Next to the TOC rise at the boundary between Grey Shales and Jet Rock (visible also in thin section), this main macrofacies transition corresponds to a sharp change in microfacies and compositional heterogeneity at millimetric to centimetric scales.

The Grey Shales represent aggradation by numerous event-beds (mostly turbidity currents, probable hyperpycnal flows and fluid-mud layers), with stacking of distinct silt-dominated and clay-dominated laminae. Occasional condensed intervals or high-energy events have resulted in thicker, silt- to fine-sand-dominated beds. Furthermore, thin sections show the possible occurrence of longer-term trends within this member, probably expressed at a scale of metres, highlighted by relative changes in the volume of massive clayey microfacies and well-bedded silty microfacies. Analysis extended over a longer stratigraphic interval (i.e. the entire Grey Shales Member) and at higher sampling resolution could show whether such patterns are recurrent and possibly corresponding to predictable 'mudstone parasequence' trends (i.e. Ghadeer and Macquaker, 2011).

By contrast, the Mulgrave Shale Member presents a uniformity of microfacies and therefore an overall greater degree of lithofacies and compositional homogeneity, although also in this case an even higher-resolution sampling would be required for a thorough quantification. However, and as with the Grey Shales, intervening periodic increases in the amount of bedded silt and relatively coarse lags probably indicate shorter-term shifts in sedimentary regime related to supply-vs.-accommodation changes ('parasequences'), and contribute a metre-scale heterogeneity to this member.

Well-established global eustatic curves and regional base-level trends in the literature (e.g. Rawson and Wright, 1995; Hesselbo and Jenkyns, 1998; Van Buchem and Knox, 1998; Hallam, 2001) show the onset of a marked transgression at the middle-base of the *tenuicostatum* ammonite biozone (middle to top Grey Shales), with a relative maximum attained during the late *falciferum*-early *bifrons* zones (Bituminous Shales into Alum Shale Member). From a purely regional perspective, and without entering the complex debate on the global Toarcian Oceanic Anoxic Event, the sedimentological trends described here are well explained by base-level control on sediment distribution over the shallow, mud-dominated shelf of the Jurassic Cleveland Basin. Whereas a relative sea-level minimum during deposition of the Grey Shales favoured direct advection of relatively coarse-clastic debris over the shelf, the gradual onset and stability of a relative sea-level maximum lengthened sediment-transport paths, reduced direct clastic supply onto most of the shelf during deposition of the Mulgrave Shale Member, and triggered a combination of enhanced productivity and intermittent stratification over a deepened water column (aided probably by the concomitant onset of an enhanced greenhouse phase; Röhl *et al.*, 2001; Van de Schootbrugge *et al.*, 2005; Wignall *et al.*, 2005), switching sedimentary from a clastic-dominated regime to a production-dominated one. In particular, the occurrence of a relative base-level maximum within the Bituminous Shales is confirmed by the near absence of silty, clastic event-beds in the basal metres of this unit; this implies a protracted phase of relatively calm conditions in a deep-water setting, farthest from

shoreline sediment sources and from the shallower shelf domain which was more easily disturbed by storm events.

Although the upper part of the WMF has not yet been analyzed in this project, field observations and a literature review predict an inverted sedimentological history for the regressive trend spanning from upper Mulgrave Shale Member to the Alum Shales and overlying, siltstone-dominated members.

We infer that the occurrence of different types of concretionary horizons within the Whitby Mudstone Formation, and especially in the Jet Rock, has important implications for the interpretation of possible carbonate interbeds recognized in subsurface core or well-log datasets. Although this topic is not been delved with in detail here, petrographic and geochemical analyses of such carbonate components may discriminate between a primary depositional origin or as secondary concretionary elements.

The distinction has potential implications for: a) an evaluation of the continuity and petrophysical relevance of carbonate horizons (barriers to fluid migration; local differentials in rock response to hydraulic fracturing, etc.); b) enhanced prediction of organic-matter concentration and distribution in the surrounding sediment (due to genetic link between carbonate phases and organic-matter diagenesis); c) enhanced prediction of vertical facies changes within a sequence-stratigraphic framework, since several early-diagenetic processes are indirectly controlled by base-level changes and phases of reduced sedimentation rates (condensed horizons at maximum transgressive surfaces, or bypass surfaces with concentration of organic debris at sequence boundaries; e.g. Taylor and Macquaker, 2000; Macquaker and Jones, 2002; Laenen and De Craen, 2004; Macquaker *et al.*, 2007; Lash and Blood, 2011); d) correlation between subsurface datasets from different parts of a prospective basin.

The distinction of advection-dominated vs. settling/production-dominated lithofacies intervals is of importance for the **prediction of lateral heterogeneity in mudstone successions**. Whereas the first are commonly more widespread and areally continuous, the latter instead imply deposition from physical processes which lose competence and capacity very gradually along the proximal-to-distal tract. Furthermore, high-volumes of sediment microfacies related to advective sediment transport implies that deposition within mud-dominated basins probably does not follow purely aggradational, easily predictable patterns with layer-cake draping of a 'basement', but is spatially distributed by lateral trends in physical processes. **Complex stratigraphic architectures** (such as clinofolds, local depocentres, etc.) are thus to be expected.

Sequence-stratigraphic principles are applicable also to mudstone successions in order to facilitate facies predictions which are probably more related to sediment composition than architectural facies distributions. In relatively distal mud-dominated settings probably a major factor controlling sequence development is the absolute distance from landmasses which act as main sediment sources, rather than the ratio of sediment supply to accommodation. Palynology

5 Palynology

All 106 samples collected in the field trip of May 2013 were processed for palynology content of the organic matter (section 5.2), but only 65 were analyzed for palynomorph assemblages (section 5.3). From each of the 65 analyzed samples, all organic matter present in the preparations is taken into account and is represented in the palynological distribution panels (section 5.4). The results are interpreted in terms of paleoenvironment and compared to the palynology from the West Netherlands Basin in Chapter 9.

5.1 Methodology

5.1.1 Samples

All 32 samples from section Runswick and all 33 samples from section Runswick North are analyzed for palynology. Together, these 65 samples comprise 11 meters of stratigraphic section, including the topmost 2 m of the Grey Shale Mb (WMF) and 9 m of the Mulgrave Shale Mb (WMF). The 9 m of Mulgrave Shale Mb include the 7m thick "Jet Rock" and the basal 2m of the "Bituminous Shales" (Fig. 5-1).

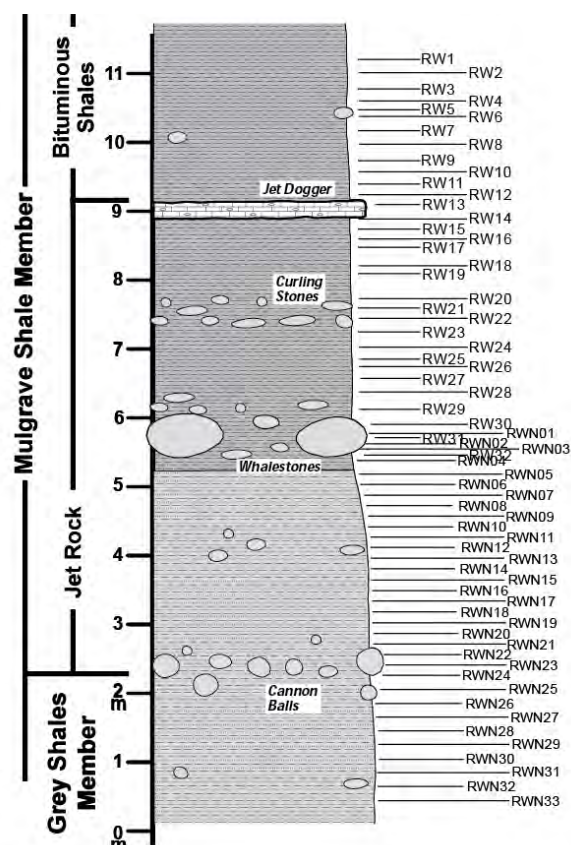


Fig. 5-1 Samples analyzed for palynology from section Runswick (RW) and Runswick North (RWN)

5.1.2 Processing

Standard palynological processing was applied for all samples, including HCl for decalcification with HCl, destruction of mineral matrix with HF and subsequent sieving over a 15 μ mesh sieve. The organic residues were mounted on glass slides using glycerin jelly. Although the samples were extremely rich in organic matter, no oxidation step was applied such that structureless organic matter is still preserved.

5.1.3 Counting

In principal, three rows were counted using the 40x objective. Illumination with ultra violet light was applied for the identification of small acritarchs and other palynomorphs. Acritarchs and other small palynomorphs are often concealed within so-called faecal pellets. Due to the bright fluorescence of these cells under ultra violet light, identification was possible. Note, that as a consequence, the relative abundances of palynomorphs are skewed towards acritarchs and other small palynomorphs. The counts of the organic matter assemblages and of the palynomorph assemblages are displayed in "closed SUM" diagrams. The counts of the dinoflagellate cysts and of the pollen and spores are displayed in saw-blade distributional panels. In 5.2., a short description of the various groups identified is provided.

5.2 Organic Matter

The organic matter or palynofacies assemblages consist of 4 groups:

Structureless Organic Matter (SOM)

This type of organic matter consists of a mid-size to large (50 to 300 μ) particle with no obvious structure, i.e. no cell walls, vessels etc. The size depends on the aggressiveness of processing: the particles tend to fall into smaller particles with more intense sieving, bleaching or shaking. Two types are distinguished, Type 1 is more or less translucent and is in general less massive than Type 2. Type 2 is dark, massive, apparently containing significantly more organic matter than Type 1. Type 2 may reach 300 μ , which is in the same range size as medium sand! Almost always, Type 2 particles reveal small mineral grains and abundant "hidden" palynomorphs when studied under ultra-violet light (instead of "normal" transmitted light). Apparently, this type represents aggregates, or faecal pellets, resulting from biological activity.

Wood

These are organic matter particles that can be attributed to wood remains. Three types are distinguished: black wood, brown wood and wood vessels.

Palynomorphs

These are (mostly uni-cellular) organic matter particles that constitute separate biological entities, such as dinoflagellate cysts, pollen and spores, cysts of prasinophyte algae, acritarchs, fresh-water algae such as *Botryococcus*, etc. This group is further subdivided and displayed in a "closed SUM" diagram.

Sheets

Sheet-like organic matter particles. Origin uncertain. This type is always very rare in abundance.

5.3 Palynomorph assemblages

Sphericals/leiospheres

Relatively small spherical particles with no obvious ultra-structure such as spines, granules or openings such as pores, slits and so on. The origin is not clear, but it is suggested that the majority can be attributed to the cysts (or *phycomae*) of prasinophyte algae. Prasinophyte algae are a class of unicellular green algae (photosynthesis) in the Division Chlorophyta.

Acritarchs

In general, acritarchs are small palynomorphs that cannot be attributed to either dinoflagellate cysts or resting cysts of known prasinophyte or other algae. Acritarchs include the remains of a wide range of quite different kinds of organisms, ranging from the egg cases of small metazoans to resting cysts of many different kinds of algae. In marine palynological assemblages, acritarchs are always present but usually quite rare. As a rule of thumb, acritarchs increase in abundance under restricted marine conditions, i.e. at the transition from non-marine to marine.

Tasmanaceae

Belong to the Prasinophyte algae, a class of unicellular green algae in the Division of Chlorophyta. Tasmanaceae and Pleurozonaria are here combined. Both make thick-walled cysts with very Hydrogen-index. Blooms of Tasmanaceae are indicative of water-column stratification.

Dinoflagellate cysts

Dinoflagellate cysts, or dinocysts, represent the acid-resistant resting cysts of a type of marine phytoplankton that makes up an important part of the primary production. These protists have so-called flagellae, that enable them to move up and down through the water-column. The fossil group appears in the Triassic and starts radiating from the Late Toarcian onward. Evolution is fast, so dinocysts are commonly used in biostratigraphy.

Sporomorphs

Sporomorphs is a general term for all occurring pollen and spores. In Jurassic times, the pollen record was only represented by gymnospermous pollen, e.g. from conifers. Angiosperm pollen appear in the Cretaceous.

Botryococcus

Botryococcus represent a type of fresh-water algae, that can tolerate brackish conditions.

5.4 Results

In general, all samples yielded abundant organic matter. As expected, a trend is observed from organic matter assemblages with abundant palynomorphs, such as

dinoflagellate cysts and pollen and spores, towards organic matter assemblages completely dominated by marine (structureless) organic matter, and back again to organic matter assemblages with abundant palynomorphs. The middle part of the section, with the very high TOC, is characterized by large and massive structureless organic matter, interpreted as faecal pellets. Based on the changes in the organic matter and palynomorph assemblages, 8 biofacies zones are distinguished, RUNS-A to RUNS-H (see Figure 4 Biofacies zonation for section Runswick Bay. The palynological results are displayed as a closed SUM diagram for the organic matter assemblages (left) and a closed SUM diagram for the palynomorph assemblages (right). and Figure 5 Biofacies zonation for section Runswick Bay. The palynological results are displayed as a closed SUM diagram for the organic matter assemblages (left) and absolute abundances [scaled from 0 to 500 specimens] of the palynomorph assemblages (right). For each sample, approximately three rows of the palynological slide are counted.). RUNS-A and RUNS-B comprise the uppermost 2 meters of the Grey Shale Member (WMF), RUNS-C to RUNS-F together make up the Jet Rock and RUNS-G and RUNS-H straddle the basal two meters of the Bituminous Shales

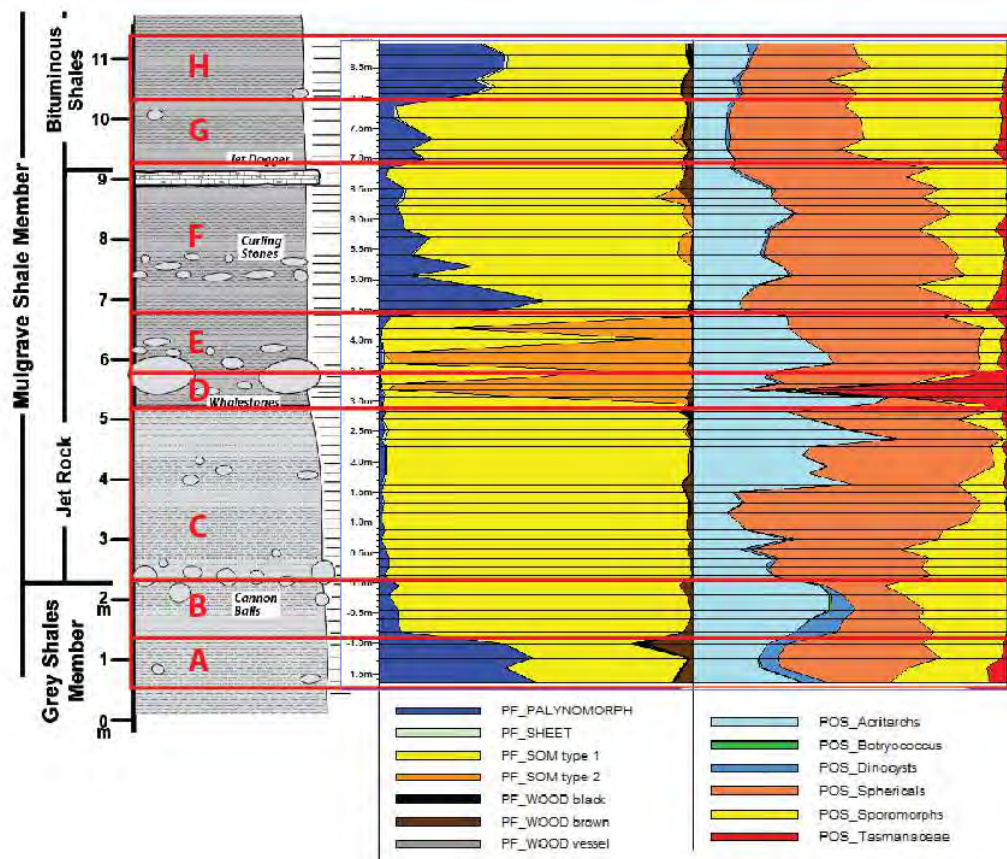


Figure 4 Biofacies zonation for section Runswick Bay. The palynological results are displayed as a closed SUM diagram for the organic matter assemblages (left) and a closed SUM diagram for the palynomorph assemblages (right).

5.4.1 *Biofacies zonation of the composite section Runswick Bay*

RUNS-A -1.65m to -1.00m [RWN 32 – RWN 29]

Organic Matter Assemblages: Abundant palynomorphs (50%). Wood is relatively common (between 5 and 20%), the highest number reached in the entire section.

Palynomorph Assemblages: Dinocysts are common. A distinct peak of Tasmanaceae is recorded at the base, which show a gradual decrease towards the top of this zone. The fresh/brackish water algae *Botryococcus* is present.

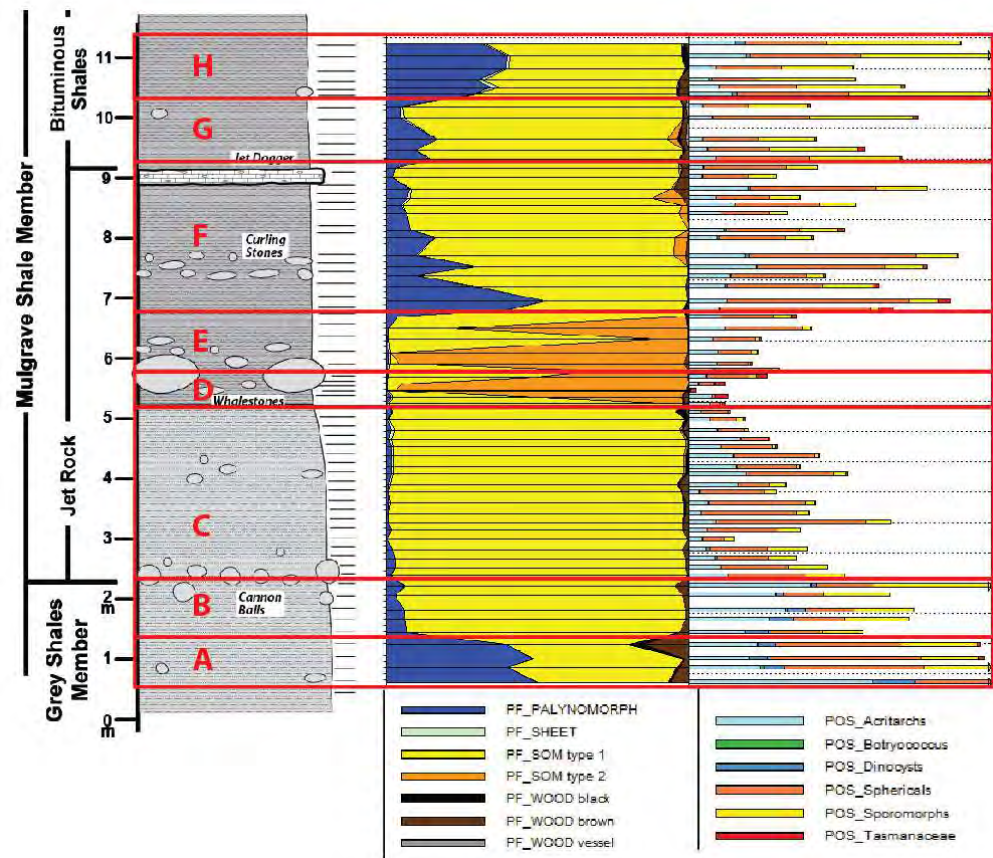


Figure 5 Biofacies zonation for section Runswick Bay. The palynological results are displayed as a closed SUM diagram for the organic matter assemblages (left) and absolute abundances [scaled from 0 to 500 specimens] of the palynomorph assemblages (right). For each sample, approximately three rows of the palynological slide are counted.

RUNS-B -0.82m to -0.05m [RWN 28 – RWN 24]

Organic Matter Assemblages: Palynomorphs are less than in RUNS-A, but nevertheless make up between 5 and 15% of the organic matter assemblage. SOM Type 1 is now the dominant component of the organic matter assemblage.

Palynomorph Assemblages: Dinocysts are common. A distinct peak of

RUNS-C 0.12m to 2.82m [RWN 23 – RWN 5]

Organic Matter Assemblages: Palynomorphs are rare, below 5%. SOM Type 1 dominates the assemblages completely.

Palynomorph Assemblages: Dinocysts are very rare and often absent. Sporomorphs are still common at the base, but decrease in abundance upwards. Sphericals dominate the palynomorphs assemblages.

RUNS-D 3.02m to 3.40m [RWN 4 – RW 31]

Organic Matter Assemblages: SOM is very dominant. Palynomorphs are very rare, below 3%. SOM Type 2 is the most abundant but SOM Type 1 also occurs.
 Palynomorph Assemblages: Dinocysts and sporomorphs are extremely rare to absent. Sphericals and acritarchs are common, but the most striking element is Tasmanaceae, which reach 80% in some of the palynomorph assemblages.

RUNS-E 3.42m to 4.40m [RWN 1 - RW 26]

Organic Matter Assemblages: SOM is very dominant. Palynomorphs are very rare, below 3%. SOM Type 2 is the most abundant but SOM Type 1 also occurs.
 Palynomorph Assemblages: Sphericals and acritarchs together dominate the assemblages to 90%.

RUNS-F 4.50m to 6.85m [RW25 – RW 12]

Organic Matter Assemblages: SOM and Palynomorphs start off equally, with 50% at the base of RUNS-F. Upwards, Palynomorphs decrease from 50 to about 10% at the top. SOM Type 2 is very rare. SOM Type 1 is abundant.
 Palynomorph Assemblages: Acritarchs and sphericals are super abundant at the base, but decrease slightly towards the top. Sporomorphs increase towards the top. Dinocysts are very rare.

RUNS-G 7.00m to 7.87m [RW 11 – RW 7]

Organic Matter Assemblages: SOM Type 1 is dominant, but palynomorphs are quite common with 15 to 20%.
 Palynomorph Assemblages: Sporomorphs are abundant, up to 50%. Sphericals and acritarchs have fallen back to 35 and 15% respectively.

RUNS-H 8.10m to 8.90m [RW 6 – RW 1]

Organic Matter Assemblages: SOM Type 1 is still dominant but palynomorphs have increased upto 30-40%.
 Palynomorph Assemblages: Sporomorphs are abundant, up to 50%. Sphericals and acritarchs make up the other 50%. Dinocysts are rare but consistently present.

5.5 Synthesis and general insights

Based on the palynological results, it is possible to arrive at the following conclusions:

The depositional environment of RUNS-C to RUNS-E is interpreted as being subjected to "persistent water-column stratification". The complete dominance of marine Structureless Organic Matter (SOM), indicates that stratification was continuous and not interrupted by prolonged periods of "normal" mixed water columns. In terms of intensity of stratification, RUNS-D and RUNS-E reflect the most intense stratification, based on the dominance of the large and massive aggregates of SOM Type 2.

Normal marine, or at least *predominantly normal marine* conditions are inferred for RUNS-A and RUNS-B, based on the common occurrence of dinocysts. In RUNS-B, the first indications for stratification are reflected by the increased amounts of marine SOM. Note that rare occurrences of dinocysts return in RUNS-F, but the amounts of dinocysts found in RUNS-A and RUNS-B are never again reached in the studied section.

A sharp boundary between RUNS-E and RUNS-F exists: the change from intense stratification to moderate stratification is abrupt. RUNS-F to RUNS-H are interpreted as being subjected to moderate water-column stratification. Normal marine conditions are not reached in this interval, but the intensity of stratification varies, reflected by the varying amounts of palynomorphs and SOM. Note the trend in the relative amount of palynomorphs: very high (50%) at the base of RUNS-F, a gradual decrease towards the top of RUNS-F and then a two-step increase through RUNS-G and RUNS-H.

6 Geochemical Analysis

A set of 125 selected samples extracted from the studied sections were subjected to various geochemical analyses, such as ICP-OES, ICP-MS, XRF and TOC (see table below). Analyses were performed for two main reasons: 1) to quantify sediment composition (mineralogy, geochemistry, organic matter), and 2) to obtain parameters of potential petrophysical significance for the derivation of “pseudo logs” from compositional data. The pseudologs can be used for comparison with subsurface logs of the PSF in order to better understand and compare compositional variations and stratigraphic trends between the Dutch and English Toarcian formations. The data presentation here is structured such that first the results are shown for the composite log of Runswick Bay, which represents most extensive stratigraphic interval studied. Analyses on partial sections from other sampling sites are subsequently described.

6.1 Methodology

6.1.1 ICP-OES and ICP-MS

Description	Inductively coupled plasma (ICP) energy source, with atomic emission spectroscopy (OES) and mass spectrometry (MS) measurement techniques.
Preparation method:	Crush and powder, fusion with alkali flux, HNO ₃ dissolution, two dilutions.
Elements (total 50)	
Major elements (10) reported as oxide % by weight	SiO ₂ , TiO ₂ , Al ₂ O ₃ , Fe ₂ O ₃ , MgO, MnO, CaO, Na ₂ O, K ₂ O and P ₂ O ₅
Trace elements (26) reported as ppm by weight	Ba, Be, Bi, Co, Cr, Cs, Cu, Ga, Hf, Mo, Nb, Ni, Pb, Rb, Sc, Sn, Sr, Ta, Tl, Th, U, V, W, Y, Zn, and Zr
Rare Earth Elements (REE) (14) reported as ppm by weight	La, Ce, Pr, Nd, Sm, Eu, Gd, Tb, Ho, Dy, Er, Tm, Yb, and Lu

6.1.2 XRF

Description	X-ray fluorescence.
Preparation method:	Crush and powder, sample made into pressed powder pellet.
Elements (total 48):	
Major elements (10) reported as oxide % by weight	SiO ₂ , TiO ₂ , Al ₂ O ₃ , Fe ₂ O ₃ , MgO, MnO, CaO, Na ₂ O, K ₂ O and P ₂ O ₅
Trace elements (27) reported as ppm by weight	As, Ba, Br, Co, Cl, Cr, Cs, Cu, Ga, Hf, Mo, Nb, Ni, Pb, Rb, S, Sc, Sn, Sr, Ta, Th, U, V, W, Y, Zn, and Zr

6.1.3 TOC

Description	TOC- total organic carbon.
Preparation method:	Crush and powder, carbonate is removed by acid leach, combustion measurement of TOC.
Major elements (1)	Total organic C

6.2 Results

6.2.1 Element affinities

Principal component analysis is used to examine clusters of chemical elements (Fig. 6-1) with affinity to potentially important mineral phases. Three main clusters are recognized from compositional data:

Organic matter related: U, V and Cu are elements that become insoluble under reducing conditions, and which thus can be concentrated during decay of significant amounts of organic matter. As such, these elements are proxies for reducing conditions.

Pyrite/metals: Fe, S, Co, Ni, Zn and Mo are elements that can be incorporated in pyrite and other sulphide minerals. The formation of the latter may be promoted by anoxic conditions; the elements can thus be used as a proxies for anoxia.

Carbonates: Ca and Sr are elements associated with carbonate minerals, in particular calcite.

Principal component analysis (PCA) performed on the detrital cluster highlights two distinct controls on composition, with implications on provenance and environmental conditions in clastic source areas:

Clay minerals: elements such as Al, K, Ga, Rb and Cs are predominantly associated with clay minerals such as kaolinite and illite.

Heavy minerals: Zr, Ta, Nb, Cr, Ti and Th are predominantly associated with a range of heavy minerals such as zircon (Zr and Th), Ti-oxides (Ta, Ti and Nb) and Cr-spinel.

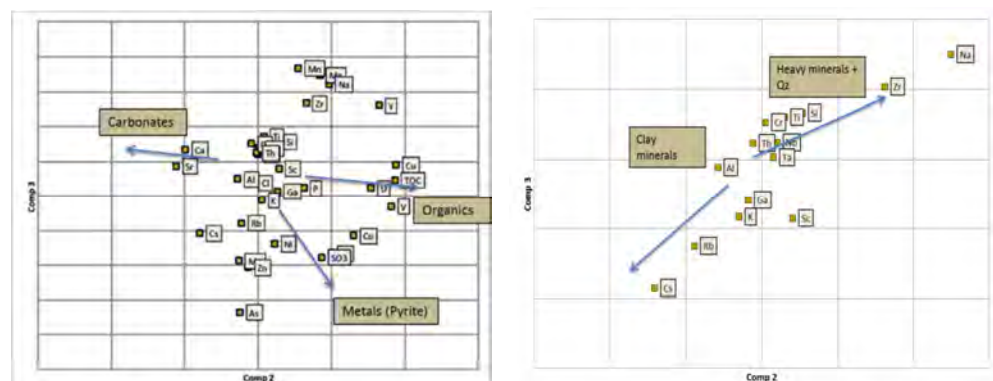


Fig. 6-1 PCA analysis showing clustering of element affinities, for A) non-detrital and b) detrital fraction.

The dendrogram analysis (Fig. 6-2) further confirms the clustering shown by the PCA. It highlights positive correlations in composition for groups of element groups with affinities for carbonate and sulphide phases, as well as for organic matter.

Elements and compounds characteristic of clay minerals and heavy minerals form a natural cluster on the left hand of the dendrogram, reflecting the occurrence of coarse- and fine-grained detrital components in the sediment.

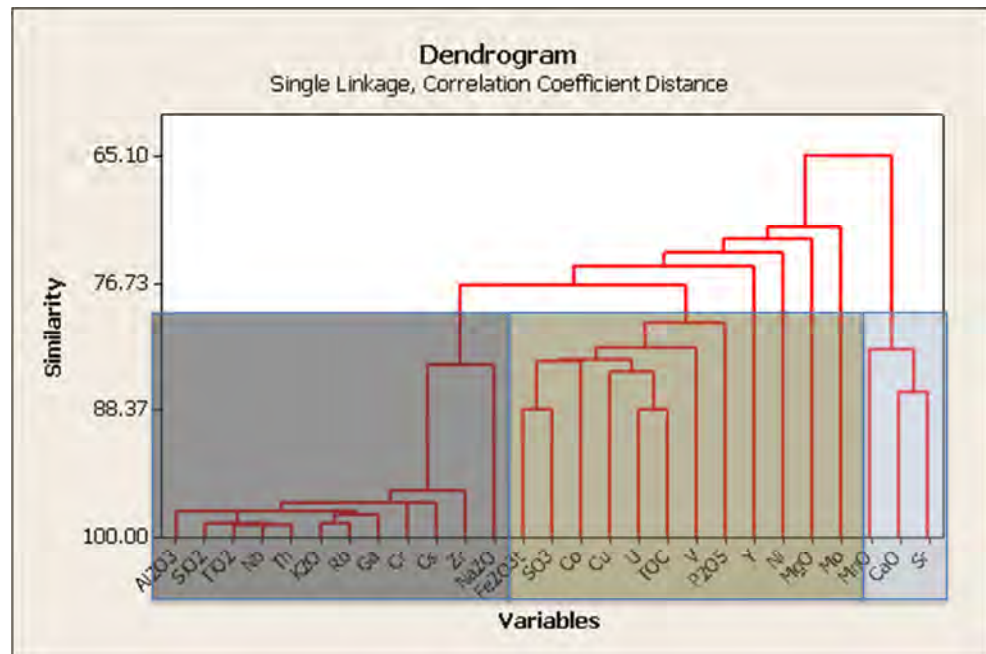


Fig. 6-2 Dendrogram showing linkage of elements based on Correlation Coefficient Distance

6.2.2 Chemostratigraphic zonation

On the basis of these methods, an unbiased chemostratigraphic zonation is obtained which relates to the research objectives, i.e. to highlight vertical and lateral heterogeneities, respectively within and between the studied sections. It is based in particular on four key elements ratios (reported below), which are proxies for variations in organic matter and heavy mineral input, the latter a proxy for detrital input of continental (fluvial) origin.

Cr/V = changes in terrestrial input (Cr) vs organic input.

Th/U = changes in clay input (Th) vs organic input (U).

Zr/Nb = trends in coarse-clastic input (subtle variations in provenance).

Mo/U = changes in pyrite vs organic content (burial efficiency vs early diagenetic oxydation of organic matter). Mo and U are considered sensitive to conditions around the redox boundary during early diagenesis (Algeo and Tribovillard, 2009). They occur as highly soluble anionic species in oxic waters but are reduced to reactive or insoluble species of lower valency under anoxic conditions. Thus, their presence or absence in sedimentary deposits has been interpreted as a signature for past reducing conditions (e.g. Wignall et al., 2007). In open-ocean systems with suboxic bottom waters, Uauth enrichment is greater than that of Moauth because Uauth accumulation begins at the Fe(II)–Fe(III) redox boundary (e.g. Helz et al., 1996) whilst Moauth accumulation becomes more important as waters become more anoxic, and especially so when they become sulfidic. Thus, in weakly oxic settings sediment Mo/U ratiosauth ratios are smaller than seawater, but increase with increasing intensity of anoxia (Algeo and Tribovillard, 2009).

The zonation (Fig. 6-3) will be used as reference in the description of the subsequent analyses.

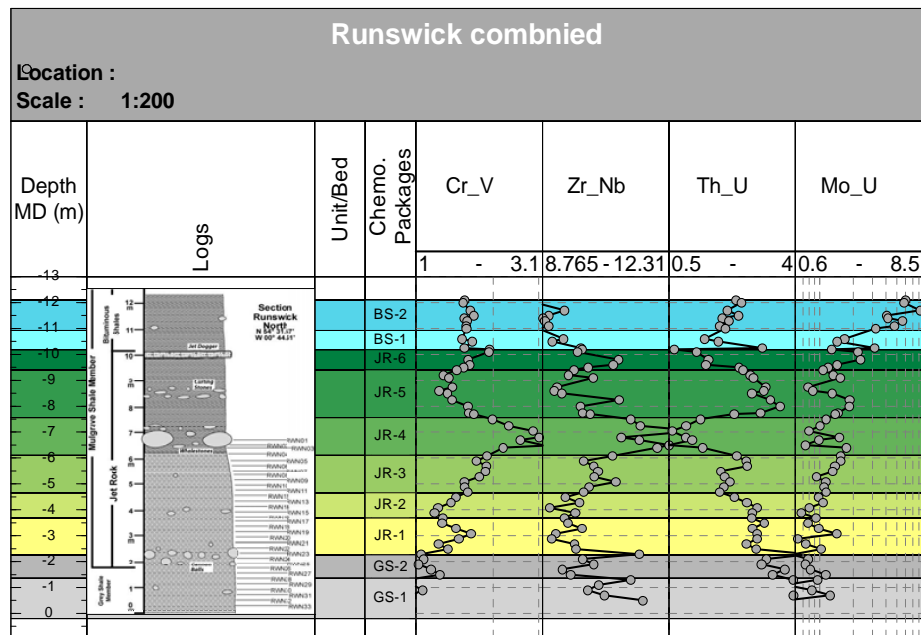


Fig. 6-3 Chemostratigraphic zonation.

6.2.3 Basic Lithology breakdown

In geochemical lithotyping (Fig. 6-4), SiO_2 is used as a proxy for quartz, while Al_2O_3 is used as a proxy for clay minerals. The relative proportion of carbonate (as CaO), the third lithology in abundance, is indicated by the size of the points shown in the scatter plots of Fig. 6-5, whereas the colour of the samples relates to the geochemical units. Other important, though minor, components such as TOC, and iron oxides (also pyrite, Fe_2O_3) are considered part of the basic lithology as well and represented in the closed SUM diagrams in Fig. 6-4. Compared to thin section analysis and normative mineralogy it is obvious that the breakdown reflects a far higher percentage of quartz, suggesting that SiO_2 is not purely a proxy for quartz but represents other minerals such as phyllosilicates as well. For this reason the latter is granted more reliability.

Further deductions are that the packages from the Grey Shale Member (grey markers) have the lowest proportions of CaO, while the packages of the Jet Rock Member (yellow/green markers) show elevated CaO values. The Bituminous Shales show a higher proportion of Al, which is related to the abundance of very fine-grained clastic fraction.

6.2.4 Basic mineralogy (normative mineralogy)

To explore the element contribution to mineral assemblages, mineral modelling was performed to calculate a normative mineralogical composition along the sampled section. The predictivity of this method depends on calibrations with actual XRD data (not available in this project). The results are presented as stacked bar plots (Fig. 6-4) and generally indicate a minor mineralogical variation along the three stratigraphic units studied: for example, the Jet Rock has slightly higher quartz

content than the Bituminous Shales, which has a higher percentage of clay; pyrite is most abundant in the Jet Rock, where it seems to volumetrically compete with the clay content. Overall, dolomite occurs irregularly in very low amount. The dolomite content seems unrelated to carbonate content, which does show distinct variations throughout the section.

This analysis is in good correspondence with 2 XRD analysis from the PSF in the Netherlands (Chesapeake report, 2011) and (Goes, 2013). Both studies show XRD results for the Loon op Zand (LOZ-01) well. Although the actual percentages differ, in general the samples are extremely clay rich (40-70 vol%) have quartz typically between 10-20%, calcite from 2-20 vol%, minor dolomite and TOC between 5-20 vol%. The clay mineralogy is composed primarily of 2:1 Al sheet silicates such as illite/mica (5-10%), smectite/illite (0-10%) and kaolinite (10-20%) and a minor amount of chlorite. This also agrees with mineralogical analysis of other PSF localities in Germany by Mann (1987), Littke et al. (1991), Kanitpanyacharoen et al. (2012) and Klaver et al. (2012)

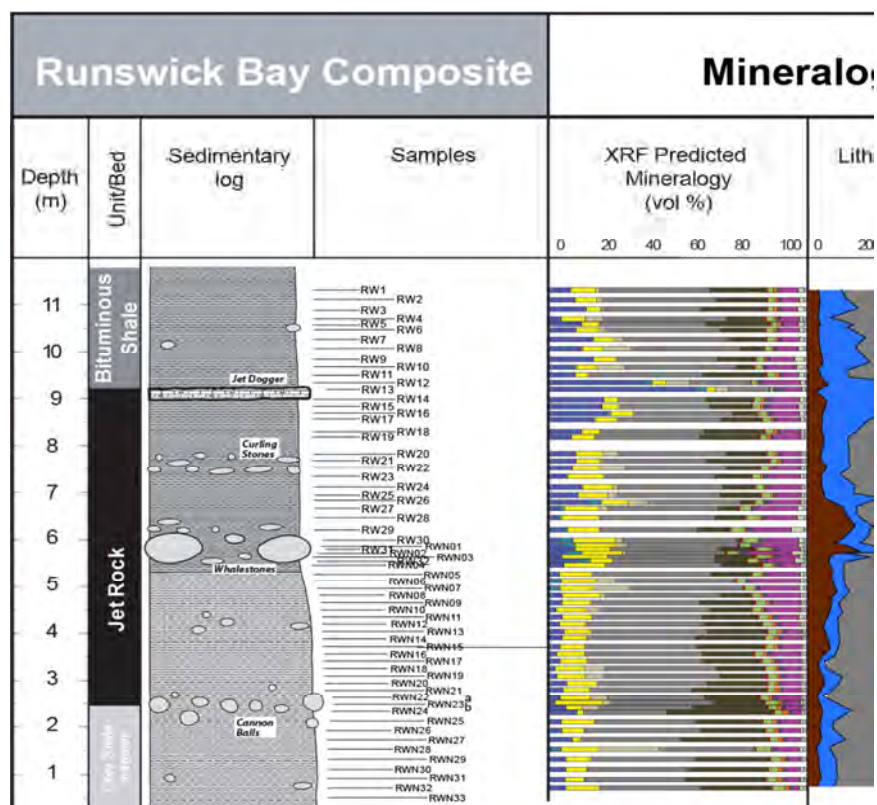


Fig. 6-4 Combined normative mineralogy (results are not XRD-calibrated, but consistent with PSF XRD data) and basic lithological breakdown. Remove the Basis lithology

6.2.5 Carbonate variation

Peaks in the concentration of Mg and Ca (Fig. 6-6) may be associated with the occurrence of dolomite and primary calcite/aragonite, respectively, while concomitant peaks in Ca and Sr are frequently associated with the presence of anhydrite, a factor which here can probably be ignored. A gradual increase in Ca abundance throughout the stratigraphic column (Fig. 6-6), from Grey Shales to the

top of the Jet Rock (top Jet Dogger) can be observed. Generally, corresponding trends in Ca and Mg suggest direct precipitation or early diagenetic substitution of carbonate by dolomite. The high Mg peak at the Whale stone layer indicate that the

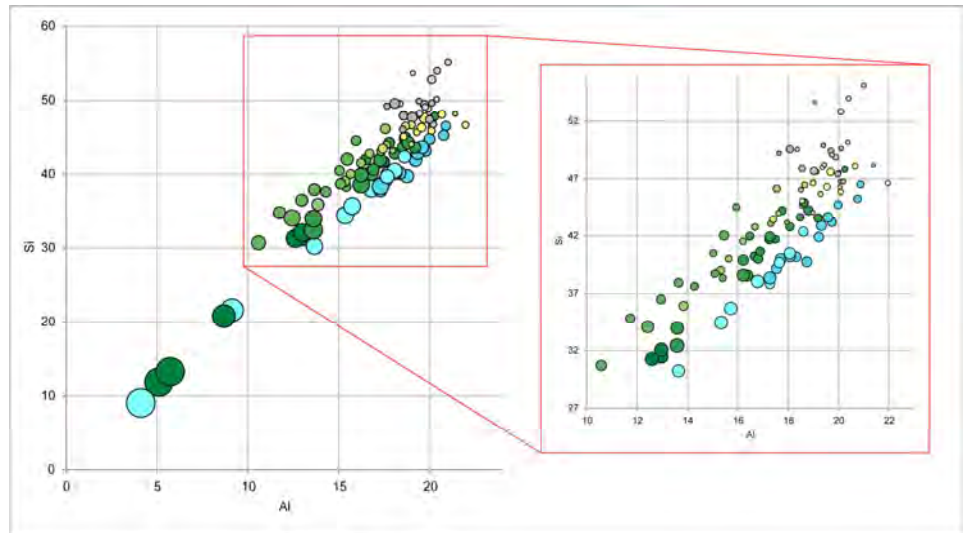


Fig. 6-5 Three component lithological breakdown with Si and Al along the axis and Ca represented by the dot size. Colors represent the geochem zone (as presented in Fig. 6-3).

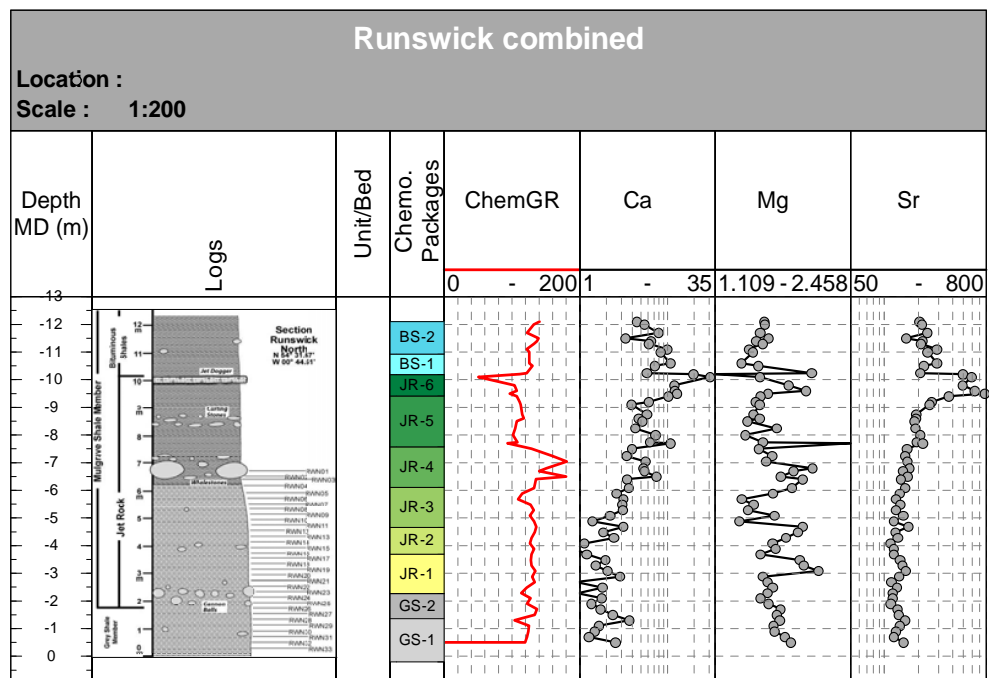


Fig. 6-6 Carbonate variation

relative depletion of Ca ions is particularly high in the presence of amounts of organic carbon. The increase in Ca correlates with a slight increase in Sr content, with maximum values in the coccolithic Jet Rock.

6.2.6 Clay changes

The relative abundances of the elements K, Rb and Cs are associated with variations in clay-mineral content. The ration K/Al is considered an important indicator for the presence of kaolinite (relatively low K/Al ratios), a clay species whose abundance points to enhanced chemical weathering (e.g. during wetter climate) in clastic source regions. The ratios K/Rb and K/Cs are commonly considered indicative of the presence of more complex clay-mineral species, such as respectively illite/montmorillonite and smectite. The evident co-variance of all three geochemical parameters () over the studied interval suggests that lower kaolinite content (high K/A), such as in the middle of the Jet Rock unit (approximately corresponding to the horizon characterized by ‘whalestone’ concretions) coincides with higher relative amounts of illite/montmorillonite and smectite.

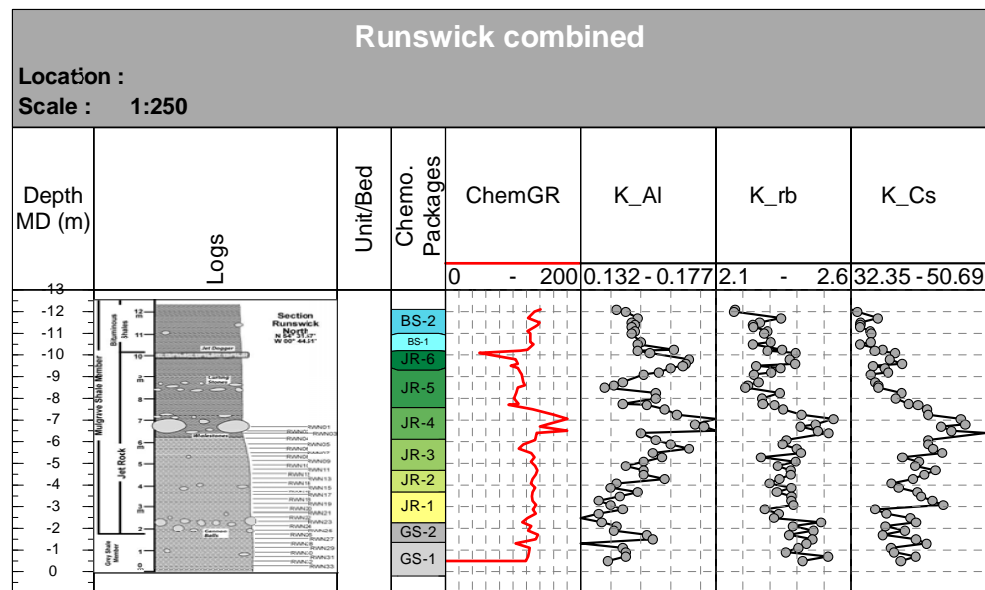


Fig. 6-7 Clay Changes

6.2.7 Changes in organic matter

Variations in elements correlated to organic-carbon content along the combined section clearly show a close correlation between TOC(%) and the elements V and U (Fig. 6-8). In the presence of reducing conditions within interstitial fluids of the surficial sediment column, vanadium (and other trace elements, such as molybdenum) is efficiently extracted from seawater and trapped as lattice substitute into various authigenic minerals, as well as adsorbed onto active surfaces (clay minerals, organic complexes). Although subject to various geochemical controls, it

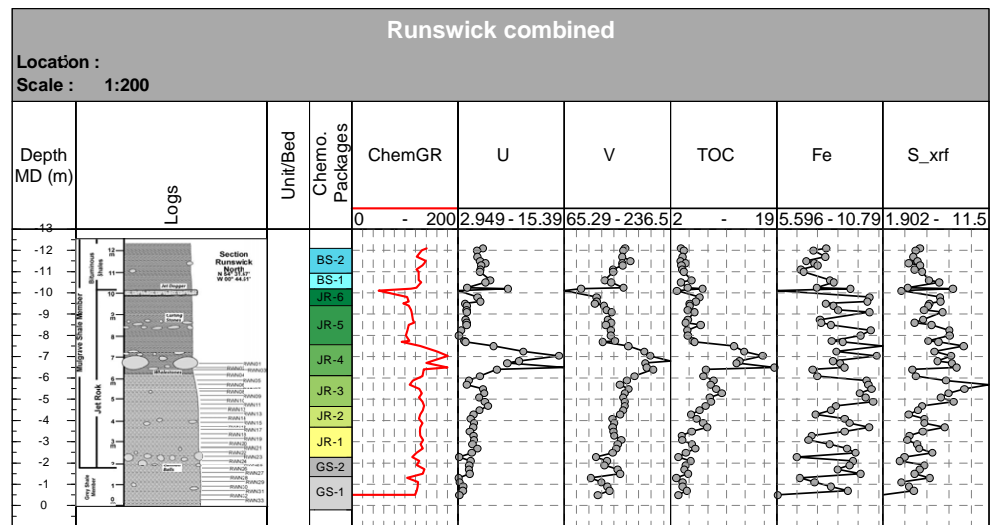


Fig. 6-8 Changes in organic matter

is thus a potential indicator of redox conditions within the bottom water column and topmost sedimentary column (Lewan and Maynard, 1982; Emerson and Husted, 1991). Uranium is also considered a very important proxy for redox conditions in seawaters, if calibrated for potential enrichment via the clastic fraction (most commonly clay minerals in Phanerozoic deposits). Uranium is extracted from interstitial solutions of organic-rich deposits in relative proximity to the sediment-water interface (early diagenesis) and fixed both within diagenetic concretions and over active surfaces (Kochenov et al., 1977; Myers and Wignall, 1987). The significance of the element for subsurface analysis is given by the potential detection of its radioactive emission in spectral gamma-ray logs, with the consequent possibility to correlate stratigraphic trends and/or organic-rich intervals between different sections at basin scale (Myers and Wignall, 1987; Parkinson, 1996).

The covariation of iron and sulphur (Fig. 6-8) is related to the affinity of the former for sulphide phases (mostly pyrite) which are produced during the advanced diagenesis of sediments with particularly high organic-matter content in anoxic conditions. However, as evident from the diagrams, trends in the abundance of secondary sulphides do not always follow TOC, because sulphide precipitation is tied to pathways and rates of organic-matter consumption in the buried sediment, and these may vary depending on sedimentation rates, geochemical conditions, sediment and prewater composition, etc. Therefore, the importance of sulphur content and sulphide-related elements for formation evaluation and correlation has to be estimated case by case for different basins and sub-basins.

6.3 Pseudo logs

6.3.1 Total and spectral GR

Using the measured K₂O (%), Th (ppm) and U (ppm) values a synthetic gamma was calculated for the studied interval, using the following equation (Ellis, 1987):

$$GR^{Tot} = a(Th) + b(U) + c(K)$$

(a,b and c = 4.0, 8.0 and 16.0)

In this way the calculated total GR mimics a well-log GR (Fig. 6-9). Note that with well-derived spectral GR logs the individual contributions of K40, Th and U are measured as well as the Total GR, hence a relationship between spectral and total data can be established and/or confirmed. Here, this is not the case since only elementary (spectral) components are available.

In order to determine if the Ellis (1987) equation is applicable, the geochemically established (synthetic) GR logs are compared with outcrop spectral GR analysis, obtained by hand-held spectrometry, of the Runswick and Kettleless North sections. In general a good relationship between the two exists, although absolute values differ up to about 25 % (Fig. 6-10).

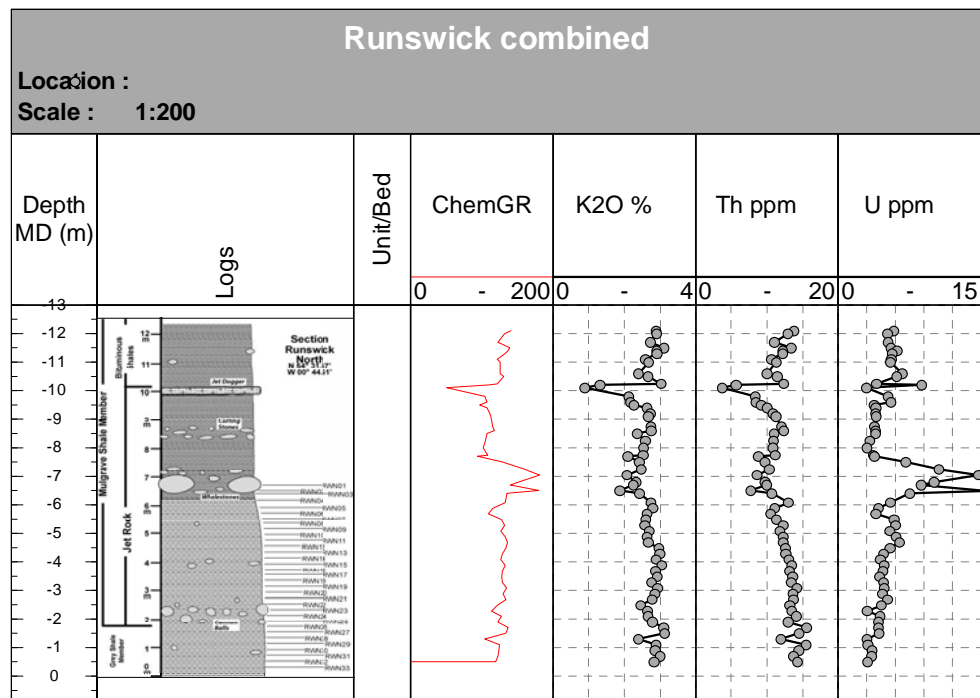


Fig. 6-9 Calculated (synthetic) GR, based on the contribution of K2O, TH, and U.

6.3.2 Density

A first proxy for density is provided by the mass coefficient (cm²/g, area over weight), which corresponds to the penetration of the x-rays of the sample, as opposed to x-ray scatter (Fig. 6-11). This was then used with the elemental data to model the density curve. In general, density is a good proxy for Quartz and Carbonate, but seems easily dominated by the presence of organic material.

6.3.3 Brittleness

Brittleness, in the geomechanical sense, is the measurement of stored energy before failure, and is function of:

- Rock strength
- lithology

- texture
- effective stress
- temperature
- fluid type
- diagenesis
- TOC

Since not all of these parameters are known a relative brittleness index (BI) is modelled using the obtained mineralogy as shown in Fig. 6-4 Combined normative mineralogy (results are not XRD-calibrated, but consistent with PSF XRD data) and basic lithological breakdown. To date, several equations exist that are applicable to different mineralogical compositions. For instance, Jarvie et al.(2007) only takes quartz, carbonate and clay into account, whereas Wang & Gale (2009) also considers the contribution of dolomite and TOC. Here we use a modified Wang equation (eq. 1, Fig. 6-11) that also includes other mineral phases present, which may contribute to the BI, such as feldspar. The total of all minerals that contribute positively or negatively to the brittleness are in the denominator, whereas the positively contributing minerals are in the numerators. Perez & Marfurt (2013) noted that TOC and Quartz positively influence the BI, although the TOC is not in the nominator of the Wang equation. Alternatively, this can be explained by a strong co-variation between Quartz and TOC, since organic material, in general, cannot be considered very brittle. For this reason an equation with negative contribution of TOC is evaluated. A weighing factor of 1.35 is applied to account for the higher contribution of carbonates to the BI, compared to, for instance, Quartz.

$$BI_{TNO} = \frac{1.35 \cdot Carb + Qz + Fsp}{Qz + Fsp + Clay + Carb + TOC} \quad (1)$$

Maximum brittleness occurs in the Jet Dogger at the top of the Jet Rock (Fig. 6-11). Fig. 6-12 shows cross plots of the various minerals that contribute to the BI. It shows that the carbonates correlate best with BI and are considered the strongest contributor. Quartz can be considered a positive, but less prominent contributor. The relationship with TOC is not evident, but a faint positive trend is present. GR relates negative with the BI, but since GR is sensitive for both high TOC and clay content, the relationship is not simple.

In the absence of rock mechanic data that give insight in the elastic properties of the studies rocks, no calibration of the mineralogically derived BI can take place. Question is if the applied shale equation is directly applicable to the JetRock. Therefore the brittleness equations will need to be revised in light of any future rock mechanic data available from the JetRock.

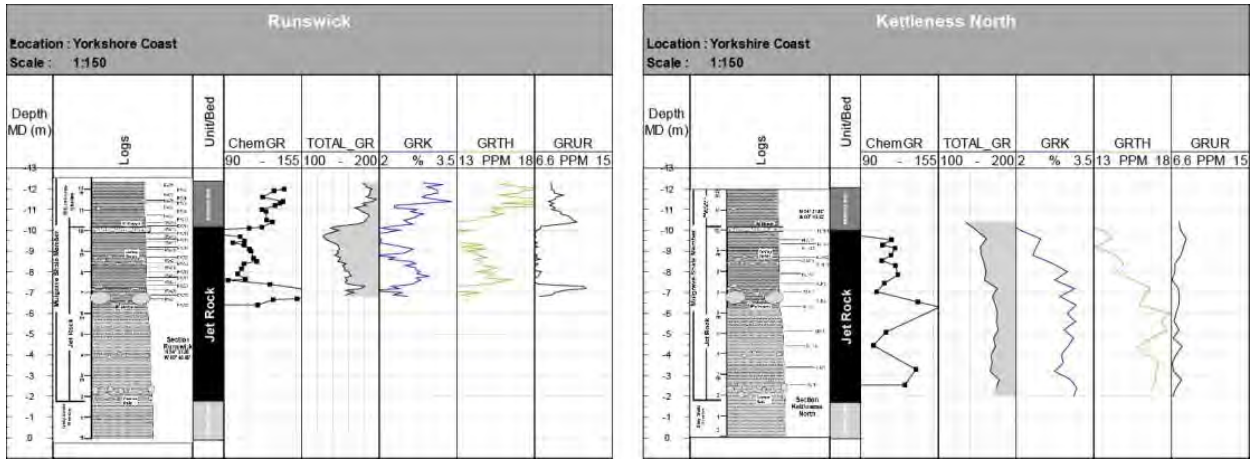


Fig. 6-10 Comparison of outcrop spectral GR and geochemically obtained (synthetic) GR.

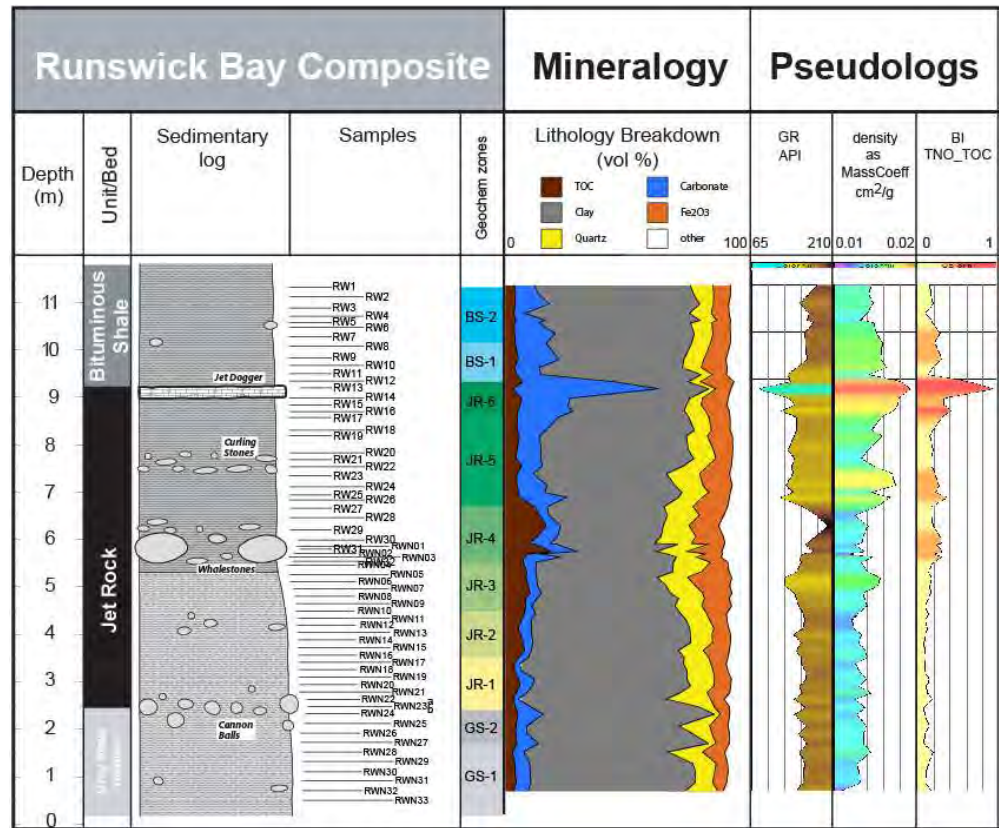


Fig. 6-11 All pseudologs combined, ChemGR – Total GR calculated from K2O (%), Th (ppm) and U (ppm) values, MassCoeff = density proxy (cm2/g), BI = TNO/chemostrat modification of the brittleness equation of Wang (2009). Input normative mineralogy(except Feldspar) is shown for reference.

6.4 Interpretation of geochemical analysis

The general, gradual increase in Ca abundance throughout the stratigraphic column, from top of the Grey Shales to the basal interval of the Bituminous Shales, is probably related to the increase in the biogenic pelagic fraction within sediments of the Jet Rock and Bituminous Shales, during the Toarcian transgression. In

particular, the pronounced increase in carbonate content evident in the topmost metres of the Jet Rock and at the base of the Bituminous Shales might reflect the enhanced efficiency in precipitation of secondary carbonates associated to the oxidation of abundant organic matter within the sediment during early burial.

Accompanying peaks in Mg concentration probably indicate direct precipitation or early diagenetic substitution of dolomite due to relative depletion of Ca ions in the presence of particularly high amounts of organic carbon (an intermediate stage between carbonate and sulphide precipitation) or of protracted diagenesis of the interested interval. Such peaks thus may correspond (or occur close) to key stratigraphic horizons characterized by high amounts of secondary concretions, close to intervals with high content in organic carbon, and corresponding to stratigraphic surfaces of reduced deposition/condensation and/or concentration of pelagic components from primary organic productivity. The concentration of strontium in carbonate phases might be related to diagenetic dissolution and reprecipitation of aragonite-rich debris, but it might be indicative also of an increase in diagenesis of carbonate material of coccolithic origin during stratigraphic intervals of pronounced pelagic contribution, since coccoliths may concentrate 3-5 times more Sr than other carbonates of inorganic/organic origin (Scotchman, 1991).

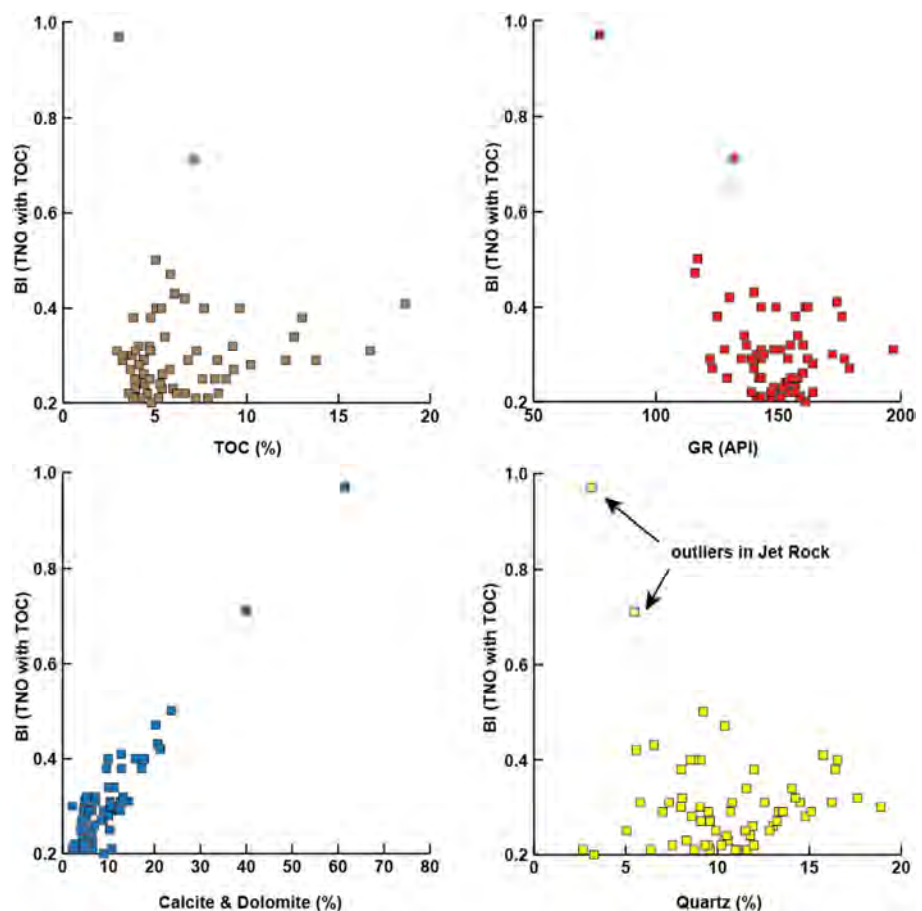


Fig. 6-12 Cross correlation plots of Brittleness Index (BI) against TOC, GR, Carbonates (Calcite and dolomite), and Quartz for the Runswick composite section.

Both the normative mineralogy and K-based clay ratios exhibit a lower contribution of kaolinite at the middle of the Jet Rock unit (approximately corresponding to the horizon characterized by 'Whalestone' concretions). Since the normative mineralogy does not indicate an enrichment of illite, the K-based clay ratios might be interpreted such that the peaks in complex clay minerals indicate relative enrichment due to an actual diminishing of the kaolinite content. The dilution effect on kaolinite may be further enhanced by higher quartz content and the higher organic content may play a role as well.

Key ratios of trace elements indicate that increased coarse clastic terrestrial input (high Cr/V) recorded at the Whale stone level is concomitant with high organic input (low Th/U) as is also shown by the high TOC at that level. The same level shows an increased Zr/Nb ratio, indicating that heavy mineral input was enhanced as well, or that subtle variations in provenance occurred. This further support the notion that the kaolinitic clay fraction is diluted by both organic content and clastic material (also shown by the Th/U ratio). An interpretation in terms of chemical weathering potential (alone) at this point is too far-fetched.

6.5 Lateral variation of results

In comparing the geochemical result of the Runswick composite with other analysed (partial) sections no pronounced difference are observable. The geochemical zonation of the Runswick site applies to the other sites as well. Results of these sections are provided digitally on the enclosed USB stick.

6.6 Synthesis and general insights

- Lithological variation is expressed mainly by variations of the three main constituents, clay, quartz and carbonate.
- Element affinity grouping shows relationships between organic matter related and pyrite/metals and clay- and heavy minerals.
- The mineralogical variation between the three stratigraphic units studied are slight.
- Lateral geochemical heterogeneity within the study area (~3 km separated localities) is not observed.
- A geochemical zonation based on variations in organic matter and heavy mineral input best displays the heterogeneities in the studied sequence.
- Density is mostly influenced by TOC (negative) and carbonate (positive) content.
- Brittleness Index (BI) is not only high for carbonate rich levels, but also is high for high TOC zones. This can be explained by high coeval siliciclastic input as deduced from the high Quartz content and also from the high Cr/V (high changes in terrestrial input (Cr) vs organic input) and Zr/Nb (change in heavy input). This suggests that high TOC and terrigenous input are linked.
- Variations in clay mineralogy based on normative mineralogy are not prominent. However, based on the K/Al, K/Rb and K/Cs ratios it shows that

relative enrichment of complex clays can be attributed to dilution of the kaolinitic clay content by organic matter and clastic material.

- TOC values and proxies for redox conditions (U, V) show a close co-variation, suggesting that there must have been a major (climatic) control on source areas (chemical weathering), sea-bottom anoxia, variations in clastic input and (early) diagenesis. Such climatic excursions are well known for the Toarcian stage (Dera et al., 2009; Hesselbo et al., 2009; Branski, 2012). Such compositional changes are thus potentially applicable for basin-wide stratigraphic correlation and have implications for a preliminary mineralogical evaluation of fine clastic fractions and of their associated geotechnical properties.
- Mo/U ratios indicate, however, that peak anoxic conditions at the seawater-bottom interface occur higher up in the succession, i.e. in the Bituminous Shales. This illustrates that peak TOC values at the Whalestone level can be mainly attributed to increased productivity in combination with suboxic bottomwater conditions.

7 Fracture Analysis

7.1 Introduction

On the scale of a field outcrop or average HC development (102-103 m scale), natural fracture networks can be laterally extreme heterogeneous, both in density and prevalent orientations. The orientation and density of genetically related fractures may also differ from one lithology to another, both laterally and vertically. Although fractures are difficult to describe and quantify in a sensible and effective way, they have a large influence on the development of fluid flow dynamics in a reservoir (effective reservoir permeability). For that reason, the presence of natural fractures in gas shale layers has large impact on the effectiveness of hydraulic fracturing. Also the orientation of fractures relative to the present-day state of stress is of major importance for planning (horizontal) wells. Thus, in attempting to make the hydraulic fracturing techniques more effective, a fracture prediction should be made that is based on the established relationship between fracture characteristics and ambient properties of the target formation. Next to this an assessment of the regional vs. local stress-strain relationship needs to be made in order to understand lateral heterogeneity as well.

Fracture analyses generally comprise four observation categories: (1) distribution and geometry of the fracture system, (2) surface features of the fractures, (3) relative timing of fracture formation, and (4) geometric relationship of fractures to other structures (Twiss & Moores, 1992). Many difficulties in interpreting fracture systems at depth occur since most fractures have sub-seismic dimensions and images of wellbores and cores have limited visibility. The study of outcrop analogues is one way to deal with these limitations, although it has its limitations as well. Outcrop studies are frequently applied in geo-engineering to describe rock strength and slope stability (e.g. Sturzenegger et al., 2007). Other applications are the description of surface analogues of buried fractured aquifers (e.g. Surrette et al., 2008) and hydrocarbon reservoirs in petroleum geology (Nelson, 1987; Odlinger et al., 1999).

It is important to keep in mind that correlation from outcrop to subsurface cannot be done straight forwardly, without considering that rock formations behave different at depth. In this study, no rheological experiments are executed. Analysis of the rheological behaviour and -parameters of the Mulgrave Shale Member are currently executed at UU (M. Houben) and TUD (A. Barnhoorn). The primary objective of this fracture study is to do a strain analysis by describing the fracture network, derive rules on mechanical stratigraphy and regional context in order to compare it to the subsurface PSF in the Netherlands (considering timing can be established).

7.2 Methodology and Dataset

7.2.1 *DigiFract and Scan-line methods*

In this study, DigiFract and the Scan-line method were used to analyze fractures. DigiFract is a software program that aims at the digital acquisition and characterization of natural fracture networks of vertical rock faces in the field. This is done by quantifying fracture densities, lengths and orientations. In 2007, DigiFract was developed to improve fracture analyses. DigiFract is a GIS-based software

package developed by the VU University Amsterdam and the Delft University of Technology to acquire and process fracture data in the field (Bertotti and Bertotti., 2007).

In the past few years, DigiFract software has been used in various studies, during which many thousands of fractures and bed surfaces have been collected in a few hundreds of different outcrops (e.g. Boro et al., 2013, Hardebol et al., 2013, Strijker et al., 2012). DigiFract was successfully used for field studies, e.g. in the Tanqua-Karoo Basin (South Africa) (Bertotti et al., 2007), for fracture characterization of a thick succession of fluvial sands in Jordan (Strijker et al., 2012) and for the Latemar carbonate platform in the Dolomites, Italy (Boro et al., 2012). To date, DigiFract was never applied on shales, especially since it is a challenge to find fresh shale outcrops with vertical rock faces.

The fractured data for this research were acquired using DigiFract 1.0 (Hardebol et al., 2013). This software contains acquisition and processing components which are designed with the general aim of acquiring fracture data such as position, orientation and height in an efficient and objective way with particular focus on vertical outcrops (Boro et al., 2013). The workflow of using the DigiFract software is outlined in Fig. 7-1. It includes an acquisition and initial processing stage (Bertotti et al., 2007). It allows for a fast and complete dataset of different outcrops. The software can perform statistical calculations using the data stored in a database management system. It can integrate different data sets while capturing complete descriptions of fracture distribution in 2D. The observational quality of field surveys can be improved by making use of light detection and ranging (LiDAR). This technique was not yet used for this study, but can be used to improve the quality of the dataset.

The scan-line method is used to quantify the density of natural fracture networks through two physical scan-lines at right angles. This technique enables the study of multiple orientations of fractures within one horizontal surface. The outcrop surfaces used for the scan-line method are horizontal wave cut platforms, which are common in the studied coastal area near Whitby.

7.2.2 *Workflow*

The first objective of the fracture analysis is to find vertical outcrops that are of acceptable quality for analysis. Next step is to upload an outcrop photo into the software and mark the area of analysis (the DigiSurface) with the software. Bedding planes and fracture planes can subsequently be added. An operator measures the orientation of each individual fracture, which is then digitized the software. Other fracture properties like direction, dip angle, aperture and mineral filling can be added as well. Fractures that are digitized with DigiFract combine a geometric description with attribute information that can be directly analysed with spatial statistical routines and presented in orientation and intensity plots.

7.2.3 Data processing

The position of the digitizing surface is defined by a basepoint, strike of baseline and dip angle of the presumably planar DigiSurface. This is done by using a digital scan-line that 'scans' the outcrops along a trackline which is placed at the base of a DigiSurface parallel to the bedding surface or semi-perpendicular to the main orientation of a selected set of fractures. This scan-line moves with a given step-size upward through the outcrop (along with the trackline) and determines the position of intersections with fractures relative to the stratigraphic succession. The fracture density can be determined by the number of fractures divided by the width of the scan-line.

Fracture units are defined on the basis of the fracture-density curve across the outcrop, i.e. fracture stratigraphy. Boundaries between fracture units are placed where the fracture density curve shows a significant break. The definition of fracture units is extended to include not only intervals with roughly constant fracture density but also sedimentary units where the fracture density shows gradual changes (a similar approach was applied by Underwood et al., 2003 and Boro et al., 2013).

The analysis of orientation distributions is a common first step in the processing of fracture data in order to find the main directions and to establish fracture subsets (Király, 1969; Fisher, 1993). DigiFract generates rose diagrams. These are used to study the oblique distribution of the azimuth of fractures. It also generates stereoplots in which the spherical orientation of planes is plotted. By using the position of fracture intersection with the scan-line, the distribution of the spacing of fractures is plotted. To include errors, mean and standard deviation of fracture spacing are plotted for each scan-line. In addition to outcrop analyses, the total distribution of fracture spacings and lengths for the same study area is grouped and frequency distribution is analyzed and plotted in a frequency histogram. Histograms are made for fracture heights and fracture spacing.

7.2.4 Outcrop description

For the fracture analysis, five outcrops at two different localities 5 km apart were selected, i.e. Runswick Bay and Port Mulgrave (WHI 1-5 in Fig. 7-2). The same outcrops were selected for the other analysis presented in this.

In both localities, two distinct sets of fracture orientations were observed and, as a consequence, two DigiFract analyses were performed. This is essential since, depending on the orientation of the rock face, one direction would dominate the results. At Runswick Bay (WHI1 and WHI3) the outcrop consists of the upper part of the Jet Rock member, with its base at ~25 cm below the Curling Stones and its top ~10 cm above the Top Jet Dogger.

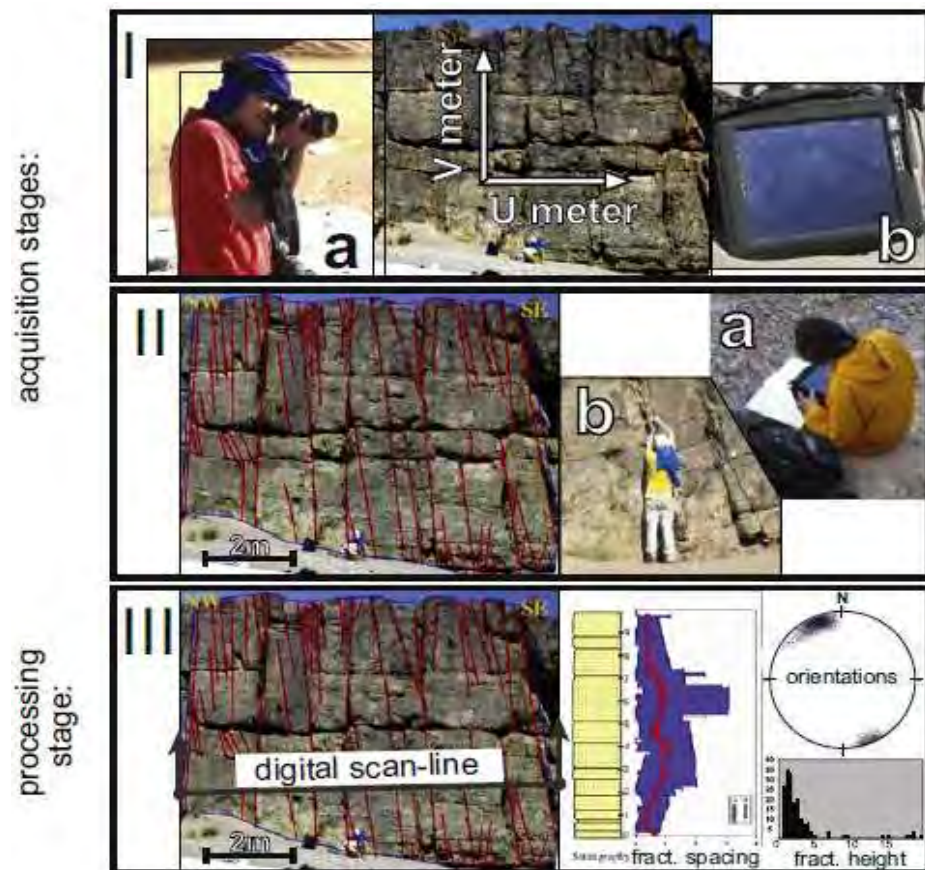


Fig. 7-1 I) The digital acquisition of the fractures, first aim is to find a valid outcrop and upload the outcrop photo into the software. II) Digitizing of the fractures and fracture characteristics (orientation measurements). III) When opening DigiFract a graphical user interface is displayed in which three different tab-windows can be opened: the location map, the digitizing surface and the processing output. A digital scan-line is projected onto the outcrop surface and all fractures that intersect with this scan-line are processed into stereoplots indicating orientations, histograms indicating fracture height distribution and diagrams which indicate fracture spacing and fracture density.

At Port Mulgrave, outcrop WHI2 consists of the middle part of the Jet Rock member, with its base ~2 m below the Whale Stones and its top at the Top Jet Dogger marker bed. The total height of this outcrop is 3.9 m with a width of 5.75 m. Outcrop WHI4, ~30 m north of WHI2, is somewhat lower in stratigraphy and includes the interval from the Canon Ball Doggers to the Curling Stones. The total height of the outcrop is 3.3 m with a width of 3 m. At Port Mulgrave also a Scanline analysis was performed in front of outcrop WHI2, on the wave cut platform formed by the top of the Canon Ball Doggers. For the pavement analysis (WHI5) two scan-lines are used with EW and NS orientations and with scan-line 1 being 20 m and scan-line 2 being 10 m.

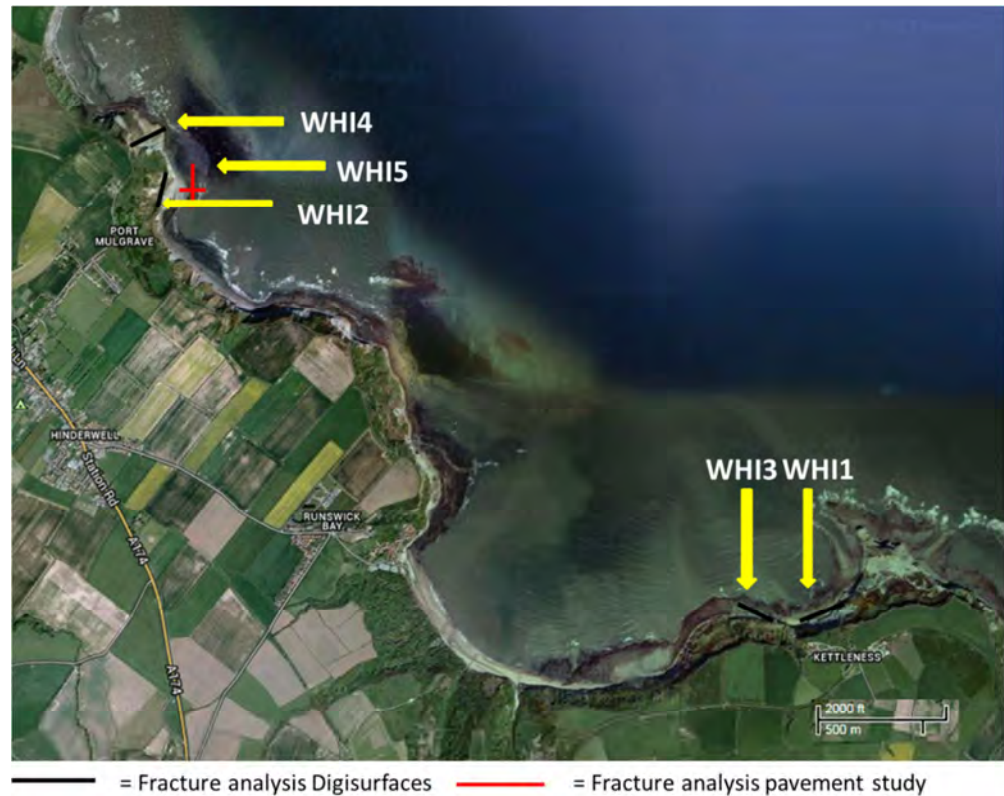


Fig. 7-2 Five outcrop locations of fracture analyses WHI1 and WHI3 are located at Runswick Bay, WHI2, WHI4 and WHI5 are located at Port Mulgrave.

7.3 Fracture characteristics

7.3.1 Whitby data overview

In total 213 fractures from 4 different outcrops were measured and afterwards digitized and processed with DigiFract. For the pavement analysis 66 fractures at outcrop WHI5 were measured analyzed using the scan-line method. An overview of outcrop names, measured fractures and number of bedding surfaces is shown in Table 7-1.

Most measured fractures are joints, i.e. open mode fractures that are not filled with minerals (Mode 1 in Fig. 7-3) and do not exhibit pronounced offsets. These fractures have been formed due to a tensional stress normal to the plane of the fracture. Open mode fractures have impact on permeability and other physical properties of rock bodies. They may enhance flow and act as a conduit when open, or hinder flow and form a barrier when filled with minerals. The degree of impact depends largely on the geometric characteristics of single fractures and their 3D spatial arrangement (Gudmondsson et al., 2001; Philip et al., 2005; Baron et al., 2008; Dockrill and Shipton, 2010).

Table 7-1 overview of number of fractures and bedding surfaces and their characteristics at all studied outcrops

DigiFract analysis Outcrop name	Number of fractures	Number of bedding surfaces	Bedding orientation (strike)	Average fracture orientation (strike)	
WHI1	64	5	262	NNE/SSW	
WHI2	83	4	060	EW	
WHI3	49	5	124	NNW/SSE	
WHI4	17	4	250	NS	
Scan-line analysis – Pavement study Outcrop name	Number of fractures scan-line 1	Number of fractures scan-line 2	Orientation (strike) scan-line 1	Orientation (strike) scan-line 2	
WHI5	43	23	N/S	E/W	

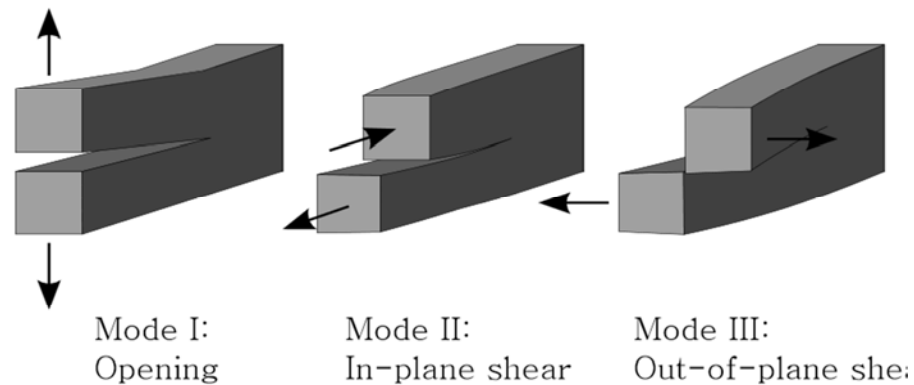


Fig. 7-3 Modes of possible fractures (Twiss & Moores, 1992). All observed fractures belong to Mode I.

7.3.2 Fracture orientations

Fracture orientations are relevant for understanding the spatial relationships between different orders of structural features and can be used to place the data in the larger structural context. Representative orientations of one fracture set in each outcrop over a large area are collected, which subsequently can be used to compare sets from one outcrop to another. In comparing datasets, the scale of observation is essential. As such it gives a sense of the strain heterogeneity in the area, which can be caused by local deviations- or perturbations of the regional stress field. Even under equal stress conditions, genetically related fractures are likely to vary in orientation, due to e.g. segmentation of the fractures, or reorientation of fractures due to local weaknesses. Also, differences in fracture orientation can be caused by slope instability processes, either natural or induced by human activities such as excavation. Because it is important to understand the relationship among fractures instead of taking the statistical analysis for granted. The fracture orientation distribution is shown in stereonet and in rose diagrams in Fig. 7-4, For each outcrop main average orientations are listed in Table 7-1. The stereoplots per DigiSurface show many differences in fracture orientation between

the different outcrops since fractures are acquired from DigiSurfaces with different orientation.

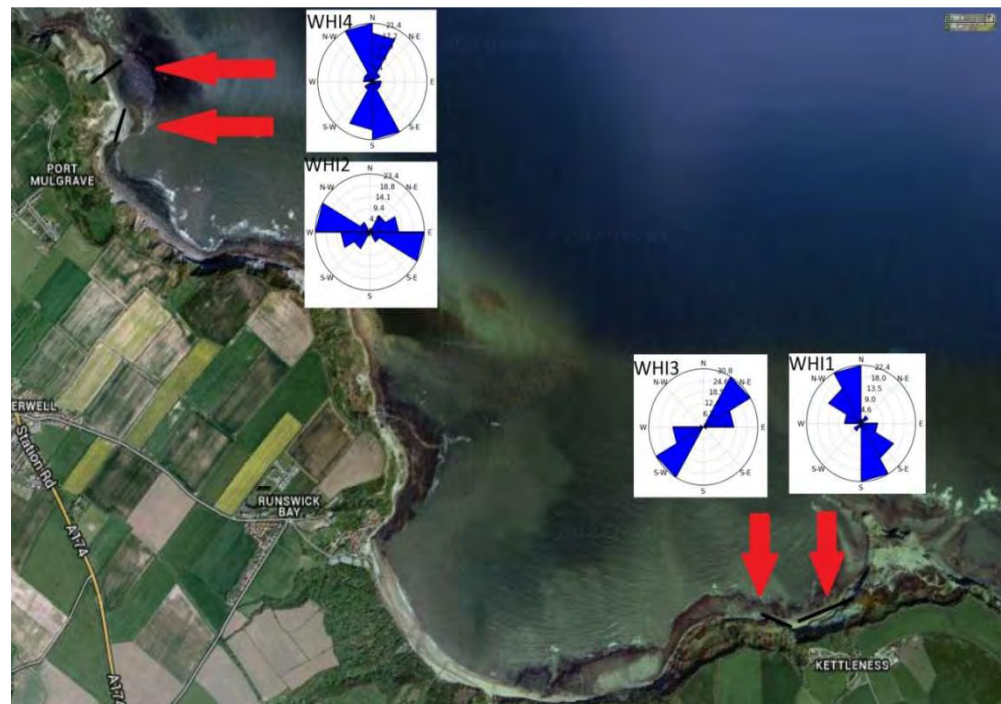


Fig. 7-4 Rosediagrams showing fracture orientations in the studied outcrops at Port Mulgrave and Runswick Bay.

7.3.3 Fracture heights

Fracture heights of all outcrops combined (except WHI4) and for each outcrop separately are shown in Fig. 7-5. The total fracture height distribution appears to be skewed towards the left. This is possibly due to the low number of large fractures observed. Only 3% of all the fractures are longer than the maximum height (3.9 m height) of the DigiFract surfaces selected, some of these cut through the entire outcrop.

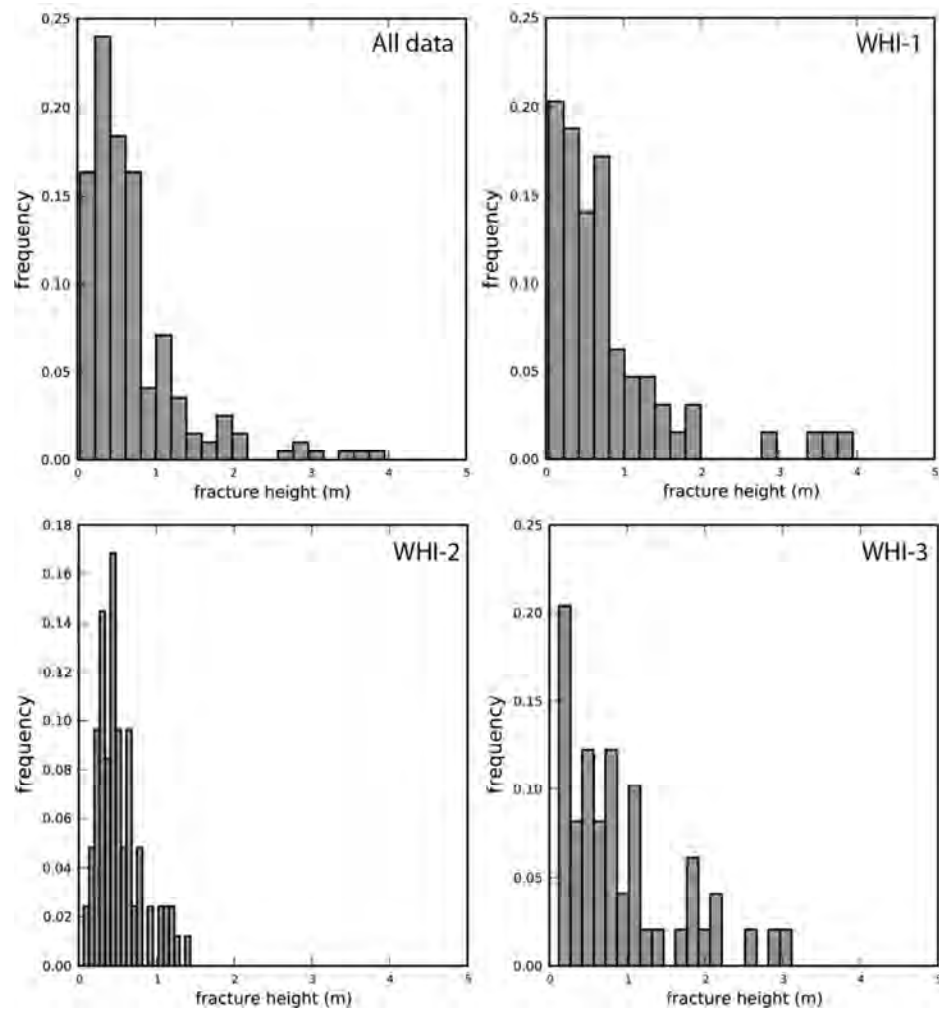


Fig. 7-5 Overview of the frequency of fracture height (m) for combined for all locations (upper left) and individual outcrops (from left to right WHI1, WHI2 and WHI3). The fractures in outcrop WHI2 show least variation in size and are more or less of the same height (in between 0.1 and 1.4 m). In WHI1 and WHI3 the fractures vary between 0-3.9 m and 0.1-3.2 m.

7.3.4 Fracture spacing and density

Fracture spacing in the different outcrops are obtained by measuring the distances between each two adjacent fractures along a perpendicular scan-line. The fracture spacing of all combined and individual outcrops can be found in Fig. 7-6. Fracture spacing distribution for all outcrops show strong asymmetrical distribution, although the actual spacing differs between all outcrops. However the spacing with the highest frequency is quite similar for all outcrops, which is in between 0.1 and 0.2 m.

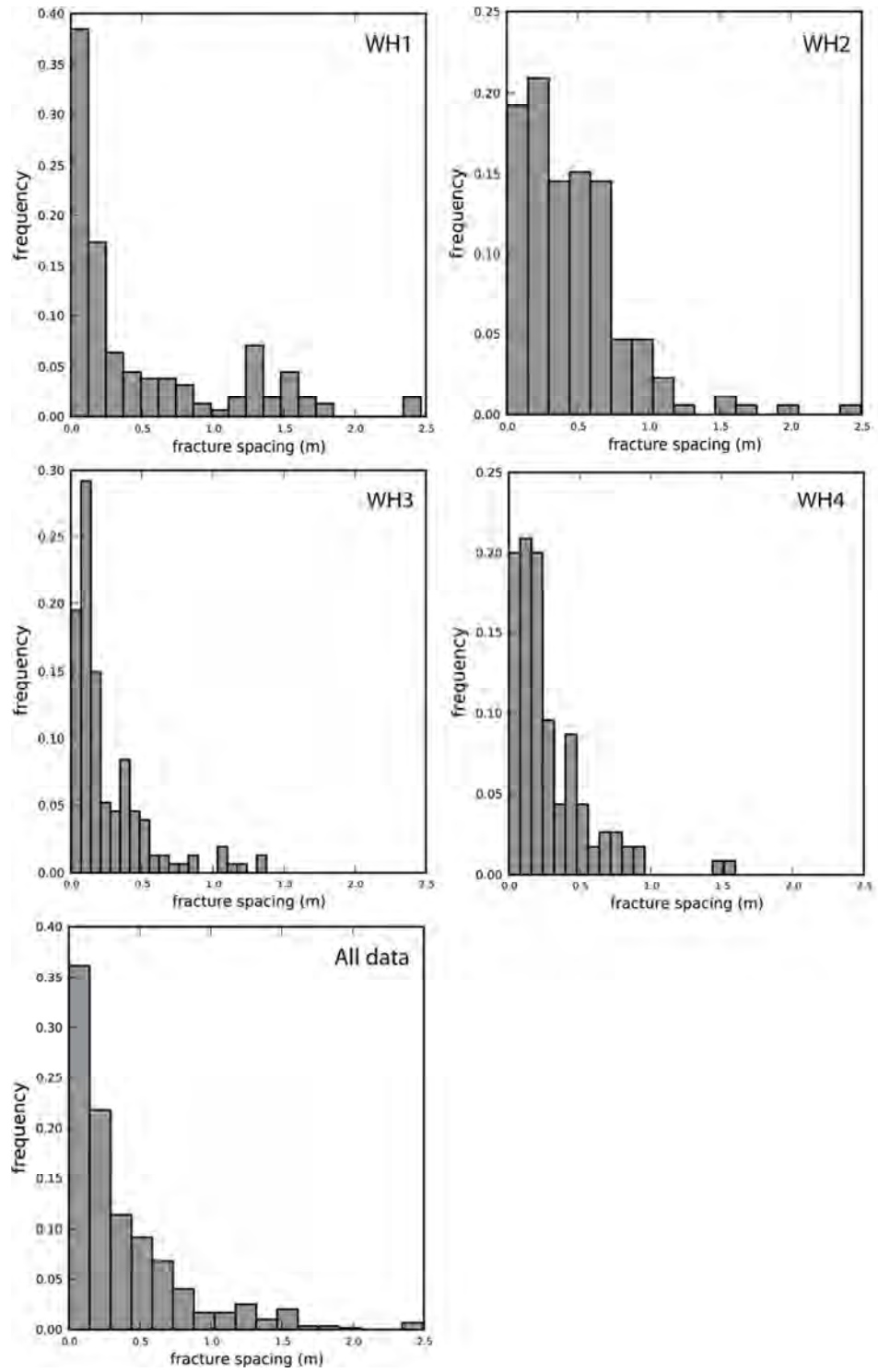


Fig. 7-6 Frequency plots of fracture spacing data (m) for all Whitby outcrops individually and combined

7.3.1 Scanline pavement study

For the pavement study performed in Port Mulgrave (locality WHI5) a scan-line analysis is executed on the wave-cut pavement formed by the Canon Ball Doggers (Fig. 7-7). Focus in the pavement study is on documenting the different fracture sets that have lengths >25 cm. In order to interpret the fracture network, one scan-line with north-south orientation and one scan-line with east-west orientation are used with a length of respectively 20 and 10 m. The spacing of fractures can be calculated using the measured data and the spacing together with the length of fractures (Fig. 7-8). The interpretation of the pavement study can be used to substantiate the observations/interpretations of the four DigiFract analysis (see section 7.4).



Fig. 7-7 Pavement area at Port Mulgrave (WHI5) with position of the N-S and E-W scan-lines.

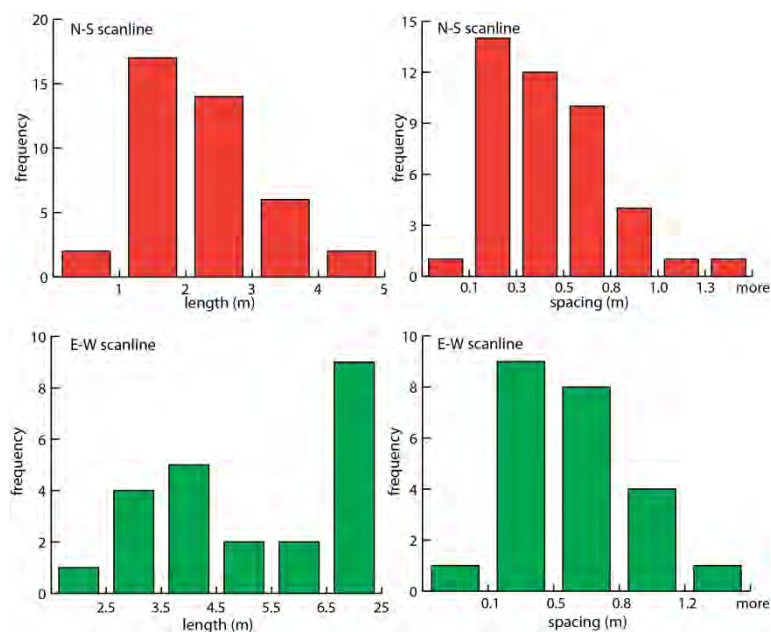


Fig. 7-8 Frequency of fracture spacings and lengths for the for the E-W and N-S oriented scan-lines.

7.4 Lithology-related fracture characteristics (DigiFract results)

7.4.1 WHI-1

Outcrop is WHI1 at Runswick Bay is oriented N-S and most of the observed fractures are oriented E-W and are perpendicular to the bedding. From the density graph (Fig. 7-9) a very high abundance of fractures below the Top Jet Dogger marker bed (arrow 3) is seen which decreases going up. The spacing increases above this layer. Overall the outcrop consists of many large fractures with most of them cutting through a large part or the entire vertical extent of the outcrop. Most of these fractures originate at the base of the DigiSurface. Some very large fractures start above the DigiSurface and have heights of minimal 3 m (arrow 1). Two fractures are present that start at the base and cut through the concretions of the Top Jet Dogger marker bed and the Curling Stone marker bed and the Curling Stone. A notable feature of this outcrop is the occurrence of a large ellipsoid concretion, which was not observed elsewhere in the Jet Rock. A few fractures terminate at the base of the Whale Stone. Some other fractures cut through the Whale Stone. These fractures are only found at the edges of the Whale Stone where the thickness of the concretion is limited (Fig. xx). Because both through-going and terminating fractures are concentrated around the concretion levels, fracture density (number per unit length) peak at his level.

7.4.2 WHI-3

WHI3 is located at 10 m distance from WHI1 (approximately 10 m apart) (Fig. 7-10), but this DigiSurface has a E-W orientation and therefore the acquired fractures are conctrated around a N-S orientation. In integrating fracture density data with other analytical results (see Chapter 9) the E-W and N-S fracture data of the WHI1 and WH3 outcrops are combined and considered as representative of one location. Several large fractures transect the entire DigiSurface including the top of the Jet Dogger although a considerable number of fractures terminate in or just above this bed. Large fractures are concentrated in sets with narrow spacing (~0.3 m) that are separated more than 1,5 m. Other than WHI1, WHI3 does not contain concretions like the Curling Stones and Whale Stone. This makes the outcrop more homogeneous (on outcrop scale) and fractures are more continuous, suggesting that the concretions have an important control on fractures terminations.

7.4.3 WHI-2

WHI2 is located at Port Mulgrave at ~5 km distance from WHI1 & WHI3 (Fig. 7-11). Most of the fractures in this outcrop are bed-confined and are shorter than in the other outcrops studied. A Whale Stone layer is present but hard to see in the figure. In the second bed of 0.5 m thickness, fractures occur with a different inclination compared to the overall vertical fractures. It is clear that these fractures are of a different style than the fractures seen in the outcrops at Runswick Bay.

7.4.4 WHI-4

WHI4 is ~30 m apart from WHI2 (Fig. 7-12) and contains a different fracture set with north-south trending fractures. In integrating fracture density data with other analytical results (see Chapter 9) the E-W and N-S fracture data of the WHI1 and WH3 outcrops are combined and considered as representative of one location. These mostly start from the bottom of the outcrop and are in many cases continuous and long. The height of the fractures in the first bed unit is ~2 m and most of the fractures in the outcrop have comparable heights. Two fractures cut throughout the entire outcrop, one terminating at the bottom of a Curling Stone and the other one cuts upward through the entire outcrop until the Top Jet Dogger marker bed and reaches a height of 4.5 m. In this outcrop no concretions are found (the first layer above the DigiSurface contains Curling Stones). The outcrop differs from outcrop WHI2 by differences in length and spacing of fractures.

7.5 Data interpretation

7.5.1 Tectonic control on fracture characteristics

The outcrops studied using the DigiSurfaces show two dominant fracture orientations. Within the pavement three typical sets of fractures were observed, the interpretation of which is shown in Fig. 7-13. The presence of multiple orientation sets is commonly explained in terms of tectonic episodes, re-activation of pre-existing faults or simultaneous development of orthogonal sets (Bai et al., 2002; Maerten et al., 2002). Rock cohesion is lost across fracture surfaces, which are thus planes of weakness within the rock. This can lead to reactivation of fractures in later tectonic events and, consequently, some combination of fractures may be genetically unrelated. In order to investigate this for the Yorkshire area the pavement study is essential. In this study all different orders of fractures are used to make an interpretation on how fractures relate to each other (fracture network connectivity and strain distribution), which can be used to infer kinematics.

Three different orders of fractures (based on fracture length) have been found in the pavement. The 1st order = 5-25m, 2nd order = 1-5m, and 3rd order = 0-1m. The fractures intersecting scan-line 2 are mostly 1st and 2nd order fractures and all of the 1st order fractures intersecting this scan-line have a length of 25 m or more. For scan-line 1 more 2nd and 3rd order fractures are intersecting and the small percentage of 1st order fractures reach maximum lengths of 5.9 m. It can be interpreted that the north-south orientated fractures intersecting scan-line 2 belong to the major set of fractures (primary fractures). They have a similar orientation to the faults present in the area (e.g. the Peak through), which are roughly north-south orientated. This reflects a similar strain distribution for both. The other set of fractures (secondary fractures), which are northwest-southeast orientated and terminate on the primary fractures have a different spacing and are shorter.

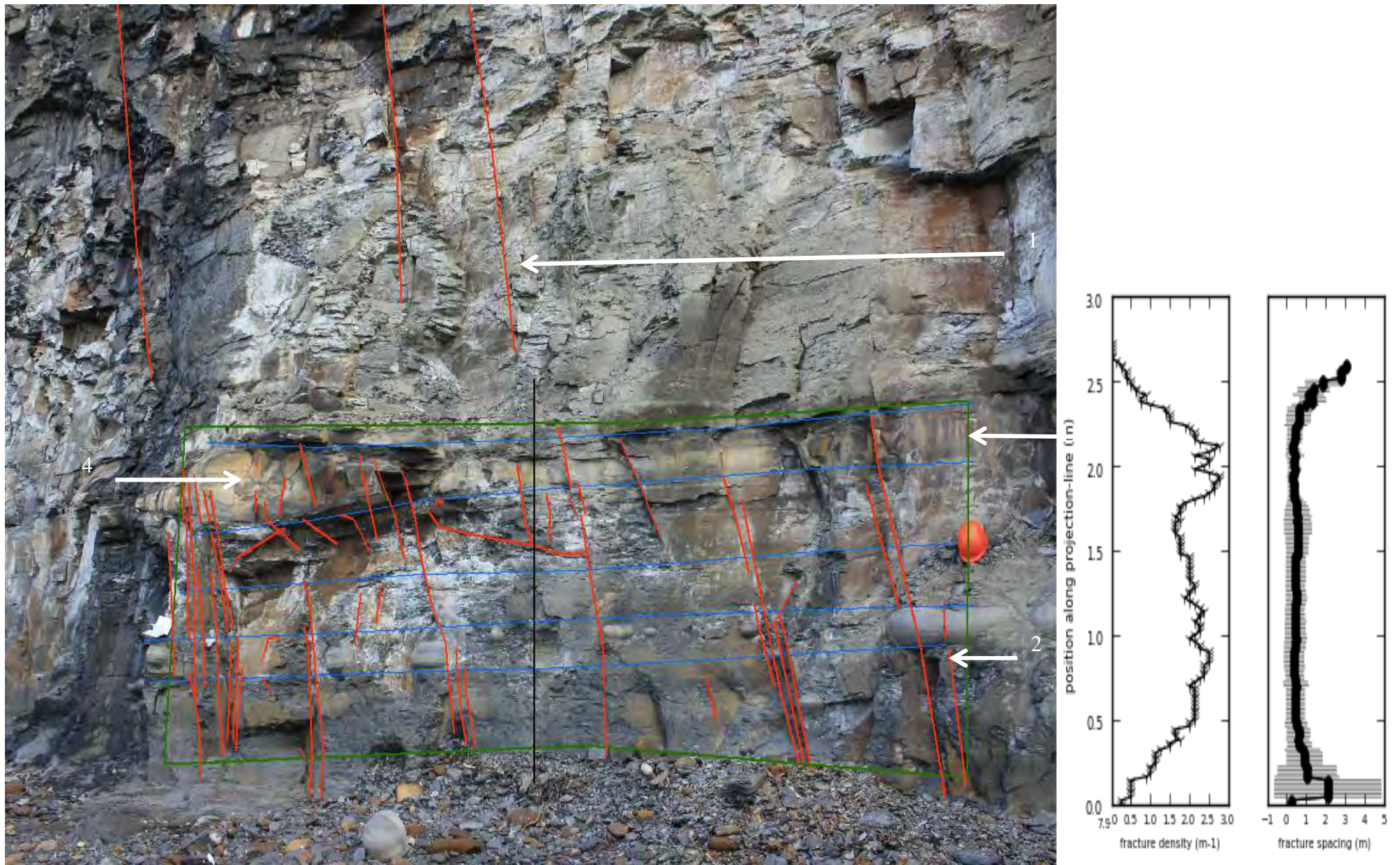


Fig. 7-9 Outcrop WHI1 at Runswick Bay, containing a typical concretion (Whale Stone) within the Top Jet Dogger maker bed (3). The DigiSurface is defined by the green area. Fractures are drawn in red, with the projection-line in black. The white arrows indicate typical features within the figure. (1) shows large fractures occurring above the DigiSurface, (2) shows fractures cutting through the limestone concretion, (3) shows the top Jet Dogger maker bed with fractures intersecting this layer, (4) shows fractures cutting through and terminating at the Whale Stone. The two diagrams on the right show the fracture density and fracture spacing (both in m) along the projection-line

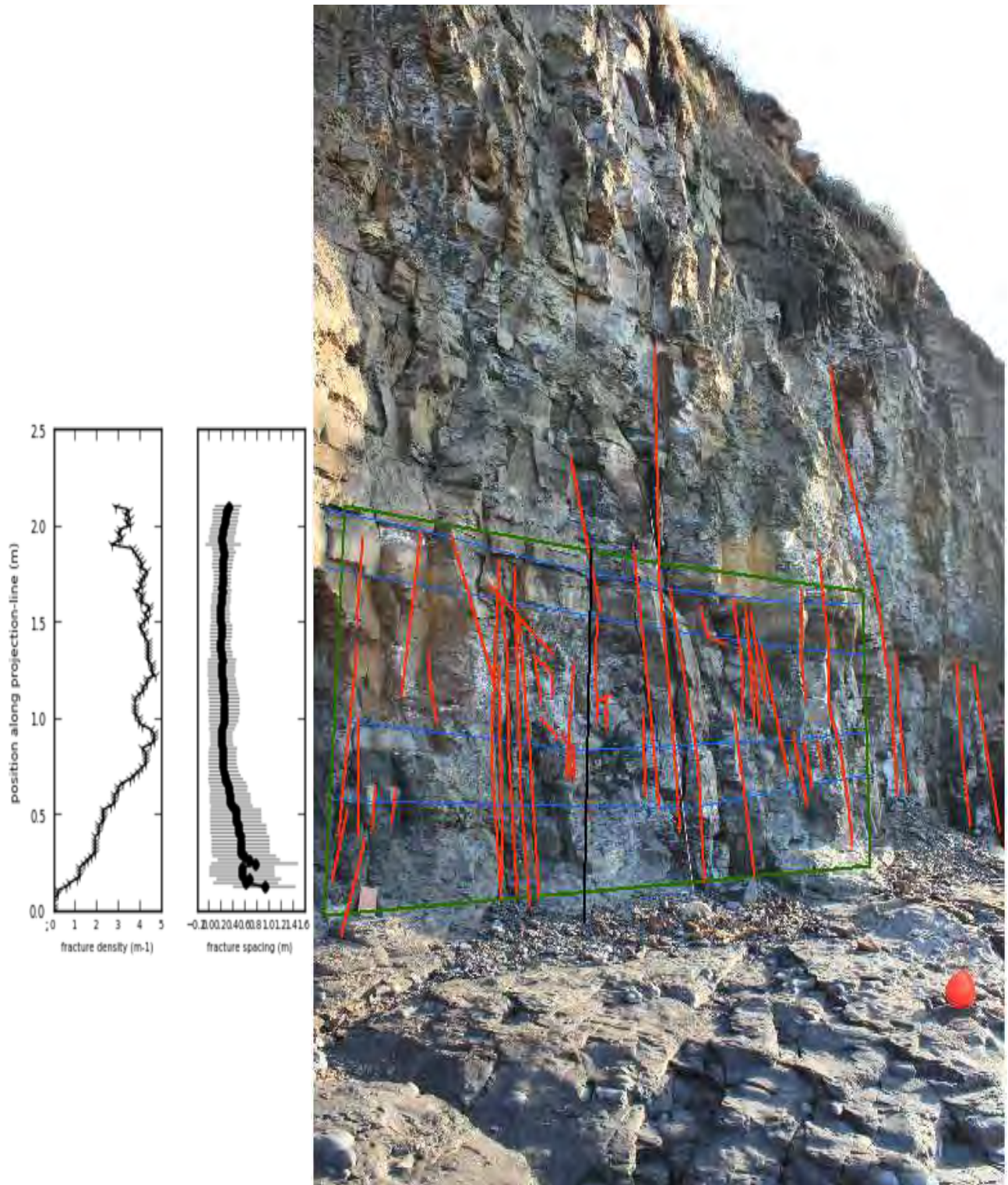


Fig. 7-10 Outcrop WHI3 at Runswick Bay. The DigiSurface is defined by the green area. Fractures are drawn in red, with the projection-line in black. On the left, two diagrams are plot showing the fracture density and fracture spacing (both in m) along the projection-line.

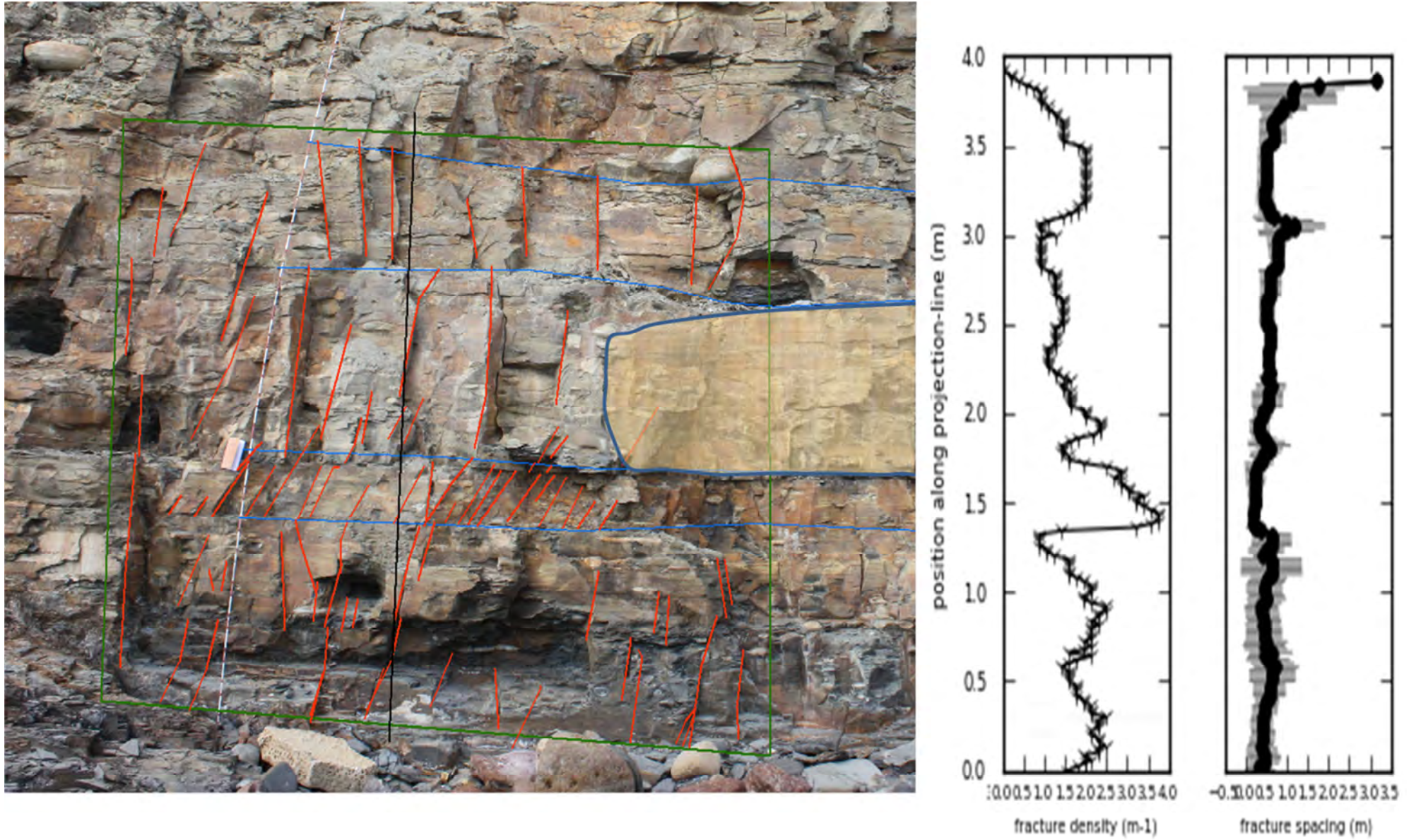


Fig. 7-11 Outcrop WHI2 at Port Mulgrave. The DigiSurface is defined by the green area. Fractures are drawn in red, with the projection-line in black. The two diagrams on the right show the fracture density and fracture spacing (both in m) along the projection-line. A Whale Stone is present in the 3rd layer and indicated by the blue line and yellow infill since visibility in this image is insufficient

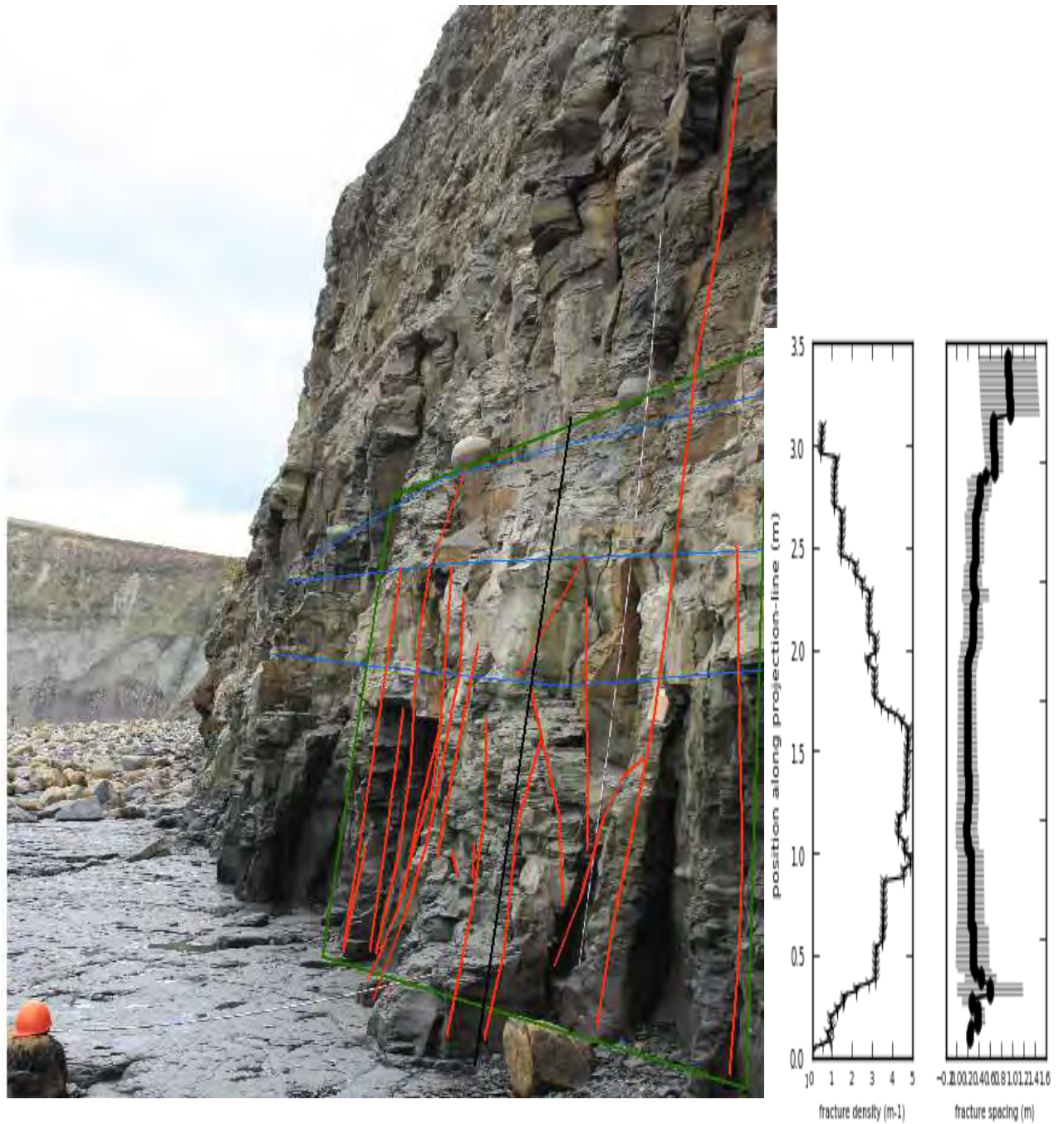


Fig. 7-12 Outcrop WHI4 at Port Mulgrave. The DigiSurface is defined by the green area. Fractures are drawn in red, with the projection-line in black. On the right, two diagrams are plot showing the fracture density and fracture spacing (both in m) along the projection-line

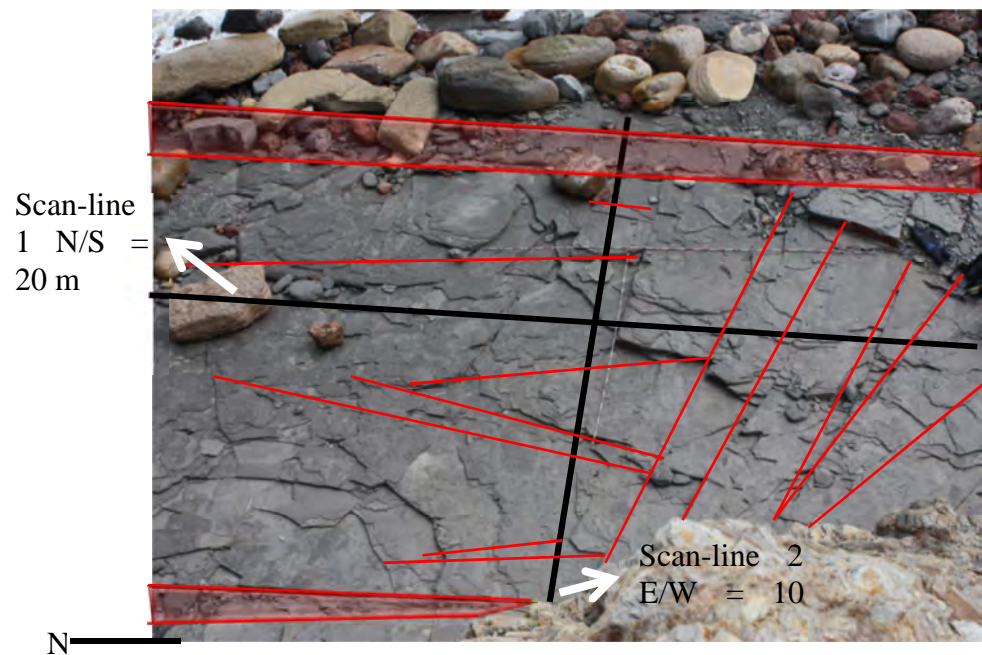


Fig. 7-13 Overview of the interpretation of fractures in the Pavement at Port Mulgrave. Red lines are the observed fractures, red coloured areas are interpreted as corridors. The black lines are scan-lines in two orientations. As is observed, fractures with an NW/SE orientation (secondary fractures that are intersecting scan-line 1) are terminated by the N/S orientated corridors (primary fractures), indicating a relation between both sets of fractures.

In outcrop WHI3 the primary faults shown in Fig. 7-13 constitute so-called fracture corridors (red coloured parts in Fig. 7-14). In the pavement study, three fracture corridors have been identified. The width of the observed corridors is ~20-30 cm, and they are north-south oriented and contain small scale (secondary) fractures oblique to the corridor bounding fractures. The northeast-southwest orientated fractures are confined (Fig. 7-13) by the north-south orientated fracture corridors, indicating a genetic relation between both sets of fractures.

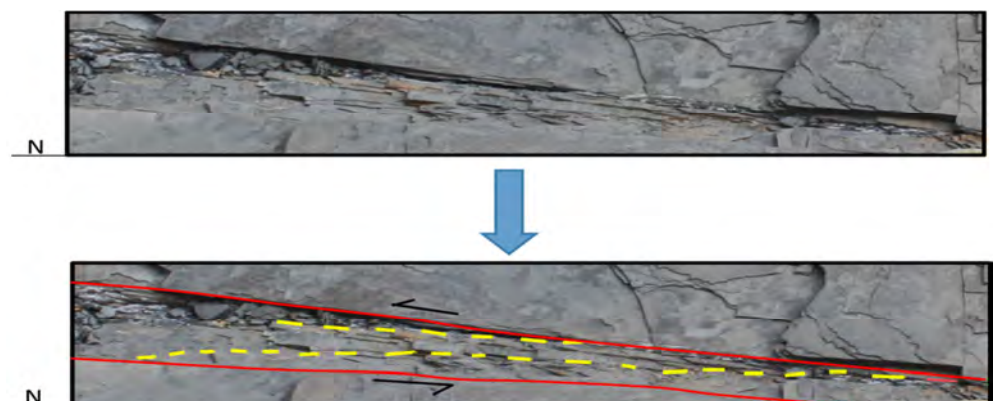


Fig. 7-14 Detail image of a corridor (red line) at the pavement of Port Mulgrave, with secondary faults (yellow) oblique to the corridor trend. The corridors are interpreted as synthetic Riedel structures, indicative of a sinistral sense of motion.

Based on the pavement analysis and the four DigiFract analyses a stress field interpretation for the Whitby outcrops can be made. Three sets of fractures were found in the studied area. The primary fractures in the outcrops and pavement study are north-south orientated. A more or less similar orientation to the faults around the study area was found, with the Peak fault as major N-S structure. The secondary fractures are found obliquely orientated (northwest-southeast) and terminating at primary fractures. No displacement along the primary fractures is observed but the secondary fractures can be interpreted as extension fractures. Signs of deformation are observed in the fracture corridors at the pavement (Fig. 7-14), in which tertiary fractures with a north northwest-south southeast orientation occur. These fractures can be interpreted as Riedel fractures. No folds or indicators of compression are observed in the study area. This observation and the presence and arrangement of extension fractures is in favour for a stress interpretation in terms of sinistral transtensional oblique slip Fig. 7-15). Unfortunately it was not possible to perform detailed studies on fault-kinematic indicators on the fracture planes (e.g. slickensides) to verify this interpretation. A quick comparison to the world stress map indicates that the paleostress conditions are dissimilar to the current stress field (north-south compressive).

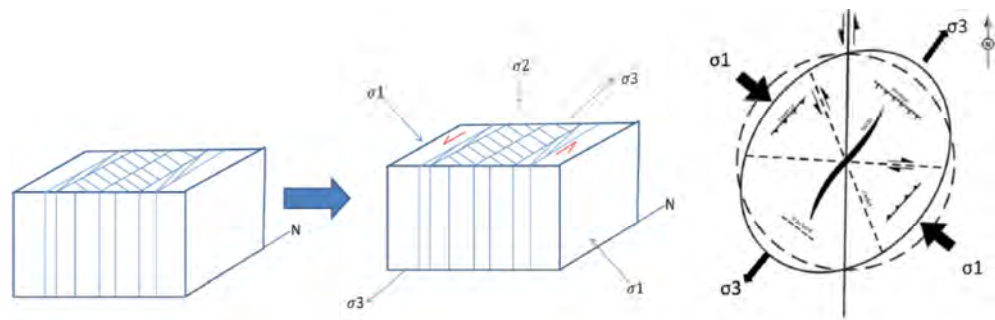


Fig. 7-15 Left: 3D block shows the observed faults and fractures in the studied area. Middle: 3D block shows the interpreted stresses responsible for faulting and fracturing. The main NS trending faults of the area (e.g. the Peak fault) are red coloured in both figures. The fractures are shown as blue lines in both figures. Right: 2D strain ellipse indicating interpreted stress regime to indicate the stress regime.

7.6.2 Lithological influences on fracture characteristics (bedding relationships)

Another objective of the study is to assess the influence of lithology and mineralogy on fracture distribution using the DigiFracxt method. The results from the four DigiSurfaces indicate that fractures are heterogeneous throughout the rock succession studied. The presence of bedding-confined fractures might indicate differences in lithology on the bed scale. In comparing the lengths and continuation between WHI2 and WHI4 (considered as one locality) it becomes clear that the lithological differences have more effect on the east-west orientated fractures (in WHI2) than on the north-south orientated fractures (in WHI4). For the beds comprising the smallest fractures (<0.4 m) the spacing is very small (~0.05-0.1 m) whereas for the larger fractures the spacing increases. Thus, the spacing of the fractures in WHI2 is proportional to the fracture length. This is also demonstrated in

WHI4, where the fracture spacing is quite regular throughout the DigiSurface since most fractures are continuous. Between the outcrops at Runswick Bay (WHI1 and WHI3) this dependency between fracture lengths and spacing is not so straightforward. Also the relationship with lithology is not that clear.

Both limestone layers and concretions act as fracture-terminating features implying that the dense calcareous layers are more resistant to fracturing than the mudstone layers. However, about 50% of the fractures do terminate at the bottom of the Whale Stone and the Top Jet Dogger member but the other 50% continues into this layer. This shows that local (paleo)stress/strain relationships can differ throughout the outcrops studied. This applies to the concretions as well. For instance, fractures terminating below the Whalestone at WHI1 (point 4 in Fig. 7-9) indicate that stress probably was not sufficient to fracture the concretions. Only at its edges, i.e. where the concretion is thin, fractures are continuous. This combination of observations suggests that the fractures developed after the formation of the concretions

7.6.3 Discussion - limitations of the applied methods

Scanline:

In the scan-line fracture analysis the smallest fractures measured are 0.25 m. Fractures smaller than this do occur but differ in scale (up to microscale) and are only visible in thin sections. A problem that occurs when taking the resolution into account is that the total lengths of most fractures running through the entire outcrop are unknown, since only fracture lengths within the outcrop DigiSurface are considered.

DigiFract:

Another limitation is the outcrop quality. Most surfaces are nearly vertical but exhibit a certain roughness which causes loss of accuracy when interpreting 3D fractures on 2D surfaces. Fractures look different on photographs as they sometimes seem to have a curved-shape while in fact they are straight. This causes digitizing surfaces to give limitations to the study of fractures. A third limitation is that the height of the outcrop is mostly higher than one can reach from the ground, which means that orientations of fractures are not always measurable. For this analysis these orientations were not added into the software.

Each DigiSurface is chosen perpendicular to the strike of the outcropping fractures as measurements perpendicular to the fracture strike are the most accurate representation of the true fracture properties. This makes mapping of multiple fracture sets that form one network not possible in one DigiSurface. This is why for every outcrop location two DigiSurfaces are analyzed which contain different fracture orientation sets.

Timing of fracturing:

Early and late diagenetic processes are likely to constrain changes in mechanical properties that affect fracture formation through time (e.g. Ortega et al., 2010). It is crucial to get insight into the burial and uplift history of the rocks studied and timing of fracture formation are useful and expand the interpretation. Marker beds are used to give indications for timing constraints by the continuity of fractures through marker beds but doing this remains a challenge, reflecting the possible error in this research.

Fault interactions:

Several faults are present in and around the study area. This causes possible stress perturbations driven by fault displacement which can result in the development of fractures with highly variable orientations (Bourne and Willemse, 2001; Maerten et al., 2002). Furthermore, variations in fault orientation can be caused by smaller scale processes as well

7.7 Synthesis and general insights

- The results from the four DigiSurfaces indicate that fractures are heterogeneous throughout the rock succession studied. The presence of bedding-confined fractures might indicate differences in lithology on the bed scale. The integration of fracture analysis results and mineralogical and geochemical presented in elsewhere in this report, elucidates on this subject.
- The discontinuity of fractures is caused by concretions or fractures are bedding confined and change with minor lithological changes. The spacing of the fractures is found to be proportional to the fracture length. Where fractures are bed-confined, a relationship between bed thickness and fracture spacing can be envisaged.
- Fracture densities are highest close to carbonate rich layers, i.e. concretions and limestone beds. Both limestone layers and concretions act as fracture-terminating features implying that most fractures developed after the formation of the concretions
- The outcrops studied using the DigiSurfaces show three different orders of fractures (based on fracture length): 1st order = 5-25m, 2nd order = 1-5m, and 3rd order = 0-1m.
- From the fracture study on mesoscale the following conclusions can be made: three types of natural fractures are identified: primary fractures, extensional fractures and riedel fractures. The arrangement of fractures represent north-south oriented fracture corridors with synthetic Reidel fractures indicating a sinistral transtensional oblique slip regime at time of deformation. This is in agreement with the general notion on paleostress conditions in the Cleveland Basin.
- The dominance of the observed fracture orientations changes laterally. This has major implications for utilizing natural fracture networks in production stimulation jobs with horizontal wells.

8 Stable isotopes and stratigraphic correlation

For this Sweetspot project, stable isotope analyses are only used to correlate the Yorkshire outcrops with the Posidonia Fm from the West Netherlands Basin and the type area in Dotternhausen, southern Germany (Fig. 8-1).

The type of stable isotope analysis applied in the project is organic Carbon-13 ($\delta^{13}\text{C}_{\text{organic}}$). Across the Early Toarcian Oceanic Anoxic event (Toarcian OAE), the $\delta^{13}\text{C}_{\text{organic}}$ displays a dramatic negative shift, which is known as the Toarcian Carbon Isotope Event (Toarcian CIE).

For the Posidonia in the Yorkshire area, an excellent stable isotope data set is available from the literature (Kemp *et al.*, 2005). Also for the Posidonia in South Germany, an excellent stable isotope data set is available from the literature (Röhl *et al.*, 2001).

In previous studies on the Dutch PSF, both palynological and stable isotope analyses were carried out on three wells from the Netherlands: Loon op Zand-01 (LOZ-01) from the WNB, and L05-4 and F11-01 from the offshore Dutch Central Graben (TNO report TNO-060-UT-2011-01497). With more than 50 meters of cored section, well LOZ-01 has become a reference section for the Posidonia in the Netherlands. Unfortunately it is an old well (1952), lacking any decent logs, including a Gamma Ray log. For that reason, it was decided to carry out some additional stable isotope analyses, in an attempt to use the stable isotope trend of WED-01 and AND-02 to correlate LOZ-01 to surrounding wells with excellent logs suites

Stable isotope analyses are carried on cored sections from two wells from the West Netherlands Basin (WNB), the Netherlands. These are Werkendam-01 (WED-01) and Andel-02 (AND-02).

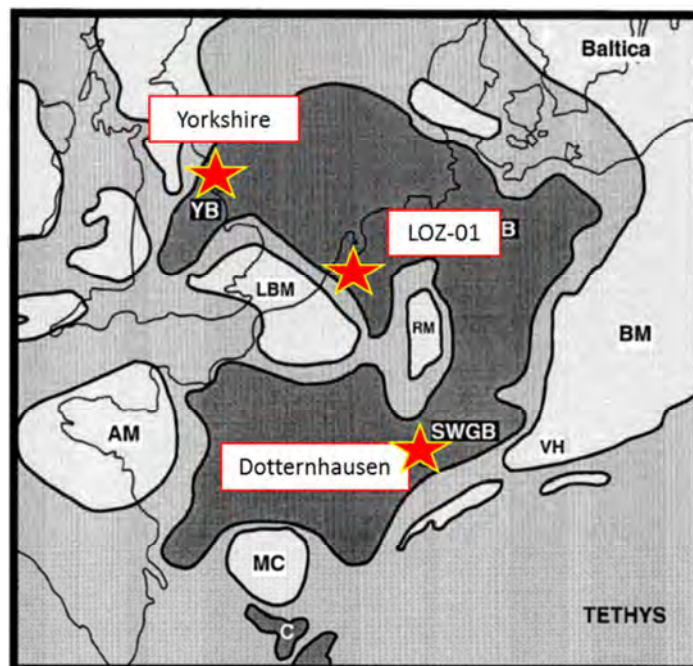


Fig. 8-1 Location map showing the positions of the Yorkshire, LOZ-01 and Dotternhausen

8.1 Methodology

Organic Carbon-13 Analysis of Rock Samples (carbonate free fractions)

The technique used for isotope analysis was Elemental Analyser - Isotope Ratio Mass Spectrometry (EA-IRMS). In this technique, samples and reference materials are weighed into tin capsules, sealed and then loaded into an automatic sampler on a Europa Scientific Roboprep-CN sample preparation module. From there they were dropped into a furnace held at 1000 °C and combusted in the presence of oxygen. The tin capsules flash combust, raising their temperature in the region of the sample to ~1700 °C. The combusted gases are swept in a helium stream over a combustion catalyst (Cr₂O₃), copper oxide wires (to oxidize hydrocarbons) and silver wool to remove sulphur and halides. The resultant gases (N₂, NO_x, H₂O, O₂, and CO₂) are swept through a reduction stage of pure copper wires held at 600 °C. This removes any oxygen and converts NO_x species to N₂. A magnesium perchlorate chemical trap removes water. Carbon dioxide is separated from nitrogen by a packed column gas chromatograph held at an isothermal temperature of 100 °C. The resultant CO₂ chromatographic peak enters the ion source of the Europa Scientific 20-20 IRMS where it is ionised and accelerated. Gas species of different mass are separated in a magnetic field then simultaneously measured using a Faraday cup collector array to measure the isotopomers of CO₂ at m/z 44, 45, and 46. Both references and samples are converted and analysed in this manner. The analysis proceeds in a batch process, whereby a reference is analysed followed by a number of samples and then another reference.

8.2 Stable isotope curves

8.2.1 *Yorkshire*

In Fig. 8-2 a high resolution stable isotope profile from the Whitby Mudstone Fm in Yorkshire is displayed (Kemp et al., 2005). The actual outcrop is Hawsker Bottoms, a cliff section about 6 km southeast of Whitby. In general, the stable isotope curve of the top part of the Grey Shale Member is flat, with average values of -26‰. In the very top of the GSM, about 2.5m below the base of the Mulgrave Shale Member (= the Canonball Doggers), the $\delta^{13}\text{C}$ values start to decrease. This decrease is the start of a pronounced negative shift, which reaches its maximum of -32‰ right at the base of the MSM. The extreme negative values last about 3 to 3.5 meters, approximately to the Whale Stone Doggers. From there, an increase in the $\delta^{13}\text{C}$ values occurs, which lasts about 3.5 to 4 meters, right up to the top of the Jet Rock (= Top Jet Dogger). In the Top Jet Dogger a value of -27‰ is reached. This point is for a long stretch the most positive value. The shape of the isotope curve at this point is typically sharp, arrow-head shaped towards the right. After this point, a very subtle decrease and increase again occurs, terminating 1.5 meters below the top of the MSM (= ovatum band). This subtle decrease-increase loop covers approximately 19 meters. The top of the loop is named X-event here. The base of the loop is named top Carbon Isotope Event (CIE) and the start of the negative shift in the top of the GSM is named base CIE.

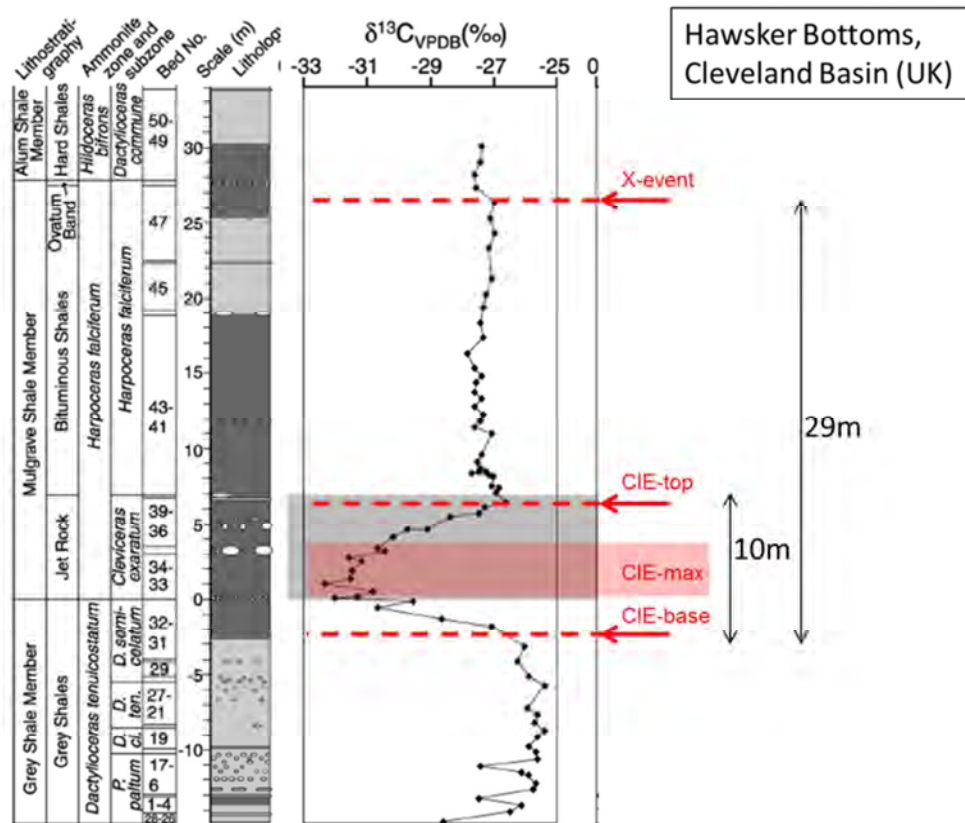


Fig. 8-2 Stable carbon isotope profile ($\delta^{13}C_{\text{organic}}$) of outcrop section Hawsker Bottoms (after Powell, 2010 and Kemp, et al. 2005)

8.2.2 Dotternhausen

Dotternhausen is a quarry section in the southwest of Germany, near Tübingen, approximately 50 km south of Stuttgart. In Fig. 8-3 the isotope curve is displayed. In Dotternhausen, the base CIE occurs 25 cm below the top of the Early Toarcian Tenuicostatum Ammonite Zone. The background levels of the stable isotope curve are slightly higher than in Yorkshire: -27‰ instead of 26 of Yorkshire. About 60 cm above the base CIE, the maximum negative value is reached: -33‰. The zone with high negative values lasts about 160 cm, to just above a continuous limestone layer which is named "Unterer Stein". Yet another 160 cm higher, the top of the CIE is reached. This level coincides with another limestone, the so-called "Oberer Stein". The X-event is placed at, or just above, the top of the section, approximately 600 cm above the top CIE.

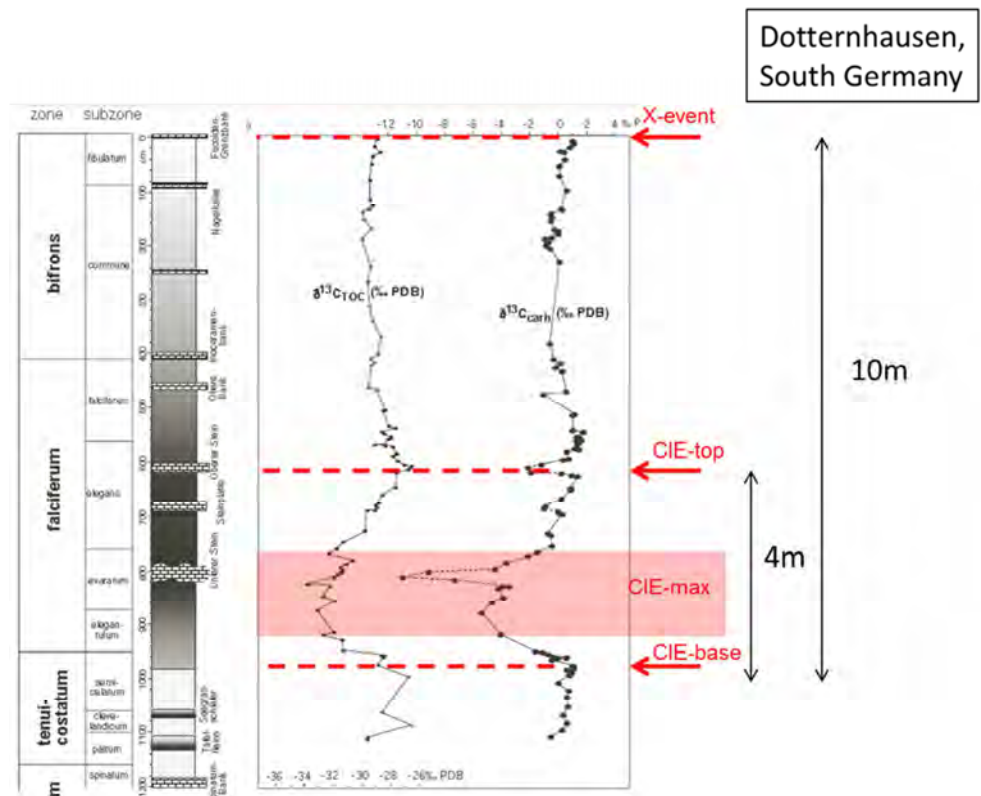


Fig. 8-3 Stable carbon isotope profile ($\delta^{13}\text{C}_{\text{organic}}$) of outcrop section Dotternhasuen (Röhl et al. 2001).

8.2.3 LOZ-01

Borehole Loon op Zand-01 (LOZ-01) is one of the few wells with a continuously cored *Posidonia* section in the Netherlands. Unfortunately, this well dates back to 1952, so there is no high-quality wire-line log suite available. A high resolution palynological and stable isotope record was established in a former project (see TNO report TNO-060-UT-2011-01497). In Fig. 8-4 the isotope curve of LOZ-01 is displayed. The base CIE more or less coincides with the base of the PSF, at 2511mAH. The average values below the PSF are around -26‰. The base of CIE-max is reached 4 meters above the base CIE and the CIE-max lasts for about 7 meters. Yet another 7 meters higher, the top CIE is reached. The X- event is positioned some 26 meters above the top CIE.

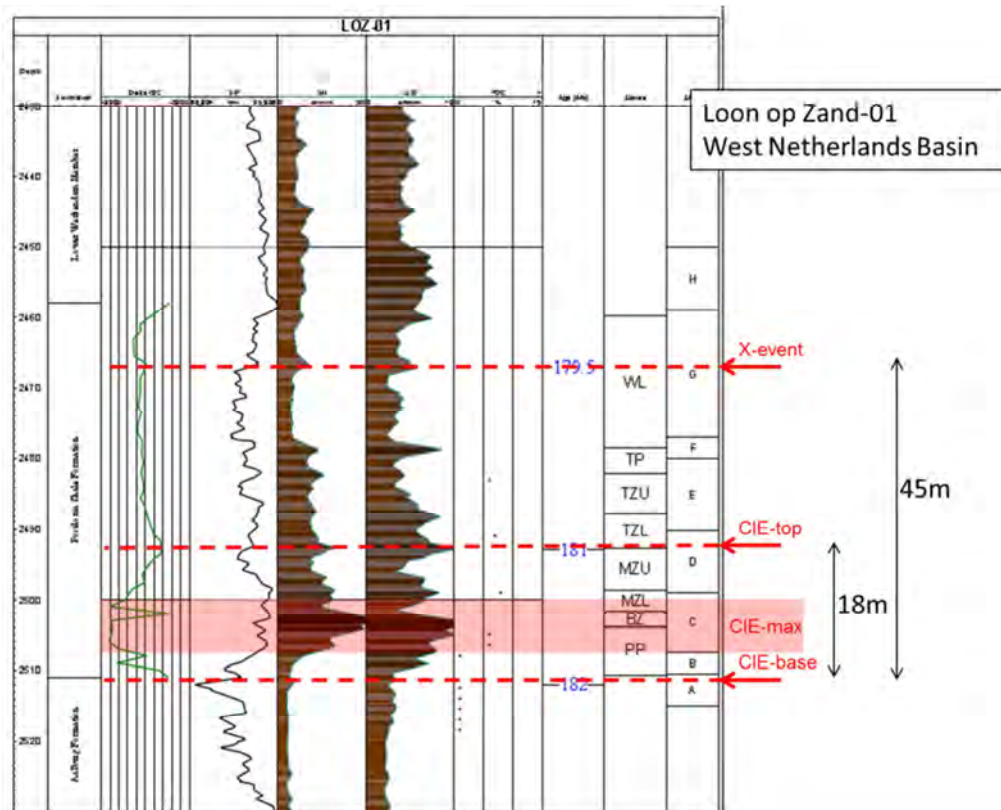


Fig. 8-4 Stable carbon isotope profile ($\delta^{13}\text{C}_{\text{Organic}}$) of well LOZ-01. The base CIE, top CIE and X-event are indicated. Columns from left to right represent: 1) lithostratigraphy, 2) stable isotope curve, 3) shallow resistivity, 4) deep resistivity, 5) TOC, 6) absolute ages, 7) log zones, and 8) biofacies zones.

8.2.4 AND-02 and WED-01

The results of well AND-02 were quite surprising: the stable isotope analyses showed absolutely no negative shift. It was quickly concluded that the cored section did not penetrate the Posidonia Fm.

The stable isotope results of well WED-01 clearly show that only the upper part of the CIE is represented in the cored section. The top CIE is very clearly expressed (see section 8.3).

8.3 Stratigraphic correlation

8.3.1 Correlation LOZ-01 to surrounding wells

In Fig. 8-5 well LOZ-01 is correlated to WED-01, based on stable isotopes, SP and LLD. These wells correlate very well, so it is feasible to interpret WED-01 in terms of isotope stratigraphy. In Fig. 8-6 well WED-01 is correlated to well WED-03, based on wire-line logs and stratigraphic thickness. Because WED-03 has a proper set of wire-line logs, including GR, DT and density, the stable isotope stratigraphy can be applied to surrounding wells in the West Netherlands Basin also. Well Meerkerk- 01 (MRK-01) has been selected as standard for the PSF in the West Netherlands Basin (Fig. 8-7).

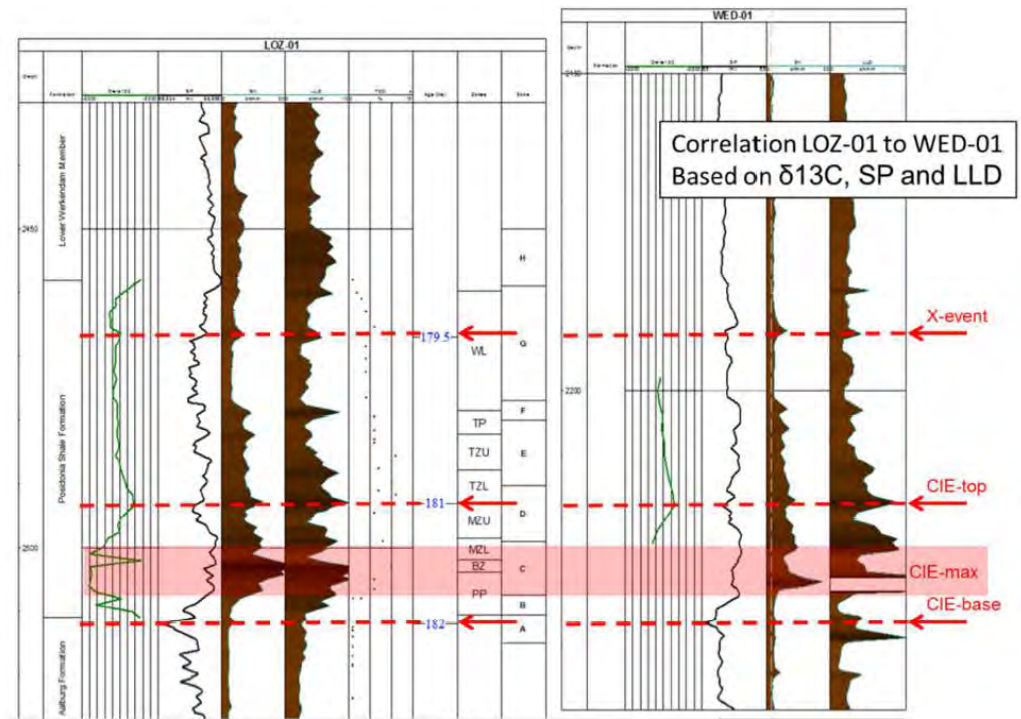


Fig. 8-5 Correlation LOZ-01 to WED-01, based on stable isotopes, SP and LLD.

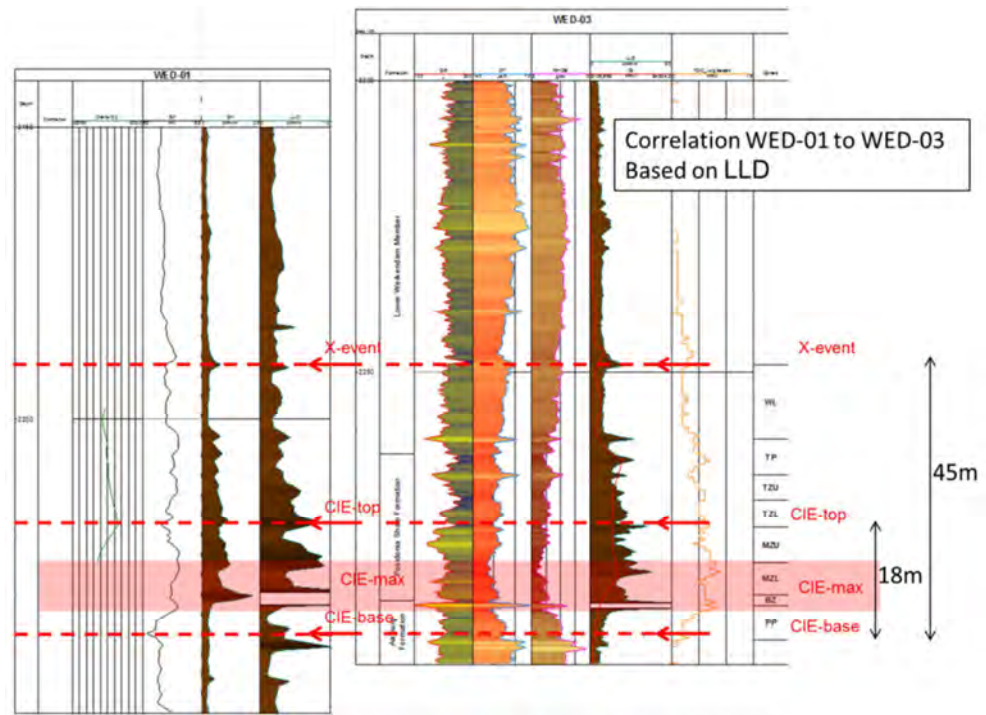


Fig. 8-6 Correlation WED-01 to WED-03, based on wire-line logs

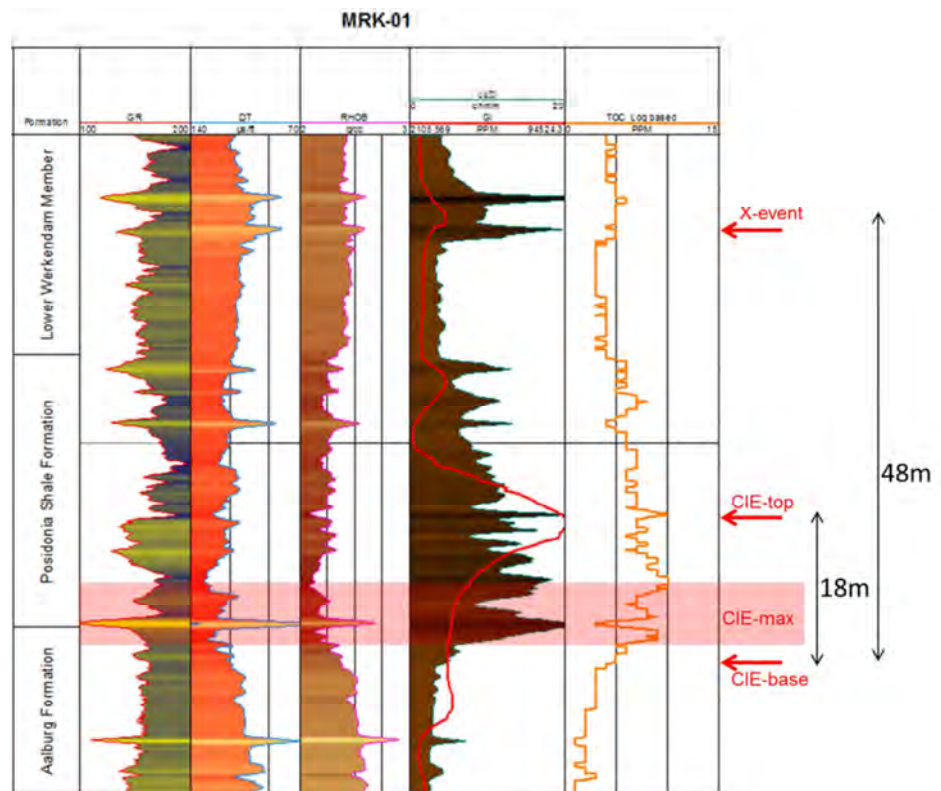


Fig. 8-7 The PSF including stable isotope stratigraphy, in well MRK-01: a standard Posidonia record for The Netherlands. Note the GI in red, indicating gas occurrences in the well.

Section 3 – Integration

The integration of the results, is organized in three chapters. In Chapter 9 all analytical results from the Whitby outcrop study are integrated. Chapter 10 integrates data and results from the Dutch onshore West Netherlands Basin, including data from previous projects and from the literature. Chapter 11 provides the overall integration, conclusions and implications for the entire project. The streamers displayed in bold and italics represent concluding statements.

9 Integration of the analytical results from the Whitby outcrop study in the UK

9.1 Heterogeneity

Macroscopic heterogeneity

The coastal outcrops of North Yorkshire are ideally suited to determine the macroscopic heterogeneity of the Toarcian black shale. The occurrence of easily identifiable marker beds, represented by conspicuous concretion horizons, enable comparison of the black shale succession on a scale of 1 to 5 kilometers. The main conclusion from a comparison of the Jet Rock between the outcrop locations of Port Mulgrave and Kettlewell, is, that there are no obvious differences in 1) overall thickness, 2) weathering profile, and 3) in the number and visual aspects of the concretion levels. Given the fact that these sections are 4 kilometers apart (Fig 3-4), the conclusion is warranted that the Jet Rock is laterally homogeneous over a distance of a couple of kilometers.

the Jet Rock is laterally homogeneous over a distance of 1 to 5 kilometers

Bear in mind, however, that it is difficult to assess how the outcrop locations between Port Mulgrave and Kettlewell are positioned relative to the paleo-coastline. The westerly thickening and amalgamation of the iron ore layers from the underlying Pliensbachian Cleveland Ironstone Formation, suggests that the paleo-coastline must have been situated towards the West in Pliensbachian times (section 3.2; see also the Whitby Excursion Field Guide, which is included in the digital data on the enclosed USB-stick). In that respect, it would be interesting to study the lateral heterogeneity of the Jet Rock on a West - East trend. Unfortunately, with the outcrops located along the WNW – ESE oriented coastline, this is not possible without additional information from cored well penetrations on land. It is important to note, however, that the Cleveland Ironstone Formation does display variation on the aforementioned WNW – ESE trend. Near Staithes, located at the far WNW end, thick ironstone concretion levels occur, indicating a near-shore marine palaeoenvironment. At Hawsker Bottoms, approximately 14 km apart from Staithes, the overall lithologies are more fine-grained and the ironstone concretionary levels have faded into indistinct horizons with separate concretions, indicating a slightly more distal palaeoenvironment than in Staithes (see section Strat Columns of the Whitby Excursion Field Guide). Surprisingly, the lateral variation of the overlying Toarcian Grey Shales Member (Whitby Mudstone Fm), between Staithes and Hawsker Bottoms, is already hardly noticeable and the lithological aspect of the member appears rather uniform. Apparently, the overall Toarcian transgression resulted in open marine conditions over the entire outcrop area, leading to an increase in the lateral homogeneity of the sediments. As a consequence, it is suggested that the Jet Rock is laterally homogeneous over -at least- 14 kilometers, but probably more.

it is suggested that the Jet Rock is probably laterally homogeneous over at least 14 kilometers and probably even more

Microscopic –vertical- heterogeneity

Based on earlier work on the PSF in the Netherlands (e.g. Trabuco-Alexandre *et al.*, 2012), it was expected to encounter significant vertical heterogeneity on a centimeter scale in the Whitby outcrop study. This expectation was mainly based on the fact that fining-upward and erosional features were observed in thin sections. In addition, measured TOC values of cored samples from wells of the West Netherlands Basin show significant spread, at least in certain intervals (see Appendix 5G and 6B). Following up on the expected microscopic heterogeneity, it was decided during the first reconnaissance field trip in March 2013, to sample big blocks of rock with the intention to study these with an extremely high resolution of 1 to 5 samples per centimeter. It was quickly decided to abandon this idea, because the available budget was not sufficient for such an elaborate study. From those thin sections studies, however the vertical heterogeneity on a microscopic scale proved less dramatic than expected.

vertical heterogeneity on a microscopic scale is small

The average sample resolution of 1 sample per 17 cm turned out to be aptly sufficient in order to capture vertical heterogeneity. The thin section analyses indicated heterogeneity on both a centimeter and a meter scale. Nevertheless, the overall outcome was that the variation can be captured in “stratigraphic domains” with shared sedimentary features, which are laterally consistent. The palynological analyses (Chapter 5) and the geochemical analyses (Chapter 6) display a low standard deviation. Overall, 1) clear trends are visible for each discipline, and 2) significant changes in these trends occur on a meter scale.

in all disciplines significant vertical changes occur on a meter scale

The significant changes in trends allow for a rough subdivision of the studied 11 meters of section into 5 units for the sedimentology, 8 units for the palynology and 11 units for the geochemistry. The only “spiky” patterns observed are the rapid changes in organic matter composition in Biofacies Zones D and E (section 5.4). In this organic rich interval with extremely high TOC values, one sample may contain very high percentage of Structureless Organic Matter Type 1, while the next sample may contain a very high percentage of Structureless Organic Matter type 2. This recorded variation corroborates with the observed distribution of the large organo-mineralic aggregates in the thin section analyses. These fairly large, up to 0.3 mm, predominantly organic particles are often distributed along horizons. Apparently, the large and massive particles originated during short-lived time intervals, perhaps during periods of extreme primary production in the upper water column. The frequency in which these phases of high productivity occur, may be seasonal, annual, decadal, centennial, or more (this cannot be determined from the dataset at hand).

a large spread in TOC values (rapid vertical changes) only occurs in the intervals with TOC > 5%

The “pulsating” frequency in the origin and deposition of the large organic

particles, might well explain the relatively large spread in TOC values in certain intervals. Clearly, the intervals with a large spread in TOC values are the intervals with high TOC values, generally above 5%. It is suggested here that strong vertical heterogeneity in TOC is related to periods with overall high primary production.

9.2 Sea level

Depositional environment in relation to sea level

The thin section analysis clearly demonstrates a fining upward trend in the Whitby Mudstone Formation, from the Grey Shales Member via the Jet Rock unit (basal part of the Mulgrave Shale Member) to the Bituminous Shales (upper part of the Mulgrave Shale Member). This trend is interpreted as a sea level rise. The (basal part of the) Bituminous Shales is very homogenous, completely dominated by clay and characterized by the absence of silt-size clastic interbeds. As a consequence, the base of the Bituminous Shales is interpreted as the maximum flooding surface. Unfortunately, the remainder of the Mulgrave Shale Member has not been studied in this project, but, based on a literature review, a regressive trend is inferred from the Bituminous Shales (Mulgrave Shale Member) to the Alum Shale Member.

the Whitby Mudstone Formation displays a large-scale transgressive-regressive trend, with the approximate maximum flooding surface at, or near the base of the Bituminous Shales.

The palynological record is more difficult to interpret in terms of sea level. This is due to the overprint of *in-situ* marine algae, such as sphericals, and on the partial absence of dinoflagellate cysts in the “death zone”, due to adverse conditions of the paleoenvironment. Nevertheless, the common occurrences of pollen and spores indicate a relatively near-shore marine environment. In combination with the general occurrences of ammonites and belemnites throughout the entire section (see Whitby Excursion Field Guide), a marine depositional environment, definitely below wave base and probably below storm wave base, is inferred for the Jet Rock. A paleo-waterdepth of 20 to 100 meters is proposed for the Jet Rock.

a paleo-waterdepth of 20 to 100 meters is proposed for the Jet Rock

9.3 Mineralogy

Carbonate

In the Whitby outcrops carbonate is present in three forms: as conspicuous concretions, the so called “doggers”, as an integral part of the sediment, and in one case as a continuous limestone layer. The continuous limestone layer is the Top Jet Dogger and this layer consists of (partly recrystallized) coccolithophores. The origin and genesis of the concretions is complex; it is related to anaerobic oxidation of methane. Methane produced in the methanogenic zone (1.5 to 3 meters below the sediment-water interface) migrates into the sulfate-methane reduction zone (0.2 to 1.5 meters below the sediment-water interface), where it is oxidized anaerobically

into HS^- and HCO_3^- ($\text{CH}_4 + \text{SO}_4^{2-} \rightarrow \text{HCO}_3^- + \text{HS}^- + \text{H}_2\text{O}$). The HCO_3^- reacts with Calcium ions, which are present in the pore fluids, to form CaCO_3 .

the genesis of the doggers (carbonate concretions) is related to anaerobic oxidation of methane in the sulfate-methane reduction zone

The biggest and highest concentration of concretions are found in biofacies zone D and E, the intervals with peak-abundances of Structureless Organic Matter, particularly type 2. This is no coincidence, as this interval with huge amounts of organic matter is expected to have generated methane from bacterial decay, immediately after deposition. Carbonate as integral part of the sediment is consistently low (<5%) in the “Death Zone” where most of the doggers occur.

the biggest and the highest number of doggers occur in the high TOC interval

Above the Whale Stone Doggers, the integral carbonate content starts to increase gradually, to reach a maximum of 70% in the Top Jet Dogger. Above the Top Jet Dogger, in the Bituminous Shales, the carbonate content drops back to around 10%, and remains essentially the same in the first couple of meters of that unit. The elevated carbonate content in the upper part of the Jet Rock is not visually expressed in the outcrops: the lower and the upper part of the Jet Rock all look the same.

the elevated carbonate content in the upper part of the Jet Rock is not visually expressed in the outcrops

Nevertheless, the increased carbonate content of the upper part of the Jet Rock has a large influence on the mechanical properties: both the Brittleness Index and the Fracture density are highest in this interval.

the Brittleness Index and the Fracture density are highest in the carbonate-rich interval – upper part of the Jet Rock –

The underlying reason for the change in carbonate preservation style, from predominant carbonate capture in concretions to predominant carbonate preservation as integral part of the sediment, is not yet entirely understood. It is important to note, however, that the change in carbonate preservation style coincides with an important change in the organic matter composition.

the change in carbonate preservation style - from concretions to integral part of the sediment - coincides with an important change in the organic matter composition, which, in turn, reflects a major drop in the primary productivity

The organic matter composition changes from ~100% dominance of Structureless Organic Matter type 1 and 2, to assemblages with 50% palynomorphs. This change in organic matter composition, basically a major drop in the primary productivity, possibly reflects a sudden decrease in the intensity of water column stratification. This change may have been induced by a sudden decrease in the amount of freshwater runoff. The elevated abundance of silt-size particles in the high TOC zone and the subsequent disappearance of silt, supports a decrease in the amount of runoff. Such a decrease in freshwater runoff (= increase in average

salinity) could also explain the sudden return of calcareous nanoplankton and dinoflagellate cysts in the system (Bucefalo Palliani *et al.*, 2002).

Quartz

In general, the amounts of quartz throughout the studied section are very low, on average 10%.

quartz content is low: 10% on average

Quartz is generally represented in the silt-size fraction. Higher amounts of quartz, particularly silt-sized particles, are present in the Grey Shales and, to a minor extent, in the high TOC-zone, in and around the Whale Stones in the middle of the Jet Rock. Typically, these stratigraphic intervals with elevated quartz display slightly higher Brittleness Index.

slightly elevated quartz content occurs in the Grey Shales and in the high TOC-zone – middle part of the Jet Rock –

Clay

Only minor variations in the clay mineralogy are observed. A decrease in the amount of Kaolinite in the high TOC interval in the middle of the Jet Rock, is interpreted to be caused by dilution.

Organic matter (TOC)

The TOC curve of the Whitby Mudstone Formation displays three discrete steps: a 5.5 m interval with a gradual but steady increase from 4% to 8%, followed by a 1.5 m interval with an extremely high mean value of 14%, followed by very long (25 m) interval with very consistent values between 2 and 5% (see Chapter 6 and Appendix 4 and 6B). Bearing in mind that the percentages are weight percentages and that the specific gravity of organic matter is very low, it is apparent that the 1.5 m interval with high TOC values, volumetrically, contains massive amounts of organic matter.

the interval with high TOC (14%) contains massive amounts of organic matter but it is only 1.5 meters thick

The palynological analysis (Chapter 5) points out that more than 99% of the organic matter is of marine origin and represented by fecal pellets or organic aggregates.

99% of the organic matter is of marine origin and is represented by fecal pellets or organic aggregates

The approach followed for the palynological analyses (section 5.1) allowed 1) to look *inside* the organic aggregates, and 2) to quantify the ratio of the aggregates versus any other occurring organic matter, such as wood particles, pollen and spores and dinoflagellate cysts. High fluorescence imaging indicates that the organic aggregates are mainly composed of structureless organic matter derived from microbial activity.

the organic aggregates are mainly composed of structureless organic matter derived from microbial activity

In addition, the fecal pellets also contain mineral grains and palynomorphs, particularly acritarchs and 'sphericals' (sphericals are probably cysts of prasinophyte algae). An important eye-opener of this study appears to be the role of primary production. It has become evident that TOC is not simply a measure of the intensity and duration of bottom-water anoxia. Instead, TOC appears to be a product of the interplay between primary production and the redox conditions at the sediment-water interface.

TOC is the product of the interplay between primary production and the redox conditions at the sediment-water interface

The ratio between the chemical elements Molybdenum and Uranium (section 6.2.2) can be used as a proxy for redox conditions. The Mo-U ratio increases steadily from the base of the Jet Rock upward. Above the Jet Rock, in the Bituminous Shales, the Mo-U ratio has become high and remains high, indicating strong redox conditions at this level. Most of the underlying Jet Rock, however, the Mo-U ratio indicates mild to weak redox conditions. Nevertheless, the highest TOC values are right in the middle of the Jet Rock, in the interval with the large fecal pellets, interpreted to be induced by extremely high primary production. In the Jet Rock, primary production appears to be a more critical factor for TOC than redox conditions.

in the Jet Rock, primary production is a more critical factor for TOC than the redox conditions

The underlying mechanism driving the primary production and bottom water anoxia is still open for discussion, but it is almost certain that palaeoclimate, in particular precipitation, plays a key role.

paleoclimate plays a key role in the underlying mechanism that drives the primary production and the bottom water anoxia

In literature, many geochemical trends are explained by increased rain fall and more intense weathering (refs). The increased amount of freshwater input in the relatively shallow sea is probably triggering the changes that lead to the extreme primary productivity and to stratification of the water column. The extreme primary production is intriguing: the surface layers of the Jet Rock marine system must have displayed productivity comparable to strong upwelling, which lasted uninterrupted for thousands of years. Judged by the huge amounts of the so-called 'sphericals', both within and outside the fecal pellets, it is suggested that the 'sphericals' (probable cysts of prasinophyte algae) were at the base of the food chain. In any case, nutrients and spore elements such as phosphate or iron, must have been omnipresent.

The pollen and spore assemblages in this study (Chapter 5 and Appendix 2) display a trend in which arid-indicating pollen types become increasingly dominant upward in the Bituminous Shales. Probably, although not studied in this project, the base of the Toarcian Grey Shale is also dominated by these arid-indicating pollen. As a consequence, a general dry-wet-dry cycle is interpreted.

the pollen and spore results indicate a dry – wet – dry paleoclimatic cycle from the Grey Shales via the Jet Rock to the Bituminous Shales

Unfortunately, the precise details with respect to environmental parameters such as the intensity in the amount of runoff, the intensity of seasonality or monsoon activity, is currently unknown. It remains enigmatic 1) why the redox conditions for the Jet Rock are relatively weak compared to the Bituminous Shales, 2) why the extreme primary production comes to an abrupt end approximately 1 meter above the Whale Stones.

9.4 Pseudologs

GR

The Total GR and Spectral GR are calculated from the geochemical results, which are called pseudologs. The aim of the pseudolog study is to be able to translate a signal back to the underlying mineralogy in case only wire-line logs are available. The Total GR displays a peak in the high TOC interval in the middle part of the Jet Rock. The peak in total GR is derived from the very high Uranium content. The GR intensity decreases slightly in the interval with increased carbonate content with the lowest GR occurring at the Top Jet Dogger.

the GR pseudolog peaks at the high TOC interval and displays a low at the Top Jet Dogger

The Total GR increases in the overlying Bituminous Shales, which is mainly due to the increased Thorium and Potassium. The GR pseudolog is compared with a field measurement of the GR from a hand-held tool. The two curves match very well for the Runswick section.

the GR pseudolog matches very well with the measured hand-held GR

It is important to note that only shale are analyzed, in other words, the pseudolog is based on shale samples only, not on the concretions. It is conceivable that the GR will display a distinct low when hitting a carbonate concretion.

the pseudolog is based on shale samples only: it is conceivable that a wire-line measured GR will display a distinct low when going through a carbonate concretion

Density

The density pseudolog displays a general increase from the middle part of the Jet Rock to the top of the Jet Rock. It appears the density is mainly steered by carbonate and quartz (increase), but is easily affected by organic matter (decrease).

10 Compilation and review of data from the Posidonia Shale Formation (PSF) in the Netherlands

10.1 Review of existing data

Sedimentology group University of Utrecht

Members of the sedimentology department of the University of Utrecht conducted several studies on the PSF (e.g. Trabucho-Alexandre *et al.*, 2012). The latter study report that the PSF is characterized by graded thin beds (<10 mm) with erosional bases and common cross-lamination within these beds. The most important conclusion drawn from these observations is that the PSF was deposited by bottom currents and that dynamic energetic conditions prevailed at the time of deposition. This finding contrasts with the traditional interpretation that deposition of the PSF took place via settling from suspension under a stagnant anoxic water column.

the PSF has been deposited by bottom currents; dynamic energetic conditions prevailed at the time of deposition

TNO reports

An internship project by Willemijn Ogg (Ogg, 2011?) carried out at TNO, focused on thin section description, macroscopically visible features and macrofossil content of core pieces of the PSF from several wells, including the long cored interval of well LOZ-01. The main conclusion corroborates with the findings of the sedimentology group, viz. a quite dynamic sedimentation process. Other interesting feature are: 1) fossils occur abundantly throughout the PSF in well LOZ-01: ammonites (e.g. *Harpoceras falciferum*), bivalves (*Bositra*), fish remains, cephalopod arm-hooks and so on. The bivalves often occur as 'sudden death' communities completely consisting of juveniles. The fish remains are often curved, in *rigor mortis*, indicating that the bottom water conditions were not suited (= no oxygen) for predators and bottom dwellers. Also calcite-filled veins are numerous throughout the PSF in well LOZ-01.

fossils occur abundantly throughout the PSF

bivalves often occur as 'sudden death' communities completely consisting of juveniles

the occurrence of curved and complete fish fossils indicate the absence of predators, and hence - at least occasional - anaerobic bottom water conditions

Mart Zijp carried out an internship at TNO on the Shale Gas potential of the PSF in the onshore West Netherlands Basin (WNB). Important conclusions and findings from this study are: 1) a log-based zonation for the PSF consisting of 4 zones, 2) above 4% TOC, a strong correlation exists between density and TOC, 3) based on mud logs, the presence of gas in the PSF over most of the WNB could be demonstrated, 4) in most of the WNB, an interval of 25 meters exists with high TOC (> 5%).

above 4% TOC, a strong correlation exists between density and TOC

mud logs always show the presence of gas in the PSF in the onshore WNB

in the onshore WNB, an interval of 25 meters exists with high TOC (> 5%)

TNO carried out a TNO-funded palynological and stable isotope study on three cored PSF intervals (TNO report TNO-060-UT-2011-01497). Two offshore wells, L05-04 and F11-01, and one onshore well, Loon Op Zand-01 (LOZ-01), were analyzed for organic matter composition and pollen and spores. The first big eye-opener was the observation that carbon-13 isotope analyses are perfectly suited to correlate the PSF wells thanks to the Carbon Isotope Event occurring in the Early Toarcian. Important conclusions from this study are: 1) in the relatively proximal location (LOZ-01) anoxia last much longer than in the relatively distal locations (F11-01 and L05-04), 2) lowering of the sea surface salinity due to fresh water influx is the main driver for stratification of the water column, 3) the highest TOC values are recorded in the Early Toarcian Carbon Isotope Event, 4) a climate change from arid to more humid conditions and back to arid again is recorded in the Posidonia Shale, 5) two types of algae dominate the Posidonia in a competitive way: Tasmanites (high HI) and sphericals (low HI). Sphericals are probably better adapted to prolonged low salinity conditions, 6) the algal blooms are not necessarily basinwide: peak occurrences of Tasmanites (acmes) cannot be interpreted as time-lines.

carbon-13 isotope analyses are perfectly suited to correlate the PSF

anoxia in the PSF last much longer in a proximal setting than in a distal setting

lowering of the sea surface salinity due to fresh water influx is the main driver for stratification of the water column

highest TOC values are recorded in the Early Toarcian Carbon Isotope Event

a climate change from arid to more humid conditions and back to arid again is recorded in the PSF

two types of algae dominate the Posidonia in a competitive way: Tasmanites and sphericals; sphericals are probably better adapted to prolonged low salinity conditions

Tasmanites acmes do not necessarily occur synchronous throughout the basin: be careful not to interpret these as time-lines.

TNO also carried out a B2B for an international operator on the PSF in the WNB. The aim was to compare the PSF with the Antrim Shale and to establish a basic workflow for shale gas research. The report itself is proprietary, but some of the results were published with the consent of the client (Verreussel *et al.*, 2012). Some important findings and conclusions are: 1) most of the PSF is oil mature but some areas exhibit higher maturity (Fig. 10-1), 2) seismic attributes should be used to identify stable fault blocks, 3) the existing log zonation is revised and a higher resolution could be established, resulting in 8 zones which allow a high resolution correlation between wells in the WNB, 4) seven biofacies zones are established in LOZ-01, 5) a correlation of the PSF in well LOZ-01 to the type section of the Posidonia Schiefer in Dotternhausen could be established. Because Dotternhausen is calibrated to the global standard (the International Time Scale), the chronostratigraphy of well LOZ-01 is now firmly established

in the WNB, the PSF is oil mature, but some areas exhibit higher maturity

seismic attributes are useful in the identification of stable fault blocks

an improved log zonation consisting of 8 zones allows a high resolution well-to-well correlation of the PSF throughout the WNB

7 biofacies zones are distinguished, reflecting environmental changes in the depositional system of the PSF

the chronostratigraphy of well LOZ-01 is now firmly established

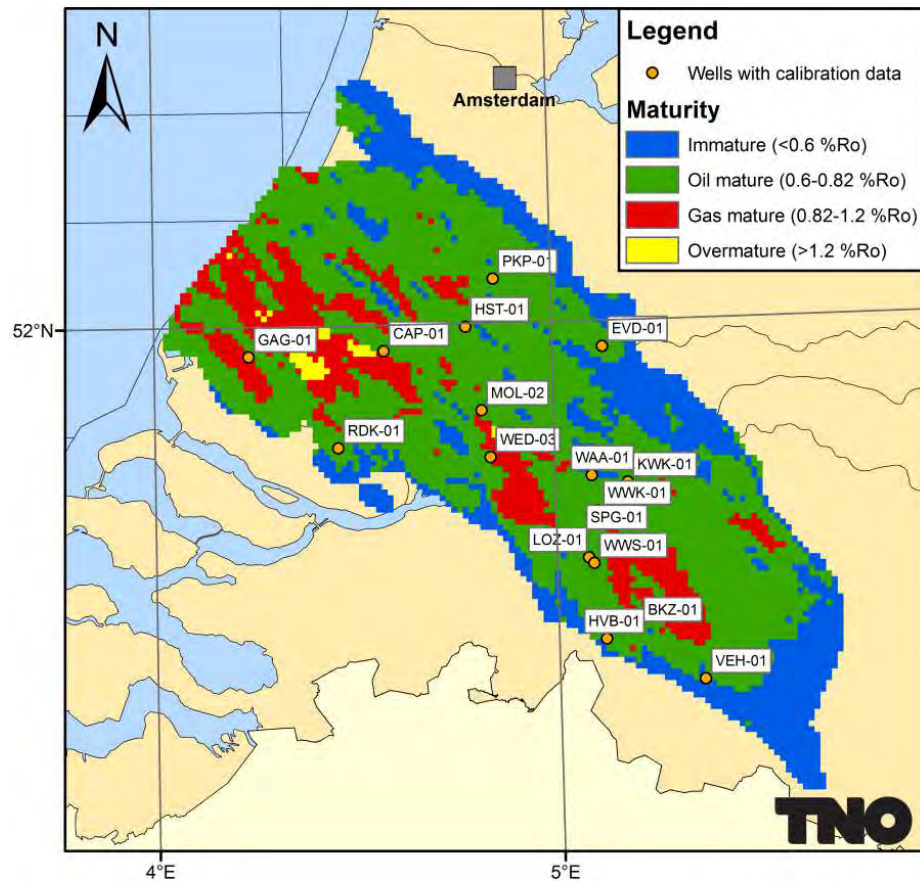


Fig. 10-1

10.2 New data: stable isotope analyses of well WED-01

The chronostratigraphy of the PSF from well LOZ-01 is firmly established, but unfortunately up-to-date wire-line logs such as GR, DT or NPHI are missing from this old (1959) well. In order to correlate this important well to the surrounding wells with excellent log suites, stable isotope analyses were carried out on a cored PSF interval from well WED-01 (Chapter 8). As a result, the stable isotope stratigraphy of the Early Toarcian, in particular the base, the maximum and the top of the Carbon Isotope Event, is now integrated with the log zonation of the PSF in the WNB.

stable isotope stratigraphy of the Early Toarcian is now integrated with the log zonation of the PSF in the WNB

The integrated and calibrated zonation of the PSF in the WNB allowed for a detailed correlation to the Whitby Mudstone Formation in Yorkshire (Chapter 8). The detailed correlation enables to apply the results of the Whitby outcrop study on the situation of the PSF in the WNB (Chapter 11).

a detailed correlation of the Whitby Mudstone Formation with the PSF in the WNB has been established

11 Discussion and conclusions

In this chapter, the findings from the Whitby outcrop study are applied to the Posidonia Shale Formation (PSF) in the West Netherlands Basin (WNB) and the outcome is discussed. The first, and most important conclusion for the analogy, is that the Toarcian black shale occurrences along the Yorkshire coast, known by the informal name 'Jet Rock', are very similar to the PSF in the Dutch subsurface with respect to age, overall thickness, depositional environment, mineralogy, and to a certain extent also the Total Organic Carbon distribution. On a trend parallel to the palaeo-shoreline, the PSF is laterally homogeneous over large distances (>50 km). Based on a number of reasons, it is expected that the PSF will be less homogeneous over large distances on a trend perpendicular the paleo-shoreline. The outcrop situation in Yorkshire does not allow to investigate the homogeneity on a perpendicular trend, and in the WNB this is not yet thoroughly studied. Another very important finding is that, in general, the vertical heterogeneity on a microscopic scale is small. An exception to this rule is the distribution of TOC, which varies dramatically on a cm scale in the interval with high TOC, albeit that the average values are consistently high. For all other variables, it is possible to distinguish stratigraphic domains with uniform character, despite the fact that the sediments of the PSF are dominated by bed-load transport processes resulting in laminae and beds on mm and cm scales. The observed lithological variation is expressed on a scale exceeding 1 meter, and allows to define a stratigraphic subdivision for both the Jet Rock and PSF of 6 to 10 units. In addition, it is evident that the observed variation in geochemistry, sedimentology and organic matter composition are related: the zonal boundaries of the individual disciplines line up. In the WNB, a detailed zonation based on the wire-line logs has been established, but detailed geochemical analyses are missing. Fortunately, it is possible to correlate the Jet Rock and PSF with high precision. Stable carbon isotope trends derived from this study and from the literature, enable correlation of the Jet Rock and PSF along at least five time lines: the base of the stable carbon isotope excursion (base CIE), base maximum CIE, top maximum CIE, top CIE and base X-event. It is attempted to compare the geochemistry and mineralogy of the Jet Rock with the PSF via pseudologs. Via geochemical analyses of the outcrop study, pseudo GR and RHOB trends for the Jet Rock are established. These are compared with wire-line GR and RHOB from the WNB. It appears that both show a similar subdivision: a peak in GR associated with a low in RHOB occurs in the maximum CIE zone and is related to the very high TOC content at that level, a low GR zone occurs in the upper part of the CIE and terminates at the top CIE. This low GR zone is related to the relatively high carbonate content of that part of the succession. Interestingly, the elevated carbonate content is not expressed visually in both the Yorkshire outcrops as in cored sections of the PSF. Carbonate occurs as integral part of the sediment, as concretions and in one case as a continuous limestone layer. The upper Jet Rock with the elevated carbonate content is also reflected in a high Brittleness Index and in a high fracture density. This observation is quite interesting, especially because the gas logs in the WNB often show a peak at or near this interval. The carbonate-rich, low GR zone is succeeded by a high GR zone. This high GR zone is characterized by low carbonate and high clay content. In the WNB, peaks in the wire-line logs occur in specific horizons, but these are not always present. These peaks are characterized by very low gamma-ray in combination with high density, high resistivity and fast acoustic. These peaks are interpreted to reflect the (near)

presence of carbonate concretions, identical to the stratigraphically defined dogger occurrences in the Yorkshire outcrops: another indication that the Jet Rock and PSF are much alike. Yet, there is one striking and important difference: the TOC trend. In the Jet Rock, the TOC quickly rises from 4 to 14%, after which the TOC falls back to 4% again. The interval with high TOC (14%) is only 1.5 meters thick. In the PSF, both in the WNB as in the offshore L05 and F11 blocks, the TOC also rises quickly to values around 15%, but the TOC remains quite high (between 5 and 8%) for quite a stretch. In the WNB, at least 25 meters of section contains high TOC (>5%), against 3 meters in the Whitby outcrops. In order to understand the reason for these diverging TOC trends, additional inconspicuous differences between these two localities are scrutinized. First of all there is a difference in overall thickness. The WNB succession is almost twice as thick as the Yorkshire succession (1.8 times to be precisely). From own observations and - rather poor - literature records, it is suggested that PSF in the WNB contains more quartz and has a higher fossiliferous content, notable in the amount of fish remains. Based on the outcome of thin section studies, it is concluded that the paleo water depth between the two locations did not differ much; estimates range from 20 to 100 meters. Therefore, it is assumed that the amount of clastic input in the WNB was much higher than in the Cleveland Basin. In other words, the catchment area of the river(s) that provided the clastic input, must have differed in terms of e.g. the areal extent, the topography, the composition of the exposed rocks and soils, and so on. In any case, both the sediment flux and the organic matter flux are much higher in the WNB than in the Cleveland Basin. It is a well-established fact, both from the literature and from the results of this study, that the anoxia of the Toarcian are triggered by a change in climate, in particular by an increase in the amount of precipitation. Most papers connect the occurrence of freshwater surface layers with the development of stratified water columns and impoverished circulation, eventually leading to bottom water anoxia and enhanced TOC content. In this study, careful comparison of the geochemical and palynological results indicates that for the Toarcian black shale, primary production is a more critical factor for TOC than the redox conditions. Almost all organic matter is of marine origin and is represented by fecal pellets or organic aggregates, which are mainly composed of structureless organic matter derived from microbial activity. In summary, the Jet Rock and PSF were deposited in sub-basins, belonging to the same shallow marine, epeiric sea, which was influenced by 1) regional and global environmental change, and 2) by local factors. The regional and global changes are primarily related to climate and are reflected in the synchronous onset of the TOC increase, in the synchronous changes in carbonate preservation style, in the assumed (but not yet confirmed) synchronous stratigraphic position of the concretion horizons, in the assumed (but not yet confirmed) synchronous changes in the geochemical composition, and in the synchronous development of other sedimentary features such as trends in quartz and clay content and bed forms. The local factors are primarily related to paleogeography and influenced the amount and extent of primary production at the site of deposition. It is concluded here that paleogeography is the underlying driving mechanism for the TOC. In that respect, the paleogeographic setting of the WNB is more prolific for shale gas or shale oil than the paleogeographic setting of the Cleveland Basin.

12 Implications and recommendations

In order to be able to predict trends in TOC in the Toarcian black shale system, a thorough understanding of the paleogeography is key. The TOC content is highly dependent on the amount and duration of the primary production at the site of deposition. Fortunately, the Toarcian black shale is homogenous across large distances. Therefore, basic knowledge derived for instance from just a few wells, will probably be sufficient to predict the properties across a large area. In the West Netherlands Basin (WNB), the Posidonia Shale Formation (PSF) exhibits a 25 meters thick interval of relatively high (>5%) TOC (log zones PP to TP, see Appendix 5 and 7). An approximately 7 meters thick part of this 25 meter interval, is assumed to be enriched in carbonate (log zone MZU). This interval is the most brittle interval of the PSF and lies directly on top of the interval with the peak in TOC. As a consequence, this interval is the most prolific for shale gas and is regarded as the prime pay zone. Yet, maturities are quite low in the West Netherlands Basin, so whether or not enough gas is present for shale gas development, remains an open question. In any case, it is recommended to investigate the paleogeography of the Posidonia system further. Property trends across the entire basin need to be established carefully, and this needs to be complemented by additional geochemical and palynological analyses on core samples from the PSF.

13 References

- Algeo, T.J. Tribouillard, N., 2009. Environmental analysis of paleoceanographic systems based on molybdenum–uranium covariation. *Chemical Geology*, 268 (2009), pp. 211–225
- Al-Suwaidi, A.H., Angelozzi, G.N., Baudin, F., Damborenea, S.E., Hesselbo, S.P., Jenkyns, H.C., Manceñido, M.O., Riccardi, A.C., 2010. First record of the Early Toarcian Oceanic Anoxic Event from the Southern Hemisphere, Neuquén Basin, Argentina. *Journal of the Geological Society of London*, 167, 633-636.
- Bai, T., Maerten, L., Gross, M.R., Aydin, A. 2002. Orthogonal cross joints : do they imply a regional stress rotation? *Journal of Structural Geology* 24 (1), p. 77-88.
- Barrow, G., 1888. *The Geology of North Cleveland*. UK Geological Survey, Memoir.
- Baron, M., Parnell, J., Mark, D., Carr, A., Przyjalowski, M., Feely, M. 2008. Evolution of hydrocarbon migration style in a fractured reservoir deduced from fluid inclusion data, Clair Field, west of Shetland, UK. *Marine and Petroleum Geology* 25 (2), p. 153-172.
- Bertotti, G., Hardebol, N., Taal-van Koppen, J., Luthi, S. 2007. Toward a quantitative definition of mechanical units: new techniques and results from an outcropping deep-water turbidite succession (Tanqua-Karoo Basin, South Africa). *AAPG Bulletin* 91 (8), p. 1085-1098.
- Bhattacharya, J.P., MacEachern, J.A., 2009. Hyperpycnal rivers and prodeltaic shelves in the Cretaceous Seaway of North America. *Journal of Sedimentary Research*, 79, 184-209.
- Boro, H., Bertotti, G., Hardebol, N.J. 2013. Distributed fracturing affecting isolated carbonate platforms, the Latemar platform natural laboratory (Dolomites, North Italy). *Marine and Petroleum geology*, v.40, p.69-84.
- Bour, I., Mattioli, E., Pittet, B., 2007. Nannofacies analysis as a tool to reconstruct paleoenvironmental changes during the early Toarcian anoxic event. *Palaeogeography, Palaeoclimatology, Palaeoecology*, 249, 58-79.
- Caruthers, A.H., Gröcke, D.R., Smith, P.L., 2011. The significance of an Early Jurassic (Toarcian) carbon-isotope excursion in Haida Gwaii (Queen Charlotte Islands), British Columbia, Canada. *Earth and Planetary Science Letters*, 307, 19-26.
- Canfield, D.E., Thamdrup, B., Hansen, J.W., 1993. The anaerobic degradation of organic matter in Danish coastal sediments: iron reduction, manganese reduction, and sulfate reduction. *Geochimica et Cosmochimica Acta*, 57, 3867-3883.
- Cohen, A., Coe, A., Kemp, D., 2007. The Late Palaeocene-Early Eocene and Toarcian (Early Jurassic) carbon isotope excursions: a comparison of their time scales, associated environmental changes, causes and consequences. *Journal of the Geological Society of London*, 164, 1093-1108.
- Curtis, C., 1987. Mineralogical consequences of organic matter degradation in sediments: inorganic/organic diagenesis. In: *Marine Clastic Sedimentology* (Eds. J.K. Leggett and G.G. Zuffa), Graham & Trotman Publishers, 108-123.

Curtis, C.D., 1995. Post-depositional evolution of mudstones 1: early days and parental influences. *Journal of the Geological Society of London*, 152, 577-586.

Curtis, C.D., Coleman, M.L., 1986. Controls on the precipitation of early diagenetic calcite, dolomite and siderite concretions in complex depositional sequences. In: *Roles of Organic Matter in Sediment Diagenesis* (Ed. D.L. Gautier), SEPM Special Publication, 38, 23-33.

Curtis, C.D., Coleman, M.L., Love, L.G., 1986. Pore water evolution during sediment burial from isotopic and mineral chemistry of calcite, dolomite and siderite concretions. *Geochimica et Cosmochimica Acta*, 50, 2321-2334.

Danise, S., Twitchett, R.J., Little, C.T.S, Clémence, M.-E., 2013. The impact of global warming and anoxia on marine benthic community dynamics: an example from the Toarcian (Early Jurassic). *PLOS One*, 8, e56255.

Demaison, G.J., Moore, G.T., 1980. Anoxic environments and oil source bed genesis. *Organic Geochemistry*, 2, 9-31.

Dera, G., Pellenard, P., Neige, P., Deconinck, J.-P., Pucéat, E., Dommergues, J.-L., 2009. Distribution of clay minerals in Early Jurassic Peritethyan seas: palaeoclimatic significance inferred from multiproxy comparisons. *Palaeogeography, Palaeoclimatology, Palaeoecology*, 271, 39-51.

Dockrill, B., Shipton, Z. 2010. Structural controls on leakage from a natural CO₂ geologic storage site: Central Utah, USA. *Journal of Structural Geology* 32 (11), p. 1768-1782.

Duarte, L.V., 1998. Clay minerals and geochemical evaluation in the Toarcian-lower Aalenian of the Lusitanian Basin (Portugal). *Cuadernos de Geología Iberica*, 24, 69-98.

Fisher, N.L. 1993. *Statistical analysis of circular data*, vol. xviii. Cambridge University Press. New York 277p.

Egenhoff, S.O., Fishman, N.S., 2013. Traces in the dark – Sedimentary processes and facies gradients in the Upper Shale Member of the Upper Devonian-Lower Mississippian Bakken Formation, Williston Basin, North Dakota, U.S.A. *Journal of Sedimentary Research*, 83, 803-824.

Emmanuel, L., Renard, M., Cubaynes, R., De Rafelis, M., Hermoso, M., Lecallonnec, L., Le Solleuz, A., Rey, J., 2006. The 'Schistes Carton' of Quercy (Tarn, France): a lithological of a methane hydrate dissociation event in the early Toarcian. Implications for correlations between Boreal and Tethyan realms. *Bulletin de la Société Géologique de France*, 177, 239-249.

Frimmel, A., Oschmann, W., Schwark, L., 2004. Chemostratigraphy of the Posidonia Black Shale, SW-Germany: I. Influence of sea-level variation on organic facies evolution. *Chemical Geology*, 206, 199-230.

Ghadeer, S.G., Macquaker, J.H.S., 2011. Sediment transport processes in an ancient mud-dominated succession: a comparison of processes operating in marine offshore settings and anoxic basinal environments. *Journal of the Geological Society of London*, 168, 835-846.

Gudmundsson, A., Berg, S., Lyslo, K., Skurtveit, E. 2001. Fracture networks and fluid transport in active fault zones. *Journal of Structural Geology* 23 (2), p. 343-353

- Gómez, J.J., Goy, A., 2011. Warming-driven mass extinction in the early Toarcian (Early Jurassic) of northern and central Spain. Correlation with other time-equivalent European sections. *Palaeogeography, Palaeoclimatology, Palaeoecology*, 306, 176-195.
- Hardebol, N.J., Bertotti, G. 2013. DigiFract: A software and data model implementation for flexible acquisition and processing of fracture data from outcrops. *Computers and Geosciences*, v. 54, p.326-336.
- Hallam, A., 2001. A review of the broad pattern of Jurassic sea-level changes and their possible causes in the light of current knowledge. *Palaeogeography, Palaeoclimatology, Palaeoecology*, 167, 23-37.
- Haq, B.U., Hardenbol, J., Vail, P.R., 1987. Chronology of fluctuating sea levels since the Triassic. *Science*, 235, 1156-1167.
- G.R. Helz, C.V. Miller, J.M. Charnock, J.F.W. Mosselmans, R.A.D. Patrick, C.D. Gardner, D.J. Vaughan, 1996. Mechanism of molybdenum removal from the sea and its concentration in black shales: EXAFS evidence. *Geochimica et Cosmochimica Acta*, 60 (1996), pp. 3631–3642
- Hendry, J.P., Pearson, M.J., Trewin, N.H., Fallick, A.E., 2006. Jurassic septarian concretions from NW Scotland record interdependent bacterial, physical and chemical processes of marine mudrock diagenesis. *Sedimentology*, 53, 537-565.
- Hesselbo, S.P., Jenkyns, H.C., 1998. British Lower Jurassic sequence stratigraphy. In: *Mesozoic and Cenozoic Sequence Stratigraphy of European Basins* (Eds. P.-C. de Graciansky, J. Hardenbol, T. Jacquin and P.R. Vail), SEPM Special Publication 60, 561-581.
- Hesselbo, S.P., Jenkyns, H.C., Duarte, L.V., Oliveria, L.C.V., 2007. Carbon-isotope record of the Early Jurassic (Toarcian) Oceanic Anoxic Event from fossil wood and marine carbonate (Lusitanian Basin, Portugal). *Earth and Planetary Science Letters*, 253, 455-470.
- Hesselbo, S.P., Gröcke, D.R., Jenkyns, H.C., Bjerrum, C.J., Farrimond, P., MorgansBell, H.S., Green, O.R., 2000. Massive dissociation of gas hydrate during a Jurassic oceanic anoxic event. *Nature*, 406, 392-395.
- Hori, R.S., 1997. The Toarcian radiolarian event in bedded chert from southwestern Japan. *Marine Micropaleontology*, 30, 159-169.
- Howard, A.D., 1985. Lithostratigraphy of the Staites Sandstone and Cleveland Ironstone Formations (Lower Jurassic) of northeast Yorkshire. *Proceedings of the Yorkshire Geological Society*, 45, 261-275.
- Howarth, M.K., 1973. The stratigraphy and ammonite fauna of the Upper Liassic Grey Shales of the Yorkshire coast. *Bulletin of the British Museum of Natural History*, 24, 238-277.
- Ichaso, A.A., Dalrymple, R.W., 2009. Tide- and wave-generated fluid mud deposits in the Tilje Formation (Jurassic), offshore Norway. *Geology*, 37, 539-542.
- Jarvie, D.M., Hill, R.J., Ruble, T.E., Pollastro, R.M. 2007. Unconventional shale-gas systems: The Mississippian Barnett Shale of north-central Texas as one model for thermogenic shale-gas assessment. *AAPG Bulletin*, V. 91, No. 4, PP. 475 - 499

Jenkyns, H.C., 1988. The Early Toarcian (Jurassic) anoxic event: stratigraphic, sedimentary, and geochemical evidence. *American Journal of Science*, 288, 101-151.

Jenkyns, H.C., 2010. Geochemistry of oceanic anoxic events. *Geochemistry, Geophysics, Geosystems*, 11, Q03004, doi:10.1029/2009GC002788.

Jenkyns, H.C., Clayton, C.J., 1997. Lower Jurassic epicontinental carbonates and mudstones from England and Wales: chemostratigraphic signals and the early Toarcian anoxic event. *Sedimentology*, 44, 687-706.

Jenkyns, H.C., Jones, C.E., Gröcke, D.R., Hesselbo, S.P., Parkinson, D.N., 2002. Chemostratigraphy of the Jurassic System: applications, limitations and implications for palaeoceanography. *Journal of the Geological Society of London*, 159, 351-378.

Kanitpanyacharoen, W., Kets, F.B., Wenk, H.-R., Wirth, R., 2012. Mineral preferred orientation and microstructure in the Posidonia shale in relation to different degrees of thermal maturity, *Clays and Clay minerals*, 60, 315-329.

Kiraly, L. 1969. Statistical analysis of fractures (Orientation and density). *Geologische Rundschau*, 125-151

Klaver, J., Desbois, G., Urai, J.L., Littke, R., 2012. BIB-SEM study of the pore space morphology in early mature Posidonia Shale from the Hils area, Germany. *International Journal of Coal Geology*, 103, 12-25.

Knox, R.W.O'B., Howard, A.S., Powell, J.H., Van Buchem, F.S.P., 1991. Lower and Middle Jurassic sediments of the Cleveland Basin, N.E. England: shallow marine and paralic facies seen in their sequence stratigraphic context. *British Sedimentological Research Group, Cambridge*, 66 pp.

Lamb, M.P., Parsons, J.D., 2005. High-density suspensions formed under waves. *Journal of Sedimentary Research*, 75, 386-397.

Lash, G., Blood, D., 2011. Sequence stratigraphy as expressed by shale source rock and reservoir characteristics – Examples from the Devonian succession, Appalachian Basin. AAPG Annual Convention, Houston, April 2011, Search and Discovery Article #80168, http://www.searchanddiscovery.com/documents/2011/40708lash/ndx_lash.pdf.

Laenen, B., De Craen, M., 2004. Eogenetic siderite as an indicator for fluctuations in sedimentation rate in the Oligocene Boom Clay Formation (Belgium). *Sedimentary Geology*, 163, 165-174.

Littke, R., 1993. Depositional history of the Posidonia Shale. In: *Deposition, Diagenesis and Weathering of Organic Matter-rich Sediments*, Lecture Notes in Earth Sciences, 47, 46-80. Springer-Verlag, Berlin.

Littke, R., Rullkötter, J., 1987. Mikroskopische und Makroskopische Unterschiede zwischen Profilen unreifen und reifen Posidonienschiefers aus der Hilsmulde. *Facies*, 17, 171-179.

Littke, R., Baker, D.R., Leythaeuser, D., 1988. Microscopic and sedimentologic evidence for the generation and migration of hydrocarbons in Toarcian source rocks of different maturities. *Organic Geochemistry*, 13, 549-559.

Littke, R., Leythaeuser, D., Rullkötter, J., Baker, D.R., 1991. Keys to the depositional history of the Posidonia Shale (Toarcian) in the Hils Syncline, northern Germany. In: *Modern and Ancient Continental*

Shelf Anoxia (Eds. R.V. Tyson and T.H. Pearson), Geological Society of London, Special Publication 58, 311-333.

Little, C.T.S., Benton, M.J., 1995. Early Jurassic mass extinction: a global long-term event. *Geology*, 23, 495-498.

Macquaker, J.H.S., 1994. A lithofacies study of the Peterborough Member, Oxford Clay Formation (Jurassic), UK: an example of sediment bypass in a mudstone succession. *Journal of the Geological Society of London*, 151, 161-172.

Macquaker, J.H.S., Gawthorpe, R.L., 1993. Mudstone lithofacies in the Kimmeridge Clay Formation, Wessex Basin, southern England: implications for the origin and controls of the distribution of mudstones. *Journal of Sedimentary Petrology*, 63, 1129-1143.

Macquaker, J.H.S., Taylor, K.G., 1996. A sequence-stratigraphic interpretation of a mudstone-dominated succession: the Lower Jurassic Cleveland Ironstone Formation, UK. *Journal of the Geological Society of London*, 153, 759-770.

Macquaker, J.H.S., Jones, C.R., 2002. A sequence-stratigraphic study of mudstone heterogeneity: a combined petrographic/wireline long investigation of Upper Jurassic mudstones from the North Sea (UK). In: *Geological Applications of Well Logs* (Eds. M. Lovell and N. Parkinson), AAPG Methods in Exploration Series, 13, 123-141.

Macquaker, J.H.S., Adams, A.E., 2003. Maximizing information from fine-grained sedimentary rocks: an inclusive nomenclature for mudstones. *Journal of Sedimentary Research*, 73, 735-744.

Macquaker, J.H.S., Taylor, K.G., Gawthorpe, R.L., 2007. High-resolution facies analyses of mudstones: implication for paleoenvironmental and sequence stratigraphic interpretations of offshore ancient mud-dominated successions. *Journal of Sedimentary Research*, 77, 324-339.

Mattioli, E., Pittet, B., Suan, G., Mailliot, S., 2008. Calcareous nannoplankton changes across the early Toarcian oceanic anoxic event in the western Tethys. *Paleoceanography*, 23, PA3208, doi:10.1029/2007PA001435.

Mattioli, E., Pittet, B., Bucefalo Palliani, R., Röhl, H.-J., Schmid-Röhl, A., Morettini, E., 2004. Phytoplankton evidence for the timing and correlation of palaeoceanographical changes during the early Toarcian oceanic anoxic event (Early Jurassic). *Journal of the Geological Society of London*, 161, 685-693.

McArthur, J.M., Algeo, T.J., Van de Schootbrugge, B., Li, Q., Howarth, R.J., 2008. Basinal restriction, black shales, Re-Os dating, and the early Toarcian (Jurassic) oceanic anoxic event. *Paleoceanography*, 23, PA4217, doi:10.1029/2008PA001607.

Milsom, J., Rawson, P.F., 1989. The Peak Trough – A major control on the geology of the North Yorkshire coast. *Geological Magazine*, 126, 699-705.

Morgans, H.S., Hesselbo, S.P., Spicer, R.S., 1999. The seasonal climate of the early-Middle Jurassic, Cleveland Basin, England. *Palaios*, 14, 261-272.

Nelson, R.A. 1987. Fractured reservoirs: turning knowledge into practice. *Journal of petroleum technology* 39, p.407-414.

- Newton, R.J., Reeves, E.P., Kafousia, N., Wignall, P.B., Bottrell, S.H., Sha, J.-G., 2010. Low marine sulfate concentrations and the isolation of the European epicontinental sea during the Early Jurassic. *Geology*, 39, 7-10.
- Pálffy, J., Smith, P.L., 2000. Synchrony between Early Jurassic extinction, oceanic anoxic event, and the Karoo-Ferrar flood basalt volcanism. *Geology*, 28, 747-750.
- Philip, Z., Jennings, J., Olson, J., Laubach, S., Holder, J. 2005. Modeling coupled fracture-matrix fluid flow in geomechanically simulated fracture networks. *Society of Petroleum Engineers Reservoir Evaluation and Engineering* 8, p. 300-309.
- Plint, A.G., Macquaker, J.H.S., Varban, B.L., 2012. Bedload transport of mud across a wide, storm-influenced ramp: Cenomanian-Turonian Kaskapau Formation, Western Canada Foreland Basin. *Journal of Sedimentary Research*, 82, 801-822.
- Pomar, L., Morsilli, M., Hallock, P., Bádenas, B., 2012. Internal waves, and underexplored source of turbulence events in the sedimentary record. *Earth-Science Reviews*, 111, 56-81.
- Powell, J.H., 1984. Lithostratigraphical nomenclature of the Lias Group in the Yorkshire Basin. *Proceedings of the Yorkshire Geological Society*, 45, 51-57.
- Powell, J.H., 2010. Jurassic sedimentation in the Cleveland Basin: a review. *Proceedings of the Yorkshire Geological Society*, 58, 21-72.
- Price, G.D., 2010. Carbon-isotope stratigraphy and temperature change during the Early-Middle Jurassic (Toarcian-Aalenian), Raasay, Scotland, UK. *Palaeogeography, Palaeoclimatology, Palaeoecology*, 285, 255-263.
- Pye, K., Krinsley, D.H., 1986. Microfabric, mineralogy, and early diagenetic history of the Whitby Mudstone Formation (Toarcian), Cleveland Basin, UK. *Geological Magazine*, 123, 191-203.
- Odlinger, N.E., Gillespie, P., Bourguin, B., Castaing, C., Chiles, J.P., Christensen, N.P., Fillion, E., 1999. Variations in fracture system geometry and their implications for fluid flow in fractured hydrocarbon reservoirs. *Petroleum geoscience* 5, p.373-384.
- Quesada, S., Dorronsora, C., Robles, S., Chalor, R., Grimalt, J.O., 1997. Geochemical correlation of oil from the Ayoluengo field to Liassic black shale units in the southwestern Basque-Cantabrian Basin (northern Spain). *Organic Geochemistry*, 27, 25-40.
- Raiswell, R., 1976. The microbiological formation of carbonate concretions in the Upper Lias of N.E. England. *Chemical Geology*, 18, 227-244.
- Raiswell, R., Berner, R.A., 1986. Pyrite and organic matter in Phanerozoic normal marine shales. *Geochimica et Cosmochimica Acta*, 50, 1967-1976.
- Raiswell, R., Fisher, Q.J., 2004. Rates of carbonate cementation associated with sulphate reduction in DSDP/ODP sediments: implications for the formation of concretions. *Chemical Geology*, 211, 71-85.
- Rawson, P.F., Wright, J.K., 1995. Jurassic of the Cleveland Basin, North Yorkshire. In: *Field Geology of the British Jurassic* (Ed. P.D. Taylor), Geological Society, London, pp. 173-208.

Rey, L., Bonnet, R., Cubaynes, A., Qajoun, A., Ruget, C., 1994. Sequence stratigraphy and biological signals: statistical studies of benthic foraminifera from Liassic series. *Palaeogeography, Palaeoclimatology, Palaeoecology*, 111, 149-171.

Riegraf, W., 1984. Mikrofauna, biostratigraphie und fazies im unteren Toarcium Südwestdeutschlands und Vergleiche mit benachbarten Gebieten. *Tübinger Mikropaläontologische Mitteilungen*, vol. 3, 232 pp.

Röhl, H.-J., Schmid-Röhl, A., Oschmann, W., Frimmel, A., Schwark, L., 2001. The Posidonia Shale (Lower Toarcian) of SW-Germany: an oxygen-depleted ecosystem controlled by sea level and palaeoclimate. *Palaeogeography, Palaeoclimatology, Palaeoecology*, 165, 27-52.

Röhl, H.-J., Schmid-Röhl, A., 2005. Lower Toarcian (Upper Liassic) black shales of the Central European Epicontinental Basin: a sequence stratigraphic case study from the SW German Posidonia Shale. In: *The Deposition of Organic-Carbon-Rich Sediments: Models, Mechanisms, and Consequences* (Ed. N.B. Harris), SEPM Special Publication, 82, 165-189.

Sageman, B.B., Lyons, T.W., 2004. Geochemistry of fine-grained sediments and sedimentary rocks. In: *Treatise on Geochemistry*, vol. 7, *Sediments, Diagenesis and Sedimentary Rocks* (Ed. F. MacKenzie), Elsevier Publishers, 115-158.

Schieber, J., 1998. Sedimentary features indicating erosion, condensation, and hiatuses in Chattanooga Shale of central Tennessee: relevance for sedimentary and stratigraphic evolution. In: *Shales and Mudstones – Basin Studies, Sedimentology and Paleontology* (Eds. J. Schieber, W. Zimmerle and P. Sethi), Schweizerbart'sche Verlagsbuchhandlung, 187-215.

Schieber, J., 2011. Reverse engineering mother nature – Shale sedimentology from an experimental perspective. *Sedimentary Geology*, 238, 1-22.

Schieber, J., Southard, J., Thaisen, K.G., 2007. Accretion of mudstone beds from migrating floccule ripples. *Science*, 318, 1760-1763.

Schwark, L., Frimmel, A., 2004. Chemostratigraphy of the Posidonia Black Shale, SW-Germany: II. Assessment of extent and persistence of photic-zone anoxia using aryl isoprenoid distributions. *Chemical Geology*, 206, 231-248.

Sælen, G., Tyson, R.V., Telnæs, N., Talbot, M.R., 2000. Contrasting watermass conditions during deposition of the Whitby Mudstone (Lower Jurassic) and Kimmeridge Clay (Upper Jurassic) formations, UK. *Palaeogeography, Palaeoclimatology, Palaeoecology*, 163, 163-196.

Shanmugam, G., 2013. Modern internal waves and internal tides along oceanic pycnoclines: challenges and implications for ancient deep-marine baroclinic sands. *AAPG Bulletin*, 97, 799-843.

Sturzenegger, M., Sartori, M., Jaboyedoff, M., Stead, D. 2007. Regional deterministic characterization of fractures networks and its application to GIS-based rock fall risk assessment. *Engineering Geology* 94, p. 201-214.

Strijker, G., Bertotti, G., Luthi, S.M. 2012. Multi-scale fracture network analysis from an outcrop analogue: A case study from the Cambro-Ordovician clastic succession in Petra, Jordan. *Marine and petroleum geology*, v.38, p.104-116.

Suan, G., Rulleau, L., Mattioli, E., Suchéras-Marx, B., Rousselle, B., Pittet, B., Vincent, P., Martin, J.E., Léna, A., Spangenberg, J.E., Föllmi, K.B., 2013. Palaeoenvironmental significance of Toarcian black shales and event deposits from southern Beaujolais, France. *Geological Magazine*, 150, 728-742.

Surette, M., Allen, D.M., Journeay, M. 2008. Regional evaluation of hydraulic properties in variably fractured rock using a hydrostructural domain approach. *Hydrogeology journal* 16, p. 11-30.

Taylor, K.G., Macquaker, J.H.S, 2000. Spatial and temporal distribution of authigenic minerals in continental shelf sediments: implications for sequence stratigraphic analysis. In: *Marine Authigenesis: From Global to Microbial* (Eds. C.R. Glenn and L. Prévot-Lucas), SEPM Special Publication, 66, 309-323.

Trabucho-Alexandre, J., Dirx, R., Veld, H., Klaver, G., De Boer, P.L., 2012. Toarcian black shales in the Dutch Central Graben: record of energetic variable depositional conditions during an oceanic anoxic event. *Journal of Sedimentary Research*, 82, 104-120.

Traykovski, P., Geyer, W.R., Irish, J.D., Lynch, J.F., 2000. The role of density driven fluid mud flows for cross shelf transport on the Eel River continental shelf. *Continental Shelf Research*, 20, 2113-2140.

Twiss, R.J., Moores, E.M. 1992. *Structural geology*, 532 pp.

Tyson, R.V., Wilson, R.C.L., Downie, C., 1979. A stratified water column environmental model for the type Kimmeridge Clay. *Nature*, 277, 377-380.

Underwood, C., Cooke, M., Simo, J., Muldoon, M. 2003. Stratigraphic controls on vertical fracture patterns in Silurian dolomite, northeastern Wisconsin. *AAPG Bulletin* 87 (1), p. 121-142.

Van Buchem, F.S.P., Knox, R.W.O'B., 1998. Lower and Middle Jurassic depositional sequences of Yorkshire. In: *Mesozoic and Cenozoic Sequence Stratigraphy of European Basins* (Eds. P.-C. de Graciansky, J. Hardenbol, T. Jacquin and P.R. Vail), SEPM Special Publication 60, 545-559.

Van de Schootbrugge, B., McArthur, J.M., Bailey, T.R., Rosenthal, Y., Wright, J.D., Miller, K.G., 2005. Toarcian oceanic anoxic event: an assessment of global causes using belemnite C isotope records. *Paleoceanography*, 20, PA3008, doi: 10.1029/2004PA001102.

Verreussel, R., Horikx, M., Donders, T., and Bunnik F.,
Vertical and horizontal characterization of the Posidonia Shale Formation in the Dutch subsurface: a palynological study. TNO report TNO-060-UT-2011-01497

Verreussel, R., Zijp, M., Nelskamp, S., Wasch, L., De Bruin, G., Ter Heege, J., Ten Veen, J., 2013. Pay-zone identification workflow for shale gas in the Posidonia Shale Formation, the Netherlands. *First Break*, 31, 63-69.

Wignall, P.B., Newton, R., 1998. Pyrite framboid diameter as a measure of oxygen deficiency in ancient mudrocks. *American Journal of Science*, 298, 537-552.

Wignall, P.B., Newton, R.J., Little, C.T.S., 2005. The timing of paleoenvironmental change and cause-and-effect relationships during the early Jurassic mass extinction in Europe. *American Journal of Science*, 305, 1014-1032.

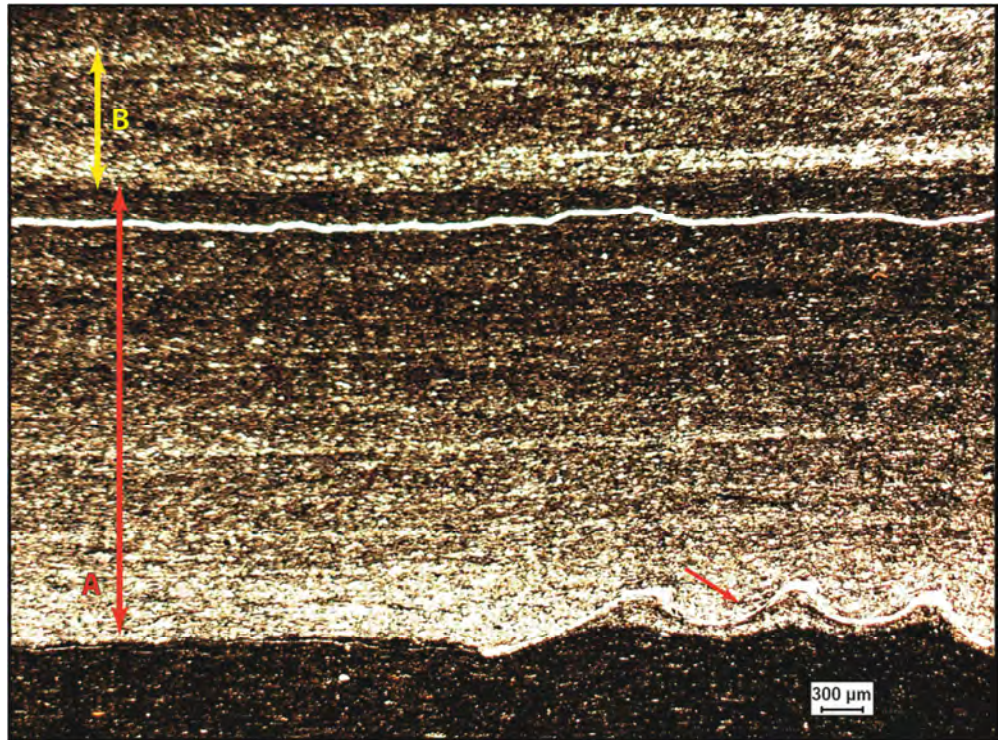
Wignall, P.B., Hallam, A., Newton, R.J., Sha, J.G., Reeves, E., Mattioli, E., Crowley, S., 2006. An eastern Tethyan (Tibetan) record of the Early Jurassic (Toarcian) mass extinction event. *Geobiology*, 4, 179-190.

Wignall et al., 2007, P.B. Wignall, J.P. Zonneveld, R.J. Newton, K. Amor, M.A. Sephton, S. Hartley. The end-Triassic mass extinction record of Williston Lake, British Columbia. *Palaeogeography, Palaeoclimatology, Palaeoecology*, 253 (2007), pp. 385–406

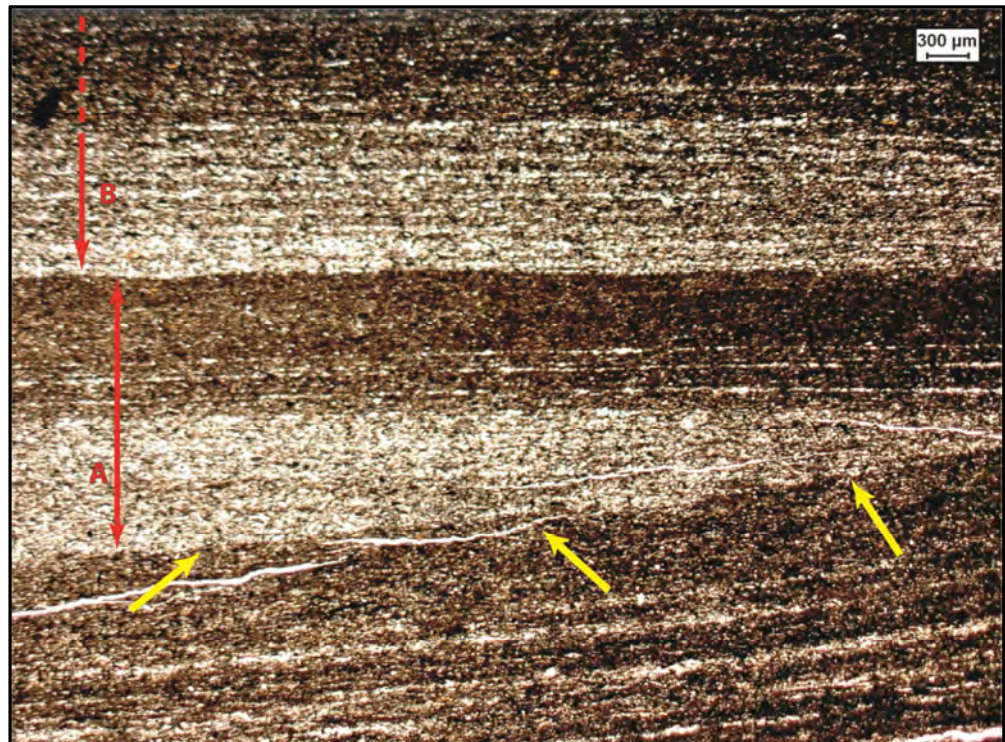
Appendix 1

Thin section analysis

Grey Shales



Sample RWN 33 – This microphotograph shows a typical association of microfacies from the topmost metres of the Grey Shales (note scale at lower right corner, approx. 0.3 mm). Two event-beds and their upper and lower boundaries are highlighted with double-headed lines; both beds feature normal grading (from silt-dominated divisions at bottom, upward to clay- and organic-rich laminae/divisions at top; transitions may be continuous or alternated through stacked coarse-fine lamination), weakly erosive to non-erosive basal surfaces, and internal plane lamination. Event A shows a typical internal ‘structure’ indicative of transport by fluid-mud layers mobilized most likely by storm waves or massive sediment supply on the proximal shelf: a basal, relatively homogeneous silt-dominated division, followed upward by alternating silt- and clay-dominated laminae, topped by a relatively homogeneous division of clay-dominated, organic-rich sediment. Note Bivalve fragment (or juvenile valve?) at lower right (red arrow), lying in a position indicating physical reworking or redeposition after probably limited transport by the initial, turbulent head of the mud layer (as indicated by the thin, laminated silt layer underlying the valve). The lower portion of the photo (~1 mm thick) consists of a homogeneous, structureless clay-dominated deposits or (hemi)pelagic origin, with associated organic matter (reddish platy particles and black, opaque spots in the ground mass) and biogenic calcareous fragments.



Sample RWN 31 – The most evident feature in thin section is a distinct erosional surface of relatively high relief and slope (yellow arrows), overlapped at a high angle by a millimetric, normally graded (silt to clay) event-bed (A). This bed shows a vertical succession of microfacies identical to bed A in the previous photo, suggesting emplacement through progressive aggradation of sediment suspended in a fluid-mud layer. The overlying bed B at top photo is not comprised completely within the image.

The lower third of the photo shows a characteristic alternation of parallel, discontinuous to continuous coarse and fine laminae inclined at a relatively high angle to the horizontal. Recent work has demonstrated that this geometry in fine sediments may be related to traction deposition of fine debris as bedforms (ripples) migrating under the effect of a unidirectional current. Alternatively, the high angle of these laminae might suggest deposition from undulose bedforms under the action of combined, oscillatory-dominant flows, most likely storm disturbances. (The restricted field of this photograph at the margin of a thin section does not consent to establish which hypothesis is the most applicable here.)

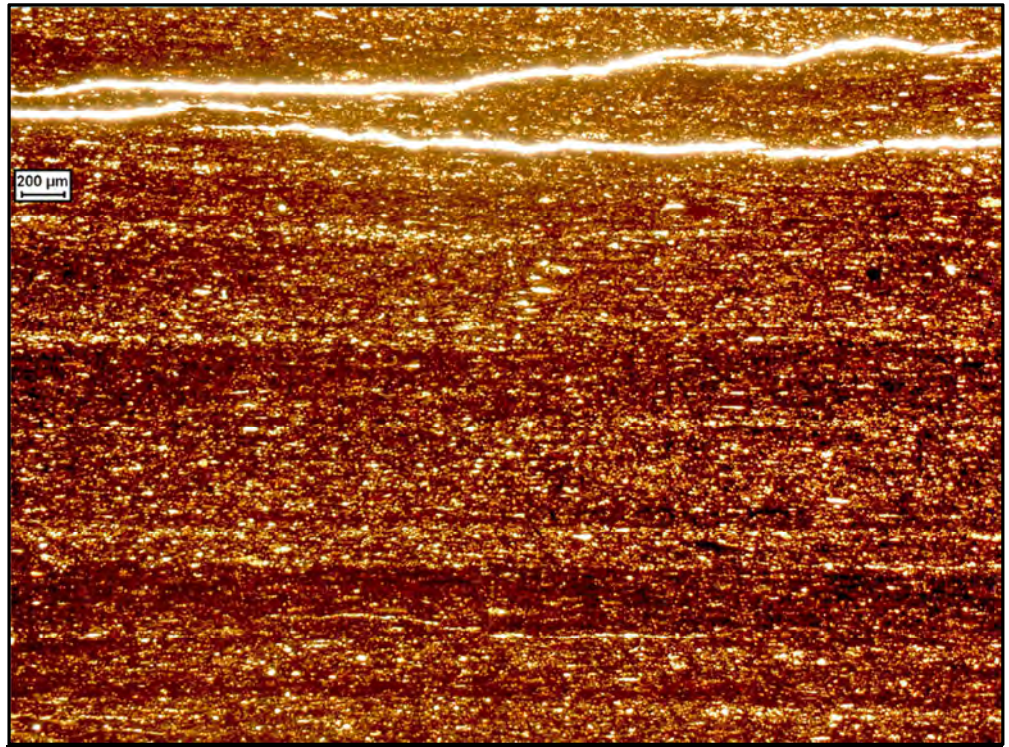
This complex association of structures indicates deposition in a shallow-marine environment dominated by sediment advection from proximal coastal sources in the form of sediment-gravity flows and shelf currents, and affected by occasional reworking and erosion by relatively high-energy events, such as geostrophic currents, storm waves, etc.

The microfacies characteristics of the Grey Shales observed here pose an interesting problem, still open for research: considering that aggradation was substantially continuous up to the overlying Mulgrave Shale Member, what is the real bathymetric range recorded by these depositional units, once universally thought to represent very deep, stagnant sea bottoms??



Sample RWN 31 – This thin section highlights very well the relationship between mechanical properties and small-scale lithologic heterogeneity within mudstones. It shows a major change in microfacies in the lower portion of the thin section, from massive, organic-rich claystone below to organic-bearing, clay-rich siltstone above; the upper half of the section probably represents a series of transport events very close in time or a single, protracted depositional event with fluctuating current velocity (unsteady), as demonstrated by the presence of discontinuous but laterally correlatable coarse-silt lags (poorly resolved at this magnification) and the lack of intervening clay-rich laminae.

The notable feature in this thin section however is represented by two coupled fractures, one of which is particularly wide (as evident by the light saturation along the centre of the image), exactly in correspondence of the change in microfacies. The major problem with extracting thin sections from mudstone samples is related to their fissility and poor resistance to mechanic stress. Numerous thin sections are commonly crossed by wide, open fractures even after sample consolidation with artificial resins. In most cases, fracture orientation is not isotropic after the sample has been worked upon, but presents some kind of systematic relationship with internal heterogeneities; even in cases of massive, homogeneous microfacies, the horizontal anisotropy due to sediment compaction tends to create a preferential plane of fissility under stress. In this case, the occurrence of two horizontally oriented fractures during thin-section preparation in exact correspondence of the microfacies transition is a good visual example of how rock texture and composition may influence macroscopic geomechanic properties.

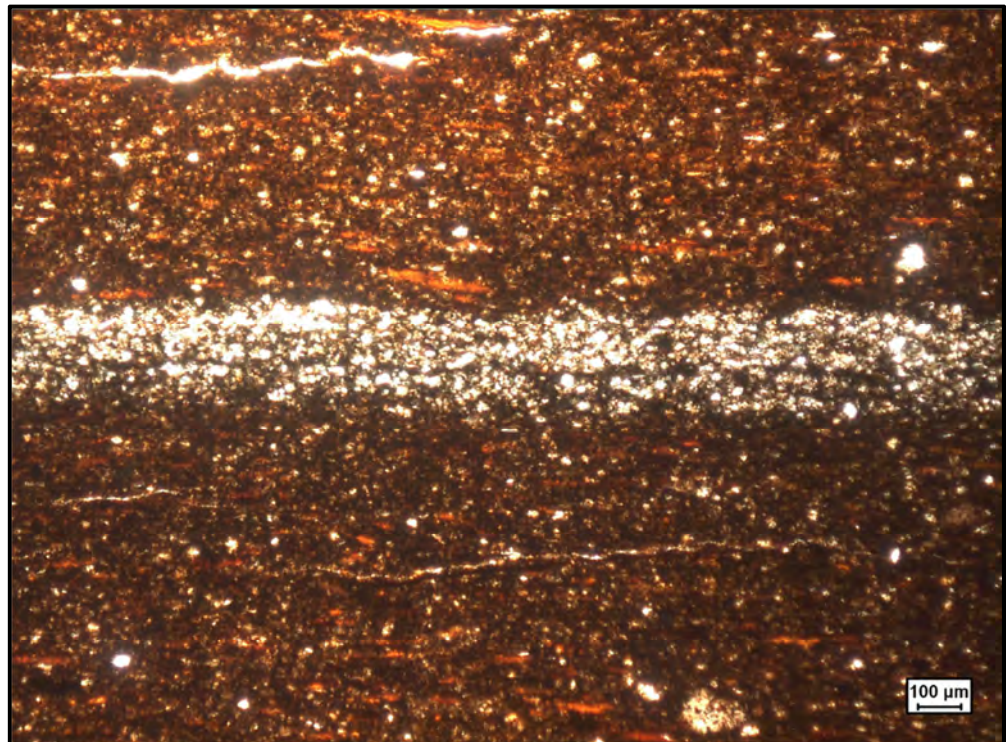


Sample RWN 23 – This sample has been collected at the transition between the Grey Shales Member and the Mulgrave Shale Member (at the base of the Jet Rock); it shows very well the heterogeneity of mudstones at a sub-millimetric scale. In this thin section, at least four, and possibly six event-beds are recognizable by the presence of sharp-based siltstone laminae grading upward into clay-rich laminae. Overall, the deposit still shows a prevalence of sediment supply from gravity- or bottom-currents which transferred relatively coarse detrital material horizontally over the shelf. The volume of productivity-related organic matter is still relatively reduced, and the volume of clay-sized fraction is subordinate to silt debris.

Jet Rock



Sample RW10 – This thin section shows the typically dominant microfacies in the Jet Rock unit: a relatively homogeneous, clay-dominated, organic- and carbonate-bearing mudstone. Most volume in the sediment is represented by clay- and silt-sized debris composed mostly of small aggregates and intraclasts of clay minerals (the low-chroma, light brown, granular background, and the larger, ellipsoidal, dark brown particles, distinctly more abundant in the lower half of the picture). Silt-sized grains, pelagic carbonate (probably foraminiferal tests) and organic matter are also present in significant quantities. Organic matter is present as dispersed, optically opaque (amorphous), wispy aggregates, poorly resolved at this magnification; and by relatively large (e.g., up to 0.2 mm at upper left in photo), flattened, high-chroma organo-mineralic particles (also known as 'marine snow') with either sharp or diffuse margins, which consist of aggregates of organic matter, clay-sized debris and autigenic pyrite (formed after deposition). These aggregates usually testify to a particularly high productivity in the photic zone and a steady supply of organic matter to the depositional interface, suggesting that local enrichment in TOC is not necessarily related to redox conditions of the lower water column, but to preservation. Note the general absence of definite bedding, indicating relatively continuous sedimentation of individual particles, but the presence of a well-developed planar fabric, due to both deposition and post-depositional compaction of soft particles, which shows the absence of effective bioturbation in this volume of sediment.



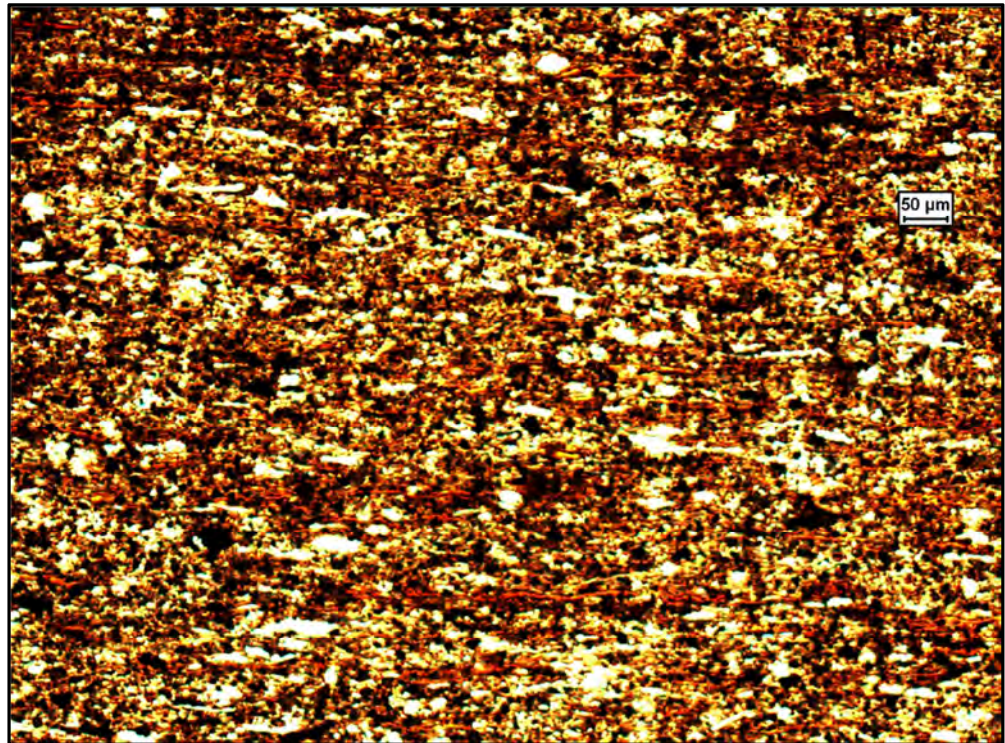
Sample RW29 – This microphotograph shows a possible facies change within the basal part of the Jet Rock, stratigraphically close to the Grey Shales Member. The lower half is substantially similar to sample RW10 above, and is truncated at top by a thin silt bed above which the modal size of individual particles and clastic content are slightly greater, while the abundance of pelleted clay aggregates is reduced.



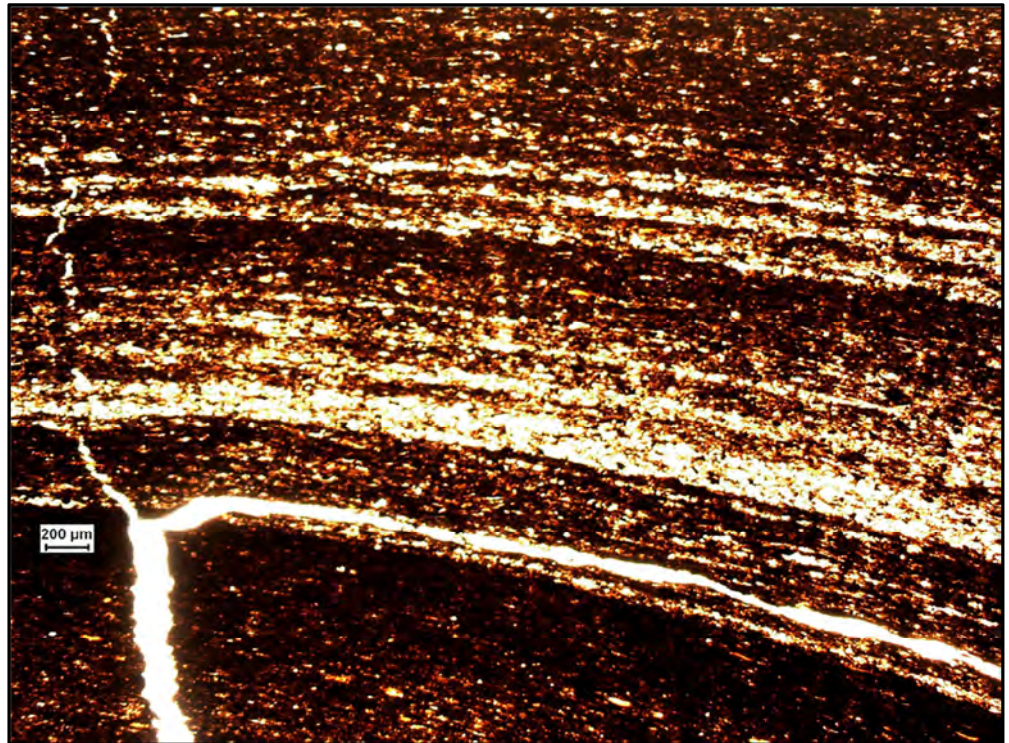
Sample RW29 – This microphotograph shows a typical example of bioturbation; the light-toned, homogenized, pelleted sediment lens in the middle of the image contrasts sharply with the encasing finer-grained, organic-rich claystone. The organism was probably a small invertebrate (note scale near upper right corner) moving horizontally through the shallow sediment column and ingesting organic matter while expelling the mineral fraction mostly in the form of pelletized aggregates. Note the deformation patterns of the encasing sediment (highlighted by highly birefringent marine-snow), subparallel to the burrow's margins. The stratigraphic position of this sample from the middle portion of the Jet Rock unit incontrovertibly demonstrates that the environment was not permanently anoxic, and oxygen levels were at least temporarily sufficient to support an active meiofauna. Note also the large length of many of the compacted organo-mineralic aggregates, some of which reach up to 0.3-.05 mm in length.



Sample RWN18 – This sample, from the basal metres of the Jet Rock unit, consists of massive, silt-bearing, organic-rich claystone. The indistinct, fine-grained background mass is composed mostly of clay minerals, microscopic organic particles, larger organic aggregates ('marine snow') and tiny calcite platelets (mostly of coccolithic origin), with scattered fine-silt-sized grains which are generally quartz (probably of aeolian origin; note the large subangular grain right at the top of the image). This dominant facies in the Jet Rock Unit represents long intervals of almost undisturbed deposition by vertical settling through the water column. The abundance of marine snow, organic matter, and calcite microdebris indicates a productive environment and biologic activity in the overlying water column, and certainly in the photic zone near the surface. Note however the presence of two thin silt streaks, probably lag deposits, highlighted by red arrows. These clearly point out the occasional activity of bottom currents removing low-density clayey and organic fractions from the soft substrate and transporting it elsewhere.

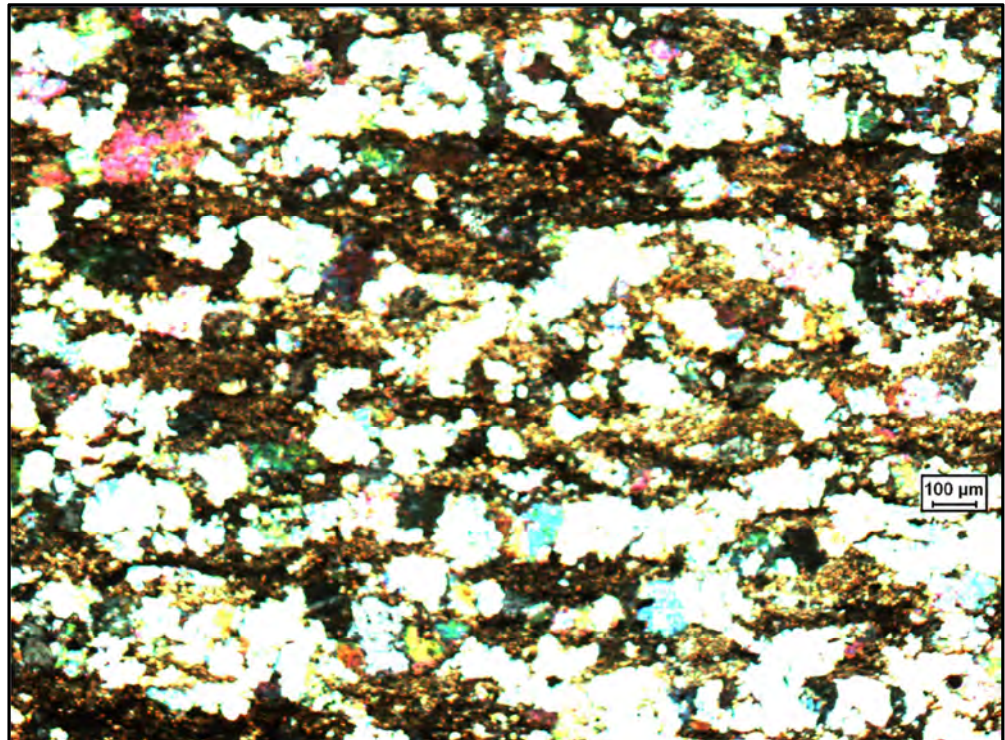


Sample RWN21 – This image shows at slightly higher magnification a similar microfacies to the one above; however, some of the basic components are more clearly visible at this magnification. Besides the lengthened, compacted organo-mineralic aggregates which highlight the horizontal reference plane within the thin-section, other coarser aggregates are visible as whitish, flattened ellipsoids whose internal structure is poorly resolved: these are pellets of organic matter and calcite (probably coccolith) platelets, produced by organisms active either within the sediment or more likely in the overlying water column. This magnification also shows abundant, optically opaque (black appearance at photo), rounded, microscopic grains: these are framboids and euhedral microcrystals of authigenic pyrite, formed during early diagenesis during partial microbial oxidation of organic matter.



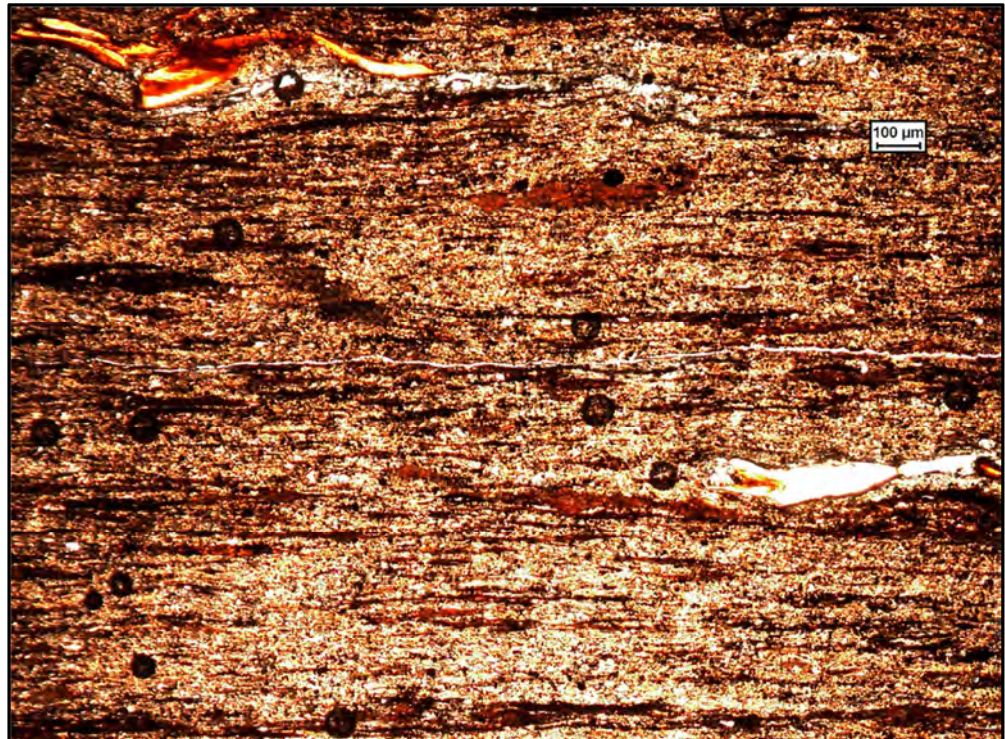
Unnumbered sample, base Jet Rock – This sample shows a typical facies transition from massive, organic-rich, silt-bearing claystone at the base, to well-bedded siltstones and organic-rich claystones alternating at sub-millimetric scale. The event bed in the centre of the photo shows a classical tripartition into a coarse basal division, a central one comprising repeated alternations of silt- and clay-rich laminae, and a topmost clayey division; this facies is most likely the product of fluid-mud redeposition after storm disturbance of the proximal shallow shelf farther to the west.

However, the most interesting aspect of this photograph is the deformation of these microbeds, dipping to the right. The lower portion of the thin section, not visible in the photo, cuts through a complete belemnite shell which lied horizontally within the sediment. This image, taken approximately 0.5 cm above the fossil, highlights the amount of differential compaction the mud has undergone during diagenesis. The sediment to the left is directly overlying the fossil's axis, and is more compacted than the sediment toward the right margin, as visible by the dip to the right of the structures, and by the slight increase in thickness of individual laminae in the same direction. The same deformation effects by differential compaction, at outcrop scale, are visible in correspondence of early-diagenetic carbonate concretions.



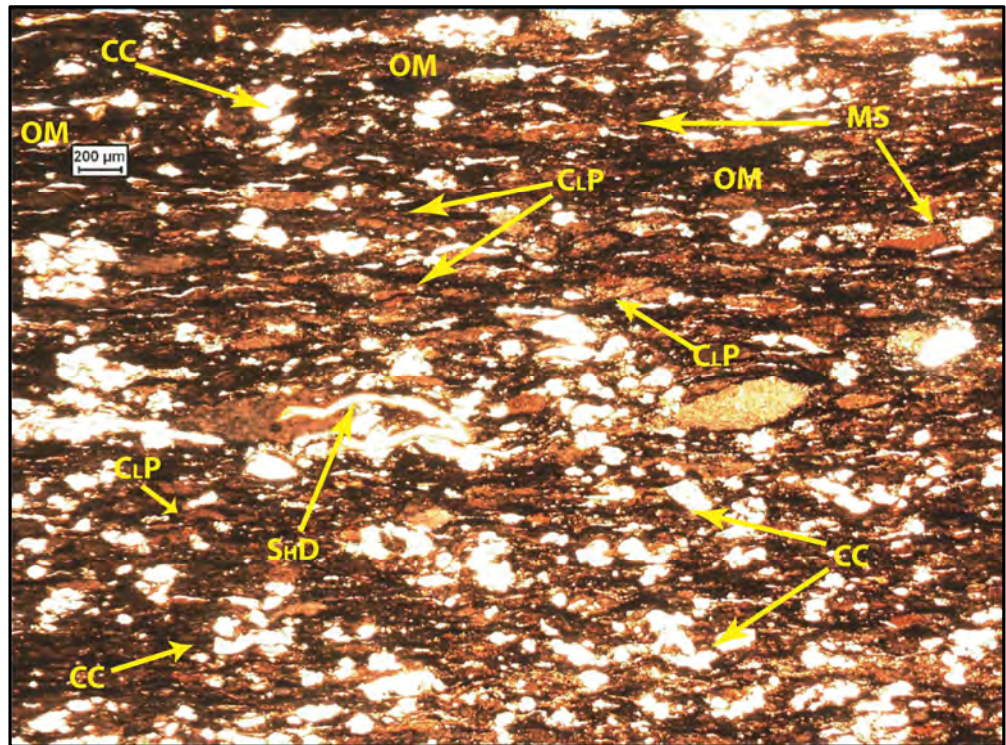
Sample RW13 (Jet Dogger bed) – The sample is taken from the so-called Jet Dogger marker bed which marks the informal stratigraphic transition between Jet Rock and Bituminous Shales units of the Mulgrave Shale Member. This is recognizable at outcrop as a laterally continuous, ‘limestone’ or ‘marlstone’ bed confidently traceable through different outcrops on the Yorkshire coast. However, the microphotograph clearly shows that the rock consists of originally clayey, organic-rich clastic sediment (dark to light brown, patchy component in the image) which has undergone pervasive cementation by calcite and locally possibly dolomite (whitish to brightly coloured, single or aggregate crystals). The size and amount of these secondary carbonate crystals probably indicate a relatively long permanence of this specific volume of mud relatively close to the sediment-water interface, allowing a prolonged accretion of early-diagenetic phases within it. Beds like this one might thus have a sequence-stratigraphic significance in the succession, indicating low rates of deposition due to changes in base level or sediment supply.

Bituminous Shales



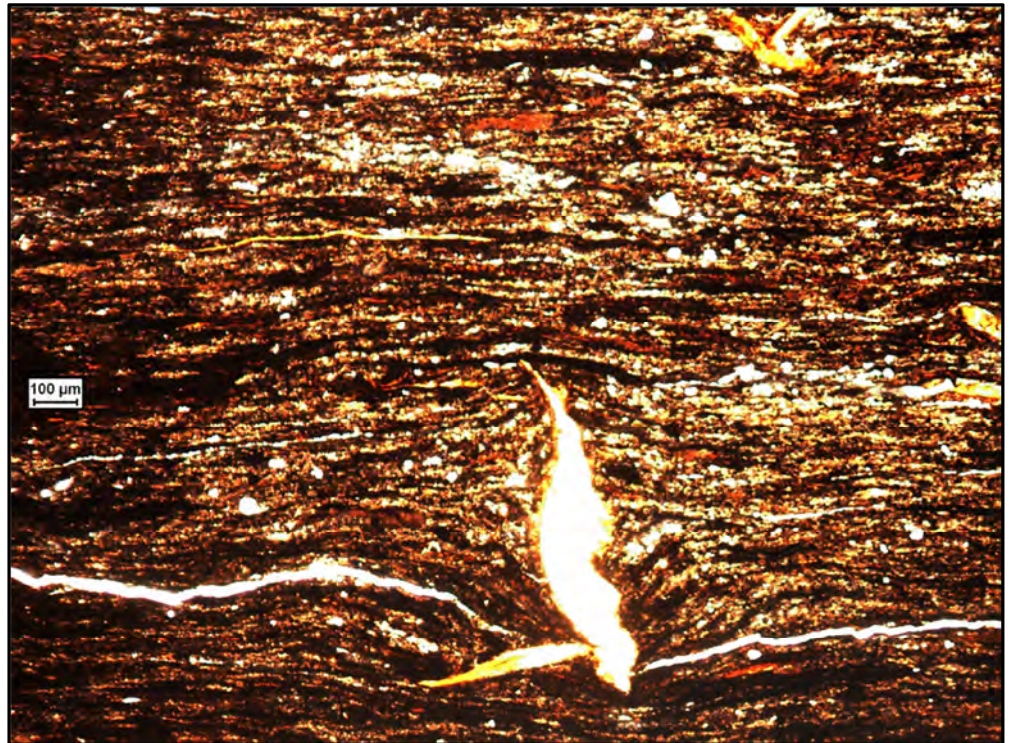
Sample RW1 – The sample has been collected at ~2 m above the Jet Dogger in stratigraphy, and stratigraphically it represents the youngest one analyzed for sedimentology. It consists of an organic-rich, carbonate-bearing massive claystone, with an almost total absence of silt-sized debris and a notable lack of pelleted fabrics compared with other samples of the Bituminous Shales. The deposit was probably accumulated in a particularly quiet environment where aggradation occurred almost entirely through vertical settling of particles along the deep water column; according to reconstructions of regional geology, the time of deposition corresponded to a maximum transgressive phase.

Besides poorly resolved clay-sized fractions and calcitic microdebris, other components recognizable in the photo are large aggregates of 'marine snow' (reddish in tone) and flattened, indistinct organic debris of possible algal origin; remains of animal origin are the two large phosphatic particles at top left and centre right in the photo.

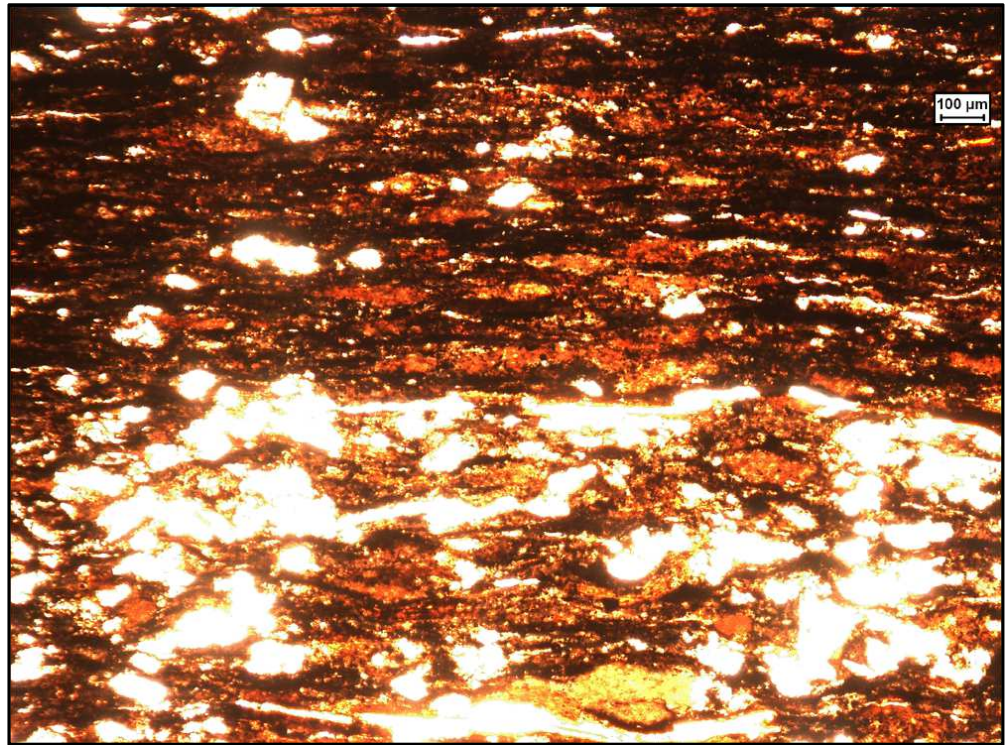


Sample PMS1 – This photograph shows another typical microfacies of the Bituminous Shales, consisting of a massive, densely pelleted, organic-rich claystone; notable in the Bituminous Shales is the frequent occurrence of sediment aggregates of various origin, probably mostly biological given the reduced evidence for physical processes of sediment transport and reworking along the original depositional interface. This sample in particular has been collected ~20 cm above the Jet Dogger bed, and presents evident incipient cementation by microcrystalline carbonate (CC), which might be related to a still relatively reduced aggradation rate and thus efficient replenishment of interstitial waters within the sediment, allowing for early-diagenetic reactions.

OM = organic matter; CLP = clay pellets; SHD = shell debris; CC = crystalline carbonate (diagenetic); MS = 'marine snow'.



Sample RW11 – This image shows a densely pelleted, massive claystone with clear evidence for the soft, watery state of the sediment-water interface at time of deposition and for low-energy environmental conditions. A (relatively) large phosphatic clast, shown at the centre low part of the photo, has reached the bottom in a vertical position which allowed it to partly penetrate it, deforming the sediment below. The clast has then remained undisturbed in a vertical position as sediment aggraded around and over it. The evidence for active sediment deformation below the clast, rather than differential compaction, is given by the difference degree of deformation of the sediment below and above the clast: the mild deformation around the upper tip of the clast is due to differential sediment compaction, and is clearly less than around the clast's lower tip.



Sample PMS11 – This sample's microfacies is similar to those observed in almost all other samples of the Bituminous Shales (massive, pelleted, organic-rich claystone); however, it presents a sharp demarcation between a lower domain, visibly affected by incipient carbonate cementation, and an upper domain with only a few carbonate microcrystals. To be noted is also the accompanying change in the relative volume of organic-matter in the two superposed domains: the upper domain presents several large organo-mineralic aggregates ('marine snow') and broadly dispersed, opaque organic debris (appearing black in the photo), whereas the lower domain appears relatively impoverished in such components. It is thus probable that carbonates were nucleated or accreted through microbial chemical mediation during gradual consumption of locally available organic debris.

Considering that the sample's position is close to the stratigraphic interval corresponding to a maximum transgression in the Toarcian Cleveland Basin, it is probable that similar intercalations of early-diagenetic, carbonate-rich facies correspond to reduced sedimentation rates. Cemented horizons within mudstone successions may be predictable on the basis of general sequence-stratigraphic principles, provided sufficient background information is available on the basin history.

Appendix 2

Charts of the palynological results

Section : Runswick composite

Interval : -9.50m - 2.00m

TNO report 2014_R10265

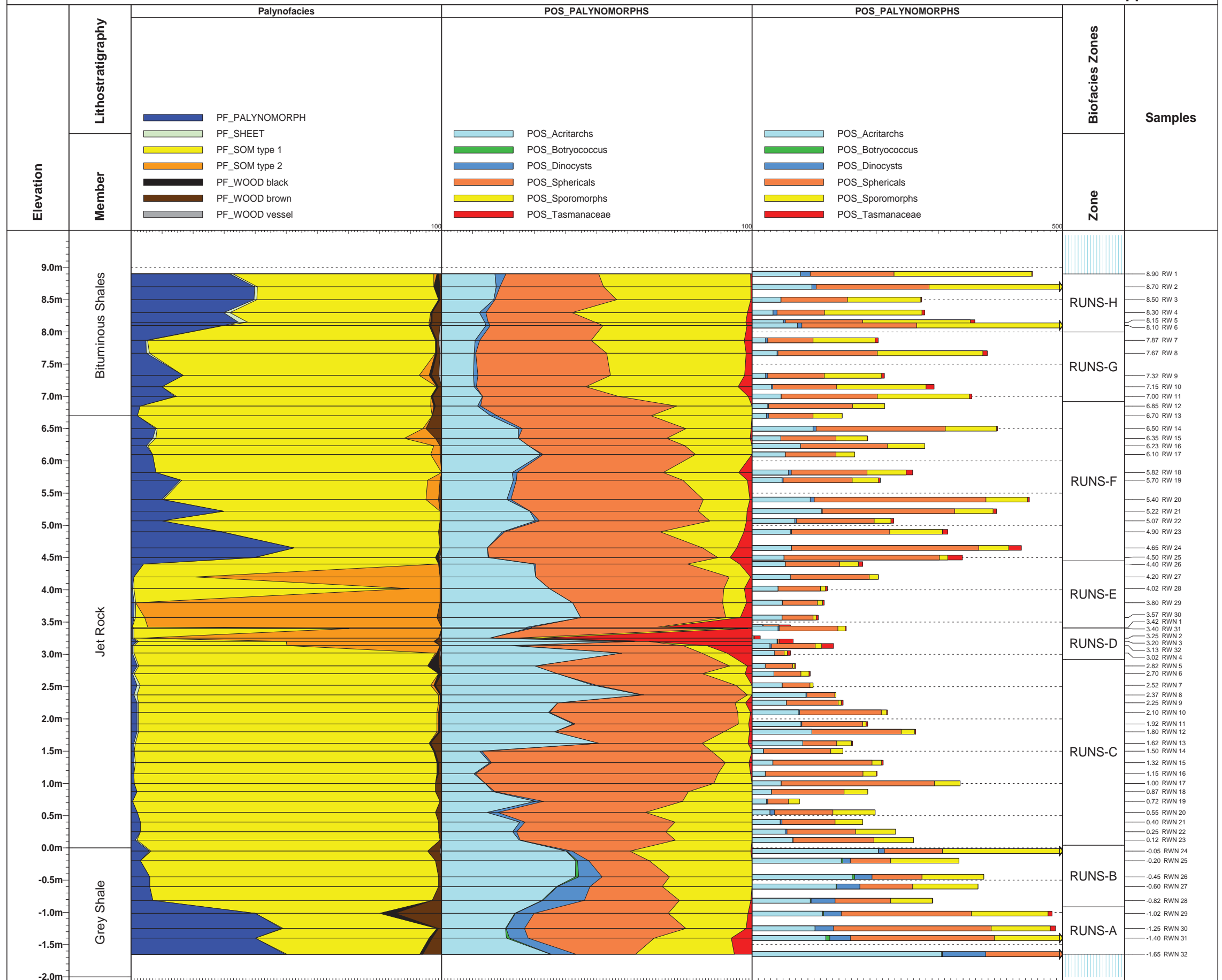
Scale : 1:50

Chart date: 24 February 2014

Runswick composite



Appendix 2A



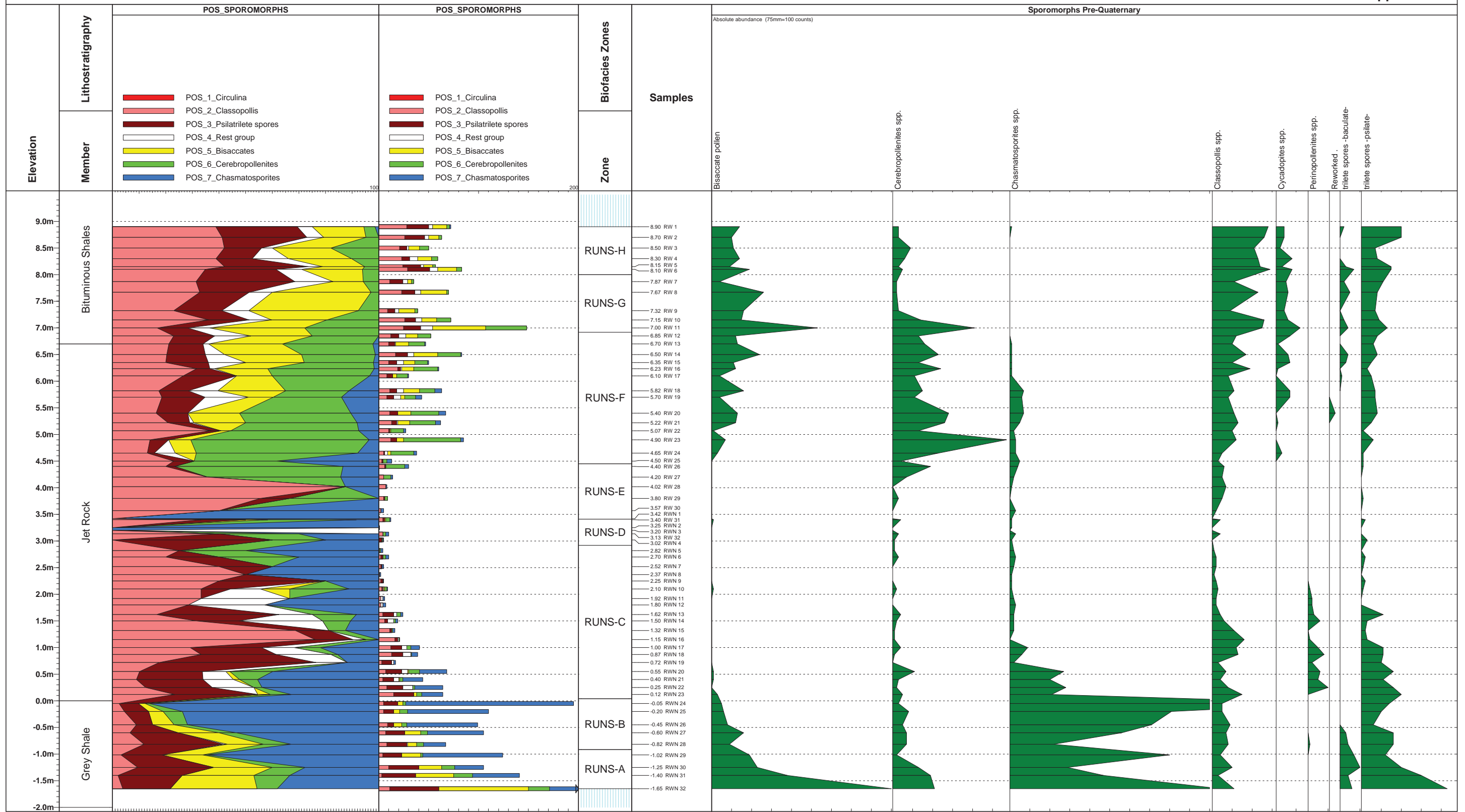
Section : Runswick composite

Interval : 9.50m --2.00m TNO report 2014_R10265

Scale : 1:50

Chart date: 14 February 2014

Runswick composite



Appendix 3

Outcrop photographs



Photo 1 The Top Jet Dogger displayed as a white band in outcrop, with the Whalestones at the base of the cliff. Hawsker's Bottoms.



Photo 2 Typical Whalestone with associated smaller concretions. Hawsker's Bottoms.



Photo 3 Typical weathering of the Middle Jurassic sandstones overlying the Whitby Mudstone Formation. The old graveyard at St. Mary's church, Whitby.



Photo 4 Cone-in-cone structures on erratic block found at the base of the cliff south of entrance to Port Mulgrave. Hammerhead for scale,



Photo 5 Top of the Jet Rock (Back packs and lower part of Linde), Top Jet Dogger (notebook and glove) and basal part of the overlying Bituminous Shales, all part of the Whitby Mudstone Formation. South of entrance to the beach at Port Mulgrave.



Photo 6 Overview of pavement studied for the fracture analysis. Port Mulgrave.



Photo 7 Top part of the Jet Rock and basal part of the Bituminous Shales. The white band above the hard hat is the Top Jet Dogger, the concretion below the hard hat belongs to the Curling Stones.



Photo 8 Runswick as seen from the South East. Note the thick Middle Jurassic sandstones at the top of the Cliff.



Photo 9 Concretion sticking out the cliff face. Note the bending of the compacted strata around it and the internal horizontal lamination reflecting the original bedding shortly after deposition.



Photo 10 The protruding cliffs at Kettleness. The thick hard layer in the base of the cliff is the last thick ironstone seam of the Pliensbachian Cleveland Ironstone Formation. The Pliensbachian-Toarcian boundary is 3 meters above the top of this layer. Typically, 6 nodular layers are present in the base of the Toarcian Grey Shale Member of the Whitby Mudstone Formation.



Photo 11 The November 2013 field trip party enduring the cold at Port Mulgrave. From left to right Peter-Jan Weijermans, Roel Verreussel, Linde van Laerhoven, Gary Graf, Jan Lutgert, Bert de Wijn, Laurent Jeannin, Johan ten Veen and Jean-Francois de Ronzier. Photograph taken by Michiel Harings.



Photo 12 The foreshore at Kettleness, showing the irregular top of an ironstone layer from the Cleveland Ironstone Formation.



Photo 13 Typical irregularly stretched shape of a concretion from the Curling Stones in the upper part of the Jet Rock, Whitby Mudstone Formation, near Runswick (vaguely visible in the background).

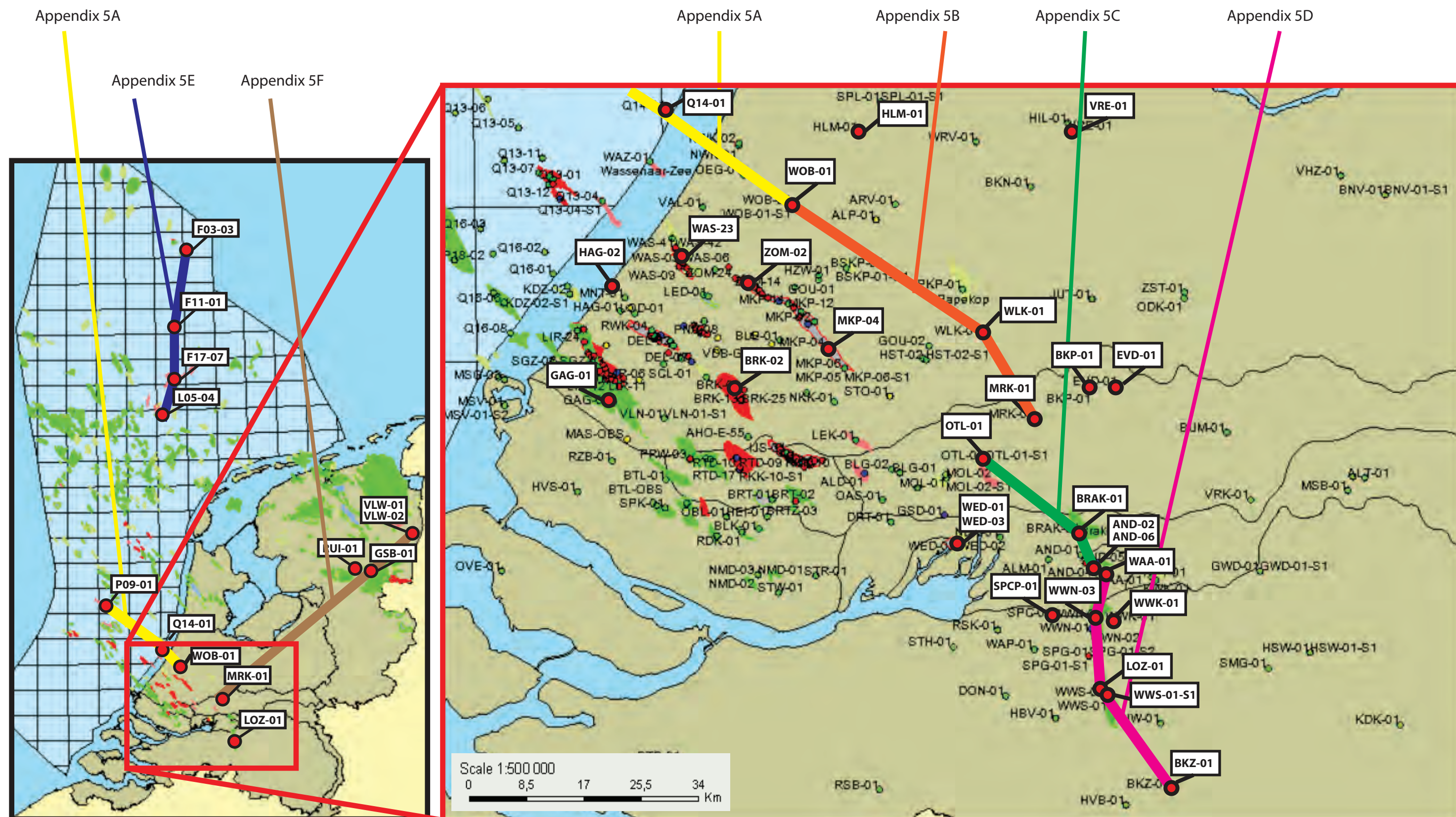
Appendix 4

Summary results Whitby

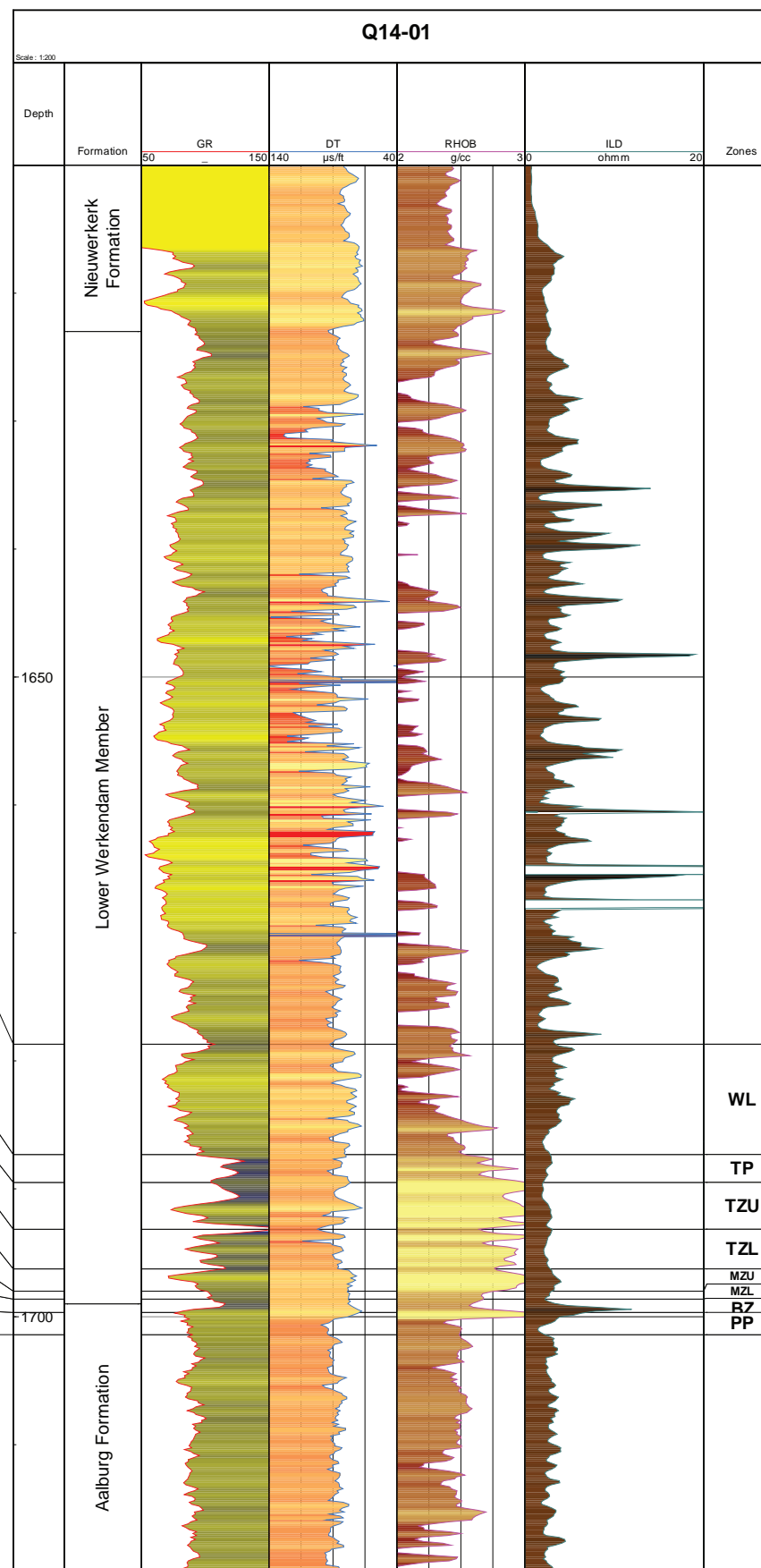
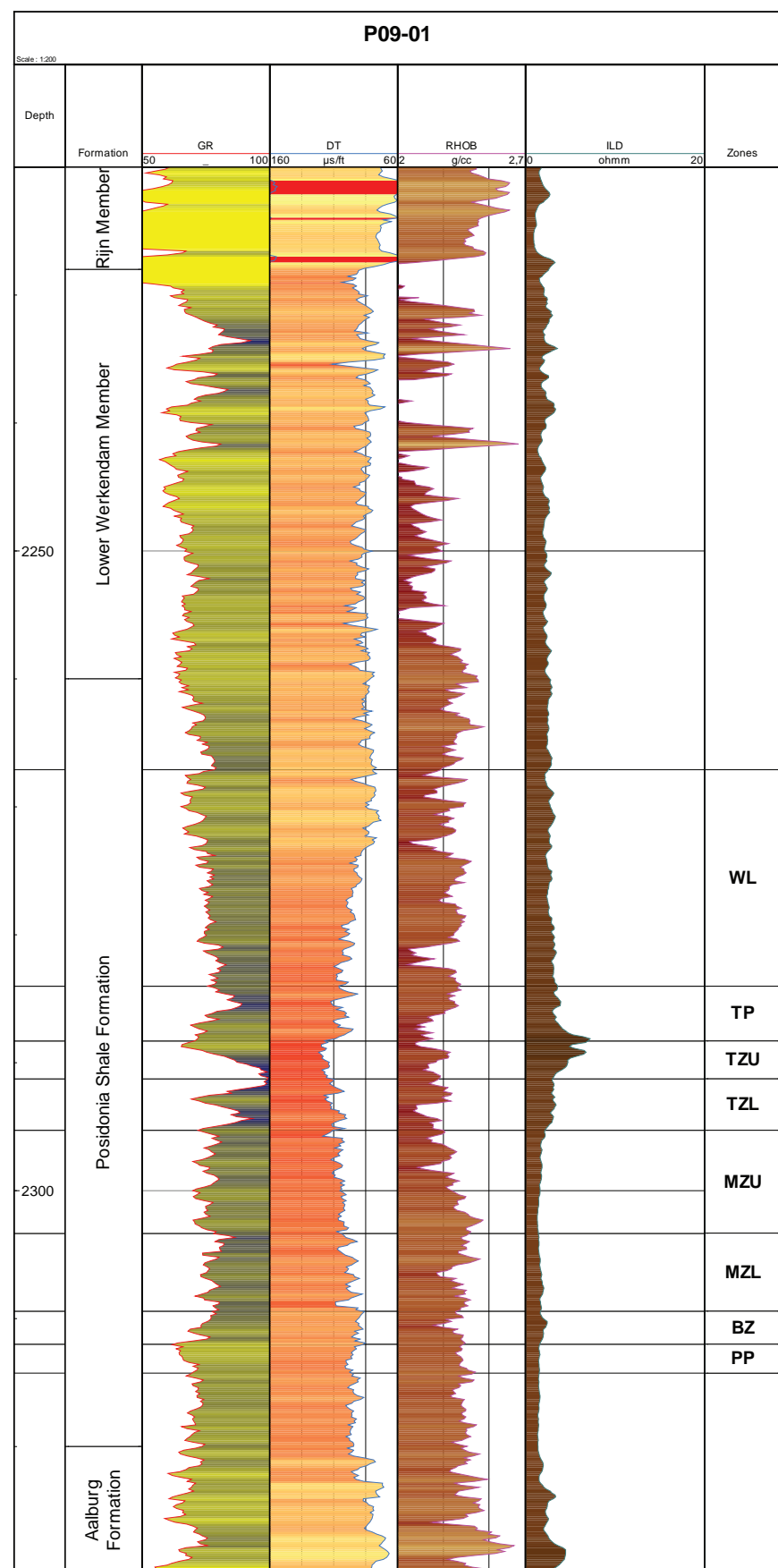
Appendix 5

Well logs Posidonia West Netherlands Basin

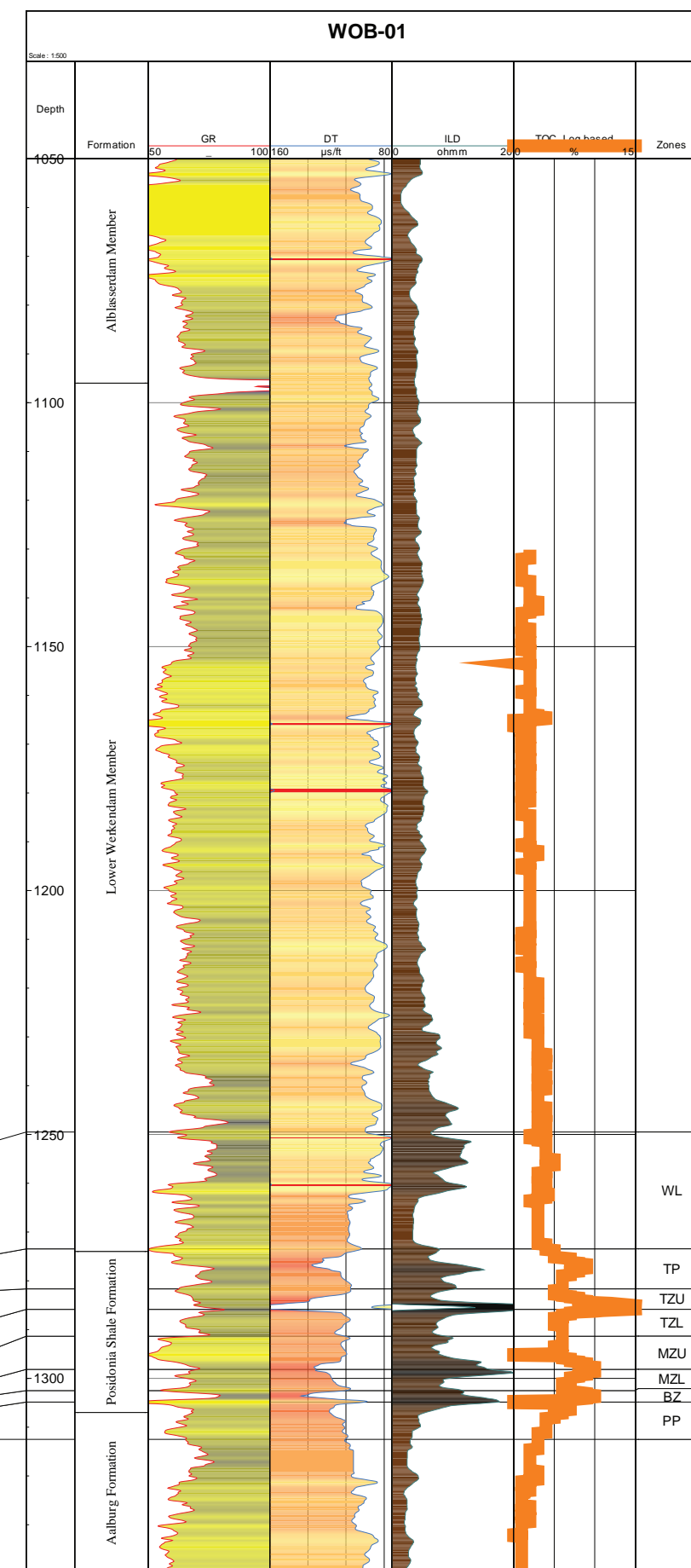
Location map displaying a selection of wells with Posidonia Shale Fm occurrences.
The transects of the correlation panels are indicated in colour.



NW

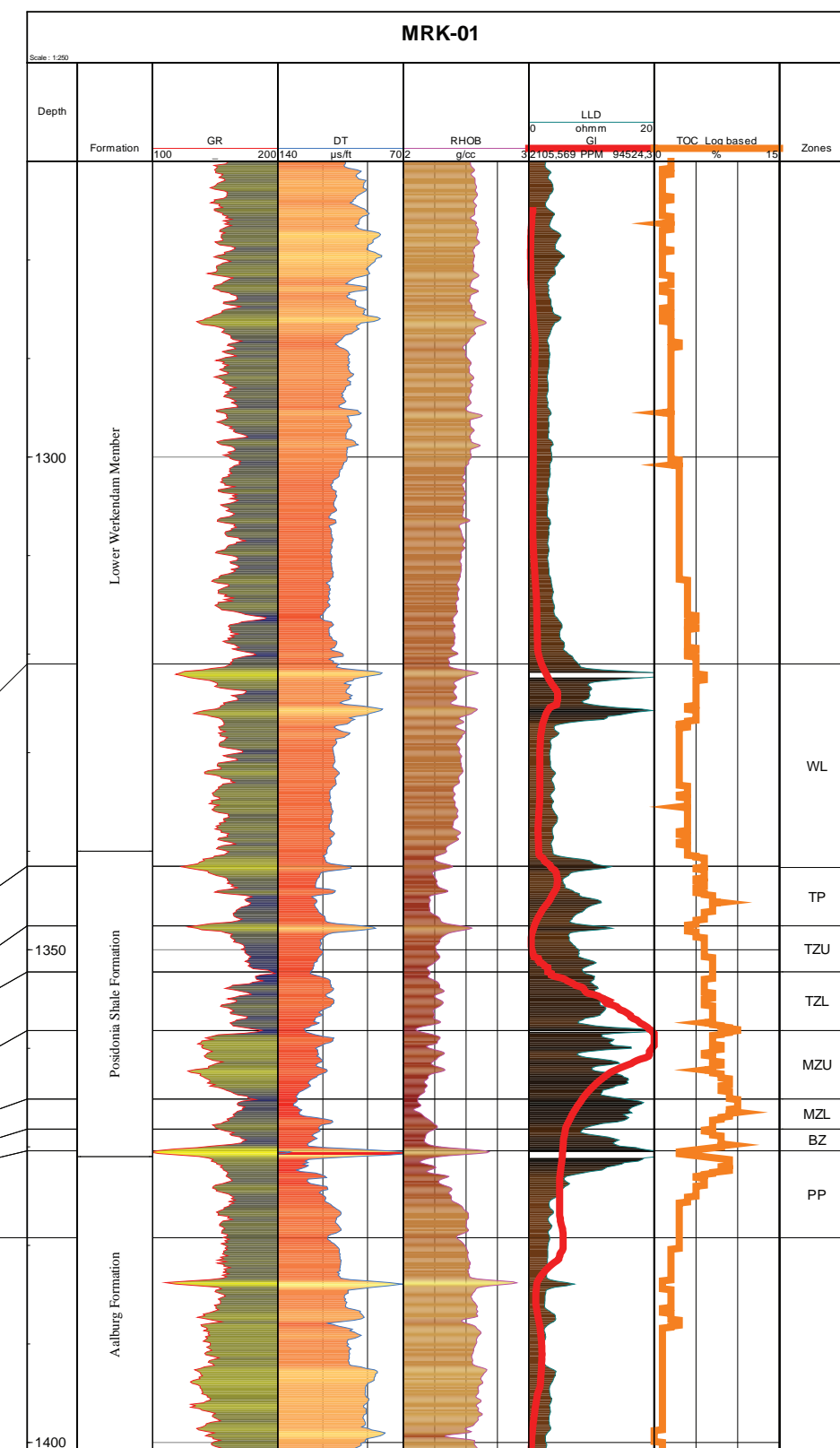
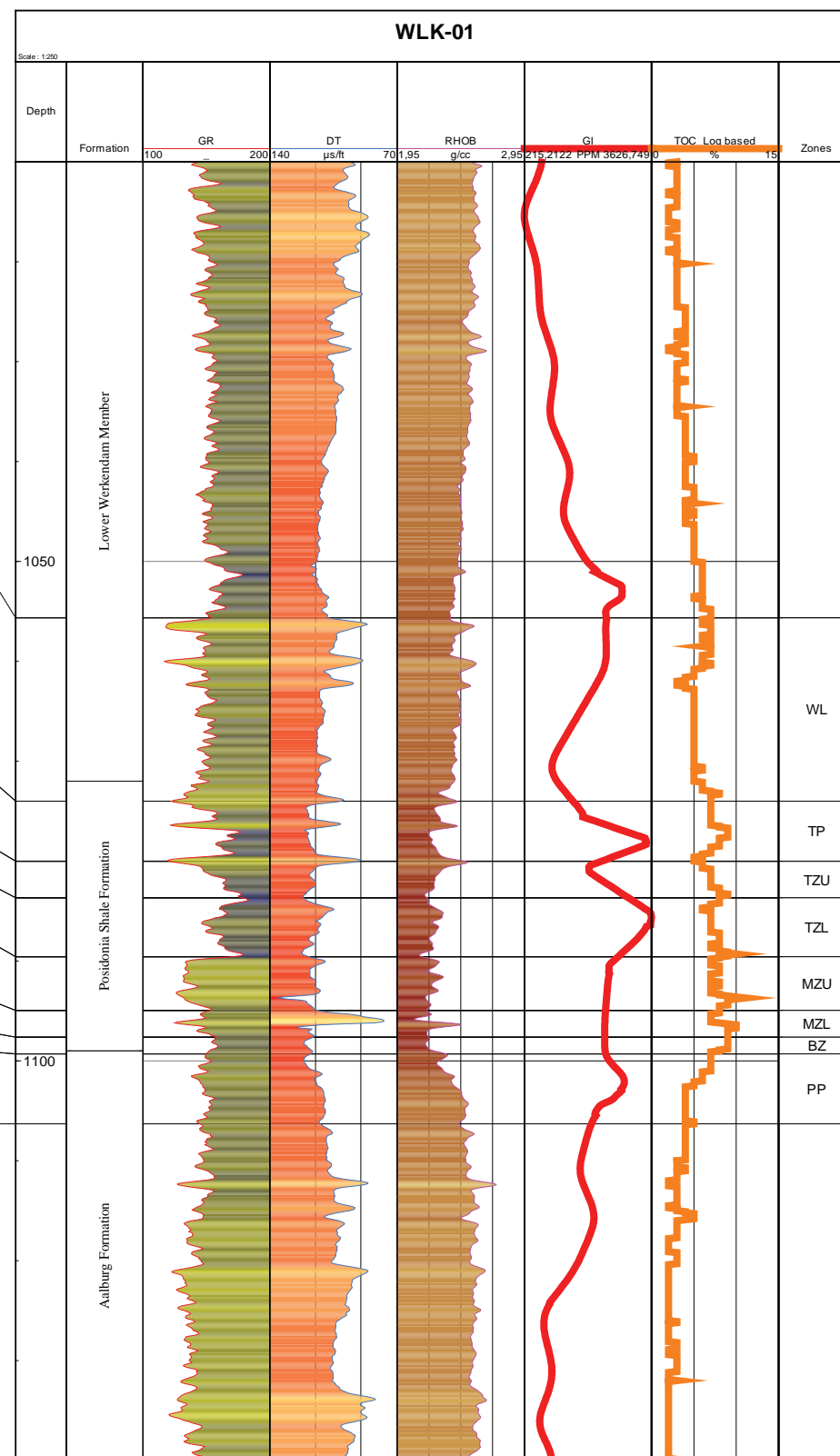
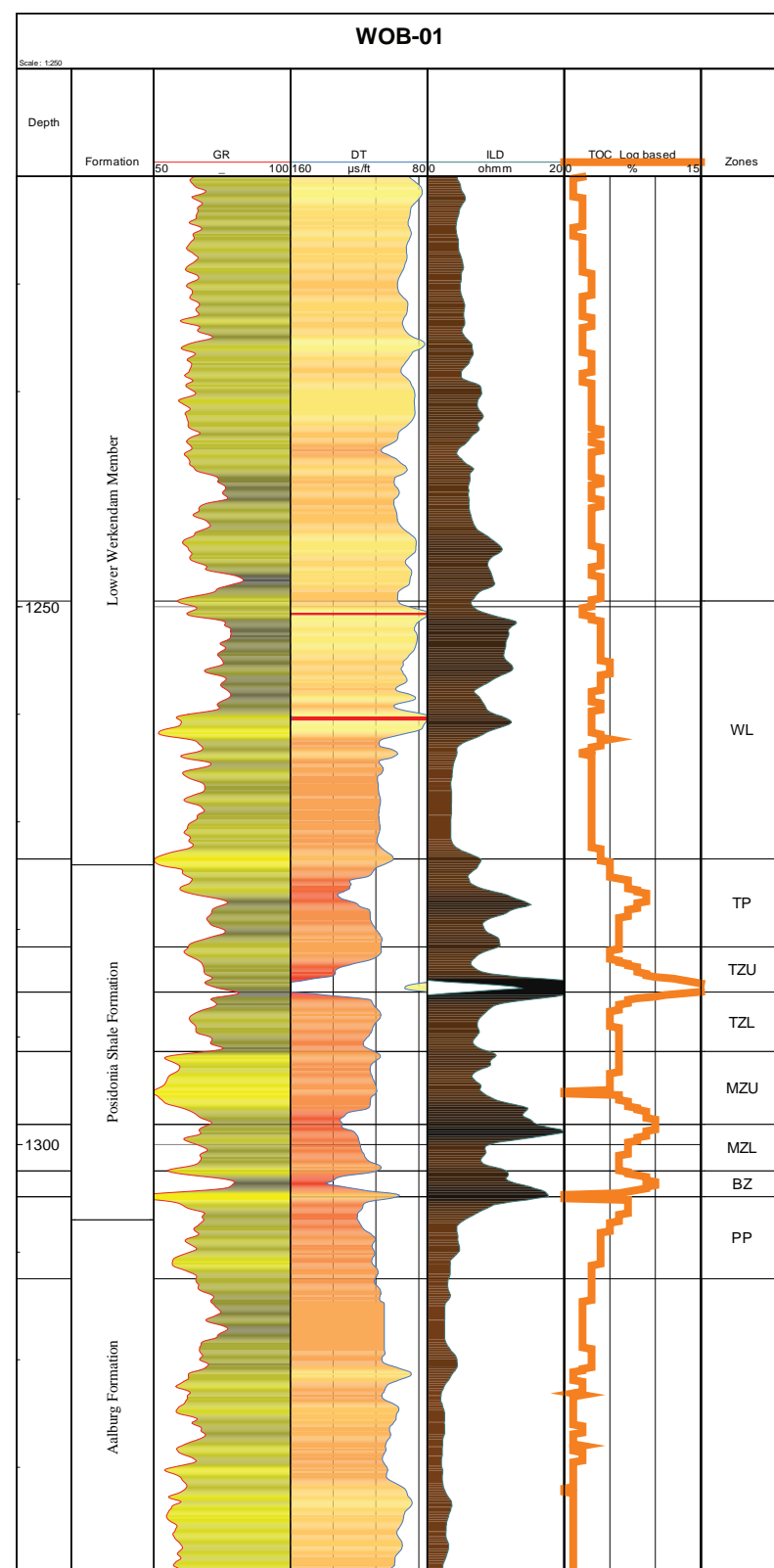


SE



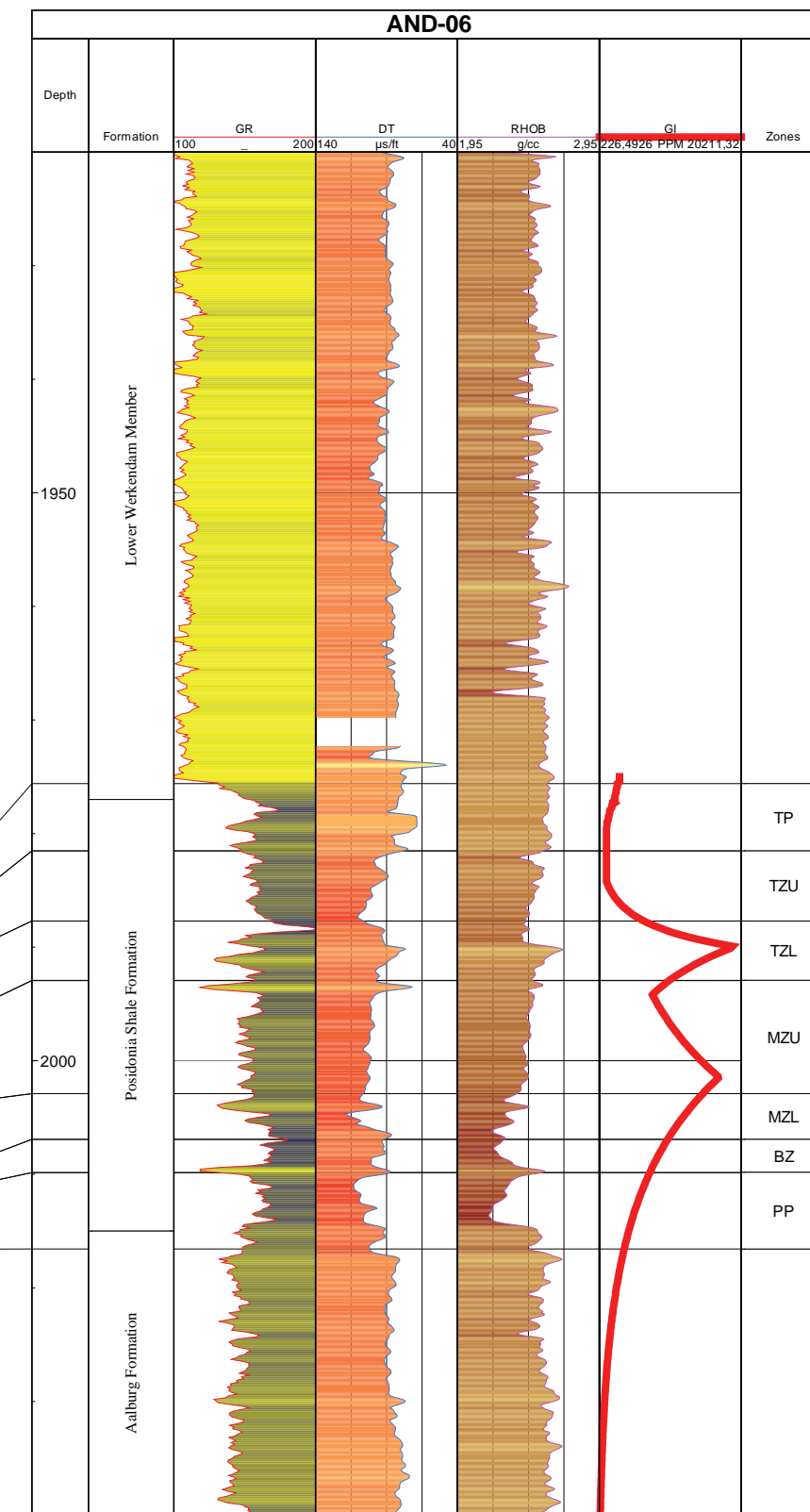
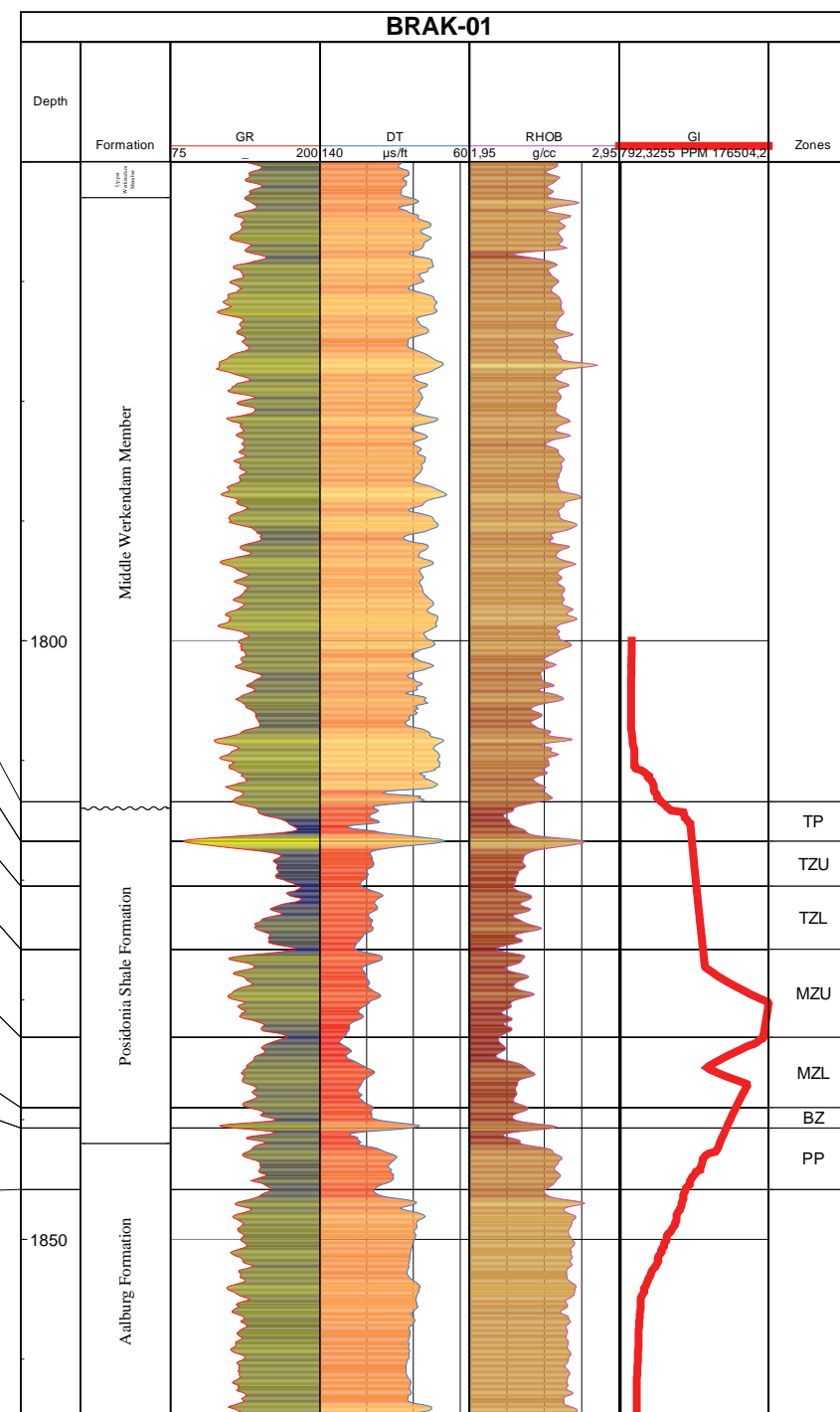
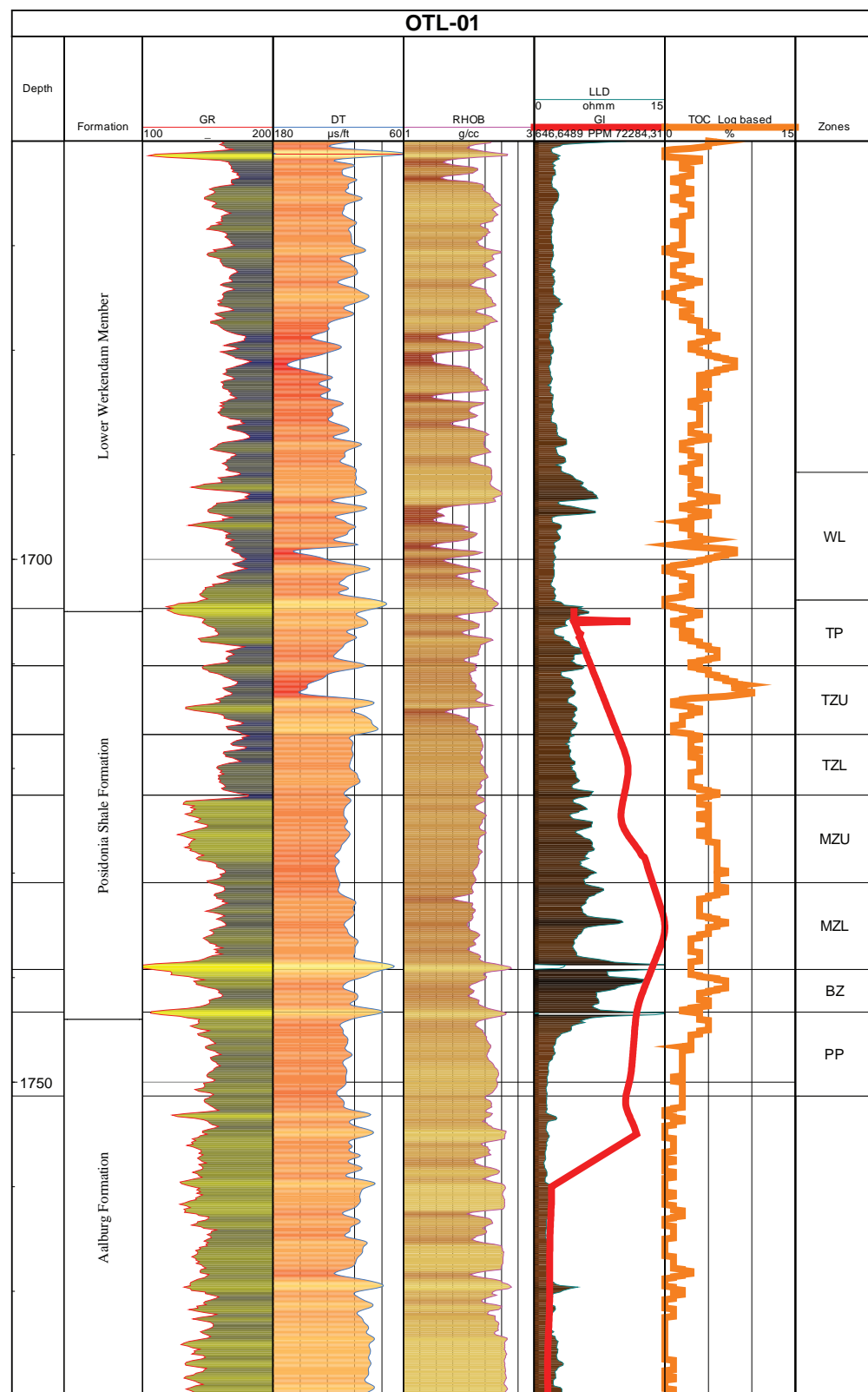
NW

SE



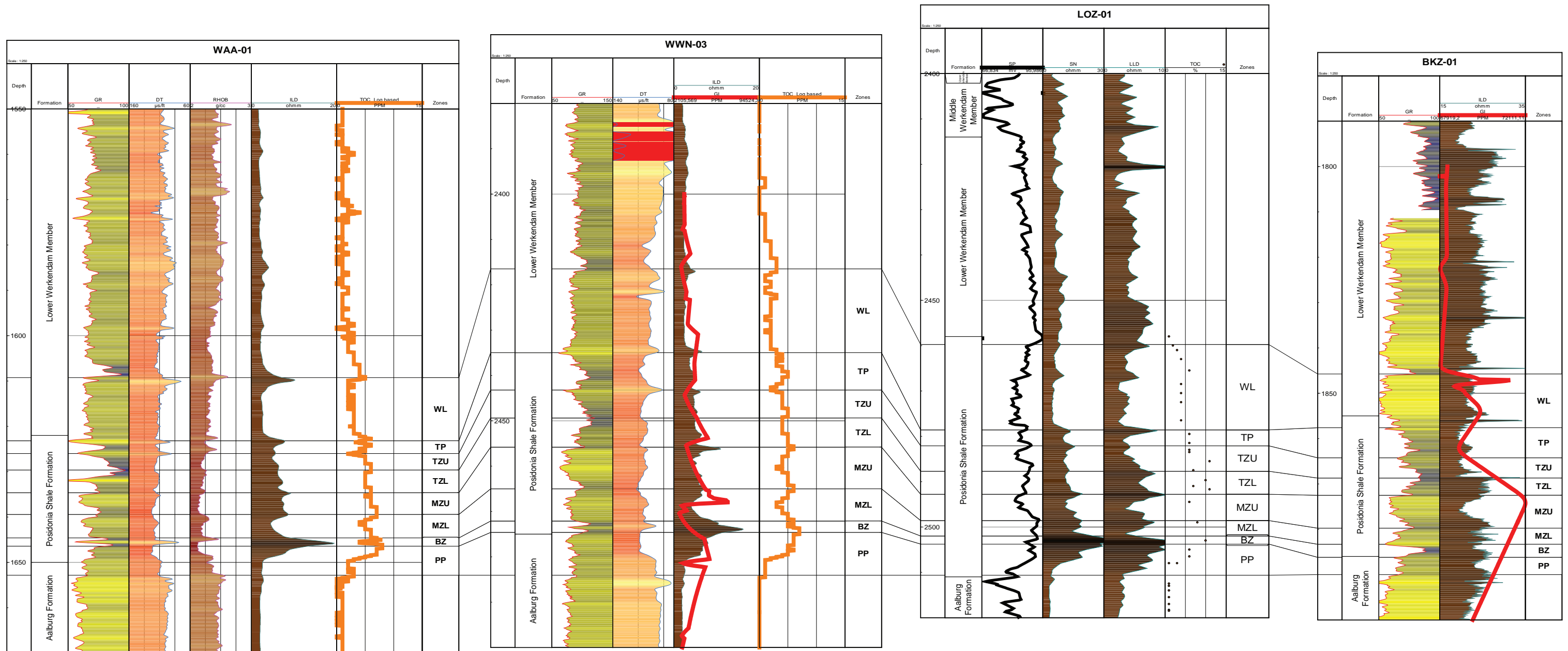
NW

SE



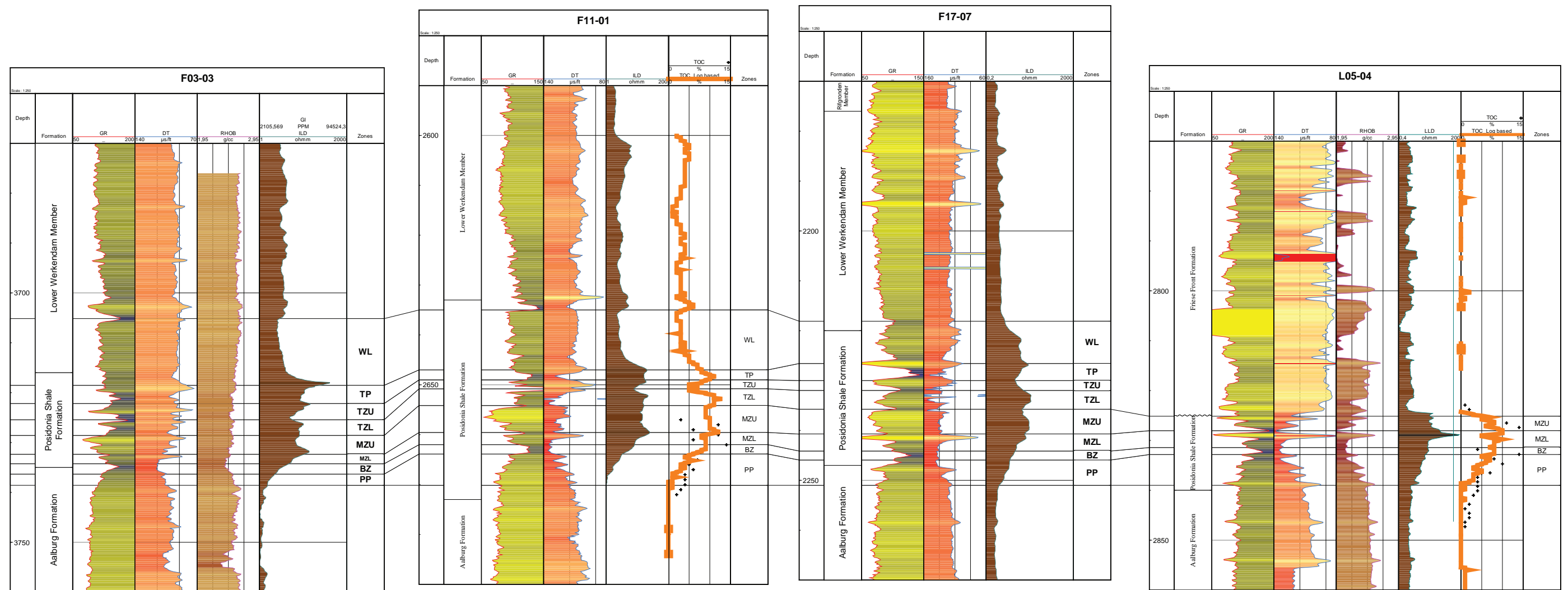
NW

SE



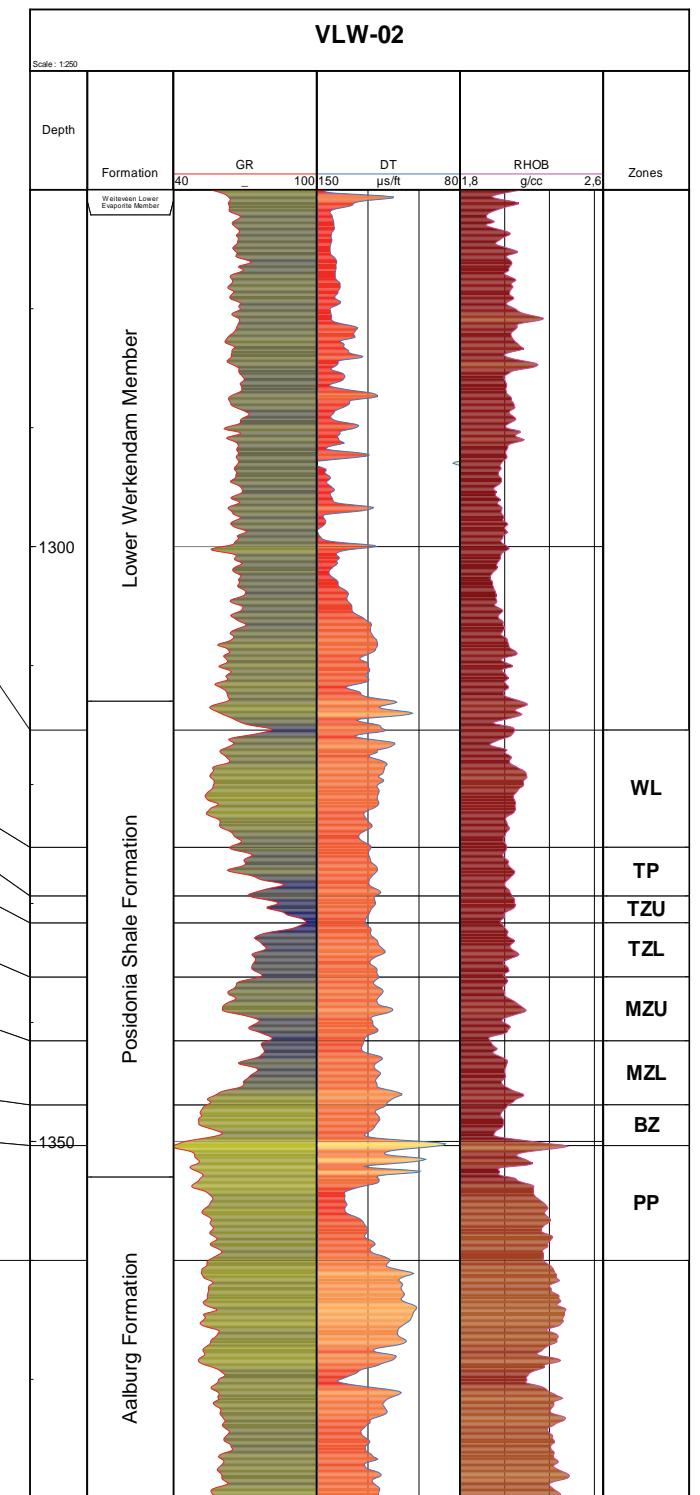
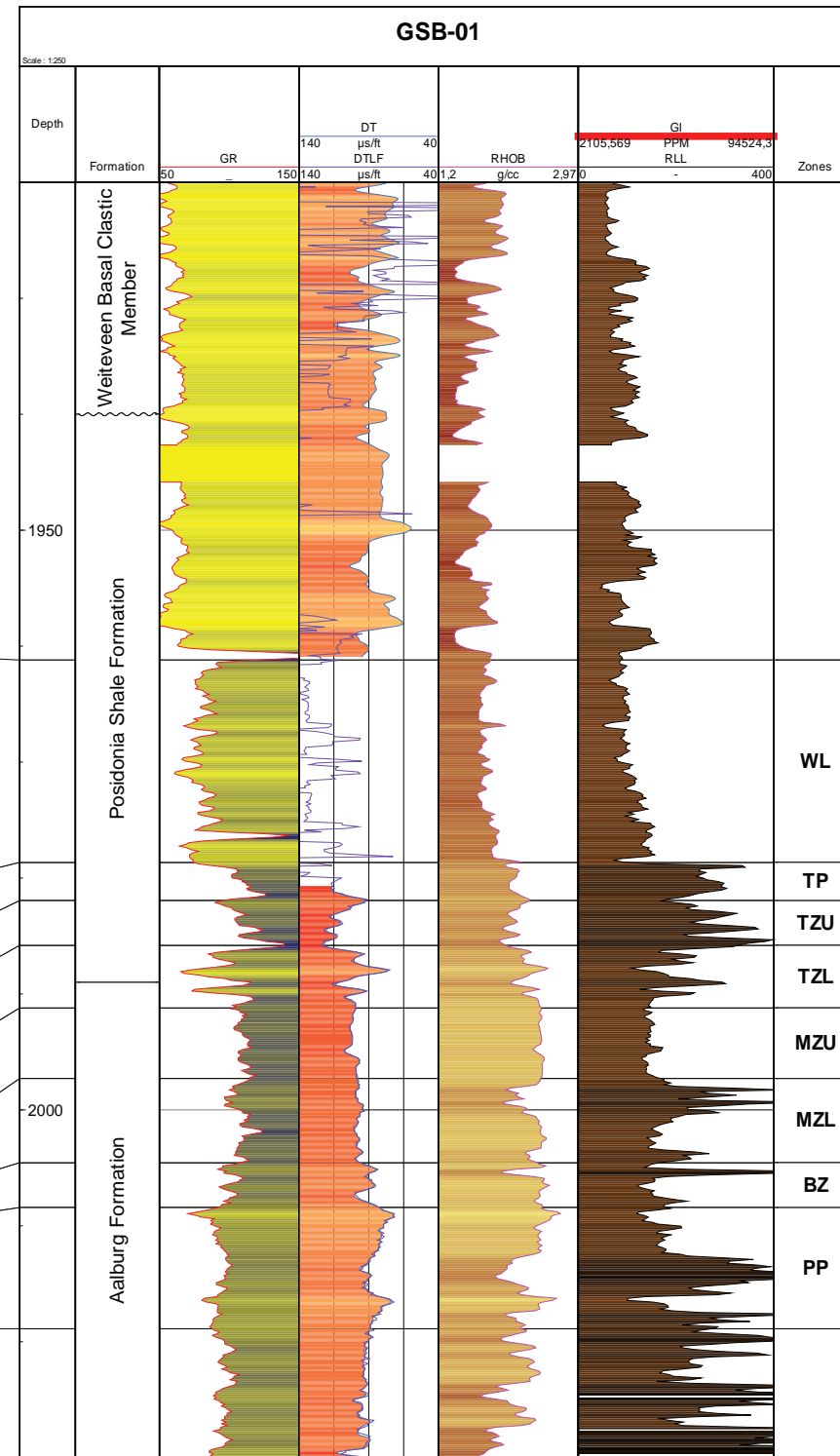
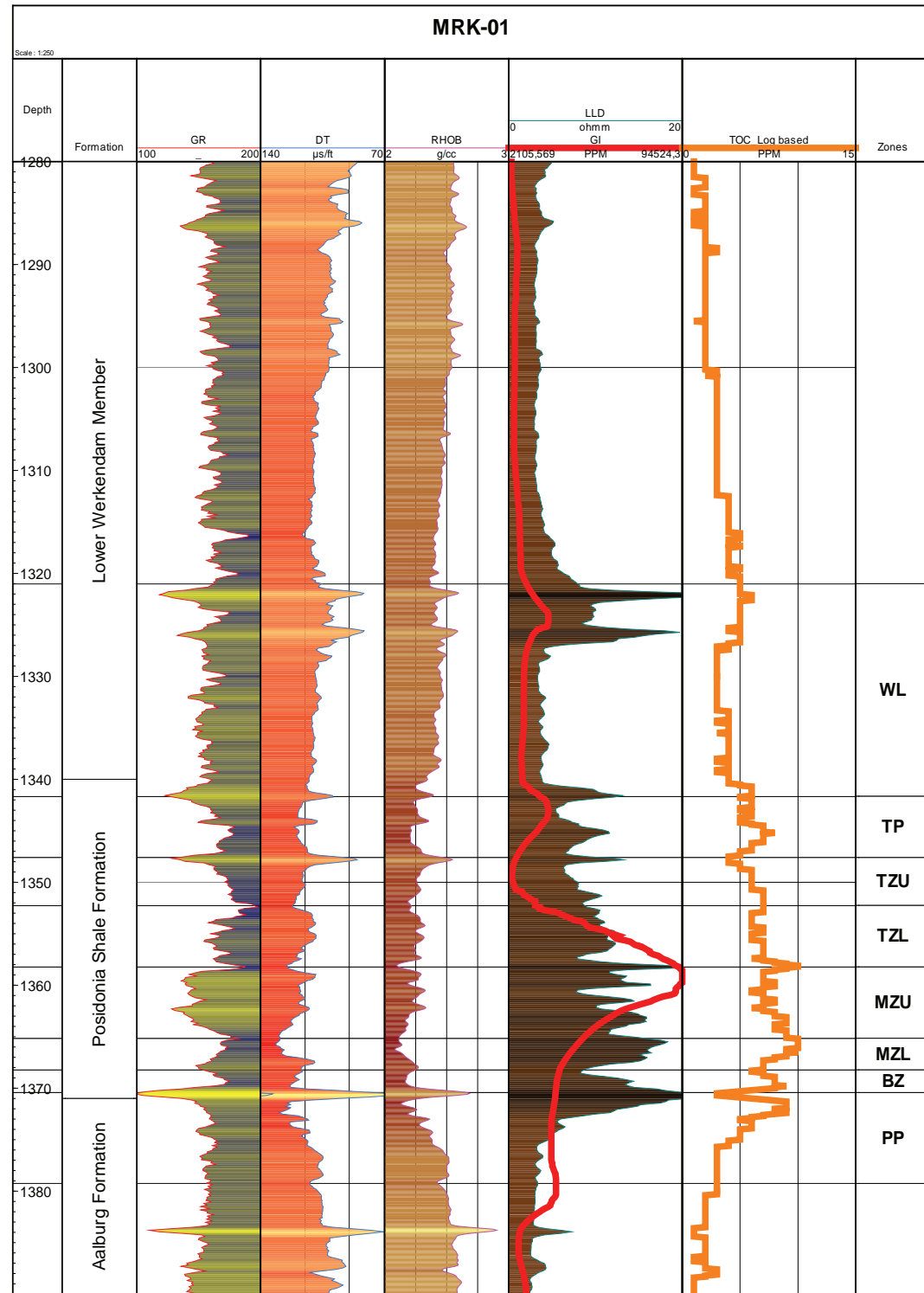
N

S



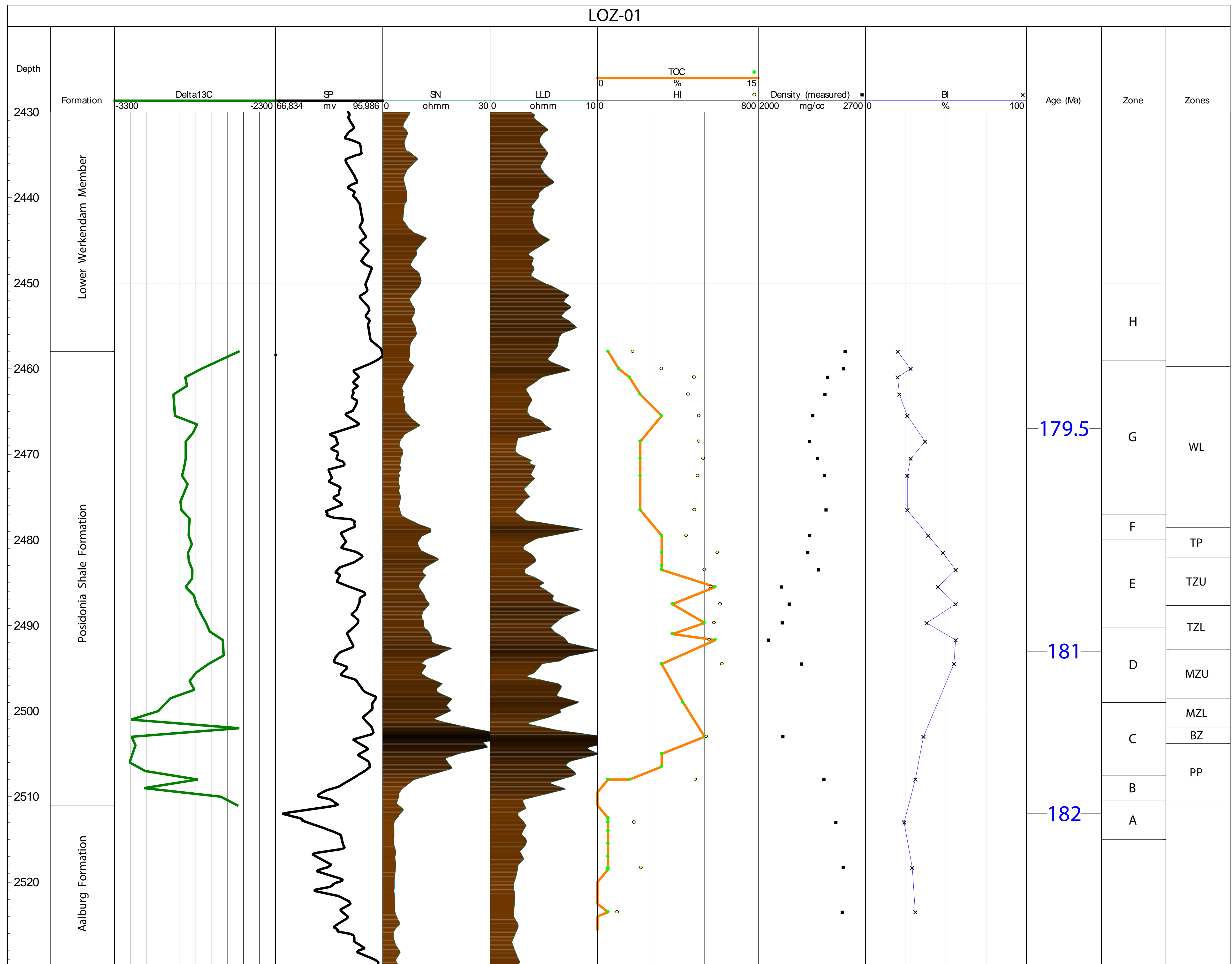
SW

NE



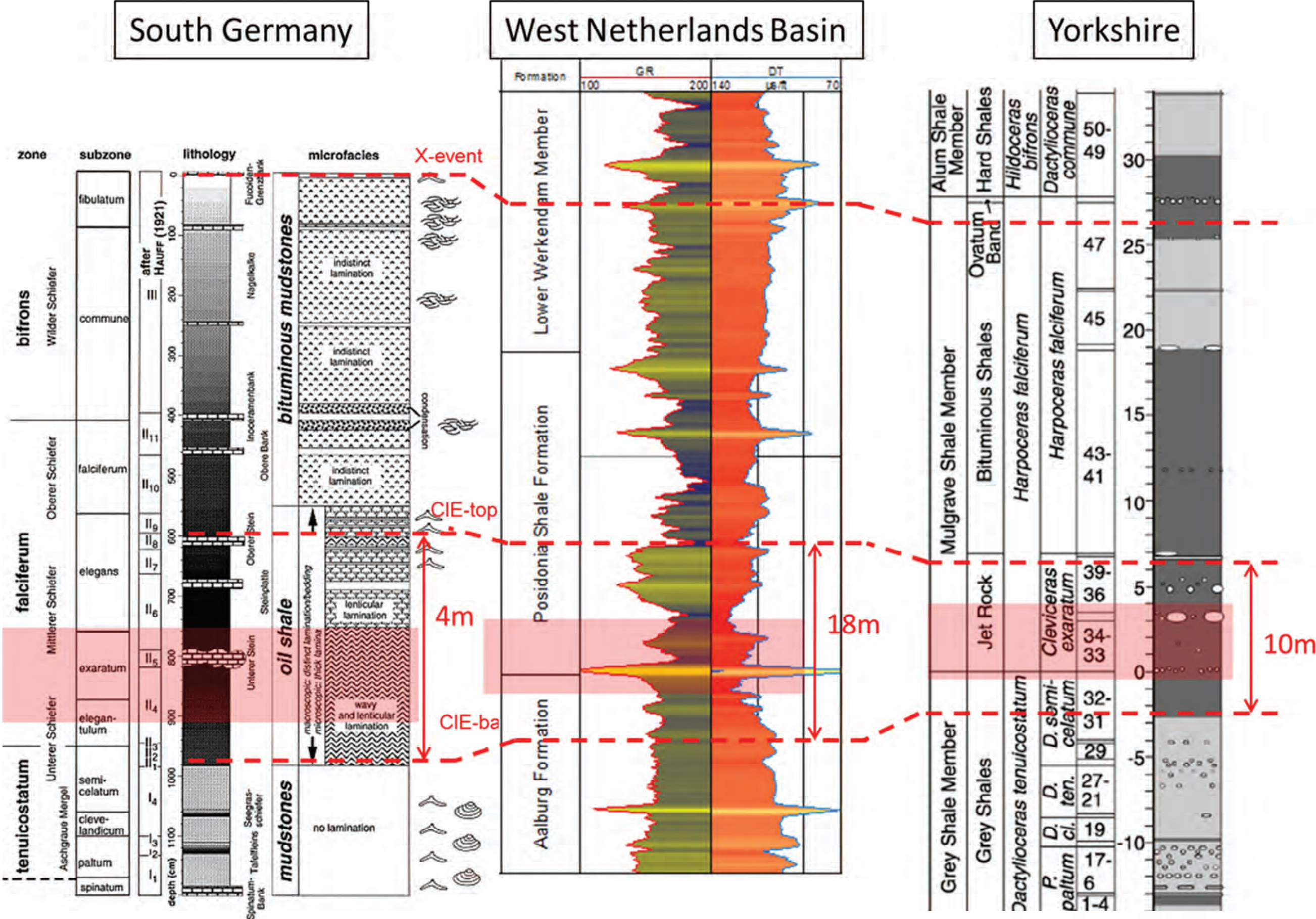
Appendix 5G Summary diagram borehole Loon op Zand-01 (LOZ-01)

Wireline logs/TOC and HI/Measured Density/Brittleness Index/Absolute Age/Biofacies Zones and Log Zones

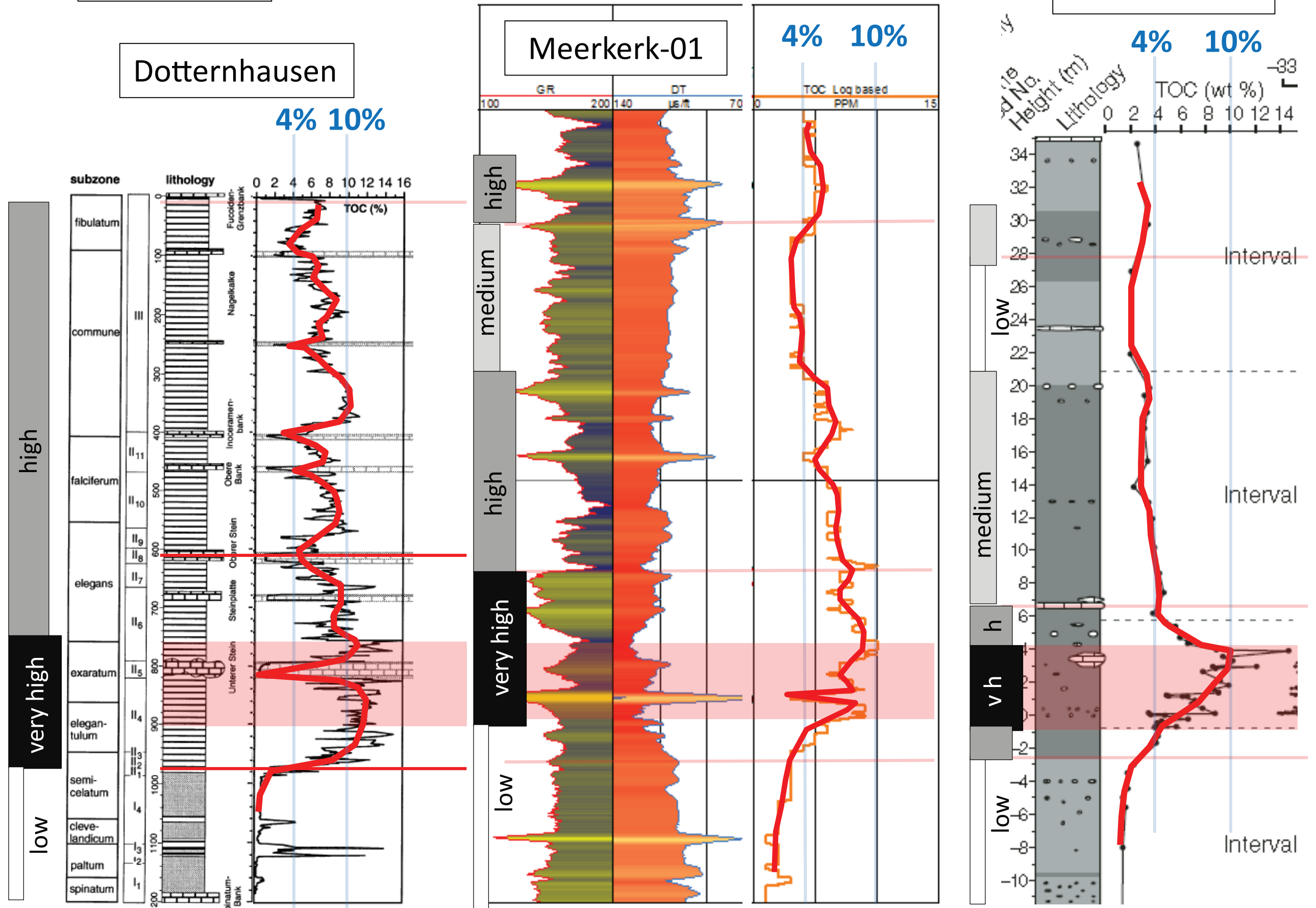


Appendix 6

Regional correlations Early Toarcian OAE



TOC profiles

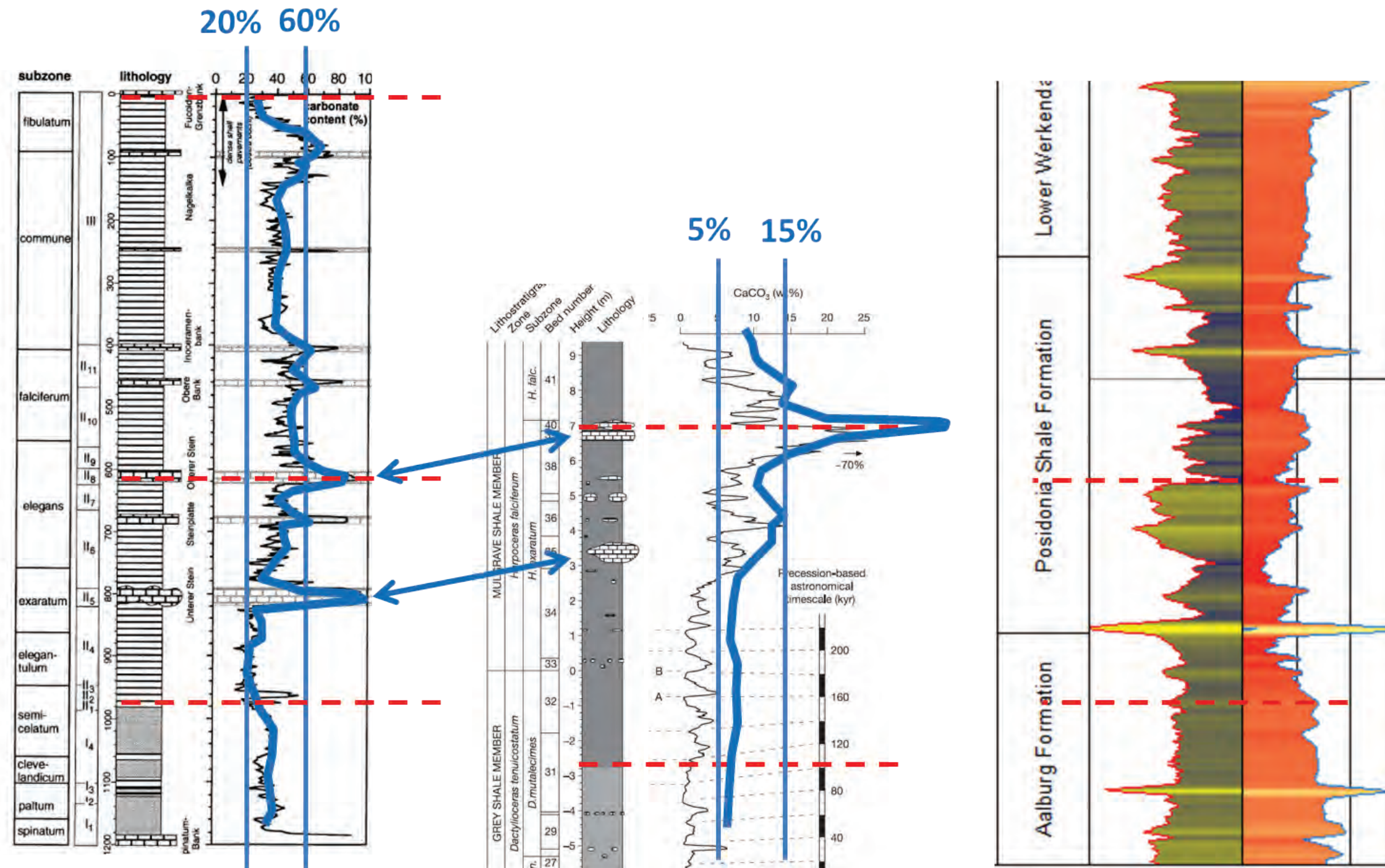


CaCO₃ profiles

Dotternhausen

Yorkshire

Meerkerk-01



Appendix 7

Log zonation of the Posidonia Shale Fm

Log Zonation

The Posidonia Shale Formation is easily distinguished from the surrounding shales of Aalburg and Werkendam formations by its distinct signature of the electric logs. On the composite well log, the Posidonia stands out by its hour-glass pattern of the gamma ray and sonic (Fig. 1). In general, the Posidonia is characterized by the following combination of log character: High GR (gamma); High DT or slow acoustic (sonic); Low RHOB (density) and High LLD or ILD (deep resistivity). The combination of log characteristics is primarily caused by the high organic matter content of the shales.

When we zoom in on the Posidonia Shale in more detail (Fig. 2), it appears that there is quite a lot of variation in the logs. In addition, repetitive patterns are observed, indicating cyclicality. These patterns can be traced from well to well and provide a means of subdividing the Posidonia Shale Formation into 'log zones'. Well Meerkerk-01 (MRK-01) is presented here to serve as a standard for the proposed log zonation.

LOG ZONES

A total of 8 log zones is distinguished. The zones are defined by specific combinations of the GR, DT, RHOB and ILD.

In general,

- the highest GR values occur in the upper half of the Posidonia
- the highest DT and lowest RHOB values occur in the lower half of the Posidonia
- the deep resistivity shows a rapid increase at the base followed by a gradual decrease
- a couple of thin, probably carbonate-rich layers (low GR, low DT, high RHOB, high ILD) occur in the Posidonia, usually near the base and in the top part
- the thin, probably carbonate-rich layers often occur in couplets, suggesting astronomical forcing
- the thin, probably carbonate-rich layers correlate on a local, not on a regional scale
- approximately 15 meters above the Posidonia (half the thickness of the Posidonia), a correlatable event in the logs occurs, characterized by i.e. a peak in resistivity

Below, the log zones are described from bottom to top.

Log Zone PP

Log Zone PP marks the transition from the underlying "normal" Aalburg Formation to the organic-rich Posidonia Shale Formation.

GR similar to underlying Aalburg shale, slight increase towards higher values
DT sharp increase towards higher values (slow acoustic), typical S-shaped pattern
RHOB sharp decrease towards lower values, typical S-shaped pattern
ILD sharp increase to high values, increase typically starts half-way the zone

Log Zone BZ

In Log Zone BZ the increasing trend in resistivity from the underlying Log Zone PP reaches its top. Quite often, Log Zone BZ is bounded at the base and/or at the top by a thin, probably carbonate rich, layer.

- GR a very high peak value is reached in the middle
- DT apart from the thin, probably carbonate rich layers, DT is high (slow acoustic)
- RHOB apart from the thin, probably carbonate rich layers, RHOB is low
- ILD very high, quite often the highest peak value of the entire Posidonia

Log Zone MZL

Log Zone MZL is quite inconspicuous except for the DT. The slowest acoustic (highest DT) is often found near the top of this zone.

- GR relatively low values, but not as low as the overlying Log Zone MZU
- DT very high (slow acoustic), often increasing and reaching a peak value near the top
- RHOB low
- ILD decreasing trend from Log Zone BZ to lower part MZL, followed by an increasing trend towards the top of MZL

Log Zone MZU

The transition from Log Zone MZU to the overlying Log Zone TZL marks the transition from predominantly low GR values to predominantly high GR values. It is the most conspicuous and probably best correlatable log event in the Posidonia.

- GR very low average values, comparable to, and in some cases even lower than, the underlying Aalburg Formation
- DT Intermediate values but usually decreasing (faster acoustic) towards the top and often a small fast acoustic peak is recorded at the top
- RHOB Intermediate values but usually increasing towards the top
- ILD not a clear trend, although in a few cases the trend appears to be similar to Log Zone MZL: decreasing trend followed by an increasing trend, only with lower overall values.

Log Zone TZL

The zone stands out for its high GR values. The zone often displays a cyclic pattern in the GR and in the DT. Often, the resistivity starts decreasing in zone TZL.

- GR high average values particularly the base and the top
- DT Intermediate values, mostly a trend of decreasing (faster acoustic) and subsequently increasing (slower acoustic) is recorded
- RHOB Intermediate values, no conspicuous trend, values on average higher than underlying zone MZU
- ILD Still high values, but mostly a trend of decreasing values is observed, except for well WOB-01

Log Zone TZU

This zone is more or less mirrors zone TZL, with the exception that the top of Zone TZU is picked on a conspicuous horizon with a low GR and low DT (fast acoustic). The base of Zone TZU often records the highest GR of the entire Posidonia and is therefore an excellent marker horizon.

- GR high average values particularly the base. The base is often the highest GR of the entire Posidonia. The top of Zone TZU is usually picked at a GR low
- DT Intermediate values, mostly a trend of decreasing (faster acoustic) is recorded. The top is often picked at a DT low (fast acoustic)
- RHOB Intermediate values, a mild trend towards higher values is observed
- ILD Relatively high values, but mostly a trend of decreasing values is observed

Log Zone TP

Log Zone TP marks the transition to the Werkendam Formation. In the ideal case, the GR and DT mirror each other and display an hour-glass pattern, but the zone is also characterized by a spikey log pattern caused by probably carbonate-rich layers. The top of Zone TP is generally selected at a conspicuous horizon with a high GR, low DT and high resistivity. Above the top of Zone TP, the normal 'background' signals of the Werkendam Formation are rapidly reached, usually within a few meters.

- GR Increasing to high values halfway the zone, and decreasing again. The top of Zone TP is usually picked at a GR low
- DT Mirrors the GR, increasing first (slower acoustic) and decreasing afterwards. The top is often picked at a DT low (fast acoustic)
- RHOB Intermediate values, a trend towards higher values is observed
- ILD Relatively high values, but mostly a trend of decreasing values is observed. The top of zone TP marks a sharp return to low background levels.

Log Zone WL

In principal, Log Zone WL is outside the Posidonia and within the Lower Werkendam Member of the Werkendam Formation. The Zone has been defined and included in this zonation, because, a) it is very consistent across large distances in its log signature and b) because the top of the zone displays relatively high resistivities which possibly reflect a high organic content.

- GR On average, quite low, normal background values for marly shale. The top is characterized by a spikey pattern of extreme lows. Above Zone WL a typical high GR (organic rich?) shale interval occurs.
- DT Mirrors the GR, normal background levels for marly shale, except for the top: spikey pattern with extreme lows (fast acoustic). Above the top of Zone WL, a low DT reflects a (organic rich?) shale interval.
- RHOB Same as GR and DT: normal background values for a marly shale. High DT spikes at the top.
- ILD Normal low background levels for marly shale, except for the top: high resistivities are observed at the top of Zone WL.

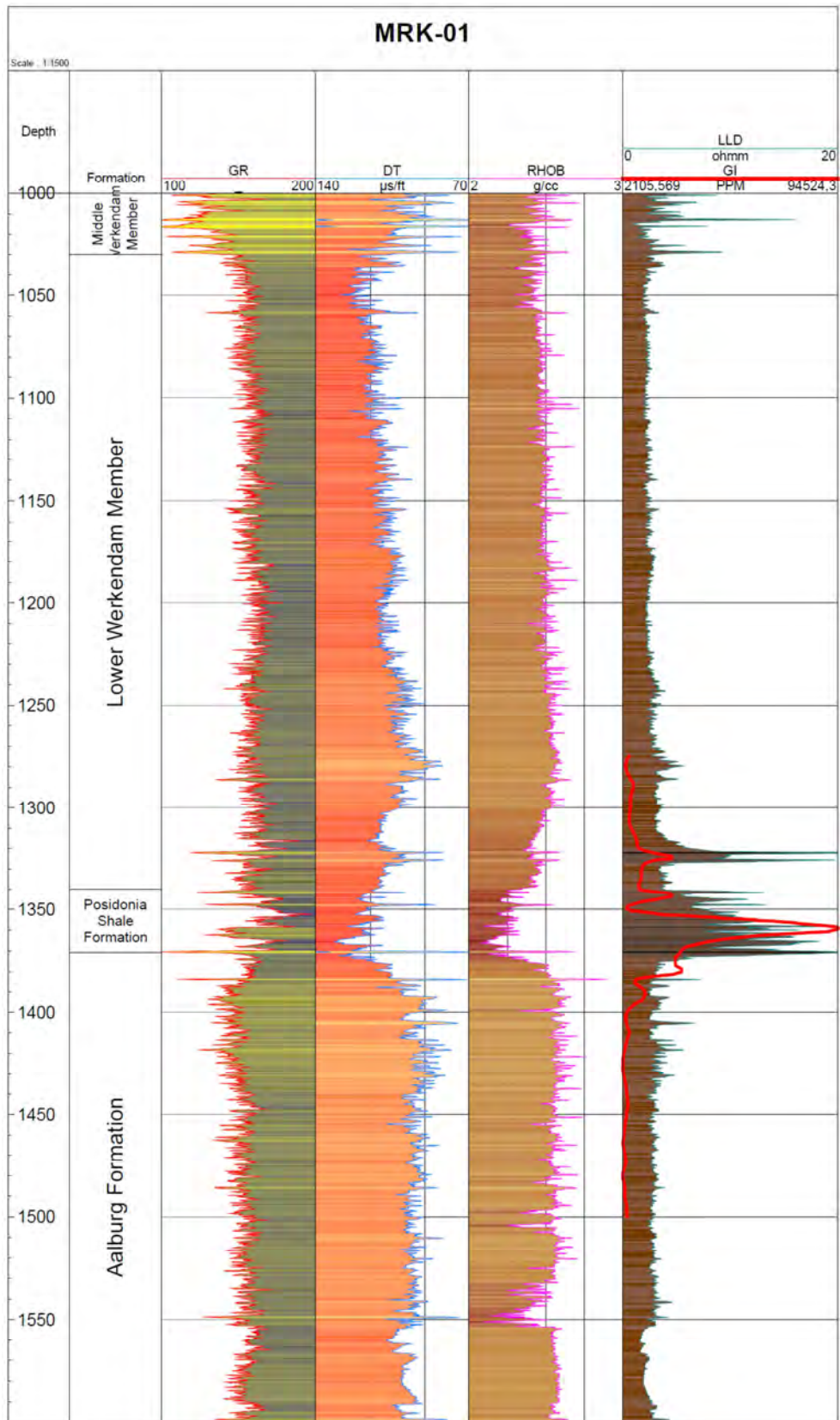


Figure 1: The expression of the Posidonia Shale Formation on electric logs.

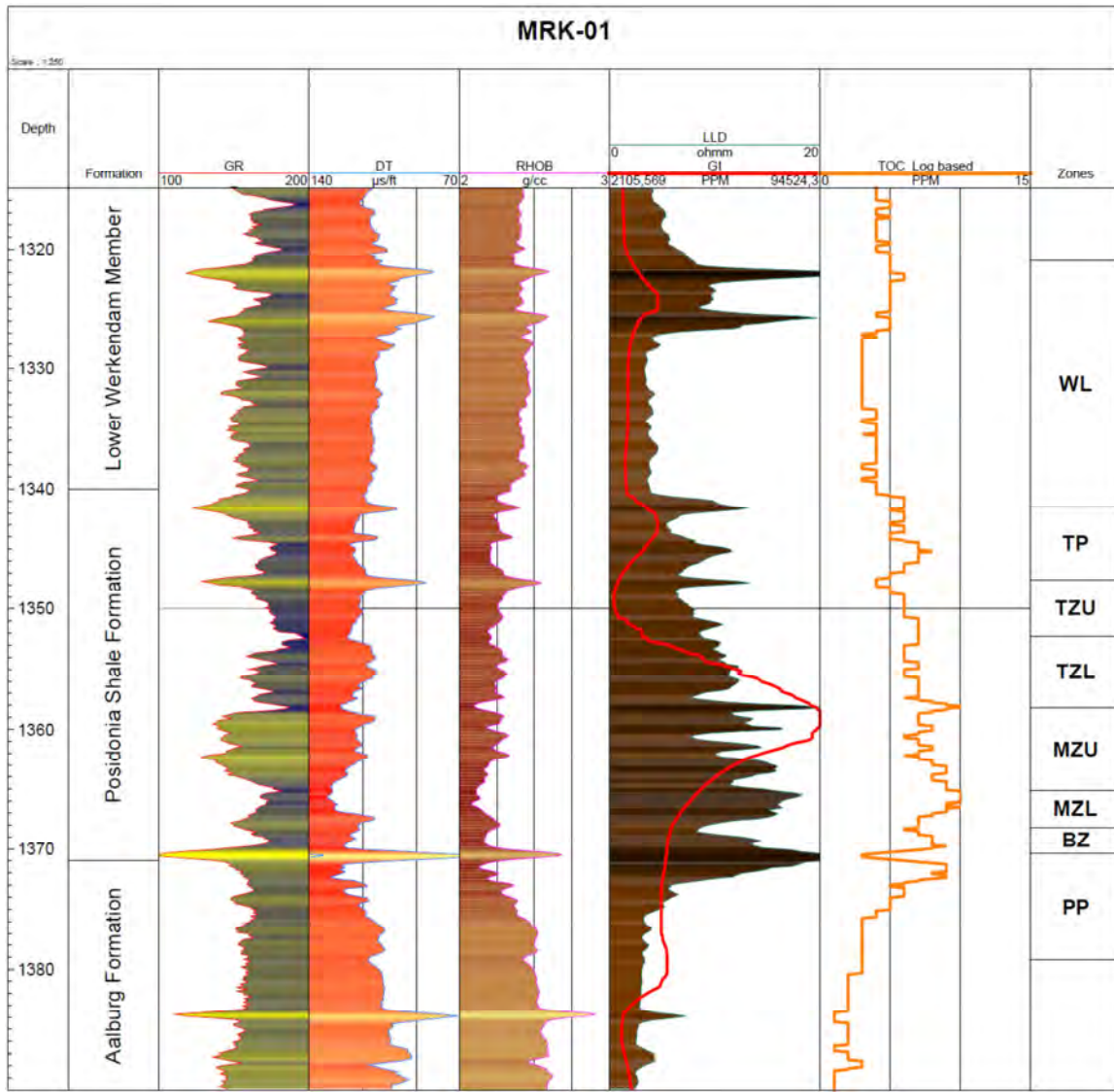


Figure 2: Log Zones of the Posidonia Shale Formation, well MRK-01